FACTORS STRUCTURING MICROBIAL COMMUNITIES ON MARINE FOUNDATION SPECIES

by

Katherine Davis

M.S., Duke University, 2014

B.S., North Carolina State University, 2010

A THESIS SUBMITTED IN PARTIAL FULFILLMENT OF

THE REQUIREMENTS FOR THE DEGREE OF

DOCTOR OF PHILOSOPHY

in

THE FACULTY OF GRADUATE AND POSTDOCTORAL STUDIES

(Botany)

THE UNIVERSITY OF BRITISH COLUMBIA

(Vancouver)

June 2022

The following individuals certify that they have read, and recommend to the Faculty of Graduate and Postdoctoral Studies for acceptance, the dissertation entitled:

Factors structuring microbial communities on marine foundation species

submitted by Katherine Davis in partial fulfillment of the requirements for

the degree of Doctor of Philosophy

in Botany

Examining Committee:

Dr. Laura Parfrey, Associate Professor, Department of Botany, UBC
Supervisor

Dr. Patrick Keeling, Professor, Department of Botany, UBC
Supervisory Committee Member

Dr. Patrick Martone, Professor, Department of Botany, UBC
Supervisory Committee Member

Dr. Mary Berbee, Professor, Department of Botany, UBC
University Examiner

Dr. Miranda Hart, Professor, Department of Biology, UBC-O
University Examiner

Additional Supervisory Committee Members:

Dr. Matthew Pennell, Associate Professor, Department of Zoology, UBC
Supervisory Committee Member

Abstract

The microbiome of marine organisms contributes to host health and ecosystem processes like nutrient cycling. Despite the importance to healthy ecosystems, little is known about the dynamics and drivers of microbiome variation on marine hosts. In this dissertation, I use longitudinal studies and field-based transplant experiments to assess the factors associated with microbiome change on four coastal foundation species. In the intertidal macroalga *Fucus distichus,* I characterize temporal dynamics and microbiome variation on host individuals. I show seasonal turnover is a highly significant predictor of microbiome change. Local environmental conditions and host developmental stage also explain some microbiome variation. I test microbiome fidelity to geographically and phenotypically differentiated *F. distichus* by exposing hosts to new abiotic conditions and microbial source pools. No immediate shifts in microbiome composition occur in five-day transplant experiments, suggesting the established microbiome is buffered against short-term environmental change. I test whether host filtering modulates the shell microbiome of the mussel, *Mytilus californianus*, and find the microbiome is not specific to living mussels. Instead, it is associated with abiotic conditions that vary across geographic locations and elevation in the intertidal zone. In cultivated kelps, I test if outplanting kelp from controlled hatcheries to open ocean sites alters the microbiome and if host and abiotic factors are correlated with microbiome variation at cultivation sites. Host-species specificity was evident throughout the cultivation process and outplanting is followed by high microbiome turnover. Microbiome variation is more strongly correlated to season than abiotic differences between cultivation sites. Altogether, my findings suggest abiotic factors and host identity influence selective microbiome assembly on coastal foundation species. Seasonal microbiome turnover

occurs in multiple hosts and coastal habitats, indicating microbes associated with the prevailing conditions may commonly replace existing members of the microbiome over weeks to months. Within host species, local abiotic conditions and host physiological state are correlated to microbiome variation. This research broadens our understanding of the tempo of microbiome turnover and factors predicting microbial community variation in marine foundation species. It provides necessary foundational knowledge for a holistic understanding of host and ecosystem response to changing oceans.

Lay Summary

The microbial communities living on marine organisms, or the microbiome, play important roles in host health. They also influence entire ecosystems as a part of food webs, by recycling nutrients, and causing disease. Ocean conditions are changing, and we expect these changes to impact which microbes are found in the microbiome. To understand the impacts of ocean change on microbiomes, we need to determine how microbiomes vary normally, especially as their hosts grow and the surrounding environment changes seasonally. I used long-term observations and experiments to study microbiome change in four coastal hosts. I show host species identity and environmental conditions are significantly associated with microbiome composition. I show limited microbiomes change over a few days but strong seasonal microbiome change. This research provides new insights on normal microbiome variation in marine hosts and contributes to a holistic understanding of healthy coastal ecosystems.

Preface

The research conducted in this dissertation has been published or is the process of being published in a peer-reviewed journal. It was carried out in collaboration with other scientists. Below I detail the contributions and publications corresponding to each data chapter.

Chapter 2: Temporal and inter-individual microbiome variation in an intertidal seaweed

This study was originally conceived and designed by Laura Parfrey, Matt Lemay, and Patrick Martone. Rebecca Piercey collected most of the field data with support from me, Laura Parfrey, and Matt Lemay. I conducted the molecular laboratory work with support from Rebecca Piercey. I carried out all bioinformatics analyses. The statistical analyses were run with support from Florent Mazel. I wrote the manuscript and created the figures under the guidance of Laura Parfrey and Florent Mazel. All authors provided valuable feedback and revisions of the manuscript. A version of this chapter has been submitted as:

Davis, K.M., Mazel, F., Lemay, M.A., Piercey, R.S., Martone, P.T., & Parfrey, L.W. (2022) Temporal and inter-individual microbiome variation in an intertidal seaweed. *In preparation.*

Chapter 3: The microbiome of the intertidal macroalga *Fucus distichus* is site-specific and resistant to change following transplant

This study was conceived and designed by me with input from Laura Parfrey. I collected the data, performed the molecular laboratory work, and carried out all bioinformatics analyses. The statistical analyses were run by me with support from Florent Mazel. I wrote the manuscript

and created the figures under the guidance of Laura Parfrey and Florent Mazel. All authors provided valuable feedback and revisions of the manuscript. A version of this chapter has been published as:

Davis, K. M., Mazel, F., & Parfrey, L. W. (2021). The microbiota of intertidal macroalgae *Fucus distichus* is site-specific and resistant to change following transplant. *Environmental Microbiology*, *23*(5), 2617-2631.

Chapter 4: Factors shaping epibiotic microbial assemblages on mussels in the rocky intertidal zone

This study was originally conceived and designed by Alyssa Gehman and Christopher Harley. Alyssa Gehman, Keith Holmes, and Olivia Schaefer collected the field data. I conducted the molecular laboratory work and carried out all bioinformatics analyses. I ran the statistical analyses. I wrote the manuscript and created the figures under the guidance of Laura Parfrey, Alyssa Gehman, and Christopher Harley. All authors provided valuable feedback and revisions of the manuscript. A version of this chapter will be submitted as:

Davis, K. M., Parfrey, L.W., Harley, C.D.G., Schaefer, O., Holmes, K., & Gehman, A.L. (2022) Factors shaping epibiotic microbial assemblages on mussels in the rocky intertidal zone. *In review.*

Chapter 5: Successional dynamics of the cultivated kelp microbiome

This study was originally conceived and designed by me and Laura Parfrey. Allison Byrne, Logan Zeinert, and Cosmo Roemer collected most of the field data with support from me and Michael Wright. I conducted the molecular laboratory work, bioinformatics, and statistical analyses. I wrote the manuscript and created the figures under the guidance of Laura Parfrey. All authors provided valuable feedback on the manuscript. A version of this chapter will be submitted as:

Davis, K.M., Byrne, A., Davis, J., Roemer, C., Wright, M., Zeinert, L., Parfrey, L.W. (2022). Successional dynamics of the cultivated kelp microbiome. *In review.*

Table of Contents

List of Tables

List of Figures

List of Abbreviations

ANOVA	Analysis of variance
ASV	Amplicon sequence variant
CKR	Canadian Kelp Resources
DNA	Deoxyribonucleic acid
KEGG	Kyoto Encyclopedia of Genes and Genomes
MRS	Manchester Research Station
NB	North Beach
NMDS	Non-metric multidimensional scaling
PB	Pruth Bay
PCoA	Principal coordinate analysis
PCR	Polymerase chain reaction
PERMANOVA	Permutational analysis of variance
rRNA	Ribosomal ribonucleic acid
UFI	Unique *Fucus* Identifier
WB	West Beach

Acknowledgements

I would like to acknowledge that the learning and research in this dissertation took place on the colonized lands of indigenous peoples including but not limited to the Homalco, We Wai Kai, We Wai Kum, Klahoose, and K'ómoks, Kwakwaka'wakw, Coast Salish, S'Klallam, Chimacum, Suquamish, Heiltsuk, Wuikinuwv, W̱SÁNEĆ, Te'mexw Treaty Association, Coast Salish, Huu-ay-aht, Musqueam, Squamish and Tsleil-Waututh. I have been present in many beautiful places throughout British Columbia and Washington as an uninvited guest. I value the relationships with oceans, lands, and living beings (even the invisible ones) that I developed through this work and the awareness I have gained of my own heritage and privilege.

I am grateful for staff, infrastructure, logistical, and grant funding support from the Hakai Institute and Tula Foundation. Thanks to Bia Segovia, Rhea Sanders-Smith, Lauran Liggan, Isabelle Desmarais, Carolyn Prentice and other Hakai Institute staff for assistance with sample collection and processing. Many thanks to Keith Holmes and the Hakai Geo-spatial team for maps, site measurements, and amazing drone imagery and photographs. I appreciate bioinformatic assistance from Evan Morien.

The work in Chapter 5 wouldn't have been possible without boat support from the Atlegay Fisheries Society. Special thanks to John Duncan for taking me out on the boat, sharing smoked salmon, and finding whales. I am grateful to Joth Davis, Charlie Delius, and Blue Dot Sea Farms for taking me out on their boat and letting me sample their cultivated kelp. Thanks to Max Calloway for facilitating sampling of hatchery kelp at the Manchester Research Station.

Additionally, I would like to express gratitude to my supervisor, Laura Parfrey, for encouraging me to pursue my research interests, for pushing me when needed, for asking tough questions, and for affording me space to have non-research adventures also. Thanks to my committee members, Patrick Keeling, Patrick Martone, and Matt Pennell for their guidance in this work. I am grateful for scholarship funding from Port Townsend organizations and opportunities presented by the Ocean Leaders Fellowship. I appreciate the peer support and friendships that have grown in the UBC Botany Department and Biodiversity Research Centre, particularly with folks from the Parfrey, Keeling, Martone, and O'Connor Labs who made this process more fun. Special thanks are owed to the friends and family who inspired me, encouraged me, showed me love, made me laugh, and ensured I got out on the water and into the mountains over the last five years.

Dedication

This work is dedicated to our connections to and through *WATER*.

Chapter 1: Introduction

The research presented here explores variation in the microbiome of marine foundation species in coastal ecosystems. Foundation species are organisms that have significant ecological impacts on their surrounding environment (Ellison, 2019), such as canopy forming macroalgae and sessile invertebrates. They create three-dimensional habitat, provision nutrient resources, and shape overall community structure. The microbiome is a collection of diverse microbial taxa and their associated genetic material found on or inside a eukaryotic host. This research focuses specifically on the microbiome of external host surfaces, which directly interface with the surrounding environment and are expected to be under some influence of spatial or abiotic factors (Schellenberg and Clarke, 2020). The microbiomes of marine foundation species affect ecosystem functioning, from the health and development of individual hosts (Morris *et al.*, 2016; Ghaderiardakani *et al.*, 2017; Ziegler *et al.*, 2017; Woznica and King, 2018) to the perpetuation of coastal biogeochemical cycles (Azam and Malfatti, 2007; Pfister and Altabet, 2019). Coastal ecosystems are currently undergoing major changes due to climate-related and anthropogenic stressors (Harley *et al.*, 2006; Halpern *et al.*, 2008). Identifying, understanding, and predicting the consequences of these changes on ecosystem functioning requires increased knowledge of the capacity for host-microbiome associations to withstand or undergo change (Shade *et al.*, 2012; Trevathan-Tackett *et al.*, 2019; Wilkins *et al.*, 2019). In this introductory chapter, I summarize existing research on the dynamics and factors associated with microbiome variation in coastal marine foundation species. I identify two major knowledge gaps in our understanding of host-microbiome associations in changing coastal oceans: 1) whether host-associated microbial communities are generally stable or undergo natural turnover and 2) whether abiotic or

biotic factors are the dominant influence over microbiome composition. Finally, I provide an overview of how my dissertation research aims to fill these gaps through observational and experimental studies on the microbiome of four marine foundation species.

1.1 Stability versus turnover in coastal marine microbiomes

Host-microbial associations in marine environments take many forms. There are classic examples of mutualistic symbioses in marine habitats involving one host and one symbiont species, like the Hawaiian bobtail squid and luminous *Aliivibrio fischeri* (McFall-Ngai and Ruby, 1991; Nyholm and McFall-Ngai, 2021) or sulfur-oxidizing bacteria in the gills of lucinid clams (Dando *et al.*, 1986). More often, hosts engage in complex associations with diverse and dynamic microbial assemblages comprising the microbiome, especially on external host surfaces (Schellenberg and Clarke, 2020). Identifying the specific interactions, or the underlying metabolic exchanges, between hosts and microbes in these high diversity communities is difficult. Still, microbial communities on marine hosts are distinct from surrounding free-living environments (Roth-Schulze *et al.*, 2016; Thompson *et al.*, 2017; Lemay *et al.*, 2021) and often host species-specific (Hernandez-Agreda *et al.*, 2018; Lemay, Martone, Keeling, *et al.*, 2018; Dunphy *et al.*, 2019; Offret *et al.*, 2020) suggesting there is determinism in microbiome assembly. Within species-specific microbial assemblages, there can be a mix of stable or 'core' members (Risely, 2020) and other intermittently present members which are only observed in association with particular environmental conditions, microbiome states, or host traits (Hernandez-Agreda *et al.*, 2018). Characterizing stable and temporally variable members of the microbiome can provide insights for future research exploring the nature of specific host-microbe interactions and their ecological functions.

Variation in microbiome composition is attributed to both positive and negative outcomes of symbiosis. Changes that cause the microbiome to diverge in diversity or structure compared to stable or healthy states are often referred to as states of "dysbiosis," and are commonly associated with host stress or disease (Egan and Gardiner, 2016). Under stressful environmental conditions, host vulnerability to invasion by specific pathogens can increase (Case *et al.*, 2011; Miller and Richardson, 2015) or microorganisms present in a healthy microbiome can become opportunistic pathogens (Burge *et al.*, 2013; Kumar *et al.*, 2016; Meistertzheim *et al.*, 2017; Zozaya-Valdés *et al.*, 2017). Yet, changes or flexibility in the microbiome have recently been proposed as mechanisms that facilitate environmental acclimatization and increase host resilience in changing oceans (Ghaderiardakani *et al.*, 2020; Voolstra and Ziegler, 2020). In this case, changes in the microbiome could expand host physiological capacities, thereby broadening environmental tolerances (Dittami *et al.*, 2016; Duarte *et al.*, 2018). Human-directed change of the microbiome on macroalgae and corals has also been shown prevent disease (Rosado *et al.*, 2019; Li *et al.*, 2021) or bolster host growth (Ghaderiardakani *et al.*, 2017; Zhang *et al.*, 2021), and may be a valuable tool to support conservation and culture of marine hosts (French *et al.*, 2021). Understanding the outcomes of microbiome change on host and ecosystem functioning holds exciting potential but remains a challenge in these complex systems.

Generalizations regarding the degree of stability in microbiomes of healthy hosts are limited by conflicting patterns of microbiome variation over time and across species. For example, a dominant habitat-forming kelp in Australia has considerable microbiome stability within geographic regions despite seasonal changes in environmental conditions (Phelps *et al.*, 2021). Some corals and other macroalgae show distinct successional or seasonal microbiome turnover (Lachnit *et al.*, 2011; Glasl *et al.*, 2016; Sharp *et al.*, 2017; Serebryakova *et al.*, 2018;

Weigel and Pfister, 2019). Lack of high-resolution sampling of individuals has required researchers to rely on inference from population-wide patterns at infrequent time points (e.g., monthly or yearly) to characterize temporal microbiome dynamics. The question remains: Is the microbiome of healthy marine hosts, or host individuals, stable over time? And if not, what is the extent and tempo of microbiome change?

1.2 Biotic versus abiotic factors associated with microbiome change

Abiotic factors such as temperature, light, and seawater chemistry (e.g., salinity and nutrients) significantly structure the temporal dynamics of free-living seawater microbial communities (Cram *et al.*, 2015; Ward *et al.*, 2017). The microbiome on marine hosts is assumed to be assembled from microbes in seawater and other microbial "source pools" on nearby substrates and hosts (Lemay, Martone, Keeling, *et al.*, 2018; Cleary *et al.*, 2019). Thus, changes in the abiotic environment and microbial source pools can determine which microbes are available to colonize a host. Correspondingly, experimental manipulations of abiotic conditions, like temperature, have elicited significant microbiome change in diverse marine foundation species (Mensch *et al.*, 2016; Li *et al.*, 2018; Minich *et al.*, 2018; Ahmed *et al.*, 2019).

The selective influence of a host can also shape microbiome assembly and turnover. Specific microbial taxa may be enriched or excluded from host surfaces based on the chemical composition of host tissues or exudates (Saha *et al.*, 2011a; Lachnit *et al.*, 2013; Longford *et al.*, 2019; Saha and Weinberger, 2019). For example, polysaccharides abundant on the surfaces and tissues of marine hosts fuel the metabolism of many heterotrophic bacteria. Variation in the types of polysaccharides produced by hosts can favor microbes with different metabolic capabilities (Roth-Schulze *et al.*, 2016; Raimundo *et al.*, 2021; Robbins *et al.*, 2021). Host morphological

characteristics (Lemay *et al.*, 2020) may also influence the microbiome, through modification of the local environment (e.g. diffusive boundary layer (Noisette and Hurd, 2018)) or via biochemical differences in tissue types (Paix *et al.*, 2020). There is evidence for tissue-specific microbiomes on macroalgae (Lemay *et al.*, 2021), corals (Pollock *et al.*, 2018), and bivalves (Musella *et al.*, 2020). Host health and immune responses (de Oliveira *et al.*, 2017; Qiu *et al.*, 2019; Posadas *et al.*, 2021) as well as defense compounds produced by the host or members of the microbiome (Egan *et al.*, 2000; Lachnit *et al.*, 2010; Longford *et al.*, 2019) seem to further impact microbiome composition.

Host selective factors can vary depending on interactions with the local environment and temporal changes in host biology. On coral reefs, the abundance and composition of available polysaccharides lead to seasonal shifts in microbiome composition and function (Glasl *et al.*, 2020). In macroalgae, seasonal variation in the dominant polysaccharide exudates and cell wall components (Dethier and Williams, 2009; Schiener *et al.*, 2015; Starko *et al.*, 2018) is hypothesized to contribute to temporal variation in the surface microbiome composition (Lachnit *et al.*, 2011; Goecke *et al.*, 2013). Similarly, seasonal shifts in the surface metabolites of the brown alga, *Taonia atomaria,* are correlated with increased seawater temperature and changes in microbiome composition (Paix *et al.*, 2019). There is also evidence that some coral and macroalgae shed their surface mucus on cyclic or seasonal timescales leading to a reset in microbiome succession (Halat *et al.*, 2015; Esther Rickert *et al.*, 2016; Glasl *et al.*, 2016). Thus, host factors that influence microbiome composition and dynamics may be tied to abiotic conditions or may be inherent to the biology of the host.

This raises the question: What is the contribution of abiotic factors versus host factors to microbiome change over time? If host factors are the dominant selective filter shaping

microbiome assembly and turnover, then we might expect the microbiome to resist change when hosts are exposed to new microbial source pools or environmental conditions. Determining if microbiome composition is sensitive to shifts in host or abiotic factors can provide insights on the resiliency of marine foundation species to environmental change and inform future mechanistic studies of host-microbiome interactions.

1.3 Research objectives

A better understanding of the tempo and drivers of microbiome variation in marine foundation species is necessary for a holistic understanding of healthy ecosystems and ecosystem response to changing oceans. Here I use a combination of longitudinal studies and experimental manipulations to determine the timescale of microbiome change in four ecologically important invertebrate and macroalgal hosts from intertidal and subtidal habitats. I assess the relative contribution of abiotic and biotic factors to observed microbiome change in these hosts. The specific goals of this research are:

1. Conduct a longitudinal study to identify the timescale of natural microbiome variation on individual hosts.
2. Experimentally test the stability of the microbiome when the host is exposed to new microbial source pools.
3. Experimentally test the role host biology plays in assembling a specific microbiome under varying abiotic conditions.
4. Conduct a longitudinal experiment to test if the microbiome acquired in early life is maintained over time, even when the host is subsequently exposed to different abiotic conditions and microbial source pools.

Chapter 2: Temporal and inter-individual microbiome variation in an intertidal seaweed

2.1 Introduction

Marine microbes form complex associations with macroorganisms (Wilkins *et al.*, 2019). The host organism likely represents protective and/or selective microbial habitats that are distinct from free-living habitats. In turn, microbes colonizing a host may directly or indirectly influence host health (Egan and Gardiner, 2016; Sweet and Bulling, 2017; Zozaya-Valdés *et al.*, 2017; Longford *et al.*, 2019), productivity (Marshall *et al.*, 2006; Tarquinio *et al.*, 2018; Mayer Pinto *et al.*, 2021), and nutrient availability in the ecosystem (Moulton *et al.*, 2016; Pfister and Altabet, 2019; Zhang *et al.*, 2019). Consequently, the ecosystem functions attributed to coastal foundation species arise from the interactions between host organisms and the associated microbial taxa and genes, or the microbiome (Trevathan-Tackett *et al.*, 2019; Wilkins *et al.*, 2019). The microbiome for a given host species, however, can vary within and across host populations (Dunphy *et al.*, 2019; Pfister *et al.*, 2019; Weigel and Pfister, 2019; Schellenberg and Clarke, 2020). Understanding the factors that shape microbial diversity on marine hosts and the cascading effects of microbiome activity on host and ecosystem functioning are key priorities in the field (Trevathan-Tackett *et al.*, 2019; Wilkins *et al.*, 2019).

Marine macroalgae (i.e. seaweeds) are foundation species and models for understanding host-associated microbiome assembly and dynamics in coastal ecosystems (Egan *et al.*, 2013; van der Loos *et al.*, 2019). Seaweed-associated microbes vary with host species (Lemay *et al.*, 2020; Quigley *et al.*, 2020), host physiological condition (Case *et al.*, 2011; Marzinelli *et al.*,

2015; Minich *et al.*, 2018; Longford *et al.*, 2019; Qiu *et al.*, 2019), disease (Zozaya-Valdes *et al.*, 2015b; Longford *et al.*, 2019), life history stage (Lemay, Martone, Hind, *et al.*, 2018), and environmental factors (Alexandra H Campbell *et al.*, 2015; Marzinelli *et al.*, 2018; Weigel and Pfister, 2019). Despite high taxonomic variability, some studies have observed consistency in the functional gene potential of seaweed microbiomes (Burke *et al.*, 2011; Roth-Schulze *et al.*, 2016). This suggests host-microbial interactions may be maintained by associations with functionally redundant taxa that are adapted to specific host or abiotic conditions. The factors driving high taxonomic variability in seaweed microbiomes and the extent to which variation is predictable or idiosyncratic across a population are poorly understood.

Microbial communities on macroalgae usually show few taxa that are prevalent across samples while the remainder of the community is highly diverse and responds dynamically to the surrounding environment (Hernandez-Agreda *et al.*, 2018; Capistrant-Fossa *et al.*, 2021). The prevalent taxa, or core microbiome, are expected to depend on host niches and are considered more likely to engage in essential metabolic exchanges with the host (Shade and Handelsman, 2012). The functions and drivers of the responsive portion of the microbiome are less clear. The responsive microbiome may be selectively assembled from a temporally variable environmental source pool, like from seawater (Fuhrman *et al.*, 2006; Gilbert *et al.*, 2012; Ward *et al.*, 2017), or may be influenced by host physiological attributes, such as growth stage or reproductive status (Tapia *et al.*, 2016; Serebryakova *et al.*, 2018; Wu *et al.*, 2018; Sacristán-Soriano *et al.*, 2019; Lemay *et al.*, 2021). Much of our knowledge on the assembly of macroalgal microbiomes is focused on bacteria, but interactions with eukaryotic microbes may also shape the community dynamics (Chow *et al.*, 2013) on macroalgal hosts and influence important ecological functions like carbon cycling (Armstrong *et al.*, 2000). High temporal resolution, repeated microbiome

sampling of host individuals is essential to gain insights on the contributions of environmental variability, microbe-microbe interactions, and host physiological cues to macroalgal microbiome assembly and variation.

In this study we used a habitat-forming, brown seaweed to characterize the microbiome on specific host individuals and across the host population over time. We sampled multiple trophic levels and the functional gene potential of the microbiome to characterize how different aspects of the microbiome respond to changes in host and abiotic factors. Our study focuses on the intertidal seaweed host, *Fucus distichus*, because it is widespread and accessible in the intertidal; the ecology is well studied (Ang, 1991; Wright *et al.*, 2004; Dethier and Williams, 2009; Wahl *et al.*, 2011); it exhibits year-round growth and reproductive capacity (Ang, 1991); its location in the intertidal exposes it to strong seasonal variation in abiotic conditions; and there are a growing number of studies exploring spatial and temporal microbiome variation for this host species and its congeners (Lachnit *et al.*, 2011; Stratil *et al.*, 2013; E. Rickert *et al.*, 2016; Mensch *et al.*, 2016; Capistrant-Fossa *et al.*, 2021; Davis *et al.*, 2021).

Disentangling the effect of seasonal turnover from host development on the microbiome can be difficult because many seaweed species display distinctive seasonal growth cycles (Schiel and Foster, 2006). In *Fucus distichus*, however, individuals of different developmental stages occur in the population throughout the year, allowing host factors and seasonality in the environment to be partially decoupled as predictors of microbiome variation. Previous microbiome of studies of fucoids have found seasonally distinct compositions (Lachnit *et al.*, 2011; Serebryakova *et al.*, 2018) while others have shown the microbiome to be relatively stable on the time-scale of days (Quigley *et al.*, 2020; Davis *et al.*, 2021). The tempo of taxonomic

turnover on *F. distichus* is not well understood and it is unclear if microbial gene functions change in concert with temporal taxonomic turnover.

To assess temporal and within-population microbiome dynamics on *Fucus distichus*, we marked specific host individuals in the field and repeatedly sampled the bacteria (16S amplicons), eukaryotes (18S amplicons), and gene functions (shotgun metagenomics) on each individual during a 10-month period. Additional juvenile individuals were included throughout the study to parse the contribution of host development and seasonal turnover to microbiome variation. We compared the seasonal dynamics of the *F. distichus* microbiome to dynamics of the surrounding microbial source pools of seawater and rock biofilms, which lack host-driven biological filtering. Characterizing the tempo and drivers of microbial turnover within and among *F. distichus* individuals provides foundational knowledge that can yield insights on the mechanisms and functions underlying seaweed-microbial interactions. Such interactions can be further explored to understand their contribution to ecosystem-functioning and the vulnerability of host-microbial associations to rapidly changing coastal oceans.

2.2 Material and methods

2.2.1 Host and site characteristics

Fucus distichus (Phaeophyceae, Fucales) occurs abundantly in the high- and mid-intertidal zones of the northeastern Pacific, ranging from southern California to Alaska. *F. distichus* is perennial and individuals generally live for 1–3 years (Ang, 1991). Throughout the year, the duration of air exposure at low tide and the environmental conditions during periods of air exposure vary significantly for this host. In winter months (November through January), the lowest low tides occur primarily at night and in April through August, low tide exposure occurs

during daylight hours (Wright *et al.*, 2004) leading to increased temperature and UV stress during exposed periods. Changes in tidal exposure due to season as well as spatial position in the intertidal zone differentially impact growth, reproduction and chemical composition of individuals in a *F. distichus* population (Ang, 1991; Wright *et al.*, 2004; Dethier and Williams, 2009). The age of an individual is positively correlated with the length of its longest blade (Ang, 1991) (Appendix A - Figure 1). Larger individuals also tend to have more dichotomies (branches), but the number of dichotomies is not the preferred metric for *Fucus* age or growth because of susceptibility to blade breakage (Keser and Larson, 1984). Reproductive thalli of *F. distichus* are found throughout the year (Ang, 1991) and individuals can remain reproductive yearlong (Wright *et al.*, 2004).

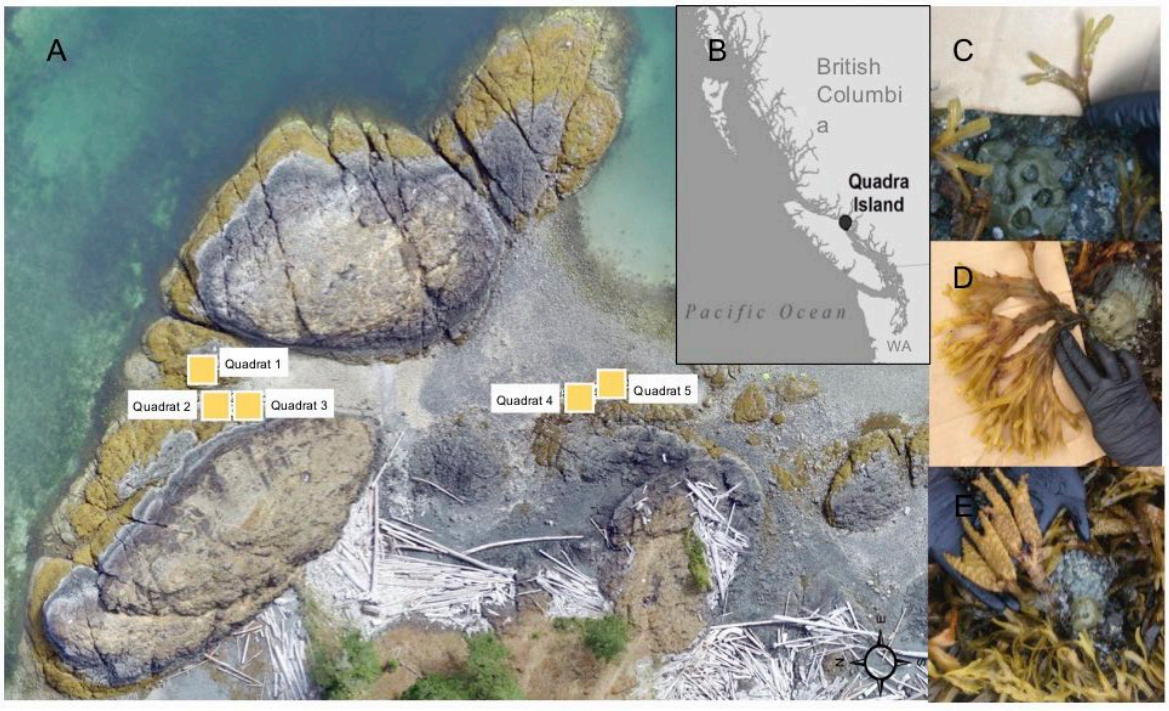

Figure 1. Map and aerial image of the study site and representative images of *Fucus distichus* sampled. A) Location of quadrats within the *F. distichus* bed; B) Study site location on Quadra Island, BC, Canada; C) Example of juvenile *F. distichus* and *in situ* UFI identification marker; D) Example of mature *F. distichus*; E) Example of reproductive *F. distichus*.

For this study, five permanent quadrats ($0.5m^2$), representing subsamples of the population, were established in the intertidal zone at the Hakai Institute Field Station, Quadra Island, British Columbia, Canada (50.1154, -125.2206) in 2017 (Figure 1A-B). Quadrats within the *F. distichus* bed were located semi-randomly, with an attempt to maximize accessibility for sampling while also minimizing variation in the tidal elevation of the host population. Effort was also made to establish quadrats in locations that had approximately 100% *F. distichus* canopy cover at the start of the study. The furthest distance between quadrats was approximately 65m and quadrats ranged from ~0m to 1m below vertical datum (CGVD 28 HT 2.0). Within each quadrat, five *F. distichus* individuals were marked with a unique *Fucus* identifier (UFI) in marine epoxy (Z-spar) attached to rock substrate next to the individual's holdfast (e.g., Figure 1C-E). The marked and resampled host individuals were frequently damaged and lost all together, presumably by wave activity, other abiotic stressors like desiccation, or biotic mechanisms such as grazing (Haring *et al.*, 2002; Dethier and Williams, 2009). When a focal *F. distichus* individual was lost, we marked and began sampling the microbiome of the smallest proximal *F. distichus*; thus, our study included individuals of different sizes and reproductive status within the same quadrat and time point (Figure 2). Canopy cover of *F. distichus* was measured during each sampling event by placing a $0.5m^2$ PVC frame with a 10x10 grid over each quadrat and using visual estimation of grid squares containing *F. distichus* to determine percent coverage.

High resolution temperature loggers were permanently attached in each quadrat to document seasonal and daily temperature variation at the site (see abiotic data collection for details). The greatest daily variation in mean maximum temperature occurred during summer months between times when the temperature logger was exposed to air at low tide and

submerged in seawater at high tide (Appendix A - Figure 2). Quadrats 4 and 5, located higher in the intertidal than quadrats 1-3, had significantly more variable daily temperature ranges (Appendix A - Figure 2). Quadrats 4 and 5 also experienced greater loss of canopy cover over time (Appendix A - Figure 2) which likely represents a positive feedback where loss of canopy cover exposed more rock substrate and led to increasingly elevated temperatures.

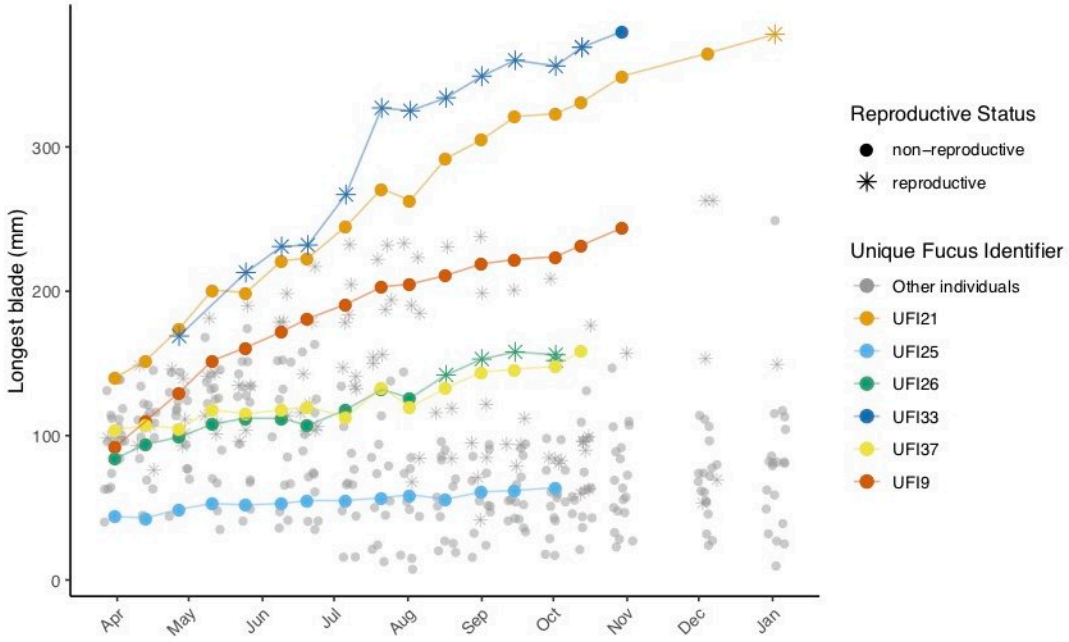

Figure 2. Variation in *Fucus distichus* size and reproductive status over time for specific individuals and across the population.

2.2.2 Sample collection

The surface microbial community of *F. distichus* individuals was characterized every two weeks using 16S rRNA gene and 18S rRNA gene amplicon sequencing and shotgun metagenomics. Briefly, the longest blade was rinsed with 0.22um filtered, sterile seawater for 10 seconds to remove transient environmental microbes and then rubbed at the apical, meristematic

tip with a Puritan® sterile swab for 10 seconds. The meristem tissue was targeted for sampling because this is the site of newest tissue growth, most recent microbial colonization, and avoids potential microbial community differences attributed to tissue age (Weigel and Pfister, 2019; Lemay *et al.*, 2021). Swabs were deposited in individual 2ml cryovials (VWR), placed in coolers on ice and upon return to the laboratory, stored at -80˚C until DNA extraction. Trait data for *F. distichus* individuals were collected at each sampling event including length of the longest blade, number of dichotomies and number of reproductive apices. Photos of *F. distichus* individuals were taken at each sampling to record host condition (e.g., grazer-inflicted or other damage and desiccation). Microbial samples from the surrounding environment were taken to provide information about the potential source community of bacteria and eukaryote colonizers of *F. distichus*. Swab samples were taken, as described above, of the "bare" rock substrate within each quadrat. Rock substrate provides a reference for how surrounding abiotic surfaces are colonized in the absence of biological filtering. Five water samples were collected from adjacent surface seawater during each sampling event to characterize the water column microbial community. Seawater samples were collected in sterile 500ml plastic bottles (Nalgene) and upon returning to the lab, filtered onto a 0.22µm Sterivex™ filter (EMD Millipore) using a Cole-Parmer MasterFlex L/S peristaltic pump; filters were in stored in sterile bags (Whirl-pak) at -80˚C.

2.2.3 Abiotic data collection

Temperature and salinity were measured at each sampling using the YSI Pro Plus Multiparameter Instrument with Quatro cable (model: 6050000, and 605790, respectively) deployed 30cm below the seawater surface at the waterline closest to the quadrats. Intertidal temperatures are known to vary on small spatial and temporal scales (Helmuth and Hofmann,

2001; Dethier and Williams, 2009) so each quadrat was equipped with a Thermochron ibutton temperature logger (model: DS1921G) to record variation among quadrats and one Onset TidbiT v2 temperature logger (UTBI-001) was deployed to record ambient temperatures. The ibuttons recorded the temperature at 2-hour intervals for the duration of the study (10 months).

2.2.4 DNA extraction

DNA was extracted from swabs and filters using the Qiagen DNeasy PowerSoil HTP 96 DNA extraction kit (QIAGEN, Hilden, Germany) following the manufacturer's recommended protocol. DNA was extracted from the seawater samples collected on Sterivex™ filters using the DNeasy® PowerWater® Sterivex™ Kit (QIAGEN, Hilden, Germany) according to manufacturer's recommended protocol.

2.2.5 16S rRNA gene and 18S rRNA gene amplicon sequencing

PCR amplification for bacterial and archaeal DNA targeted the V4-V5 region of the 16S rRNA gene using primers, 515f: 5'–GTGYCAGCMGCCGCGGTAA–3' and 926r: 5'–GGACTACNVGGGTWTCTAAT–3' (Comeau *et al.*, 2011). PCR amplification for eukaryotic DNA targeted the V4 region of the 18S rRNA gene using primers, E572f: 5'–CYGCGGTAATTCCAGCTC–3' and E1009r: 5'–AYGGTATCTRATCRTCTTYG–3' (Comeau *et al.*, 2011). Amplicon library preparation and sequencing with Illumina MiSeq using paired-end (2 × 300 bp) v3 chemistry was performed at the Integrated Microbiome Resource (IMR), Centre for Comparative Genomics and Evolutionary Bioinformatics (CGEB) at Dalhousie University according to published protocols (André M. Comeau *et al.*, 2017).

Quality filtering, trimming, dereplication, chimera removal, inference of true amplicon sequence variants (ASVs), and taxonomic assignment against the SILVA database (v.1.3.2) was done with DADA2 (Callahan *et al.*, 2016). For DADA2 processing the filter and trim step was set to a minimum read length 150bp forward and 120bp reverse. Reads were truncated after a quality score of less than or equal to two. Reads with higher than 8 forward and 10 reverse maxEE "expected errors" were discarded. Chimera detection was done using the pooled method. Singletons in each sample and sequences with less than 100 reads across the entire dataset were removed. For the 16S rRNA gene amplicon dataset, reads unassigned at the domain-level and reads assigned as chloroplast or mitochondria were removed for downstream analyses. For the 18S rRNA gene amplicon dataset reads unassigned at the domain-level and reads assigned to the host family, Fucales, were removed for downstream analyses. Sequence data is available from the European Nucleotide Archive under project accession: PRJEB50052.

2.2.6 Shotgun metagenomics

Shotgun metagenomic libraries were constructed for a subset of samples. We specifically selected samples of *F. distichus* individuals with the longest consecutive sampling coverage to capture intra-individual differences and host changes that could explain dynamics of microbial functional traits over time. Five *F. distichus* individuals, three rock substrate and three seawater samples were sequenced at each of four time-points (n= 20 *F. distichus*, n= 12 Rock, n= 12 Seawater). Metagenomic libraries were prepared with the Illumina Nextera XT kit. 150-bp fragments were sequenced on an Illumina NextSeq 550 at the IMR facility at Dalhousie University. Quality statistic generation, paired-end read merging, and quality filtering were performed on the raw sequencing reads via the SqueezeMeta pipeline (Tamames and Puente-

Sánchez, 2019). Annotation of genes sequences to the Kyoto Encyclopedia of Genes and Genomes (KEGG) IDs was conducted in SqueezeMeta and assignment of KEGG ID orthologs to KEGG level B and KEGG level C categories was done with the collapse_table.py script from FAPROTAX (Louca, Parfrey, *et al.*, 2016). Metagenomic data is available from the European Nucleotide Archive under project accession: PRJEB50052.

2.2.7 Statistical analyses

All statistical analyses were performed using R version 3.6.2 (R Core Team, 2019). 16S rRNA amplicon datasets were rarefied to 5000 reads per sample and 18S rRNA amplicon datasets were rarefied to 1000 reads per sample for most downstream analyses. For metagenomic reads (KEGG Orthologs), abundances were square root transformed for most downstream analyses. Differences in microbiome structure among habitat types (*F. distichus*, rock substrate, or seawater), sampling date, or host traits were analyzed with the vegan package (Oksanen *et al.*, 2019) using PERMANOVA with 999 permutations on Bray-Curtis dissimilarities and visualized using non-metric multidimensional scaling plots made with phyloseq (McMurdie and Holmes, 2013) and ggplot2. To test for significant differences in microbial communities between specific habitats we used pairwise PERMANOVAs on Bray-Curtis dissimilarities with the wrapper function pairwise.adonis for vegan (Martinez Arbizu, 2020); p-values were adjusted with the Benjamini–Hochberg correction for multiple comparisons. We used month of sampling as our measure of time in the PERMANOVA analysis. This aided visualization in NMDS plots and minimized the impact of samples missing for individual *F. distichus*. We used quadrat as a random variable that represents small-scale variation in space and in environmental conditions across the population. For host traits, we used the presence of one or more receptacles to indicate

reproductive activity and length of the longest blade as a coarse metric of size and age. We also conducted statistical analyses using number of dichotomies of the host as an alternative metric of host size which captures host three dimensional structure. The length of the longest blade and the number of dichotomies for a host were positively correlated (p-value < 0.001; SI Figure 1); so, we present only length of the longest blade in our models as a predictor of host development and size because this metric is generally better correlated with host age (Ang, 1991).

We tested for differences in microbial community composition within a host individual and across the population over time by comparing Bray-Curtis dissimilarity between pairs of samples from different sampling days. The same approach was used to assess differences in community composition at single timepoints. Here, we made pairwise comparisons of samples taken on the same day from within the same quadrat. We also assessed community similarity of pairs of samples taken from the whole population on the same day. Plotted dissimilarity values were assessed visually for differences.

To identify microbial ASVs or gene functions (KEGG level B and C) that were significantly associated with each habitat type (*F. distichus*, rock substrate, or seawater), we applied indicator species analysis, IndVal (Cáceres and Legendre, 2009). Indicator species analysis determines significant associations based on the fidelity and specificity of a taxa or gene function to a group, in this case, habitat type. Fidelity is the probability of being found in all samples of a given group, and specificity is the probability being found in only one group given its presence in that group.

We visualized the dynamics of compositional turnover on an individual (UFI) and across the population by plotting the relative abundance of the most abundant taxa or gene functions

over time. For population-level plots, we calculated the mean relative abundance across all samples taken at each timepoint and present the summary value in stacked bar plots.

Two samples taken at different times are predicted to harbor microbial communities that are less similar than two samples taken at the same time based on the time-decay relationship. The time-decay relationship should lead to a decreasing relationship of community similarity over time. However, if there is a seasonality effect, two samples taken at different times in the same season (e.g., 10 months apart) should be more similar than two samples taken at different times in different seasons (e.g., 6 months apart). As a result, there would be a non-linear time decay relationship. To test for this, we added a quadratic term to the mantel test of the relationship between microbial community similarity and the time elapsed between samples. We tested the significance of the quadratic term using randomization in the MRM approach (Lichstein, 2006) and the function MRM in the ecodist package. We also recorded the number of days apart which the community similarity values switched from decreasing to increasing using the fitted coefficients of the MRM model.

Code for the statistical analyses can be found at https://github.com/katherine-m-davis/FucusTimeseries

2.3 Results

We collected longitudinal data on the microbiome of *Fucus distichus* and the surrounding rock substrate and seawater every two weeks from March 2017 to January 2018. After quality filtering and removal of low coverage samples the dataset included 227 *Fucus distichus*, 95 rock substrate, and 43 seawater samples. Shotgun metagenomics was conducted on a subset of samples: 96 *F. distichus*, 48 rock substrate, and 40 seawater samples.

We found the *Fucus distichus* microbiome to be distinct from surrounding habitats. Habitat type was the most important factor explaining overall differences in microbial community composition and functions across the dataset (Figure 3). Seawater, rock substrate and *F. distichus* harbored distinct bacterial communities (Figure 3A) (PERMANOVA 16S: df = 2, F = 42.25, p-value < 0.001), eukaryotic communities (Figure 3C) (PERMANOVA 18S: df = 2, F = 14.89, p-value < 0.001) and functional repertoires (Figure 3E) (PERMANOVA metagenomics: df = 2, F = 15.95, p-value < 0.001). Pairwise comparisons showed the microbiome of *F. distichus* was more similar to biofilm communities on rock than to planktonic communities in seawater both in terms of microbial taxa and functional gene categories (Appendix A - Table 1).

We used indicator species analysis to determine which taxa or gene functions were statically associated with differences between habitat types. Bacterial genera significantly associated with *F. distichus* included *Blastopirellula, Granulosicoccus, Litorimonas, Croceitalea, Rubritalea, Roseibacillus, Hellea*, and *Dokdonia* (IndVal statistic > 0.75; p-value < 0.001); many of these taxa are commonly found on seaweeds (Appendix A - Table 2). 18S rRNA amplicon sequence data, which capture protists as well as epiphytic algae and animals, revealed weaker associations between eukaryotes and *F. distichus* compared to bacteria (no genera at IndVal statistic > 0.75). At a lower threshold (IndVal >0.5) there were twenty-one eukaryotic taxa significantly associated with *F. distichus*, including seaweeds (Ulvaphyceae*, Ulvella, Halothrix, Pylaiella*), animals (Harpacticoid copepods*),* ciliates (*Aspidisca* and *Trochilia*) (Appendix A - Table 3). Although seaweeds and invertebrate animals are not typically considered members of the microbiome, we include them here because these organisms have microscopic life forms. We acknowledge, however, that the detection of these organisms could have resulted from free DNA shed into the environment by excretion or other biological

processes. There were more bacterial and eukaryotic genera specifically associated with rocks and seawater compared to *F. distichus* (Appendix A - Table 2 and 3). Functional genes, as defined by KEGG level C categories, significantly (p-value < 0.01) associated with *F. distichus* included those involved in biosynthesis of secondary metabolites, signaling molecules, cell motility, antibiotic resistance, membrane transport, and carbohydrate metabolism (Appendix A - Table 4). Significant differences between habitats were primarily driven by variation in the relative abundance and seasonal turnover of sequences assigned to specific KEGG categories (Appendix A - Figure 5). The percentage of shotgun metagenomic reads mapped to KEGG IDs also differed significantly by habitat type. The majority of unmapped reads occurred in rock and seawater samples (Welch test p-value < 0.001) (Appendix A - Table 5).

The *Fucus distichus* microbiome was not composed of a stable set of bacterial or eukaryotic ASVs at the population level. No ASVs (based on 16S rRNA or 18S rRNA amplicons) were present on all individuals in the population at all time points sampled. Although we detected no taxa with one hundred percent prevalence on *F. distichus* at the ASV level, we found the population-level *F. distichus* microbiome consisted of the same dominant bacterial genera across individuals. At a given timepoint, there were differences in the relative abundance of the dominant bacterial genera among host individuals (Appendix A - Figure 3) but the overarching temporal patterns were similar across the *F. distichus* population (Appendix A - Figure 3). For eukaryotes, there was higher variability than in the bacterial community when considering either ASVs or the dominant families found on *F. distichus* over time (Figure 4B; Appendix A - Figure 4).

We tested for stable members of the microbiome on individual hosts through time and found high turnover in ASVs overall. The mean prevalence of an ASV on a single host

individual was in 14.03% (bacteria) and 21.4% (eukaryotes). While no bacterial ASVs were one hundred percent prevalent on any host individual that was repeatedly sampled more than five times during the study, some taxa were consistently present on specific individuals over time. The most prevalent bacterial ASV occurred in 91.67% of samples of the host with the unique *Fucus* identifier (UFI) UFI25 (99.52% sequence similarity to uncultured *Granulosicoccus* isolated from the surface of *F. vesiculosus*; GU451366.1 (Lachnit *et al.*, 2011)). For eukaryotes, 18S rRNA gene amplicons from *Balanus glandula* (barnacle)*, Zaus unisetosus* (copepod)*,* and *Cylindrotheca closterium* (pennate diatom) were 100% prevalent on three unique host individuals. The next most prevalent protist ASVs occurred in 83.33% of samples of host UFI16 (93% sequence similarity to uncultured *Aspidisca* ciliate (Laurin *et al.*, 2008)) and UFI35 (100% sequence similarity to *Pseudoperkinsus tapetis* isolated from oyster and sea cucumber hosts in Barkley Sound, BC (Marshall and Berbee, 2010)).

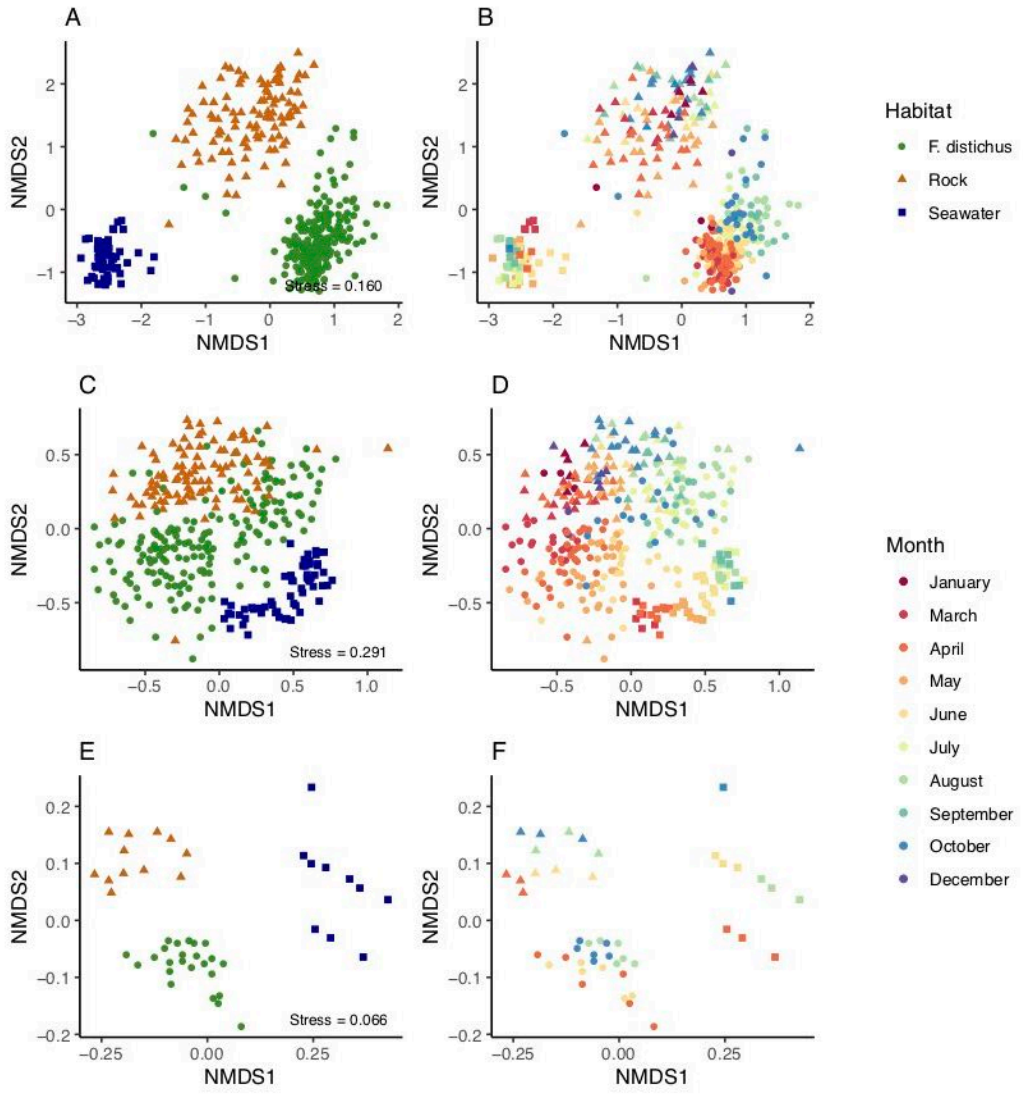

Figure 3. Bray–Curtis dissimilarity of *Fucus distichus* and environmental microbial communities visualized with NMDS showing microbiome variation correlated with habitat type (A, C, E) and month of sampling (B, D, F).

Strong seasonal variation in the *Fucus distichus* microbiome is apparent in the NMDS plots (Figure 3B, D, F) and in time-decay plots (Figure 4). For a given host individual and across the population, samples taken from consecutive months (e.g. January and February) or months closer together in the year were more similar than samples taken further apart (e.g. January and August) (Figure 5). Microbial community similarity did not, however, strictly decrease over

time. Samples taken more than four to five months apart became increasingly more similar over time instead of more dissimilar. This parabola-shaped time-decay relationship (Mantel test, p-value < 0.001) was observed for both bacterial and eukaryotic communities in all habitat types (Figure 4) albeit more weakly in rock substrate. Microbial communities on rock substrate had consistently low community similarity between sampling dates. In contrast to the taxonomic composition, the microbial gene functions were highly similar and temporally consistent for samples from each habitat type (Appendix A - Figure 5). Despite the higher similarity of functional genes compared to taxa, the relative abundances in functional gene profiles exhibited statistically significant variation over time on *F. distichus* and in seawater (Figure 3F; Appendix A - Table 6).

While the *Fucus distichus* microbiome is predominately correlated with time or season, the host individual is also a significant predictor of microbiome composition (two factor PERMANOVA analysis with month and individual, Table 1). Taxa summary plots of the dominant genera illustrate the layered influence of seasonality and community stability on individual hosts (Appendix A - Figure 3 and 4). The relative abundances of common genera change over time across the whole population; for example, *Granulosicoccus* decreases in late summer while *Dokdonia* increases (Appendix A - Figure 3). Within the population-level trends, compositional summary plots for *F. disitchus* individuals show distinct compositions with some taxa that are relatively stable over time (Appendix A - Figure 3). To further probe the stability of the microbiome on host individuals compared to the host population, we compared microbiome similarity (1 – Bray-Curtis dissimilarity) at a single timepoint as well as over time between individuals, quadrats, and across the population. The microbiome of a focal individual was most similar to other host individuals sampled at the same timepoint, especially within the same

quadrat. This inter-individual similarity value for a given date was greater than the mean community similarity on one focal individual over time (Figure 5). High inter-individual similarity at a single timepoint, despite differences in host size or reproductive status, suggests a strong influence of local environmental conditions on the microbiome. Over time, however, microbiome similarity was highest on a given focal individual and lowest when comparing samples from across the entire population. This indicates each individual *F. distichus* is colonized by a unique microbiome with its own successional trajectory, but the tempo of community turnover is similar across the population (Figure 5).

We asked to what extent host factors and the local environment are correlated to within-population variation in the *F. distichus* microbiome. We used quadrat as a measure of the local environment, the length of each focal individual's longest blade as a proxy for host size and age, and the presence of receptacles anywhere on an individual to represent reproductive maturity of the host (see methods for details). We found quadrat explained the second largest share of variation (after month of sampling) in the taxonomic composition of the *F. distichus* microbiome for both 16S and 18S amplicons (Table 1). Reproductive status and host size were also significant explanatory factors. Reproductive status and size both explained a significant and larger share of variation for bacteria. For eukaryotes, length of the longest blade had more significant explanatory power (Table 1). There were significant interactions between month of sampling and host factors for bacterial and eukaryotic community composition (Table 1). Overall, eukaryotic communities were more variable than bacterial communities and had less variation explained by temporal, host, or environmental factors (Table 1).

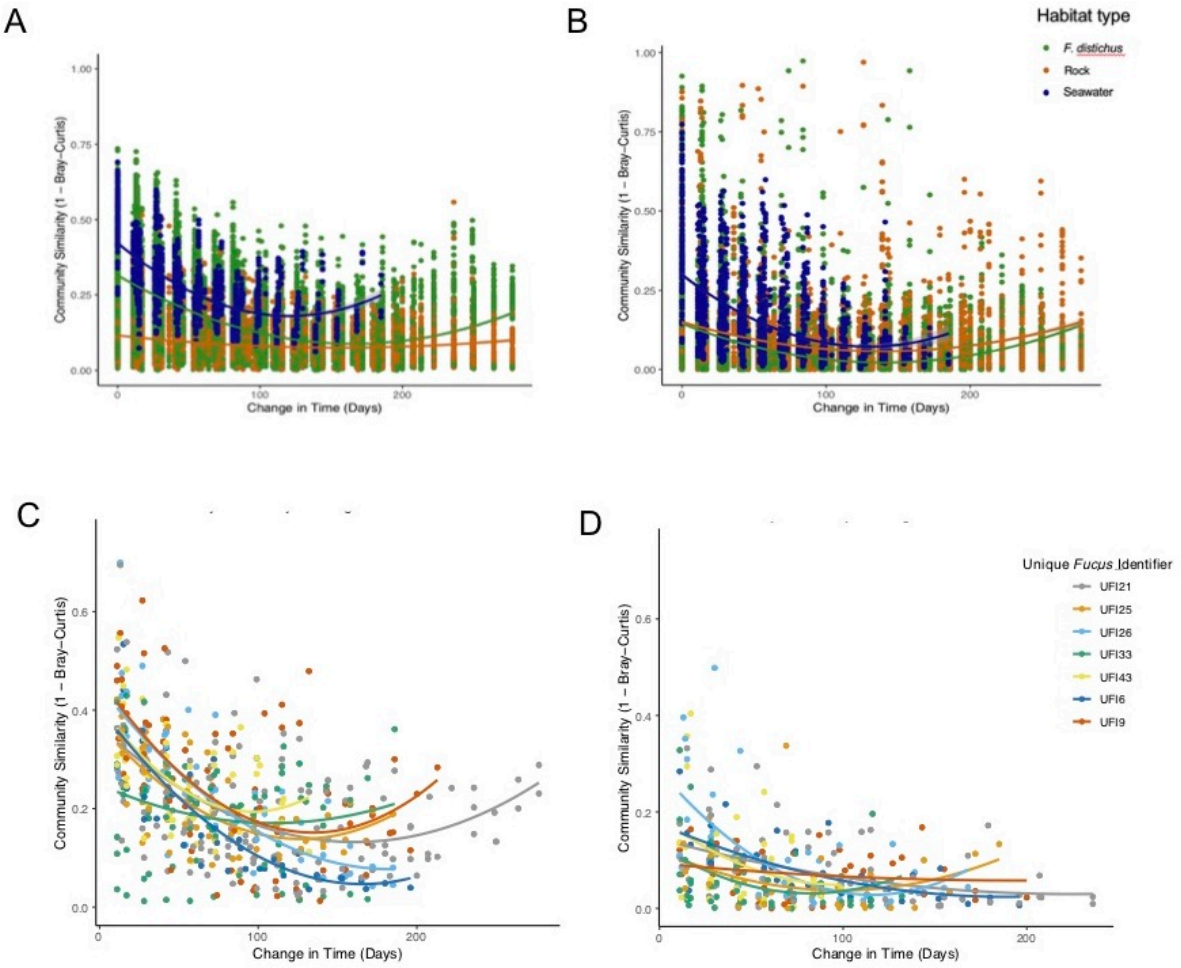

Figure 4. Pairwise sample comparisons showing the time-decay relationship of community similarity across habitats and *Fucus distichus* individuals. Each point represents a pairwise sample comparison of community similarity (1 - Bray-Curtis dissimilarity) as a function of how many days apart the samples were taken for the *Fucus distichus* population or surrounding rock and seawater habitats (A, B) or within longitudinally sampled *Fucus distichus* individuals (UFIs) (C, D). Panels A and C are bacteria communities (16S); B and D are eukaryote communities (18S).

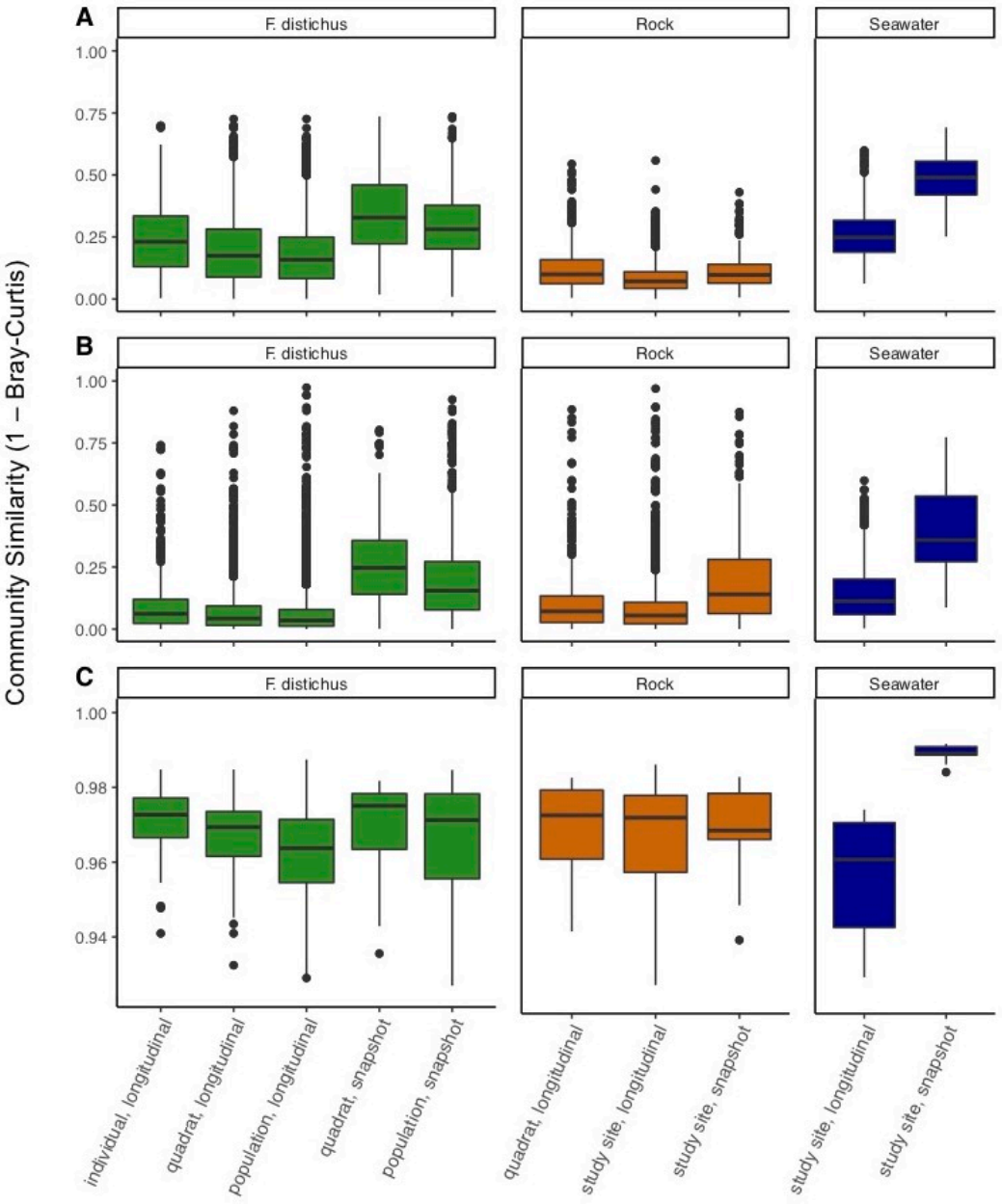

Figure 5. Comparisons of microbiome similarity (1 - Bray-Curtis) on host individuals and across the *Fucus distichus* population in contrast to microbial communities in the surrounding environment. Longitudinal comparisons are between samples taken on different dates. Snapshot comparisons are between samples taken on the same date.

Bacteria (16S)							
	Df	**SumsOfSqs**	**MeanSqs**	**F Model**	**R^2**	**p-value**	**Significance**
Month	9	15.56	1.7289	8.4645	0.2075	0.001	***
Quadrat	4	4.293	1.0733	5.2548	0.0573	0.001	***
Reproductive status	1	1.066	1.0661	5.2198	0.0142	0.001	***
Longest blade length	1	1.21	1.2105	5.9264	0.0161	0.001	***
Month:Quadrat	27	10.97	0.4063	1.9893	0.1463	0.001	***
Month:Reproductive status	7	2.162	0.3088	1.5121	0.0288	0.002	**
Quadrat:Reproductive status	4	1.478	0.3695	1.8092	0.0197	0.001	***
Month:Longest blade length	8	2.693	0.3366	1.6478	0.0359	0.001	***
Quadrat:Longest blade length	4	1.389	0.3473	1.7002	0.0185	0.002	**
Reproductive status:Longest blade length	1	0.364	0.3644	1.7839	0.0049	0.021	*
Month:Quadrat:Reproductive status	12	2.845	0.2371	1.1608	0.0379	0.045	*
Month:Quadrat:Longest blade length	22	5.407	0.2458	1.2032	0.0721	0.007	**
Month:Reproductive status:Longest blade length	6	1.488	0.248	1.2141	0.0198	0.057	.
Quadrat:Reproductive status:Longest blade length	3	0.925	0.3082	1.5088	0.0123	0.011	*
Month:Quadrat:Reproductive status:Longest blade length	5	1.086	0.2172	1.0635	0.0145	0.305	
Residuals	108	22.059	0.2043	0.2941			
Total	222	74.995	1				
Eukaryotes (18S)							
	Df	**SumsOfSqs**	**MeanSqs**	**F Model**	**R^2**	**p-value**	**Significance**
Month	9	16.477	1.8308	5.6045	0.2124	0.001	***
Quadrat	4	3.268	0.8171	2.5013	0.0421	0.001	***
Reproductive status	1	0.428	0.4279	1.31	0.0055	0.083	.
Longest blade length	1	0.538	0.5377	1.646	0.0069	0.01	**
Month:Quadrat	26	11.78	0.4531	1.387	0.1518	0.001	***
Month:Reproductive status	8	2.628	0.3285	1.0055	0.0339	0.461	
Quadrat:Reproductive status	4	1.658	0.4144	1.2686	0.0214	0.017	*
Month:Longest blade length	8	2.193	0.2741	0.8391	0.0283	0.987	
Quadrat:Longest blade length	4	1.469	0.3672	1.1241	0.0189	0.114	
Reproductive status:Longest blade length	1	0.354	0.3544	1.0849	0.0046	0.282	
Month:Quadrat:Reproductive status	12	4.078	0.3398	1.0402	0.0526	0.27	
Month:Quadrat:Longest blade length	19	5.668	0.2983	0.9133	0.0731	0.959	
Month:Reproductive status:Longest blade length	6	2.314	0.3857	1.1806	0.0298	0.011	*
Quadrat:Reproductive status:Longest blade length	2	0.716	0.3582	1.0966	0.0092	0.227	
Month:Quadrat:Reproductive status:Longest blade length	1	0.507	0.5069	1.5517	0.0065	0.007	**
Residuals	72	23.52	0.3267	0.3031			
Total	178	77.596	1				
Signif. codes: 0 ‘***’ 0.001 ‘**’ 0.01 ‘*’ 0.05 ‘.’ 0.1 ‘ ’ 1							

Table 1. The contribution of temporal, spatial, and host factors to variation in microbiome diversity (Bray-Curtis) among *Fucus distichus* samples using PERMANOVA.

2.4 Discussion

We investigated the sources of variation in the microbiome of a *F. distichus* population and on specific host individuals over time. We show that seasonal temporal turnover is strongly associated with *F. distichus* microbiome composition as well as the non-host-associated biofilm and planktonic microbial communities in the surrounding environment. Within the context of seasonal turnover, we find that variation in the *F. distichus* microbiome is further correlated to differences in the local environment, host individuals and host developmental traits.

Our finding that habitat type is a dominant selective filter for the taxonomic and functional composition of intertidal microbial communities is consistent with findings from other coastal environments (Roth-Schulze *et al.*, 2016; Lemay, Martone, Keeling, *et al.*, 2018). Within each of the three habitats sampled, there is strong temporal turnover in microbial taxa and, to a lesser extent, functional repertoire. This suggests seasonal filtering by abiotic factors occurs widely among microbial habitats in the intertidal zone, consistent with findings from other macroalgae (Sieburth and Tootle, 1981; Lachnit *et al.*, 2011; Stratil *et al.*, 2013; Saha *et al.*, 2014), marine foundation species (Sharp *et al.*, 2017; Weigel and Erwin, 2017) and seawater microbial communities (Gilbert *et al.*, 2012; Cram *et al.*, 2015; Ward *et al.*, 2017).

We aimed to understand the tempo of microbiome turnover on *F. distichus* and to determine if microbial gene functions change in concert with taxonomic turnover. We found a synchronous effect of time on the *F. distichus* microbiome across the host population, consistent with observations of population-level turnover in other host-associated microbiomes (Kolodny *et al.*, 2019; Stone and Jackson, 2021). Recruitment of microbes specifically adapted to seaweed-associated niches from seasonally variable source pools (Gilbert *et al.*, 2012; Ward *et al.*, 2017)

may be responsible for this effect. Throughout this work we refer to recruitment as it is used in the biofilm literature, meaning the active colonization and community assembly on a surface, agnostic of the surface type, host-, or microbial-control over this activity (Dang and Lovell, 2016). We found the timescale of turnover on individual *F. distichus* hosts and across the host population is weeks to months, consistent with previous experimental work reporting relative stability of the *Fucus* microbiome over days to weeks (Quigley *et al.*, 2020; Davis *et al.*, 2021). We predict that the biofilm on *F. distichus* is a protective habitat which buffers microbes against shorter-term abiotic variation occurring over hours to days, such as throughout tidal cycles. Further research is needed to understand the generality and mechanisms of short-term stability in host-associated microbial communities in highly variable intertidal environments.

In contrast to the variation in microbial taxa observed on *F. distichus*, we found microbial functions to be highly consistent across individuals with small but significant population-level changes in relative abundance of gene functions seasonally. High functional consistency is congruent with previous findings from phylogenetically diverse macroalgae in other ecosystems (Roth-Schulze *et al.*, 2016) and seasonality is an emerging pattern in ocean and coastal metagenomes (Glasl *et al.*, 2020; Yoshitake *et al.*, 2021). It is possible that the microbial functions consistently maintained through time provide insurance against stochastic population fluctuations or seasonal loss of taxa in the *F. distichus* microbiome (Rosenfeld, 2002; Biggs *et al.*, 2020). Describing the persistent functions in the *F. distichus* microbiome can aid in identifying ecological interactions between the host and its associated microbial community. A portion of the gene functions we characterized are undoubtedly consistent across habitats and over time because they are essential components of all microbial life and/or have high phylogenetic conservatism (Louca *et al.*, 2018). However, not all microbial genes sequenced

here via shotgun metagenomics were annotated by the KEGG database (Appendix A - Table 5), indicating that some functions of the *F. distichus* microbiome have not yet been characterized, similar to metagenomes sequenced from ocean microbial communities (Sunagawa *et al.*, 2015) and animal hosts (Youngblut *et al.*, 2020). These undescribed functions could represent microbial traits that are responsive to changes in host factors, that shape symbiotic interactions with the host, and/or that drive important ecological processes, such as carbon cycling. Further culture-based and (meta)genome assembly-based research is needed to describe and understand the relationship between microbial taxa, specific uncharacterized gene functions, and putative contributions they make to host and ecosystem functioning.

While the time effect was the strongest measured correlate to *F. distichus* microbiome variation, we specifically aimed to understand if any component of the *F. distichus* microbiome is stable over time and what factors are associated with microbiome variation between host individuals. We did not find evidence stability at the ASV-level across the population. There were also very few ASVs with high prevalence on an individual over time. The lack of a temporally stable microbiome on *F. distichus* contrasts with some terrestrial crop plants (Stopnisek and Shade, 2021), marine bivalves (Neu, Hughes, *et al.*, 2021), and corals (Hernandez-Agreda *et al.*, 2018) where tens of ASVs persist on all members of a host population over time. The common assumption is that taxa with 100% prevalence on the same individual through time or in the population represent obligate symbioses, whether mutualistic or parasitic. The lack of highly prevalent ASVs in this population indicates *Fucus*-microbe associations are facultative and responsive to environmental change. The microbial colonizers of *F. distichus* are likely broadly adapted to seaweed-associated niches, supported by the observation that many of the prevalent genera on *F. distichus*, such as *Granulosicoccus* and *Blastopirellula*, are shared

across seaweed species (Lage and Bondoso, 2014; Lemay, Martone, Keeling, *et al.*, 2018; Capistrant-Fossa *et al.*, 2021). These taxa are likely adept at utilizing host-derived, complex polysaccharides (Martin *et al.*, 2015; Faria *et al.*, 2018), forming biofilms (Bengtsson and Øvreås, 2010), and tolerating the high oxygen environment of the seaweed tissue surface (Weigel and Pfister, 2020).

We initially hypothesized that sources of inter-individual microbiome variation could arise from 1) stochastic differences among hosts that are maintained over time or 2) differences that are associated with host developmental traits (i.e. size or reproductive status) which vary consistently but asynchronously across the population. Both appear to be correlated with the *Fucus distichus* microbiome. We found higher levels of community similarity within an individual over time compared to the population (Figure 4) and high variability between individuals pointing towards stochastic differences that are maintained by priority effects (Fukami, 2015). We also found host factors, including size and reproductive status, explained small, albeit significant, amounts of variation in microbial community composition. These findings indicate microbial community assembly on *F. distichus* may be shaped by both stochastic recruitment and deterministic filtering attributed to host biology. We propose that the order of stochastically and deterministically arriving taxa influences the unique successional trajectory on a given host and our observations reveal the tempo of this succession is relatively consistent across the host population.

Interestingly, the host factors statistically associated with taxonomic composition of the *F. distichu*s microbiome differed for bacteria and eukaryotes. For eukaryotes, size of the host was the measured biological factor that explained the most variation in this study. This suggests the age of the host tissue or structural complexity of the host may be important to habitat

formation for eukaryotic taxa. Similar results have been found in the anatomical and morphological features of other macroalgae (Christie *et al.*, 2009; Lemay *et al.*, 2020, 2021). For bacteria, however, reproductive status also contributed significantly to compositional variation. We hypothesize that chemical defenses, which could be specific to or differentially abundant in reproductive tissue relative to other host tissues (Van Alstyne *et al.*, 1999; Hemmi *et al.*, 2005), exert a stronger selective filter on bacteria compared to overall structural complexity or size of the host like for eukaryotes.

In keeping with a strong relationship between environmental context and the *F. distichus* microbiome, we found evidence for a significant spatial effect on the taxonomic composition of the F. *distichus* microbiome at the quadrat level. Data from high resolution temperature loggers provided evidence for significant temperature variation among quadrats (Appendix A - Figure 2). The disparate canopy cover loss between the quadrats also suggests a gradient of host-stress across the studied population (Appendix A - Figure 2). Taxonomic variation in the microbiome on *F. distichus* individuals in different quadrats, separated by a few meters, could potentially be caused by temperature differences and thermal preferences of microbes (Yung *et al.*, 2015; Mensch *et al.*, 2016). Other abiotic factors that vary across spatial scales of centimeters to meters in the intertidal, such as wave action, insolation and desiccation, can also change the levels of stress in *F. distichus* individuals within in a population (Haring *et al.*, 2002; Dethier and Williams, 2009). Consequently, significant taxonomic differences in the microbiome between host individuals in different quadrats could be a direct result of spatial habitat heterogeneity or an indirect result of variation in host stress levels (Qiu *et al.*, 2019).

There was a significant amount of unexplained microbiome variation in the host population that could be due to unmeasured temporal, spatial, or host factors. For example,

seasonal alterations in host storage compounds could drive changes in the microbiome. Brown macroalgae, including *Fucus* species, store carbon as mannitol and laminarin, which support growth during times of reduced photosynthesis (Lehvo *et al.*, 2001). Dethier and Williams (2009) found that the major storage compound in *F. distichus* shifts from mannitol in spring, to laminarin in fall. While host tissue chemistry and physiology were not measured in this study, we expect seasonal shifts between mannitol and laminarin storage to occur in *F. distichus* at our study site. These shifts could selectively favor different microbial taxa or metabolic pathways, similar to the strong seasonal effects seen in the microbiome other *Fucus* species (Esther Rickert *et al.*, 2016) and macroalgae in coral reef ecosystems (Glasl *et al.*, 2020). Polyphenolic defense compounds like phlorotannins could also account for some of the unexplained variation in the *F. distichus* microbiome, as phlorotannins can vary within *Fucus* populations, particularly between juveniles and adults (Pavia *et al.*, 2003; Dethier and Williams, 2009). These and other surface-associated compounds have been shown to exert seasonal deterrent effects on specific microbes and other colonizing organisms (Lachnit *et al.*, 2013; Saha and Wahl, 2013). Further, grazing pressure can affect regulation of host defense compounds (Van Alstyne, 1988; Rohde *et al.*, 2004) and temporal variation in grazing could have cascading effects on host-associated microbial communities (Tan *et al.*, 2020). Unfortunately, we did not measure grazing or record variation in grazer abundance among quadrats in this study. Further research, for example in controlled laboratory or mesocosm settings, will be needed to parse out how the abiotic environment, host biotic interactions and host tissue chemistry influence spatial and temporal variation in the *F. distichus* microbiome.

2.5 Conclusion

In summary, we show that the taxa and gene functions of the microbiome of an intertidal foundation species are strongly correlated to seasonal abiotic variation. Layered within seasonal turnover, our findings suggest habitat heterogeneity at the quadrat scale coupled with stochastic recruitment and priority effects may produce within-population microbiome differences. We show host factors such as size and reproductive status are statistically associated with variation in the microbial assemblages on different *F. distichus* individuals. In contrast to the unique and temporally variable microbial taxa associated with individual hosts, we find far less gene function turnover in the population-wide microbiome. As seaweed hosts and their associated microbiomes come under heightened stress from climate and anthropogenic change (Marzinelli *et al.*, 2018; Minich *et al.*, 2018), a baseline understanding of the temporal dynamics and factors associated with microbiome taxonomic and functional composition in healthy seaweed populations, as provided here, is critical to track impacts of environmental change.

Chapter 3: The microbiome of *Fucus distichus* is site-specific and resistant to change following transplant

3.1 Introduction

There is widespread evidence of host species-specificity in the microbial communities associated with diverse marine eukaryotes, suggesting that selective mechanisms maintain host-microbial associations that are distinct from microbial assemblages in the surrounding environment (e.g. seawater, sediment, other organisms) (Adair and Douglas, 2017; Cleary *et al.*, 2019). These host-associated microbes can play roles in modulating growth, settlement, nutrition and defense in marine organisms (Egan and Gardiner, 2016; Morris *et al.*, 2016; Apprill, 2017; Ugarelli *et al.*, 2017; Woznica and King, 2018) but microbial functions important to host biology or biogeochemical processes are often performed by diverse and functionally redundant microbial taxa (Burke *et al.*, 2011; Roth-Schulze *et al.*, 2016; Louca *et al.*, 2017). Within a host species there can be seasonal turnover in the taxonomic composition of associated microbes (the microbiome) (Bengtsson *et al.*, 2010; Lachnit *et al.*, 2011; Serebryakova *et al.*, 2018) and variation across geographic and/or environmental gradients (Pantos *et al.*, 2015; Pfister *et al.*, 2019; Weigel and Pfister, 2019; Schellenberg and Clarke, 2020). This taxonomic variation in time and space suggests the environment plays a strong role in the composition of host-associated microbial communities (Adair and Douglas, 2017; Louca *et al.*, 2018). In keeping with a strong role of the environment and its influence on a shared microbial source pool, the strength of microbiome host specificity is often reduced for host species in sympatry (Lemay, Martone, Keeling, *et al.*, 2018; Cleary *et al.*, 2019). Yet, other factors are also known to

influence the microbiome, including host genetics (Griffiths *et al.*, 2019; Díez-Vives *et al.*, 2020), phenotypic traits (Carrier and Reitzel, 2018; Lemay *et al.*, 2020), organismal behaviors (Pratte *et al.*, 2018), as well as biotic interactions such as microbial cooperation or competition (Coyte *et al.*, 2015). Identifying the contribution of extrinsic (e.g. abiotic conditions and source pool of potential microbial colonizers) versus intrinsic (e.g. host traits and biotic interactions) factors to the diversity and structure of the microbiome within and among host species and in changing environments is a major priority in microbial ecology (Trevathan-Tackett *et al.*, 2019; Wilkins *et al.*, 2019).

Alterations in the microbiome have been linked to disease (Zozaya-Valdes *et al.*, 2015a; Kumar *et al.*, 2016; Zozaya-Valdés *et al.*, 2017; Qiu *et al.*, 2019) and stress responses (Marzinelli *et al.*, 2015; Minich *et al.*, 2018) of many marine hosts and could potentially disrupt biogeochemical cycles (Moulton *et al.*, 2016; Säwström *et al.*, 2016; Pfister *et al.*, 2019) and marine food webs (Campbell *et al.*, 2014). Changes in the microbiome can also positively impact the host through protective effects (Longford *et al.*, 2019; Rosado *et al.*, 2019) or facilitation of adaptation (Dittami *et al.*, 2016; Lynch and Hsiao, 2019; Voolstra and Ziegler, 2020). Hosts populations may further benefit from microbiome turnover via functional redundancy where microbial functions essential to the host are maintained through associations with diverse microbial taxa from the same functional guild (Burke *et al.*, 2011; Louca, Jacques, *et al.*, 2016). As it is unclear how changing ocean conditions will impact marine hosts or their microbiome, characterizing how marine microbiomes differ across sites with varying environmental conditions and assessing the stability of the microbiome in response to alterations in the environment is a critical step towards understanding and predicting outcomes of change on host-associated microbial communities.

Intertidal macroalgae are informative host systems for studying natural variation in the microbiome because these organisms experience marked variation in abiotic conditions on short timescales (i.e., tide cycles) and short distances (i.e., high versus low intertidal zone) in addition to longer seasonal timescales and larger geographic distances. Intertidal macroalgae are also phenotypically diverse and display trait plasticity across intertidal gradients (Johannesson *et al.*, 2012; Mueller *et al.*, 2015) which could selectively influence the microbiome (Balakirev *et al.*, 2012). Further, functional redundancy is increasingly studied in the microbiome of marine macroalgae (Burke *et al.*, 2011; Roth-Schulze *et al.*, 2016, 2018), yet there is limited existing research on how microbiomes vary across the mosaic of habitats and changing environmental conditions experienced by members of the same intertidal, macroalgal host species.

Here we focus on *Fucus distichus,* an ecologically important species of macroalgae in the northeastern Pacific. It is often the dominant primary producer in the high to mid- intertidal zone of rocky shores and forms dense canopies which serve as habitat for diverse organisms. *Fucus distichus* thrives across a wide range of intertidal conditions and displays phenotypic variation corresponding to environmental conditions (Schonbeck and Norton, 1978; Blanchette, 1997; Dethier and Williams, 2009). Early attempts to propagate other *Fucus* species in the absence of microbes were unsuccessful or showed irregular growth, suggesting microbes are essential for host development and survival (Fries, 1984, 1993). The microbiomes of other *Fucus* species show temporal and spatial variation (Stratil *et al.*, 2013; Saha *et al.*, 2014, 2020; Quigley *et al.*, 2020) and regulation via surface metabolites and defense compounds produced by the host (Saha *et al.*, 2011b; Saha and Wahl, 2013; Saha and Weinberger, 2019). This existing research indicates associations with microbes are important to the ecology of fucoid hosts, but little is known about microbial communities on *F. distichus* throughout the intertidal zone.

We characterized the microbiome on *F. distichus* from multiple habitats within a small geographic area (< 5 km). We hypothesized that environmental variation, and the corresponding host morphological variation across *F. distichus* habitats, would be accompanied by compositional differences in the microbiome because of the selective filters exerted by differing abiotic conditions. We used common garden and reciprocal transplant experiments to test the stability of associations between *F. distichus* and the microbiome. Field-based transplant studies are a crucial yet underutilized tool to understand host-microbiome associations in ecologically realistic conditions (Greyson-Gaito *et al.*, 2020). We hypothesized that the microbiomes of transplanted *F. distichus* would rapidly shift to reflect the contemporary environment of the host because environmental conditions pose a strong selective filter and also alter the microbial source pools available to colonize the host. Characterizing the interactions between foundation species and their microbiomes, particularly in highly variable intertidal habitats, is a necessary step towards understanding how host-microbiome associations and their ecosystem functions will respond to environmental fluctuations associated with changing oceans (Smale and Wernberg, 2013; Harris *et al.*, 2018; Trevathan-Tackett *et al.*, 2019; Wilkins *et al.*, 2019).

3.2 Materials and methods

3.2.1 Site and *Fucus distichus* morphotype description

We sampled *F. distichus* from five sites within the Hakai Lúxvbálís Conservancy at the Hakai Institute's Calvert Island Ecological Observatory on Calvert Island, BC, Canada in June 2018 (Figure 6). The high intertidal, wave-exposed site at West Beach (WB high) is characterized by *F. distichus* with short blades that twist slightly (morphotype A). This high intertidal morph grows attached to boulders, approximately 1m above mean lower low water

(MLLW) (Appendix B - Figure 1). The low intertidal, wave-exposed site at West Beach (WB low) is characterized by *F. distichus* with deeply forked receptacles, long blades and a flat growth habit (morphotype C). WB low *F. distichus* grows attached to large boulders approximately 1m below MLLW (Appendix B - Figure 1). The WB low site has the highest macroalgal diversity of all sites in this study (Lemay *et al.*, 2018). WB high and WB low sites are in the same boulder field on West Beach, with a clear vertical zonation pattern between *F. distichus* morphs (personal observation). The high intertidal morph is separated from the low intertidal morph by a zone of boulders and cobble where little to no *F. distichus* grows (Appendix B - Figure 1). A high intertidal, wave-exposed site was sampled at the opposite end of West Beach (WB west wall). The WB west wall *F. distichus* has short, twisting blades (morphotype A) and grows on boulders and vertical rock walls 0-1m above MLLW (Appendix B - Figure 1).

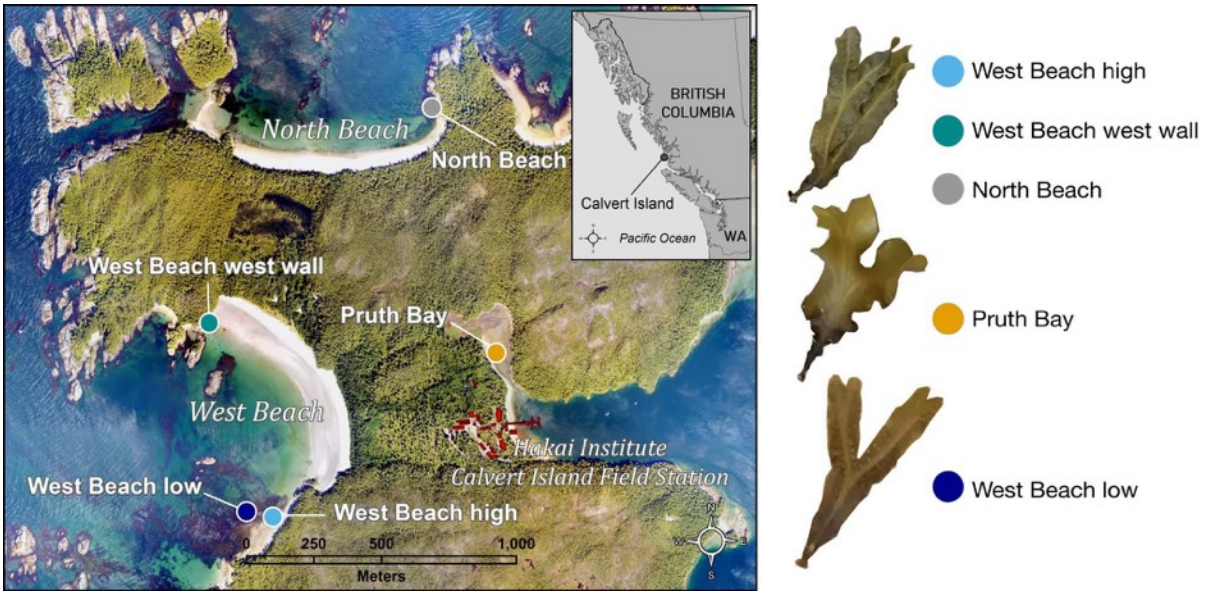

Figure 6. Map of sampling sites on Calvert Island, BC (colored circles) and corresponding *Fucus distichus* morphotypes. High intertidal sites with morphotype A are North Beach (grey), West Beach west wall (teal), West Beach high (light blue). The high intertidal site with morphotype B is Pruth Bay (yellow). The low intertidal site with morphotype C is West Beach low (dark blue).

The North Beach (NB) *F. distichus* is from a high intertidal, wave-exposed site on the north end of Calvert Island (Figure 6). This is a short-bladed, twisting morph (morphotype A) growing on rock walls approximately 1m above MLLW (Appendix B - Figure 1). The Pruth Bay (PB) *F. distichus* occurs in a shallow, protected bay with a freshwater stream at the head of the bay. *F. distichus* at this site has wide blades with undulate margins and upright growth habit (morphotype B) and is found attached to cobble in the high intertidal, 0-1m above MLLW (Appendix B - Figure 1). Similar morphological differentiation between habitats is well documented within other species of *Fucus* (Anderson and Scott, 1998; Scott *et al.*, 2001; Kucera and Saunders, 2008).

3.2.2 Common garden experiment

For the common garden experiment, we combined *F. distichus* from the five sites described above in a controlled environment (Appendix B - Figure 1) to see if individual microbiomes converged to a common composition when the microbial source pool and environmental conditions were homogenized. *F. distichus* (n=10) were collected from each site by selecting individuals that could be easily dislodged without damaging the holdfast (e.g. *F. distichus* growing attached to small barnacles). All individuals were roughly the same size; less than 10cm long at the longest blade. Collected individuals were brought back to the lab, rinsed with 0.22µm filtered sterile seawater and sampled by rubbing the first 2-3cm from the apical tip (the site of new growth) with a Puritan® sterile swab for 10 seconds to characterize the initial microbial community (sample day 1). Swabs were deposited in individual 2ml cryovials (VWR) and stored at -80˚C until DNA extraction.

A random subsample of individuals (n = 8 per site) were attached to small, 10% bleach sterilized rocks (~7cm in diameter) using Splash Zone Epoxy (Z-Spar, New Jersey, USA) and allowed to air dry until the epoxy hardened (~ 1hr). Samples from each site were marked with a unique identifier on the rock substrate using enamel paint. Each experimental unit (sterile rock with attached *F. distichus* individual) was randomized in a continuous flow seawater table to account for variability in experimental conditions (Appendix B - Figure 1). Seawater was pumped directly from Pruth Lagoon at the Calvert Island Ecological Observatory dock (51°39'17.2"N,128°07'45.1"W). The seawater table was completely drained for three to four hours every day to mimic tidal exposure. Light was provided by natural light through one window and four 75W fluorescent bulbs. Light averaged 499 ± 20.2 umol/m^2/s at the light source, 9.24 ± 1.65 umol/m^2/s at the top of the seawater table, and 7.80 ± 1.38 umol/m^2/s below the seawater surface. *F. distichus* individuals in the flow-through table were sampled daily for five consecutive days by rinsing a blade with 0.22µm filtered sterile seawater for 10 seconds to remove transient environmental microbes and then rubbed at the first 2-3cm from the apical tip (the site of new growth) with a Puritan® sterile swab for 10 seconds. The sterilized rock substrate was swabbed in a 2-3cm^2 patch as above to see how biofilm communities developed on an abiotic surface in the common garden. Swabs were deposited in individual 2ml cryovials (VWR) and stored at -80˚C until DNA extraction. Experimental *F. distichus* individuals were routinely inspected visually for tissue necrosis or other evidence of negative effects of the experimental conditions but none were observed. On average, individuals in the common garden increased in length of the longest blade by 0.80 ± 0.52mm over five days (0.16mm/day).

3.2.3 Reciprocal transplant experiment

We tested if strong differences in environmental conditions and associated biotic interactions are correlated with *F. distichus* microbiome composition with a reciprocal transplant experiment. We asked if transplanting *F. distichus* hosts from one habitat to a new habitat would lead to the acquisition of a different microbiome, more similar to the *F. distichus* microbiome of the new habitat, either by transmission from the new abiotic environment (e.g., seawater or rocks) or nearby *F. distichus* native to the new habitat. We compared compositional stability (or change) of the *F. distichus* transplants to the biofilm communities on the rock substrate where *F. distichus* individuals were attached. Rock substrate represents an abiotic surface which also has an environmentally acquired microbial community but lacks biologically driven selective filtering. As a result, we hypothesized that transplanted rock substrate would be more readily influenced by the abiotic conditions and microbial source pool of the new environment than *F. distichus* transplants.

Two sites on Calvert Island, BC with marked differences in physical and ecological characteristics and distinct *F. distichus* morphotypes were selected for the reciprocal transplant experiment: Pruth Bay (PB) and West Beach low intertidal zone (WB low) (Figure 6). These sites are the same as included the common garden experiment, but different individuals were selected for the transplant experiment. PB and WB low are separated by approximately 15 km of coastline and due to the geography and prevailing ocean currents, these sites are expected to have limited seawater exchange in the short term (hours to days). At each site, juvenile *F. distichus* individuals (non-reproductive; length of longest blade from holdfast 5-8cm) growing attached to rocks 30cm or smaller in diameter, were selected for transplanting (n = 16 *F. distichus* individuals per site; n = 8 rocks per site). Selected *F. distichus* individuals were sampled by

rinsing the length of a thallus blade with 0.22µm filtered sterile seawater for 10 seconds to remove transient environmental microbes and then rubbed along the first 2-3cm from the apical tip with a Puritan® sterile swab for 10 seconds. Swabs were deposited in individual 2ml cryovials (VWR), placed in coolers on ice and, upon return to the lab (4 hours or less after collection), stored at -80˚C until DNA extraction. The rock substrate to which these individuals were attached was gently scraped with a sterile blade to remove other macroalgal species and sessile invertebrates and then rinsed and sampled by swabbing a 2-3cm^2 patch as detailed above. Transplanted rocks were marked with unique identifiers using enamel paint for identification in the field. Additional rocks with attached juvenile *F. distichus* individuals were selected, marked and swabbed, but not transplanted (n= 16 individuals per site); these served as origin site controls. Transplants (*F. distichus* attached to rocks) were moved to the non-native, destination site in 5-gallon buckets and swabbed again at time of transplant (day 0). Transplants and unmanipulated *F. distichus* comparisons were swabbed every 24 hours within two hours of the lowest low tide for five consecutive days. Corresponding rock substrate swabs were also collected at each sampling.

3.2.4 DNA extraction and 16S rRNA gene amplicon sequencing

DNA was extracted from swabs and filters using the MoBio PowerSoil®-htp 96 well DNA extraction kit (Carlsbad, CA) following the manufacturer's recommended protocol. Extracted DNA was sent to Integrated Microbiome Resource (IMR), Centre for Comparative Genomics and Evolutionary Bioinformatics (CGEB) at Dalhousie University for PCR amplification and library construction. Primers targeted the V4-V5 region of the 16S rRNA gene for bacteria and archaea, 515f: 5'–GTGYCAGCMGCCGCGGTAA–3' and 926r: 5'–

CCGYCAATTYMTTTRAGTTT –3' (Comeau *et al.*, 2011). Amplicon library preparation and sequencing with Illumina MiSeq using paired-end (2 × 300 bp) v3 chemistry was performed at the Integrated Microbiome Resource at Dalhousie University, Halifax, Nova Scotia, Canada according to published protocols (André M Comeau *et al.*, 2017). Quality filtering, trimming, dereplication, chimera removal, inference of true amplicon sequence variants (ASVs), and taxonomic assignment against the SILVA database (v.1.3.2) was done with DADA2 (Callahan *et al.*, 2016).

For DADA2 processing the filter and trim step was set to a minimum read length of 150bp forward and 120bp reverse. Reads were truncated after a quality score of less than or equal to two. Reads with higher than 8 forward and 10 reverse maxEE "expected errors" were discarded. Chimera detection was done using the pooled method. Singletons and 16S reads from chloroplast or mitochondria were removed for downstream analyses. We detected signals of contamination in our amplicon sequencing reads from mammalian gut microbiomes. All samples that contained more than one ASV from any member of Clostridia or Negativicutes were excluded from downstream analysis, as those taxonomic groups are known to be prevalent in the mammalian gut but not in marine ecosystems. Sequences and metadata are deposited in the European Nucleotide Archive (ENA) under the project accession PRJEB42717.

3.2.5 Statistical analyses

All statistical analyses were conducted in R (R Core Team, 2019; version 3.6.2). 16S amplicon data were rarefied to 1500 reads per sample. To test for differences among bacterial communities between morphotypes and sample sites, we performed permutational analysis of

variance (PERMANOVA) on Bray-Curtis dissimilarities of initial samples from both experiments using the vegan package (Oksanen *et al.*, 2019) in R.

To test for differences in microbiomes of samples originating from different habitats in the common garden experiment, we used PERMANOVA on Bray Curtis dissimilarity and performed independent analyses for each sampling day (initial sample before individuals were placed in the common garden, two days, and five days after the start of the experiment). To test for significant differences in microbiome composition between specific sites of origin or morphotypes at the start and end of the common garden experiment we used pairwise PERMANOVAs with Bray Curtis dissimilarities using the wrapper function pairwise.adonis for vegan (Martinez Arbizu, 2020) and adjusted p-values with the Benjamini–Hochberg correction for multiple comparisons. Community differences by site and sampling day in the common garden were visualized with principal coordinates analysis (PCoA) using the phyloseq (McMurdie and Holmes, 2013) and vegan (Oksanen *et al.*, 2019) packages in R.

If microbial community composition in the common garden became homogenized across all *F. distichus* individuals over time, we would expect microbial community dissimilarity between samples from different sites to decrease from the start of the experiment to day five and to increase between samples originating from the same site over time. To test for this, we used the Jaccard dissimilarity metric, based on the presence or absence of bacterial ASVs, for *F. distichus* individuals from each of the five sites. We used paired t-tests of Jaccard distance to determine if more ASVs were shared between *F. distichus* individuals originating from the same site or between those originating from different sites at the start (day 1) or end (day 5) of the common garden experiment. We used indval analysis from the indicspecies package (Cáceres and Legendre, 2009) to identify ASVs that were indicative of each site of origin (WB low, WB

high, WB west wall, NB, PB) as well as ASVs that were shared among all *F. distichus* in the common garden at initial sampling and on day five of the experiment. The indval analysis assesses the relationship between ASV occurrence or abundance values from a set of samples and the classification of the same samples into groups, which may represent habitat types, sampling points, experimental treatments, etc. The method calculates an IndVal index value based on specificity, or the proportion of samples of in a group where the ASV is found, and the fidelity, or the proportion of the number of individuals (abundance) of the ASV that are in the group (Dufrêne and Legendre, 1997). An index value is calculated for every ASV in each group and then ASVs with the highest association value for a particular group are identified using permutation tests to assess the statistical significance of the relationship.

To test for differences among bacterial communities between treatments in the reciprocal transplant experiment, we used PERMANOVA on Bray Curtis dissimilarity for transplanted samples (transplants) compared to *F. distichus* native to the transplant location or site of origin (controls). To visualize the PERMANOVA results, we conducted principal coordinates analysis (PCoA) using the phyloseq package. Independent PERMANOVAs were performed on samples from each sampling day (initial sample to 5 days after the start of the experiment) with treatment as the explanatory variable. To determine if microbial communities on transplanted *F. distichus* changed in compositional similarity relative to *F. distichus* controls from the site of origin or destination site over time, we used ANOVA on a linear model of pseudo-F statistics from PERMANOVAs regressed against sampling day.

In the reciprocal transplant experiment, we wanted to know if bacterial ASVs specific to one site (PB or WB low) readily colonized *F. disitichus* which were transplanted to that site. We used indval analysis to identify specific bacterial ASVs that prevail in a site of origin (PB or WB

low) while being absent or having low/irregular abundance elsewhere, suggesting a significant, stable and site-specific association with *F. distichus* at that origin or indicator site. After identifying significant indicator ASVs for each site of origin (PB and WB low controls), we examined the relative abundance of significant indicator ASVs on *F. distichus* individuals from the transplant treatments to determine if indicator ASVs colonized individuals transplanted to the indicator site (increased in relative abundance) or were lost from individuals transplanted away from the indicator site (decreased in relative abundance).

All PERMANOVA analyses were run with 999 permutations. All R code associated with these analyses is available on GitHub: https://github.com/katherine-m-davis/Fucus_transplant.

3.3 Results

3.3.1 *Fucus distichus* microbiome composition is correlated with site and host morphology.

We examined the microbiome composition on the surface of 52 *F. distichus* individuals from five sites on Calvert Island, British Columbia, Canada, by comparing *in situ* unmanipulated, initial samples from our two independent experimental studies conducted in the same week. These samples included the high intertidal, wave-exposed host morphotype A at three sites: West Beach (WB) high (n = 7), WB west wall (n = 8), North Beach (NB) (n = 7); the high intertidal, wave-protected morphotype B at one site: Pruth Bay (PB) (n = 17); and the low intertidal, wave-exposed morphotype C at one site: WB low (n = 13) (Figure 6). Each site is characterized by a distinct physical habitat (Appendix B - Figure 1). Morphotype and site explained significant variation in microbiome composition (PERMANOVA: morphotype pseudo-$F_{2,47} = 18.591$, p-value < 0.001; morphotype:site pseudo-$F_{2,47} = 4.552$, p-value < 0.001).

We examined the effect of site alone by testing for a site effect within the one morphotype that was sampled at multiple locations separated by hundreds of meters to kilometers.

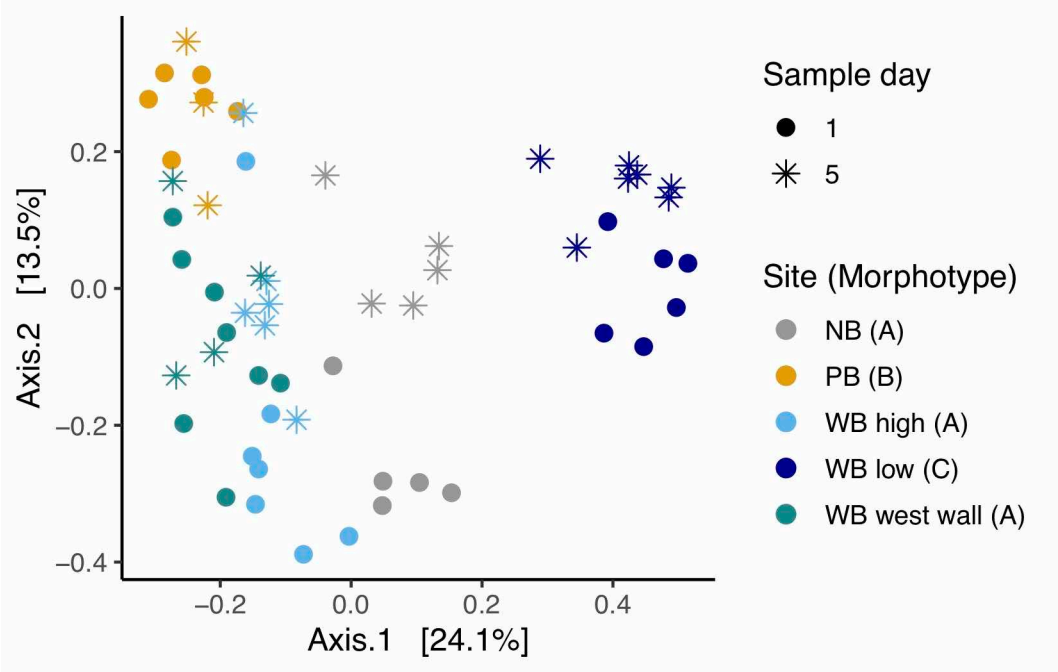

Figure 7. *Fucus distichus* microbiomes in the common garden remain differentiated by site over time. PCoA of Bray-Curtis dissimilarities for *F. distichus* microbiomes in the common garden from initial sampling on day 1 (circles) and final sampling on day 5 (stars).

The high intertidal, wave-exposed morphotype A (sampled at WB high, WB west wall, and NB) also showed significant variation in microbiome composition among sites (PERMANOVA: pseudo-$F_{2,19} = 4.086$, p-value < 0.001) (Figure 7). We sampled underlying rock substrate for a subset of sampling sites (PB and WB low) and found that *F. distichus* microbiomes (PB, n = 23; WB low, n = 17) were significantly different from biofilm communities on rocks sampled at those sites (PB, n = 15; WB low, n = 17) (PERMANOVA: pseudo-$F_{1,70} = 18.605$, p-value < 0.001) (Fig. 4A). Rock biofilm communities also showed significant site-specificity (PERMANOVA: pseudo-$F_{1,34} = 15.059$, p-value < 0.001).

3.3.2 Differences in *Fucus distichus* microbiome compositions are maintained in a common environment.

To determine if a shared microbial source pool and consistent environmental conditions would result in *F. distichus* individuals converging to a common microbiome, regardless of site of origin, we performed a common garden experiment. From the individuals sampled *in situ*, we selected a subset of 8 individuals from each of the five sites, transported them to the lab, and attached them to sterilized rocks (see Experimental procedures; Appendix B - Figure 1). At the start of the experiment (sample day 1), before transplanting them into a common flow-through seawater tank, we confirmed that *F. distichus* microbiomes from each site of origin were statistically different from *F. distichus* microbiomes from every other site, in agreement with above. There was no significant effect of experimental manipulation and transportation to the lab [PERMANOVA: pseudo- $F_{4,27} = 6.958$, p-value < 0.001] (Figure 7). The most abundant ASVs associated with *F. distichus* from each site were predominantly from the same families: Flavobacteriaceae, Rhodobacteraceae, Rubritaleaceae, Saprospiraceae, and Thiohalorhabdaceae; although the relative abundances of dominant genera within these families varied by site (Figure 8A). After five days in a common environment, differences in microbiome composition between sites remained significant (PERMANOVA: pseudo-$F_{4,20} = 5.787$, p-value < 0.001) (Figure 7). Strikingly, we did not observe convergence to a similar or shared microbiome composition over time (Figure 7 and 8A).

We used pairwise comparisons of microbial community composition on *F. distichus* individuals from the same site versus between individuals from different sites to determine if more ASVs were shared between sites after five days in the common garden compared to original microbiome compositions at the time of collection from the field. If all *F. distichus*

individuals were colonized by the same microbial taxa in the common garden, or if microbes were transmitted between hosts from different sites, we would expect to see significant increases in community similarity between samples from different sites over time. Pairwise comparisons of Jaccard beta-diversity, a metric based on presence/absence of shared ASVs, showed more shared ASVs for individuals from within the same site than comparisons between hosts from different sites; these results were similar at the start and end of the experiment (Figure 8B). When comparing Jaccard metrics from the initial day in the common garden to day five, paired t-tests showed no significant change in beta-diversity within or between sites, with the exception of comparisons between PB and other sites and comparisons within WB low and WB west wall. The samples from WB low became significantly more dissimilar to each other from day one to day five in the common garden (Figure 8B; Appendix B - Table 1).

Indicator species analysis was used to identify ASVs that had colonized all individuals in the common garden, regardless of site of origin, by the end of the experiment (day 5). Indicator species analysis assesses the specificity and fidelity of ASVs to specific sites or groups of sites via permutation tests (see Experimental procedures) (Cáceres and Legendre, 2009). We found few ASVs that indiscriminately colonize *F. disitchus* regardless of site of origin (Appendix B - Table 2), these included members of Bdellovibrionaceae. Most indicator ASVs were significantly associated with specific sites of origin, even at the end of the experiment (Appendix B - Table 2). These indicator ASVs belong to clades typically associated with *Fucus* species and other marine macroalgae, including Saprospiraceae, Granulosicoccus, and Piruellaceae (Appendix B - Table 2) (Bondoso *et al.*, 2017; Parrot *et al.*, 2019; Weigel and Pfister, 2019). The site-specificity of indicator taxa further highlights the strong distinction between *F. distichus*

microbiomes from different sites and the persistence of those distinct microbial communities throughout the experiment.

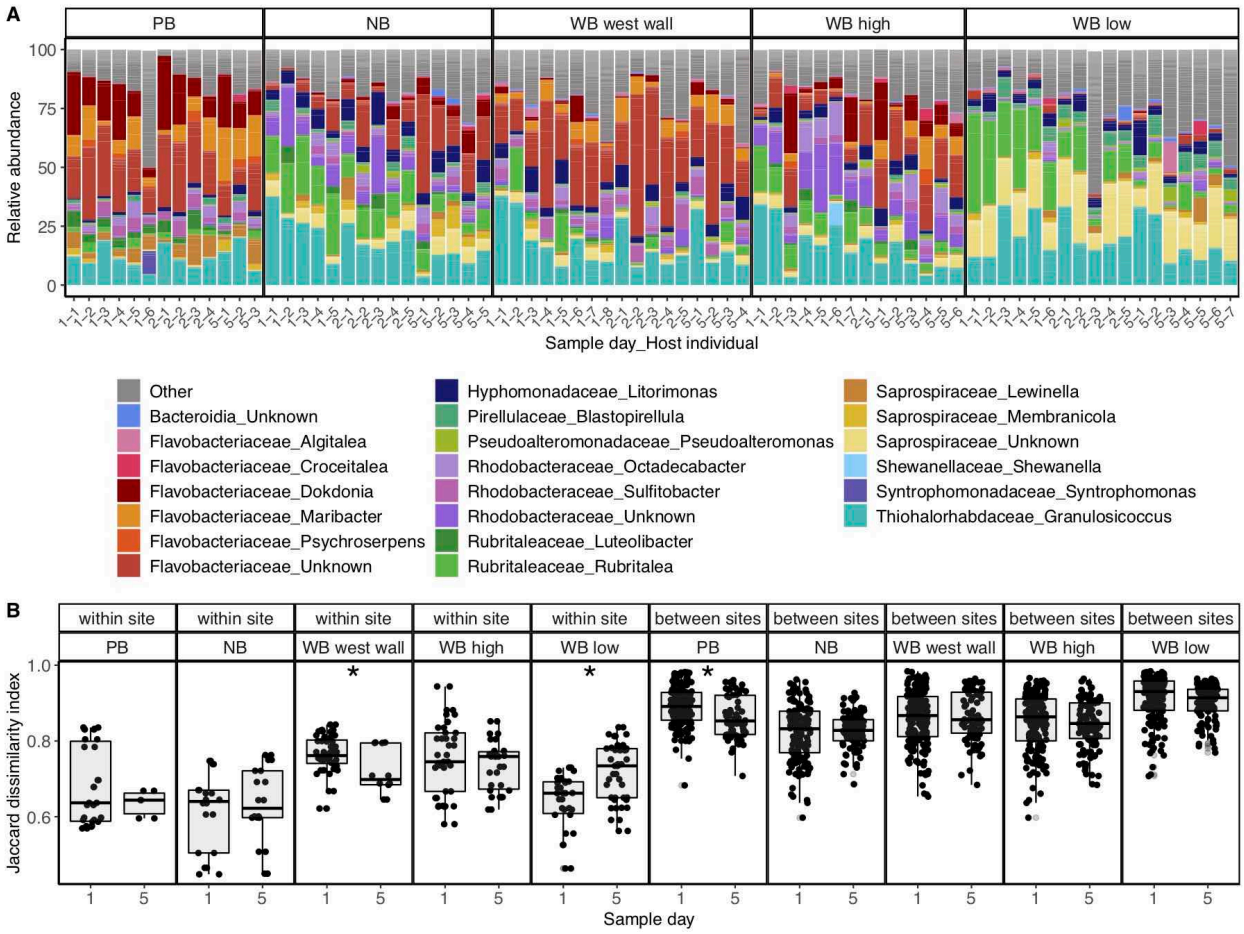

Figure 8. Broad taxonomic groups are common to all Fucus distichus sampled but compositional differences based on the presence/absence of specific ASVs (as measured by the Jaccard dissimilarity index) are greater between sites than within sites at the start and end of the common garden experiment. A) Stacked bar plots of the most abundant ASVs on *F. distichus*, grouped by family and genus. Each column represents an individual *F. distichus* sample; samples are ordered by day of sampling and grouped by origin site. The first number of x-axis labels is sampling day, the second number is a unique *F. distichus* identifier. B) Jaccard dissimilarity values for pairwise comparisons of *F. distichus* microbiome samples from within the same site or between different origin sites at the initial sampling (1) and fifth, final day in the common garden (5). We represent between-site comparisons for each site independently, plotting the dissimilarity values between a focal site and all the others. Asterisks indicate a significant difference in Jaccard dissimilarity between initial and final time points for a given site based on paired t-tests.

3.3.3 Differences in *Fucus distichus* microbiome and rock biofilm communities are maintained following transplantation to novel environments.

To determine if the stability observed in the common garden experiment translates to natural conditions, we performed *in situ* transplantation between the two sites with the most divergent environmental conditions: high intertidal protected bay (PB) and low intertidal wave-exposed site (WB low). Among the individuals initially sampled *in situ*, we selected a subset of 16 individuals (and 8 rocks) from each of the two sites to transplant. Some samples of specific individuals and timepoints during the experiment were lost in the field to natural processes such as wave action and grazing. Others were excluded to due to poor sequencing quality or sample contamination (for details see Experimental procedures), and ultimately, we analyzed 162 high-quality samples (103 *F. distichus* and 59 rock samples taken over the 5-day experiment). We observed resistance to rapid change in the biofilm community of *F. distichus* individuals (Figure 9B) and rock substrate (Figure 9C) following transplant to a new environment. Over the course of the experiment, both *F. distichus* and rock biofilm microbial communities remained more similar in composition to controls in the native, origin site than to *F. distichus* individuals (or rock substrate) in the environment to which they were transplanted (i.e., transplanted microbiomes stayed clustered with microbiomes of the origin site rather than the destination site) (Figure 9B and C) (Appendix B - Figure 2). For transplants from PB to WB low, we found no significant difference in microbial community composition over time (all 3 days) on *F. distichus* (n = 13) or rocks (n = 9) (PERMANOVA PB->WB low rock transplants by sample day: pseudo-$F_{1,7}$ = 0.913, p-value = 0.543, brown shapes in Figure 9C; PB->WB low *F. distichus* transplants by sample day: pseudo-$F_{1,11}$ = 1.391, p-value = 0.164, brown shapes in Figure 9B). In contrast, for transplants from WB low to PB, we found a significant difference in microbial community

composition over time (over all 6 days) on *F. distichus* (n = 47) and rock (n = 15) (PERMANOVA WB low ->PB rock transplants by sample day: $F_{1,13} = 2.415$, p-value = 0.016, green shapes in Figure 9C; WB low->PB *F. distichus* transplants by sample day: $F_{1,45} = 5.102$, p-value < 0.001, green shapes in Figure 9B). We also compared the pseudo-F statistic of PERMANOVA models that compare *F. distichus* microbiomes composition to origin and destination site controls across sampling days with regression; we found no significant relationship between pseudo-F statistic and day of sampling at either site (Appendix B - Figure 3). This supports our finding that transplanted hosts did not become progressively, and significantly, more similar (i.e. less differentiated and smaller pseudo F-value) to *F. distichus* hosts native to the destination site over time.

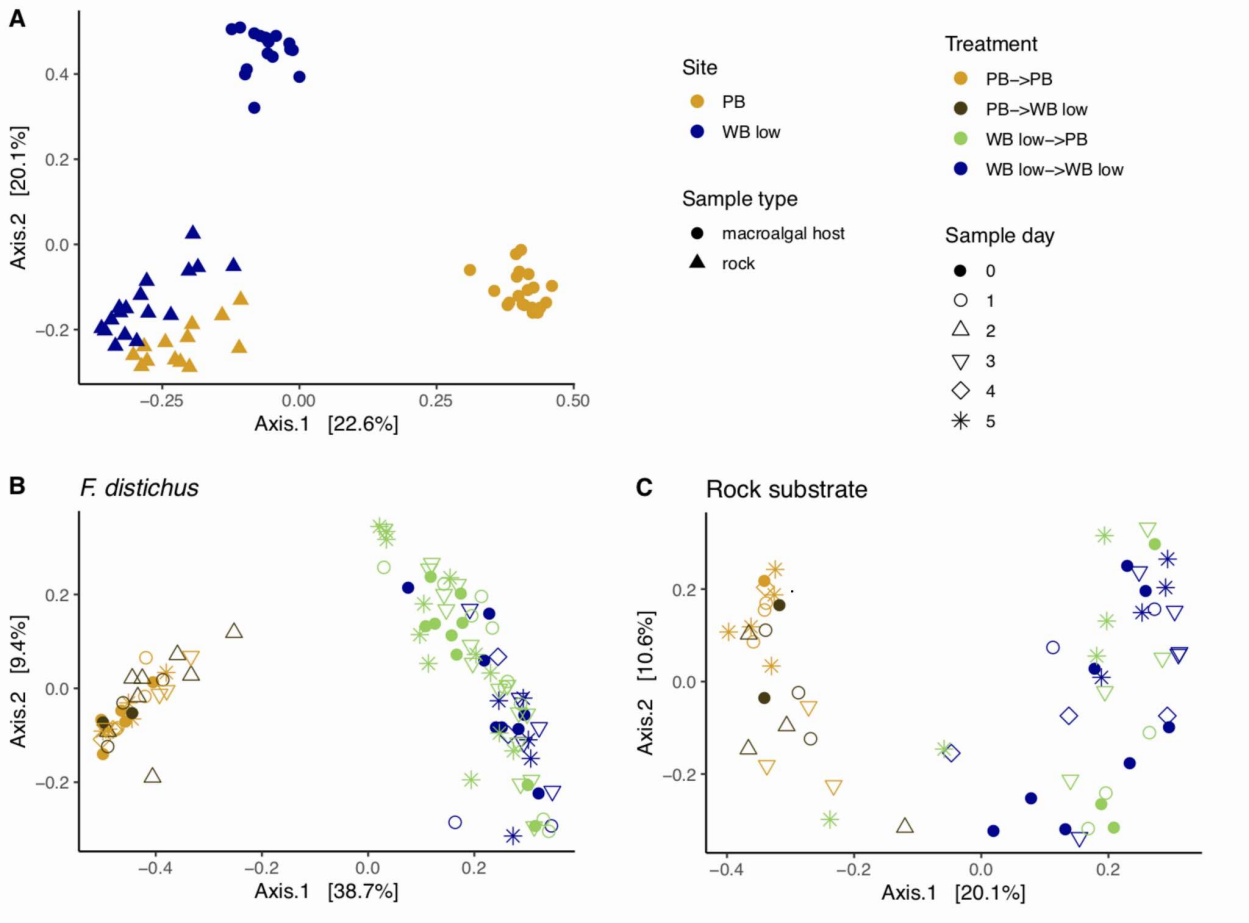

Figure 9. Microbial communities on *Fucus distichus* and rock substrate from wave-protected and wave-exposed habitats are distinct and experimental transplants remain more similar to the origin site than to the destination site. A) PCoA plot based on Bray-Curtis dissimilarity of microbial communities on unmanipulated *F. distichus* and underlying rock substrate from wave-exposed West Beach low (WB low) and protected Pruth Bay (PB). PCoA plots of reciprocally transplanted (WB low -> PB and PB -> WB low) and unmanipulated controls at each site (WB low -> WB low and PB -> PB) over time (initial sample = day 0 to final sample = day 5) for B) *F. distichus* and C) rock substrate.

Indicator species analysis found numerous ASVs significantly associated with *F. distichus* from both WB low and PB (Figure 9). The majority of ASVs significantly associated with an origin site (indicator group) did not rapidly colonize *F. distichus* transplanted to that indicator site. Instead, most ASVs identified as indicators from the origin site remained associated with transplants originating from that site when transplanted to the new environment (Figure 10). Visual inspection revealed few indicator ASVs from the destination site that

consistently colonized individuals transplanted there; for example, Rhodobacteraceae ASV29 and ASV37 and Saprospiraceae ASV332 characteristic of WB low colonized transplants from PB; Flavobacteriaceae ASV4, Rubritaleaceae ASV25, and Saprospiraceae ASV177 characteristic of PB notably colonized transplants from WB low (Figure 10; Appendix B - Table 3). Instead, we noted shifts in the community of *F. distichus* originating from WB low and transplanted to PB were characterized by a systematic loss of taxa. Taxa that were lost on WB low to PB transplants included ASVs from Leucothrix, Granulosicoccus, Rubritalea, and unknown members of Saprospiraceae and marine group NS11-12 (Figure 10). A similar loss of ASVs was not apparent in transplants from PB to WB low.

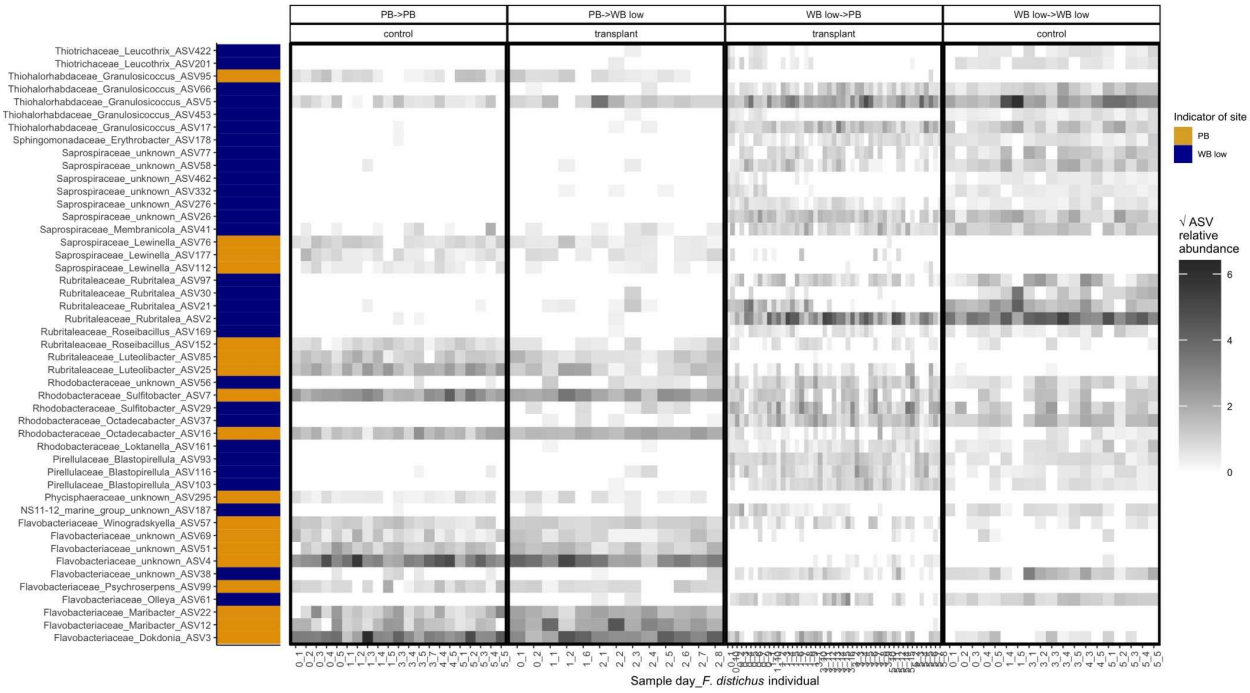

Figure 10. Indicator ASVs for a given site do not readily colonize *Fucus distichus* transplanted to that site. ASVs (with family and genus-level taxonomic assignments) significantly associated with Pruth Bay (PB, yellow label) or West Beach low intertidal (WB low, dark blue label) with an Indval statistic ≥ 0.9 (SI Table 3 for all indicator ASVs). Each column represents an individual *F. distichus* sample. Samples are grouped by treatment (transplant or unmanipulated control), origin location and sampling day following transplant (initial = 0 to final = 5). The higher relative abundance an ASV is in a sample, the darker the grey rectangle. Relative abundance of ASVs per sample were square root transformed to better visualize right-skewed abundance distributions.

3.4 Discussion

We investigated variation in the surface microbiome of *Fucus distichus* with three distinct morphotypes from five sites that are separated by small spatial distances on Calvert Island, BC, Canada (Figure 6). Morphological variation in *F. distichus* is correlated with prevailing environmental conditions such as wave exposure and vertical position in the intertidal (Coyer *et al.*, 2009; Pearson *et al.*, 2010; Wahl *et al.*, 2011). Much like macroalgal morphology, microbial communities are also shaped by environmental conditions at local (Weigel and Erwin, 2016; Pfister *et al.*, 2019; Quigley *et al.*, 2020) and regional spatial scales (Campbell *et al.*, 2015; Marzinelli *et al.*, 2018; Weigel and Pfister, 2019). We predicted that abiotic factors and correlated host characteristics across sites influence the source pool of microbes colonizing *F. distichus* such that microbiome composition would be differentiated in accordance with host morphology. As expected, morphotype A individuals from three high-intertidal, wave-exposed sites hosted microbiomes that were more similar to each other than to morphotype B or C (Figure 7). The clear differences we observed between *F. distichus* microbiomes from WB low (morphotype A) and WB high (morphotype C), sites that are separated by only tens of meters, emphasizes the role selective filtering by local environments (e.g. host morphology and/or tidal height) plays in establishing microbiome differences on *F. distichus* compared to other mechanisms such as dispersal. Unexpectedly, we also found strong and significant differences in microbiome composition by site within a single morphotype, morphotype A, for sites separated by hundreds of meters to kilometers (Figure 6 and 7). The site-specific microbiome on *F. distichus* with the same morphology is surprising as macroalgal hosts at these sites are likely experiencing similar wave action, seawater immersion time and UV exposure due to their position at roughly the same tide height. It is possible that more subtle differences in local abiotic

conditions, such as levels of desiccation, UV exposure, and temperature extremes, known to vary within an *F. distichus* population and throughout a tidal cycle (Joux *et al.*, 1999; Wright *et al.*, 2004; Rothrock and Garcia-Pichel, 2005; Alster *et al.*, 2018), could affect the success of specific microbes on a host individual. Host factors, such as morphological complexity (Lemay *et al.*, 2020), exudate composition (Bengtsson *et al.*, 2011; Saha *et al.*, 2011b; Parrot *et al.*, 2019), and tissue chemistry (Dethier and Williams, 2009; Weigel and Pfister, 2020) that vary across space (Van Alstyne, 1988; Saha and Wahl, 2013) and season (Esther Rickert *et al.*, 2016) in *Fucus* species can also promote or inhibit the growth of particular microbes (Stratil *et al.*, 2013; Saha *et al.*, 2014) and drive the significant variation in microbiomes within *F. distichus* we report. We expect that the varied microbial taxa contributing to intraspecific differences in the microbiome are filling similar ecological roles on *F. distichus*; functional consistency and taxonomic variability are commonly observed in the microbiome of macroalgae (Burke *et al.*, 2011; Louca, Jacques, *et al.*, 2016; Roth-Schulze *et al.*, 2016, 2018; Louca *et al.*, 2018) and in other systems (Louca *et al.*, 2016, 2018). Whether intraspecific differences in microbiome composition would be maintained after abrupt environmental change is not well known.

To test the stability of site-specific differences in *F. distichus* microbiome composition in the face of changing environmental conditions we used experimental transplants. We hypothesized that transplantation to a common garden would homogenize site-specific microbiome differences due to rapid community turnover driven by selective filtering imposed by the common abiotic environment (Hernandez-Agreda *et al.*, 2017; Marzinelli *et al.*, 2018; Lemay *et al.*, 2018; Weigel and Pfister, 2019), recruitment from a shared microbial source pool, or transmission between hosts. We can reject this hypothesis, at least for short time scales (hours to days), as we found that microbial communities on *F. distichus* originating from different sites

did not converge to a shared composition in our common garden environment. Site-specific microbiome differences remained significant after five days; showing that resident *F. distichus* microbiome are not quickly replaced or outcompeted in new environmental conditions. The constructed environment of our common garden had continuous flow of natural seawater but did not fully mimic the variation typical of natural intertidal habitats and microbial source pools. Thus, we used reciprocal transplants in the field to investigate the stability of the *F. distichus* microbiomes in ecologically realistic conditions (Greyson-Gaito *et al.*, 2020). Again, we found that existing differences by site of origin were resistant to change over the six-day experiment (Figure 9) and significant differences in the microbiome by site of origin persisted. Further, we found little evidence that bacterial taxa significantly associated with the new (destination) site colonized transplants (Figure 10). This implies the microbiome of *F. distichus* does not rapidly turnover in response to altered environmental conditions or microbial source pools at both the community level and with respect to individual bacterial taxa. Surprisingly, we observed this pattern of site-specificity and resistance to immediate colonization by microbes in a new environment in both *F. distichus* and the underlying rock substrate. Again, these results point to selective filtering by local abiotic conditions and priority effects (Fukami, 2015) or the dynamics of biofilm turnover as factors that shape the structure and stability of marine surface-associated microbial communities whether they are on living hosts or inert substrates such a rock.

Biofilm dynamics may be a particularly important determinant of the timescale of turnover in host-associated microbial communities. Rapid microbiome turnover, on the order of hours to days, has been demonstrated for highly disturbed or previously uncolonized host surfaces and substrates in marine systems including corals (Ziegler *et al.*, 2017, 2019); macroalgae (Rao *et al.*, 2006; Longford *et al.*, 2019); seagrass (Wang *et al.*, 2021); artificial

macroalgal substrates (Lemay *et al.*, 2020; Weigel and Pfister, 2020); and marine particles (Datta *et al.*, 2016). Long-term observations of transplanted marine hosts with mature and unmanipulated biofilms see more gradual microbiome turnover, if any. In these studies, transplanted microbiomes often become more similar to the new, destination environment on the timescale of months or years (Ziegler *et al.*, 2017, 2019). In some cases, however, long-term microbiome change is attributed to seasonal turnover (Weigel and Erwin, 2017) or effects of transplantation (Alexandra H Campbell *et al.*, 2015; Casey *et al.*, 2015; Uren Webster *et al.*, 2020) while signatures of origin-site specificity are maintained. In this study, where we do not find evidence of rapid microbiome turnover, we propose that new colonization of mature biofilm communities could be constrained by slow microbial growth and recruitment rates (Kirchman, 2016) as well as competition and antagonism among microbes. We surmise that transplantation to a new environment did not represent a disturbance to the biofilm community severe enough to facilitate rapid colonization by new microbial taxa. There is evidence for antagonism among microbes also defending *Fucus* species against new microbial colonization; for example, by antibiotic producing Rhodobacteraceae (Dogs *et al.*, 2017). We observed high prevalence and relative abundance of Rhodobacteraceae and other microbes in the *F. distichus* microbiome that have been shown to produce antibiotics (Wiese *et al.*, 2009; Singh *et al.*, 2015; Chakraborty *et al.*, 2017), suggesting active competitive strategies may be a stabilizing force against taxonomic turnover in new environments (Hibbing *et al.*, 2010). More experimental studies on microbially-mediated mechanisms of microbiome assembly are needed to understand the importance of biotic interactions in the structure and stability of the macroalgal microbiome.

We predict that natural microbial community turnover occurring on longer timescales of weeks to months might eventually lead to shifts in microbiome composition on experimentally

transplanted *F. distichus*. In support of this prediction, we observed a trend toward increasing similarity to the destination environment in the transplants that were sampled for a longer duration (WB low to PB = 6 days) compared to the reciprocal transplants of PB to WB low which were sampled over 3 days (Figure 9B).

There is an emerging pattern across marine systems of greater resistance to turnover in microbiomes originating from more variable environments following experimental manipulation. Subtidal sponges show greater turnover following transplant than sponges from the more variable intertidal environment (Weigel and Erwin, 2017); corals adapted to cooler, more constant thermal regimes show greater turnover following transplant than corals adapted to hotter and more variable thermal regimes (Ziegler *et al.*, 2017, 2019); and offshore, surface bacterioplankton communities show greater turnover in response to environmental change than bacterioplankton from more dynamic nearshore waters (Wang *et al.*, 2020). Our findings of general stability in the microbiome of host species adapted to highly dynamic intertidal environments, are congruent with this pattern. Within our study, *F. distichus* individuals that underwent the greatest amount of microbiome change following transplant to a new environment were from the WB low site (Figure 8B; Figure 9B). *Fucus distichus* from the WB low intertidal site experience overall more stable conditions compared to individuals at higher intertidal sites. These individuals and their associated microbes are exposed to the air for less time during a given low tide event and also experience fewer low tide cycles overall, resulting in decreased exposure to desiccation and temperature extremes (Wright *et al.*, 2004; Wahl *et al.*, 2011). Thus, exposure to environmental variation, even within a single host species, may influence the sensitivity of associated microbial communities to environmental change. Correspondingly, we observed a loss of some taxa significantly associated WB low on transplants from WB low to PB

but not on transplants from PB to WB low. This suggests certain ASVs may be more sensitive to environmental change, even on time scales of a few days, especially if they are adapted to less variable abiotic conditions. Additional experiments run for longer durations and specifically designed to test if adaptations to more variable environments decrease sensitivity to environmental change are needed to better understand the timescales and drivers of microbiome turnover on macroalgae.

3.5 Conclusion

In conclusion, we have shown that *Fucus distichus* hosts a surface microbiome that differs significantly over small spatial scales (meters to kilometers), probably in response to different environmental conditions (e.g., wave action, tidal exposure, salinity) and/or host factors (e.g., physiology, tissue chemistry). Following transplantation to a new, natural environment or controlled common garden we found the microbiome of this intertidal host is stable over a short period of time (5 days). Our findings imply that the native and site-specific microbiome is resistant to invasion by microbes from distinct microbiomes on conspecific hosts or novel environmental source pools. Our findings expand current understanding of microbial community assembly in highly variable environments and show surprising stability of the microbiome in response to environmental change over a few days to a week. Future work on macroalgae and other systems are needed to test the generality of our findings and the hypothesis that variable environments harbor microbial communities that are more resilient in the face of changing environmental conditions.

Chapter 4: Factors shaping epibiotic microbial assemblages on mussels in the rocky intertidal zone

4.1 Introduction

Mussels are important intertidal foundation species. The microbial communities living on or in mussels, i.e. the microbiome, play a central role in host health as well as nitrogen and carbon cycling (Pfister, 2007; Heisterkamp *et al.*, 2013; Pfister and Altabet, 2019) in coastal ecosystems. The intertidal zone where mussels live is a heterogeneous habitat with abiotic gradients of temperature, salinity, nutrients, ultraviolet (UV) light, wave action, and rainfall (Connell, 1972; Helmuth and Hofmann, 2001; Harley and Helmuth, 2003). The position of a mussel within the intertidal zone can affect its physiology (Place *et al.*, 2012) and biotic interactions (Paine, 1974; Lubchenco, 1980); all of which could influence the microbiome. Characterizing the abiotic and biotic drivers of host-microbiome associations in foundation species, like mussels, is critical for understanding the contribution of the microbiome to diverse physiological and ecological functions. It can also aid in predicting the potential outcomes of environmental change on host-microbiome associations (Wilkins *et al.*, 2019).

Mussels have long been a model of ecological zonation in the intertidal (Paine, 1966, 1974) and are increasingly susceptible to mass mortality events (Harley, 2008; Seuront *et al.*, 2019) and other climate change related stressors (Frölicher *et al.*, 2018). Thus, natural populations of intertidal mussels represent a valuable system for studying host-microbiome associations across heterogenous environmental gradients which are under heightened pressures from climate change. Previous studies of the mussel microbiome have investigated the microbial

diversity of internal tissues and fluids (Li *et al.*, 2018; Vezzulli *et al.*, 2018), especially in relationship to disease-causing agents (Li *et al.*, 2019), because of their economic value and impacts on human health (Rubiolo *et al.*, 2019). Less is known about the factors shaping the epibiotic shell microbiome which serves as an interface or protective cover between mussels and the abiotic environment.

Some constituents of the mussel shell microbiome, endolithic cyanobacteria, have received research attention because of the role these organisms play in host survivability. Endolithic cyanobacteria are parasitic microbes that bore into mussel shells causing decreased shell thickness and strength. The energetic costs to repair shell damage can compromise mussel growth, byssal attachment strength, and increase mortality (Kaehler, 1999; Zardi *et al.*, 2009). The boring activity by endolithic cyanobacteria removes the dark, outer periostracum of mussel shells exposing the light gray prismatic layer. The lighter-colored, eroded shells reflect UV radiation and the porosity of eroded shells helps mussels retain more water compared to uneroded mussel shells (Gehman and Harley, 2019). Consequently, high levels of endolithic cyanobacteria infestation and resultant erosion reduce stressful heat gain and mussel mortality during high temperature events at low tide (Zardi *et al.*, 2016; Gehman and Harley, 2019). Thus, the parasitic shell-boring cyanobacteria become mutualistic in a context-dependent manner during intense thermal stress (Gehman and Harley, 2019). There is some evidence that infestation by endolithic cyanobacteria increases with elevation in the intertidal zone because photosynthesis of these organisms is enhanced by the prolonged exposure to light (Marquet *et al.*, 2013). The relationship between endolithic cyanobacteria abundance, shell erosion, and intertidal elevation in the northeastern Pacific is not well understood and the composition of endolithic cyanobacteria assemblages on mussel shells in this region have not yet been examined

using molecular tools (Bower *et al.*, 2002). We characterized the cyanobacterial assemblages on the California mussel, *Mytilus californianus*, using 16S rRNA amplicon sequencing and examined the relationship between host, parasite, shell erosion and overall microbiome composition across elevation gradients in the rocky intertidal zone at four sites in British Columbia, Canada.

It is possible that host biology acts as a selective filter on microbial colonization of mussel shells, as demonstrated for the internal compartments of diverse hosts (Woodhams *et al.*, 2020) and protective outer layers of marine host species like corals (Glasl *et al.*, 2016). For example, the biochemical composition (Bers *et al.*, 2006) or microtopographies (Bers *et al.*, 2005) of an intact periostracum or waste products excreted by the host (Pfister *et al.*, 2014) could influence which microbes colonize mussel shells. Alternatively, the shell may represent a calcium carbonate surface on which the microbiome is strictly shaped by abiotic factors that constrain microbial growth or productivity (Palinska *et al.*, 2017). Experimental manipulation is a necessary tool for determining the role of host control and abiotic variation in shaping the composition of the mussel shell microbiome.

In this study, we experimentally tested the hypothesis that shell microbiome composition and shell erosion caused by endolithic cyanobacteria is influenced by the biology of a live host. We transplanted uneroded pairs of live and killed mussels across an intertidal elevation gradient at four sites and characterized the shell microbiome 2-3 months later using 16S rRNA gene amplicon sequencing. We predicted 1) that the shells of transplanted live mussels would be less susceptible to erosion by endolithic cyanobacteria and 2) that the microbiome on live mussel shells would be significantly different than the microbiome on killed mussel shells when exposed to different abiotic conditions because of the selective filtering of microbes by host biology.

4.2 Materials and methods

4.2.1 Experimental conditions

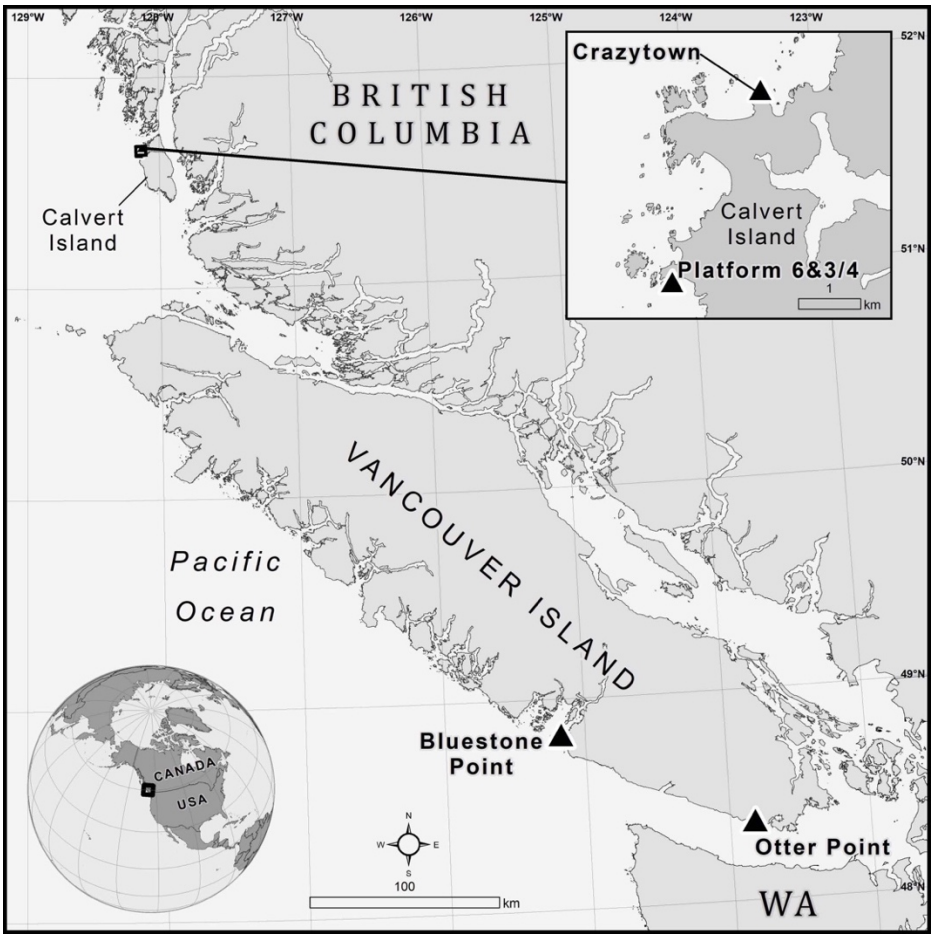

Figure 11. Map of mussel transplant sites.

Mussel transplant experiments were conducted in 2017, at four sites around coastal British Columbia, Canada that are dominated by the California mussel, *Mytilus californianus* (Figure 11). Two sites were on Calvert Island near the Hakai Institute Ecological Observatory: one on the north side of the island (Crazytown, Table 2) and one on the west side of the island (Platform 6 ¾, Table 2). The other two sites were located on Vancouver Island; Otter Point in Sooke and Bluestone Point near the Bamfield Marine Sciences Centre (Table 2).

Site	Region	Latitude	Longitude	Initial experimental pairs (n)	Transplant date	Microbiome sampling date	Microbiome samples analyzed		
					(2017)	(2017)	Live (n)	Killed (n)	Unmanipulated controls (n)
Bluestone Point	Vancouver Island	48.82304	-125.1617	11,10	28 April, 27-28 June	18-Sep	19	24	10
Otter Point	Vancouver Island	48.35714	-123.8231	11,12	26-27 April, 21,23-24 June	18-Sep	19	22	11
Crazytown	Calvert Island	51.66751	-128.1333	19	26-28 May	21-Sep	14	13	15
Platform 6 and 3/4	Calvert Island	51.63939	-128.1525	23	26-30 April	20-Sep	12	13	10

Table 2. Mussel transplant study locations, number of experimental transplants, key dates, and microbiome sample numbers.

Individual mussels used in this experiment were collected from low elevation mussel beds (donor beds) near the experimental transplant sites. Small mussels (25-30mm) with minimal erosion (<20%) were selected for transplanting. Each individual experimental plot contained two mussels: one live mussel set in epoxy in an orientation that allowed the shell to continue to open and close, and one killed mussel with one half of the shell set into the epoxy so the exterior of the shell faced outward. A total of 19 to 23 plots were established per site over a range of dates between April and June 2017. Microbiome samples of transplanted and unmanipulated live control mussels from the donor beds were taken in September 2017, at the conclusion of the experiment (Table 2). Of the experimental plots sampled, 10 to 12 transplanted pairs per site had sufficient amplicon sequencing read coverage for paired microbiome data analysis. Plots where only one mussel from the experimental pair had sufficient read coverage were included in some downstream analyses.

4.2.2 Abiotic measurements

Roughly half the experimental plots at each site were inlaid with iButton temperature loggers which recorded temperature hourly during the study. Temperature data was extracted

from each iButton and separated into measurements of exposed rocky substratum (subaerial) and seawater (immersed) based on whether the plot was submerged during that measurement using tide charts and the elevation (tide height) of the plot. For each plot, the average and 90^{th} quantile temperature values were calculated for subaerial and immersed time periods. Elevation in the intertidal zone was calculated using tide charts, combined with measures of seawater height and the height of each plot against the stationary position of a laser level. On Calvert Island, elevation and tide height was measured using a combination of Real Time Kinematic (RTK) positioning survey and drone based digital surface elevation models. Using a geographic information system, we extracted elevation data for all survey plots and temperature loggers not directly measured with the RTK survey.

4.2.3 Mussel and erosion data collection

The area of mussel shell eroded was quantified for each transplanted individual at the start and end of the experiment. The eroded area of the upper mussel shell and the total area of the upper mussel shell were measured using ImageJ () and used to calculate percent of shell area eroded. Erosion rate (change in proportion eroded*w^{-1}) was calculated based on start and end values. Mussel shell length was measured in the field and growth rate (mm*$week^{-1}$) was calculated which demonstrated that live transplanted mussels maintained normal growth during the experiment (Gehman and Harley, 2019).

4.2.4 Microbiome sample collection and DNA extraction

To characterize the microbiome of transplanted and live control mussels, we sampled the shells *in situ* for 16S rRNA gene amplicon sequencing. Sampling involved rinsing each shell

with 0.22µm filtered, sterile seawater for 10 seconds to remove transient environmental microbes and then rubbing with a Puritan® sterile swab for 10 seconds. Swabs were deposited in individual 2ml cryovials (VWR), placed in coolers on ice, and upon return to the lab (6 hours or less after collection), stored at -80˚C until DNA extraction.

4.2.5 16S rRNA gene amplicon sequence processing

DNA was extracted from swabs using the MoBio PowerSoil®-htp 96 well DNA extraction kit (Carlsbad, CA) following the manufacturer's recommended protocol. Extracted DNA was sent to Integrated Microbiome Resource (IMR), Centre for Comparative Genomics and Evolutionary Bioinformatics (CGEB) at Dalhousie University for PCR amplification and library construction. Primers targeted the V4-V5 region of the 16S rRNA gene for bacteria and archaea, 515f: 5'–GTGYCAGCMGCCGCGGTAA–3' and 926r: 5'–CCGYCAATTYMTTTRAGTTT –3' (Comeau *et al.*, 2011). Amplicon library preparation and sequencing with Illumina MiSeq using paired-end (2 × 300 bp) v3 chemistry was performed at the Integrated Microbiome Resource at Dalhousie University, Halifax, Nova Scotia, Canada according to published protocols (André M Comeau *et al.*, 2017). Quality filtering, trimming, dereplication, chimera removal, inference of true amplicon sequence variants (ASVs), and taxonomic assignment against the SILVA database (v.1.3.2) was done with DADA2 (Callahan *et al.*, 2016). For DADA2 processing, the filter and trim step was set to a minimum read length of 150bp forward and 120bp reverse. Reads were truncated after a quality score of less than or equal to two. Reads with higher than 8 forward and 10 reverse maxEE "expected errors" were discarded. Chimera detection was done using the pooled method. Singletons and reads assigned as mitochondria were removed for downstream analyses.

4.2.6 Statistical analyses

All statistical tests were conducted in R (R Core Team, 2019; version 3.6.2). 16S amplicon sequencing data were rarefied to 1763 reads per sample. To test if the mussel shell microbiome composition varied among geographic locations we compared Bray-Curtis dissimilarity metrics of live control mussels using PERMANOVA in the vegan package (Oksanen *et al.*, 2019) and conducted pairwise comparisons between sites using the pairwiseAdonis wrapper function (Martinez Arbizu, 2020). To determine if the shells of killed mussels had different overall microbiome composition compared to live hosts, we used PERMANOVA on Bray-Curtis dissimilarity metrics with sampling location as strata. All PERMANOVA tests were conducted with 999 permutations. Differences in alpha diversity between live controls from each of the sites were evaluated with Kruskal-Wallis tests for both richness (total observed amplicon sequence variants (ASVs)) and Shannon-Weaver index (H'). Differences in alpha diversity between live and killed mussel shells were quantified with paired Wilcoxan tests for each of the four sites.

To examine the community structure and relative abundance of putative shell-boring cyanobacterial taxa, we analyzed the relative abundance of reads assigned to cyanobacteria in experimental treatments and geographic sites after excluding chloroplast sequences. Chloroplast reads from micro- and macroalgae are assigned to the phylum cyanobacteria based on 16S rRNA gene amplicon sequencing. We analyzed chloroplast sequences separately to gain an understanding of eukaryotic algal colonizers on mussel shells which can also be endolithic (Palinska *et al.*, 2017). We tested for differences in the relative abundance of cyanobacteria reads

and chloroplast reads between treatments at all sites combined and between treatments at each site using Kruskal-Wallis tests.

We used IndVal analysis from the indicspecies package (Cáceres and Legendre, 2009) to identify ASVs that were significantly associated with live or killed experimental transplants that differed in shell erosion. We also identified taxa significantly associated with transplant and live control hosts. The IndVal analysis assesses the relationship between ASV occurrence or abundance values from a set of samples and classification of those samples into groups, which may represent habitat types, sampling points, experimental treatments, etc. The method calculates an IndVal index value based on specificity, or the proportion of samples in a group in which the ASV is found, and fidelity, or the proportion of the counts of that ASV (abundance) that are exclusive to the group (Dufrêne and Legendre, 1997). An index value is calculated for every ASV, in every group, and the ASVs with the highest association value for a particular group are identified using permutation tests to assess the statistical significance of the relationship.

The envfit function in the vegan package was used to assess the contribution of site, shell erosion, and abiotic variables to variation in the PCoA ordination of samples based on Bray-Curtis dissimilarity values. The calculated or continuous abiotic variables included in the model were intertidal elevation, immersed temperature (90^{th} quantile values), and exposed temperature (90^{th} quantile values). A Mantel test was used to confirm the statistical significance of correlations between continuous abiotic variables and microbial community similarity between samples.

4.3 Results

We sampled 46 live unmanipulated control and 136 experimentally transplanted mussels across four geographic sites in British Columbia, Canada (Table 2). A total of 6647165 reads were kept after processing via the DADA2 pipeline which included 5126 unique amplicon sequence variants (ASVs).

4.3.1 Live mussels experience less erosion by endolithic cyanobacteria.

We tested whether shell erosion by endolithic cyanobacteria is potentially modulated by live mussel hosts at four rocky intertidal sites. The area of mussel shell eroded over the course of the experimental period was significantly lower for live transplants compared to killed transplants across the dataset (Wilcoxan $p = 0.0004$; Figure 12A). Variation in erosion between experimental treatments was driven by significant differences at Otter Point (p-value < 0.001) and Crazytown (p-value = 0.031) (Appendix C - Figure 1). We used IndVal analysis to identify bacterial taxa differentially associated with live and killed mussel transplants that experienced significant differences in erosion at Otter Point and Crazytown. Killed mussel shells with increased erosion were more likely to be colonized by uncharacterized Rhodobacteraceae and *Maribacter* spp. Live mussel transplants with significantly less erosion than the killed transplants were associated with *Maribius* spp (Appendix C - Table 1). The relative abundance of reads from photosynthetic taxa (cyanobacteria and eukaryotic algae) did not differ between live and killed mussel transplants (p-value = 0.17; Figure 12B). The relative abundance of reads from potentially endolithic taxa did not differ between live and killed mussel transplants (Figure 12 C) and was not significantly correlated with elevation in the intertidal zone (Pearson's R, $R^2 = 0.059$, p-value = 0.5; Appendix C - Figure 2 and 3).

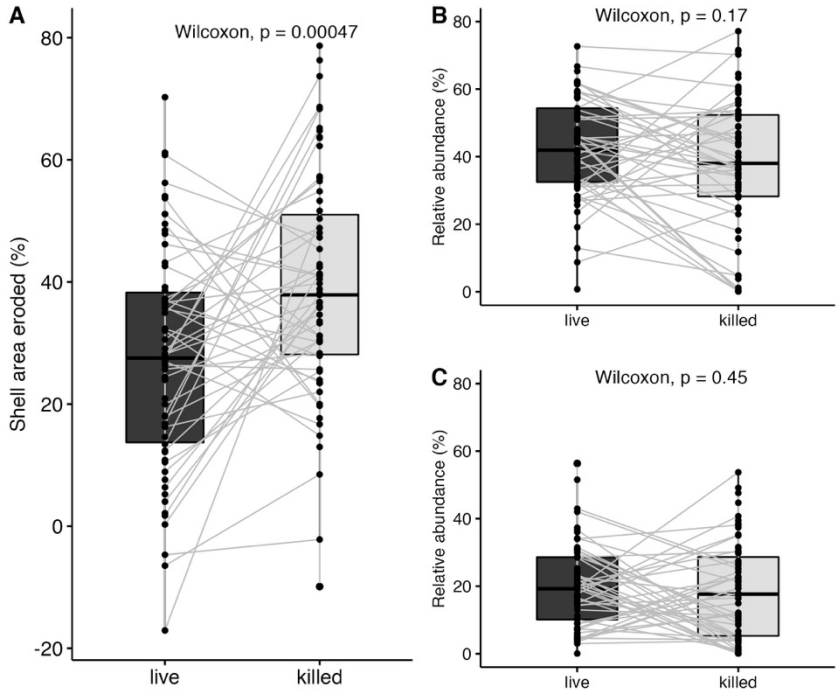

Figure 12. Paired Wilcoxan tests examining differences in A) percentage of shell area eroded, B) relative abundance of 16S rRNA reads from all cyanobacteria and eukaryotic algae, and C) relative abundance of 16S rRNA reads from potentially endolithic taxa for pairs of live and killed mussel transplants.

4.3.2 Mussel shell microbiomes are correlated with abiotic factors rather than biotic interactions.

We examined patterns of beta diversity across all four sites to understand the contribution of geographic location to variation in the mussel shell microbiome. Site contributed significantly to the structure of the mussel shell microbiome on unmanipulated live controls (PERMANOVA: $R^2 = 0.200$, pseudo-F = 3.49, p-value = 0.001; Appendix C - Figure 4) and pairwise comparisons showed significant differences in composition between all sites except for between Crazytown and Platform 6 & 3/4 (Appendix C - Table 2). Alpha diversity, as quantified by ASV richness and Shannon-Weaver index (H'), was significantly higher in mussels from the donor beds on Vancouver Island compared to those from Calvert Island (ASV richness: F = 43.22, p-value <

0.001; H': F = 27.19, p-value < 0.001). Site also explained significant variation in microbiome beta-diversity of experimentally transplanted mussels based on the Bray-Curtis metric (PERMANOVA: R^2 = 0.079, pseudo-F = 5.059, p-value = 0.005; Figure 13).

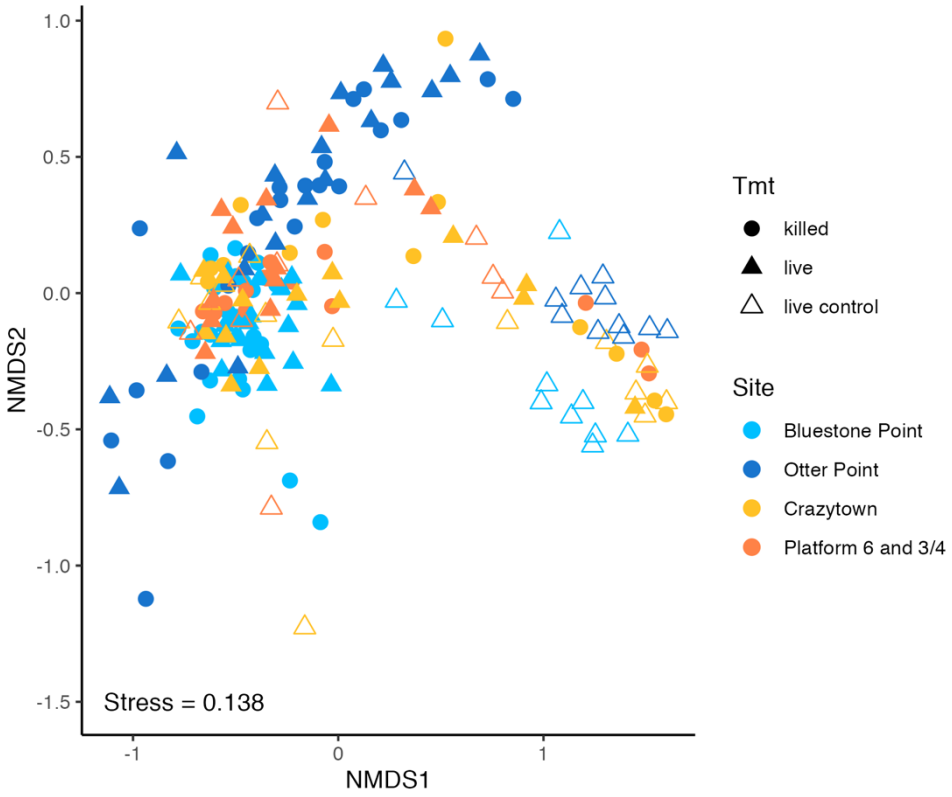

Figure 13. Non-metric multidimensional scaling analysis of Bray-Curtis dissimilarity for mussel shell microbiome samples.

Experimentally transplanted live and killed mussel shells did not have significantly different microbial communities in terms of alpha diversity (Shannon-Weaver index (H'): p-value = 0.23; ASV richness: p-value = 0.81) (Appendix C - Figure 5). Beta-diversity based on Bray-Curtis dissimilarity was also not significantly different between live and killed transplanted mussels (Figure 13; Table 3). The microbiome of transplanted mussels, regardless of host viability, was significantly different from those of live control mussels (PERMANOVA: R^2 = 0.040, pseudo-F

= 7.506, p-value = 0.001; Table 3; Figure 13 and 14). IndVal analysis between transplant and live control mussels identified many ASVs, including those assigned to *Lewinella* and undescribed Rhizobiaceae, as well as *Pleurocapsa, Phormidesmis* and chloroplast ASVs as significantly enriched on the shells of transplanted mussels (Appendix C - Table 3).

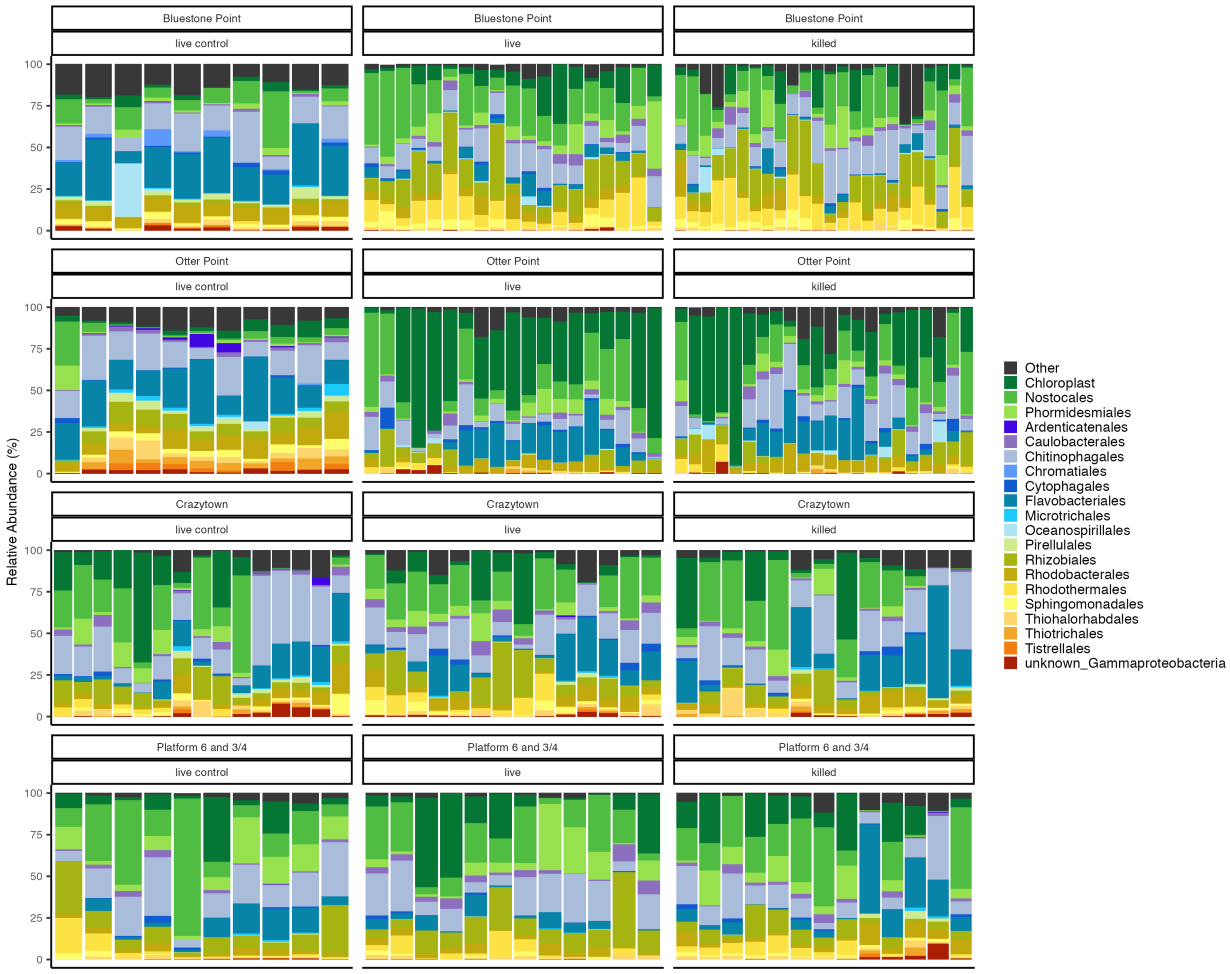

Figure 14. Bar plots of the relative abundance of dominant microbial families on mussel shells across sites and treatments. Each bar represents an individual mussel shell sample. Samples from live and killed transplants are arranged from left to right by increasing elevation in the intertidal zone. Samples from live control mussels were all taken from the lowest extent of the mussel bed at each site.

Treatment comparison	Df	SumsOfSqs	F Model	R^2	p-value	p-adjusted
killed vs live	1	0.304	0.863	0.006	0.6	1
killed vs live control	1	2.103	5.581	0.046	0.001	**0.003**
live vs live control	1	2.39	6.53	0.057	0.001	**0.003**

Table 3. Pairwise PERMANOVA results of Bray-Curtis dissimilarity between live transplants, killed transplants, and live control mussels for all sites combined.

To understand the effect of abiotic conditions that vary within the intertidal zone on the mussel shell microbiome, we tested for differences in diversity metrics on experimentally transplanted mussels across the continuous range of intertidal elevations to which they were transplanted. There was a significant negative relationship between alpha diversity and elevation at Otter Point for the shell microbiome of both live and killed mussel transplants (Appendix C - Figure 6). There was not a significant relationship between alpha diversity and elevation at any other sites. The relationship between microbiome beta diversity, based on the Bray-Curtis metric, and tidal elevation of mussel transplants was significant when considering all sites combined (PERMANOVA: $R^2 = 0.047$, pseudo-F = 6.64, p-value = 0.005; Appendix C - Figure 7).

To further explore the effects of biotic and abiotic variation on the mussel shell microbiome, we examined the role of geographic location, shell erosion, intertidal elevation, subaerial (substratum), and immersed (seawater) temperatures in explaining differences in the composition of the mussel shell microbiome. Temperature data were collected for approximately half of the transplanted mussel pairs at each site. There was, however, significant loss of temperature loggers during the study, so we examined microbiome variation for a subset of transplant pairs with available iButton temperature data (n = 21 pairs; Bluestone Point, n = 4; Otter Point, n = 4; Crazytown, n = 7; Platform 6 & 3/4, n= 6). The variables site, intertidal

elevation, 90th quantile immersed temperature and 90th quantile subaerial temperature explained significant variation in the first two axes of the multi-dimensional ordination space for Bray-Curtis dissimilarity of transplanted mussels (Table 4; Figure 15). A Mantel test confirmed significant dissimilarity of shell microbiomes between mussel transplants of increasing distance apart along vertical elevation gradients in the intertidal (p-value < 0.001). Measured shell erosion was not significantly correlated to elevation of transplants in the intertidal zone (Pearson's R, R^2 = 0.028, p-value = 0.75) nor was it a significant predictor of microbiome differences (Table 4).

	R^2	**p-value**
Site	0.2361	**0.001**
Treatment	0.0173	0.426
Elevation	0.1434	**0.027**
Immersed temperature (90th quantile)	0.1298	**0.035**
Subaerial temperature (90th quantile)	0.3118	**0.001**
Shell area eroded (%)	0.0042	0.896

Table 4. Envfit results of the explanatory variables contributing to mussel shell microbiome dissimilarity (Bray-Curtis) for transplanted mussels with available iButton data corresponding to the PCoA plot presented in Figure 15.

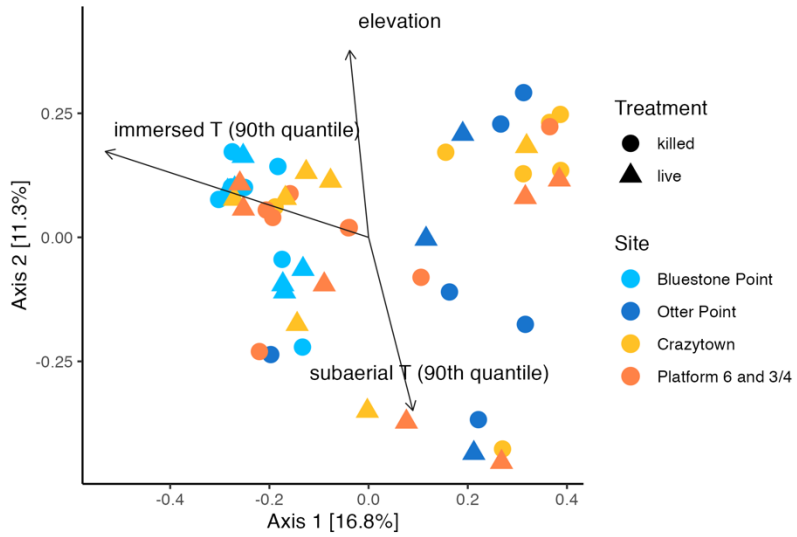

Figure 15. Drivers of dissimilarity in shell microbiome diversity among transplanted mussels. Significant continuous explanatory variables (arrows) from Table 4 are displayed on the PCoA plot based on Bray-Curtis metric. Plotted samples are transplanted mussels with available iButton temperature (T) data.

4.3.3 A few taxa dominate cyanobacteria assemblages on mussel shells.

We characterized the cyanobacterial assemblages on shells of *Mytilus californianus* to understand the composition and distribution of these organisms in coastal British Columbia (Appendix C - Figure 8). We found the relative abundance of cyanobacteria reads was higher on transplants than live controls at the two sites on Vancouver Island (Appendix C - Figure 3) but there was no difference in the relative abundance of cyanobacteria reads between live and killed treatments across the dataset (Appendix C - Figure 3). The cyanobacteria assemblages were dominated by reads from two genera, *Pleurocapsa* and *Phormidesmis,* which consistently cooccurred at roughly the same ratio across the dataset (Appendix C - Figure 9). In a few samples, *Pleurocapsa* was detected but *Phormidesmis* was not (Appendix C - Figure 8). The 16S rRNA gene primers also amplify sequences from chloroplasts of eukaryotic algae, so we also examined these communities on mussel shells because some marine eukaryotic algae are

endolithic (Marcelino and Verbruggen, 2016). We found chloroplast reads were significantly higher on experimental transplants compared to live controls (Appendix C - Figure 3) and exhibited a significant negative correlation with tidal elevation (Appendix C - Figure 2).

4.4 Discussion

4.4.1 Erosion activity by endolithic cyanobacteria depends on host condition.

We hypothesized that live mussels would be less susceptible to erosion by endolithic cyanobacteria because live hosts have the potential to influence cyanobacteria colonization and erosion activity by modulating the shell surface. Such modulation could come from active shell surface maintenance, alteration of the shell thermal environment via evaporative cooling, or other biochemical mechanisms. In agreement with our hypothesis, we found significantly less erosion on live mussel shells compared to paired killed transplants. This pattern was evident in the significant differences in the percentage of shell eroded between live and killed mussel transplants at two out of the four sites. The site-specificity of these results is supported by findings that endolithic erosion rates can depend on abiotic conditions (Kaehler, 1999; Zardi *et al.*, 2009). Alternatively, abiotic factors that varied between sites could have weakened the periostracum and facilitated erosion on killed mussel shells in a site-specific manner (Kaehler, 1999). Still, differences in erosion between live and killed mussels in some abiotic contexts suggests that live mussels may have the capacity to influence the activity of shell-boring parasites.

Interestingly, we did not find a significant difference in the relative abundance of cyanobacterial reads between live and killed mussels at any site. We expected that increased shell erosion would be correlated with a more abundant cyanobacteria community. It is possible

that our sampling method did not capture endolithic cyanobacteria cells that are localized inside small bore holes on highly eroded shells, leaving out a significant proportion of the cyanobacteria community in the amplicon sequencing data.

4.4.2 Known endolithic taxa dominate cyanobacteria assemblages on mussel shells in the northeastern Pacific.

The cyanobacteria assemblages on mussel shells were dominated by *Pleurocapsa spp.* and *Phormidesmis spp*.; *Pleurocapsa* are usually late-successional stage endolithic taxa (Ndhlovu *et al.*, 2021). They have previously been described as members of endolithic assemblages that are responsible for significant shell erosion in other mussel species (Kaehler, 1999). *Phormidesmis* are filamentous cyanobacteria with few records of endolithic activity in marine hosts. Cooccurrence of these two taxa at a relatively consistent ratio on mussel shells, and the infrequent observation of *Pleurocapsa* in the absence of *Phormidesmis* suggests that *Pleurocapsa* may facilitate shell colonization by *Phormidesmis.* While we did not take samples at the start of this experiment to examine this hypothesis, future research could take samples over time to test for successional dynamics or facilitation in the algal communities on mussel shells. It is not clear why relative abundance of the putative shell-boring taxa was not positively correlated with measured shell erosion or intertidal elevation as predicted (Kaehler, 1999). It is possible that recruitment dynamics of endolithic cyanobacteria might be confounded with the abiotic drivers of their erosion activity. Since we selected low elevation mussels with little to no erosion for transplantation, the experimental mussels could have had a very reduced endolithic community at the start of the experiment, and thus cyanobacteria detected on transplanted mussels were recruited to mussel shells over the course of the experiment. In this case, the microbiome

samples may have been taken before significant erosion took place under site-specific abiotic conditions. Abiotic factors including water movement and air temperature have previously been shown to affect the distribution and activity of endolithic cyanobacteria (Kaehler, 1999). Nonetheless, this study makes an important contribution showing *Pleurocapsa*, a known shell boring cyanobacterium, dominates the 16S rRNA sequence reads of cyanobacterial assemblages on California mussels in British Columbia, Canada which have not previously been characterized using molecular techniques (Bower *et al.*, 2002). It is noteworthy that we detected a high relative abundance of chloroplast reads, many without family-level or finer taxonomic assignment, on mussel shells across the dataset. Given that marine eukaryotic algae can also be endolithic (Marcelino and Verbruggen, 2016; Pernice *et al.*, 2019), it would be interesting to further characterize phototrophic eukaryotic taxa on mussels to determine if these organisms are euendoliths, contributing to shell erosion in the northeastern Pacific, or if their colonization of mussel shells is merely facilitated by endolithic cyanobacteria.

4.4.3 Shell erosion and host condition are not significant predictors of the overall mussel shell microbiome taxonomic structure.

We found differences among sites to be the most significant correlate with mussel shell microbiome composition in unmanipulated controls. These results are aligned with observations of strong differences in the microbiome of whole mussels between marine lakes and open marine waters (Cleary and Polónia, 2018) and increasing dissimilarity in the gill and shell microbiome of *Mytilus californianus* across a latitudinal gradient (Neu, Allen, *et al.*, 2021). Microbiome variation across spatial or geographic locations indicates that prevailing environmental conditions and microbial source pools strongly impact mussel shell microbiome assembly.

By transplanting mussels across elevations in the intertidal zone, we provide additional evidence for the role of abiotic filtering in shaping the mussel shell microbiome. Particularly, we show elevation, subaerial substratum temperature, and immersed seawater temperature, are significantly associated with observed differences in the mussel shell microbiome. Intertidal elevation has been shown to influence the digestive gland microbiome of oysters and clams in a recent transplant study (Offret *et al.*, 2020) and the microbiome of sympatric macroalgae (Lemay *et al.*, 2020; Quigley *et al.*, 2020) and benthic microbial communities (Rothrock and Garcia-Pichel, 2005; Okamoto *et al.*, 2022) are also shaped by geographic location and position in the intertidal zone. We suspect that thermal or other abiotic factors that vary across intertidal gradients can select for microbial taxa with distinct abiotic preferences (Yung *et al.*, 2015) and lead to spatial microbiome variation across the intertidal zone. For example, the mussel and oyster gut microbiomes are shown to exhibit temperature-driven compositional convergence at distinct geographic locations (Pierce and Ward, 2019). Likewise, the effect of intertidal abiotic gradients is recognized to influence the distribution of macroorganisms and microeukaryotes (Connell, 1972; Okamoto *et al.*, 2022). Our research provides novel evidence for similar abiotic structuring of microbial communities on the external surface of an intertidal foundation species. The distinct shifts in transplanted mussel shell microbiomes observed at different elevations in the intertidal zone may indicate the potential for future extreme weather events and predicted ocean warming to dramatically impact the mussel shell microbiome and its ecological functions.

4.5 Conclusion

In this study we find experimental evidence of differential erosion by endolithic cyanobacteria on killed mussel shells compared to on live hosts, suggesting some potential for

host biology to influence erosion by shell-boring parasites. We identify potential endolithic cyanobacteria taxa occurring broadly on mussel shells and surprisingly find the overall shell microbiome composition is not affected by shell erosion or interactions with living hosts. Transplanting mussels throughout an elevation gradient in the intertidal zone caused marked shifts in microbiome composition for both live and killed hosts. Our findings demonstrate that the shell microbiome of the California mussel is correlated more strongly to spatially variable abiotic factors than biotic interactions with the host or shell-boring parasites. The results from our experimental transplants further indicate that alterations in abiotic conditions have the potential to significantly impact the mussel shell microbiome with unknown consequences for host health and ecosystem functions.

Chapter 5: Successional dynamics of the cultivated kelp microbiome

5.1 Introduction

Kelp are important primary producers and habitat-forming species in coastal ecosystems (Teagle *et al.*, 2017). Kelp tissues are colonized by diverse microbial communities with genetic repertoires involved in vitamin synthesis, host settlement and developmental cues, defense and stress responses, polysaccharide metabolism, and nutrient cycling. The functional capacity of the kelp microbiome suggests it plays essential roles in both host biology and coastal biogeochemical cycles (Ji *et al.*, 2017; Vollmers *et al.*, 2017; Lin *et al.*, 2018). Thus, increased knowledge of the composition and dynamics of kelp-microbial associations is critical to for a holistic understanding of kelp health and coastal ecosystem functioning.

Globally, many kelp populations are in decline (Krumhansl *et al.*, 2016). Some of the factors negatively impacting kelp, like disease, fouling, marine heat waves, and anthropogenic disturbance, also affect the kelp microbiome (Morris *et al.*, 2016; Marzinelli *et al.*, 2018; Minich *et al.*, 2018; Qiu *et al.*, 2019; James *et al.*, 2020; Zhang *et al.*, 2020). In corals, marine foundation species also facing global declines, the microbiome has been shown to mitigate effects of negative stressors on the coral host. Extensive research on the composition, functions, spatial, and temporal dynamics of the coral microbiome (reviewed in van Oppen and Blackall, 2019) has helped identify specific microbial taxa or consortia that can be inoculated onto corals to enhance host growth, survivability, or resilience (Rosado *et al.*, 2019; Zhang *et al.*, 2021). A similar approach utilizing the microbiome to benefit kelp under changing ocean conditions holds great promise (Ghaderiardakani *et al.*, 2020), but additional research is needed to understand the factors influencing kelp-microbial associations and microbiome assembly.

Cultivation of kelp is gaining research attention as a method to restore declining kelp populations (Wood *et al.*, 2019) and to diversify the sustainable aquaculture sector (Grebe *et al.*, 2019). Kelp cultivation could be an ideal application of microbiome manipulation to enhance production and restoration outcomes, but little is known about the composition and turnover of the kelp microbiome during the cultivation process. The kelp cultivation process involves collecting reproductively mature, parental sporophytes and releasing zoospores from parental sorus tissue which settle onto seedstring in hatchery aquaria (Forbord *et al.*, 2018) (Figure 16). The microscopic kelp on seedstring are grown in filtered seawater (i.e., near-sterile conditions) amended with artificial nutrients and light at the hatchery until they reach a target blade size as juvenile sporophytes (Redmond *et al.*, 2014). The macroscopic juvenile sporophytes are then outplanted from the hatchery to anchored lines at open ocean cultivation sites where they continue to grow in natural seawater (Forbord *et al.*, 2018) (Figure 16). The hatchery would be the easiest stage in the cultivation process for changing kelp-associated microbial communities because of the controlled abiotic conditions, small scale, and protocols to reduce extraneous microbial colonizers (i.e., microbial source pool). Changing the kelp microbiome in the hatchery has the potential for long lasting impacts on the host. Evidence for this effect is based on findings from corals (Damjanovic *et al.*, 2019; Epstein *et al.*, 2019) and terrestrial crops (Barret *et al.*, 2015; Walsh *et al.*, 2021), where microbiome assembly in early life stages sets the overall microbiome successional trajectory for the host. The microbiome on early life stages of kelp has received little research attention, and it is not known if microbes colonizing juvenile kelp persist on host tissues as they grow. It is also unknown if there are differences in cultivated kelp microbiome dynamics across a range of ecologically and economically valuable kelp species that differ in life history strategies and tissue chemistry. The limited previous studies have focused

only on one species, *Saccharina japonica* (Zhang *et al.*, 2020; Han *et al.*, 2021). For microbiome manipulation to be a useful tool in kelp cultivation, it is important to characterize the extent and predictability of microbiome change throughout the cultivation process across a range of hosts. This will allow assessment of whether microbial benefits can be transferred from controlled conditions to complex ecological settings (Sessitsch *et al.*, 2019; French *et al.*, 2021).

In this study we tested whether microbes that colonize cultivated kelp in the hatchery persist or shape microbial community succession over time. We hypothesized that the microbiome of kelp in the hatchery would be low in taxonomic richness and very consistent between replicate samples because the hatchery conditions are highly controlled compared to natural seawater. We hypothesized that host species-specific microbiome differences would be observed in the hatchery, despite the similar growing conditions. We expected that some host species-specific microbial associations established in the hatchery would persist on hosts after outplanting. We predicted those stable associations would be rare but detectable within a background of overall microbiome change following outplanting to open ocean cultivation sites. We hypothesized that microbiome change occurring after outplanting would involve an overall increase in taxonomic richness and reflect different microbial source pools at each cultivation site. We expected cultivation site-specific communities to emerge on outplanted kelp because wild kelp show variation in microbiome composition driven by abiotic and regional factors (Weigel and Pfister, 2019; Wood *et al.*, 2022).

To test our hypotheses, we outplanted replicate seedstring spools of two brown algal species, *Saccharina latissima* and *Alaria marginata,* grown in the same hatchery, to five environmentally distinct cultivation sites in British Columbia, Canada. We sampled the hatchery microbiome of the young sporophyte kelp and took samples at three timepoints (approximately

every six weeks) after outplanting the kelp (Figure 16) to characterize microbiome changes throughout the cultivation process at each cultivation site. We compared our results from BC to a similar study in Washington, USA. This allowed us to assess the generalizability of our findings in kelp originating from different parental populations that were grown in different hatchery and field cultivation conditions. Understanding how different abiotic conditions affect kelp microbiome assembly in cultivation is important because site selection is an integral part of kelp cultivation or habitat restoration efforts (Bruhn *et al.*, 2016). Identifying persistent microbial associations and putative benefits in diverse environmental contexts will be necessary for widespread adoption of kelp microbiome manipulation (Clouse and Wagner, 2021).

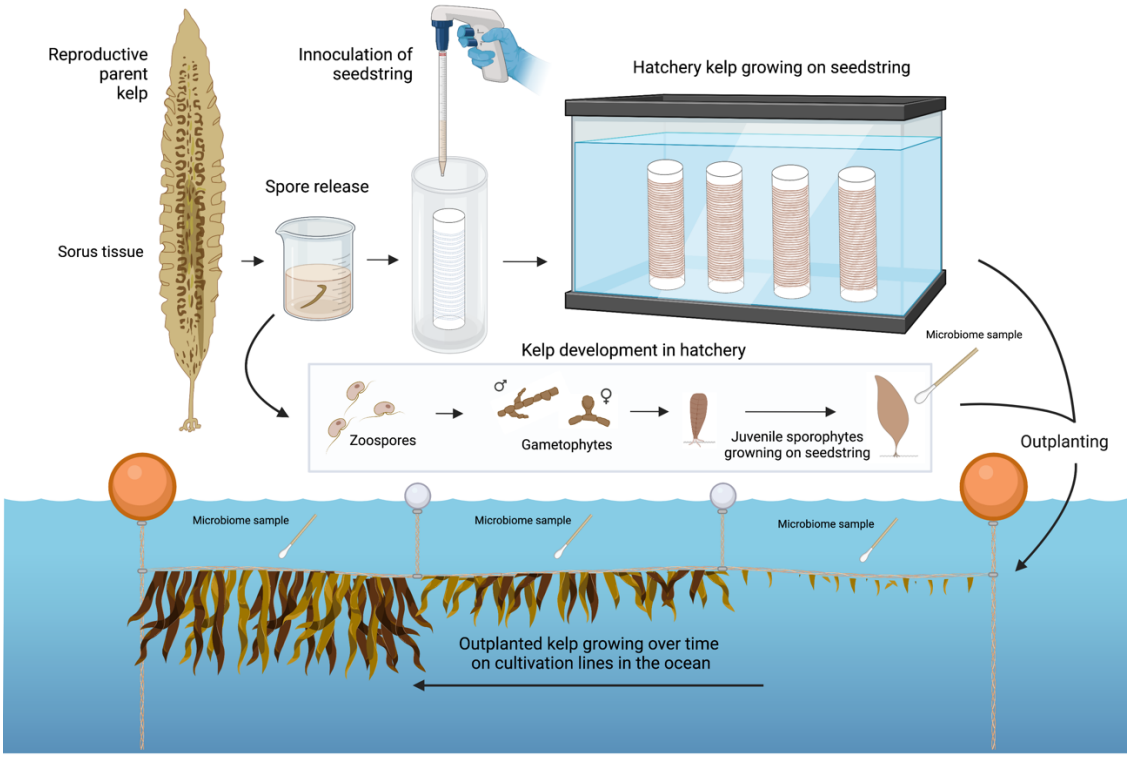

Figure 16. Overview of kelp cultivation and study sampling design.
Artwork of reproductive *Saccharina latissima* by Jungsoo Park.

5.2 Materials and methods

5.2.1 Study area

Kelp seedstring cultures were started from spores obtained from wild parental populations collected near Bamfield Marine Sciences Centre in British Columbia, Canada (48.839, -125.140) and Hood Head in Washington, USA (47.883, -122.614). Settled spores went through germination and fertilization on seedstring using batch culture in indoor aquaria at two hatcheries: Canadian Kelp Resources (CKR), Bamfield, BC, Canada and Manchester Research Station (MRS) NOAA Lab, Manchester, WA, USA. Kelp on seedstring were grown in the hatcheries until they became macroscopic juvenile sporophytes (1-4 mm blade length). Juvenile sporophytes of *Saccharina latissima* and *Alaria marginata* were outplanted at five sites in BC: Site 1 and Site 2 in Loughboro inlet, Interfor, East West Bay, and Talbot Cove (Figure 17). The BC *Alaria marginata* seedstring was outplanted 25-26 November 2020 and the *Saccharina latissima* seedstring was outplanted 16-17 December 2020. In WA, *Saccharina latissima* seedstring was outplanted to one site at Hood Head on 11 January 2019 (Figure 17).

Figure 17. Map of kelp hatchery and field cultivation sites.

5.2.2 Microbiome sample collection

Seedstring microbiome samples were collected from juvenile sporophytes (1-4 mm blade length) just prior to outplanting by swabbing a 3 cm^2 area of the seedstring on PVC spools at MRS with a sterile swab or by cutting 5 cm lengths of seedstring from CKR into sterile Whirlpak bags. Hatchery seawater and aquarium tank walls were sampled at MRS to compare colonization of living kelp tissue to the microbial source pools in seawater and non-host hatchery surfaces. Seawater samples were collected from the hatchery aquaria by filtering 500ml of water through a

0.22µm Sterivex filter (Millipore Sigma) using a sterile syringe. Tank wall swabs were collected over a 5 cm^2 area near the center of immersed vertical aquarium wall. In WA, outplanted kelp were sampled two months after outplanting, on 21 March 2019, by rinsing meristematic tissue (site of newest blade growth and recent microbial colonization) with 0.22µm filtered, autoclaved seawater for 10 seconds and then swabbing 2 cm^2 of the rinsed area with a sterile swab. In BC, whole blades of outplanted kelp were collected into individual sterile bags during the February and April 2021 sampling. At the final sampling for the BC study (22-24 June 2021), both swabs and whole blade samples were taken to compare microbiome composition between swab and whole-tissue sampling methods (Appendix D - Figure 1). Triplicate seawater samples were taken at cultivation sites ~30cm below the surface and filtered onto Sterivex filters as described above. Swabs of the cultivation line, on which the seedstring was outplanted, were used to characterize and compare the microbiome of non-host substrate at the cultivation sites. Field collected swabs, whole tissue samples and Sterivex filter cartridges were immediately placed on ice until return from the cultivation sites (< 6 hrs) and then temporarily stored at -20ºC until transportation on ice to the laboratory for long-term storage at -80ºC.

5.2.3 DNA extraction and 16S rRNA amplicon sequencing

DNA was extracted in random order from swabs, Sterivex filters, 2 cm lengths of seedstring, and 2 cm^2 pieces of meristematic tissue excised from frozen whole kelp blades with sterile razor blades. DNA extraction was performed using the DNeasy 96 Powersoil Pro Kit (Qiagen) following the manufacturer's guidelines. Extracted DNA was cleaned of PCR inhibitors using the OneStep-96 PCR Inhibitor Removal Kit (Zymo Research) according to the manufacturer’s protocol prior to PCR amplification. We used dual-index barcoded primers 515F

and 806R to amplify the V4 region of the 16S rRNA gene (Apprill *et al.*, 2015; Parada *et al.*, 2016) with the addition of a plastid peptide nucleic acid PCR blocking clamp (PNA Bio) to minimize contamination from 16s rRNA sequences originating from chloroplasts in the eukaryotic hosts (Lundberg *et al.*, 2013). Agarose gel electrophoresis and a Qubit 2.0 Fluorometer (Thermo Fisher Scientific) were used to check the quality and quantity of amplicons. PCR products were cleaned using the UltraClean 96 PCR Cleanup Kit (Qiagen) and fluorometrically quantified using the Quant-iT PicoGreen dsDNA Assay Kit (Invitrogen) for library pooling. A Bioanalyzer trace was performed at the BRC Sequencing Core, University of British Columbia to assess the quality and target size of the pooled libraries before being sending to the Hakai Institute Marna Genome Lab, Quadra Island, BC for sequencing via the Illumina MiSeq Platform.

5.2.4 16S rRNA gene amplicon sequence processing

To process demultiplexed raw paired-end sequencing reads, primers sequences were removed using Cutadapt (Martin, 2011). We then used the DADA2 pipeline (Callahan *et al.*, 2016) with sequences filtered and trimmed using the following settings: (truncLen=c(250,180), maxEE=c(2, 2), truncQ=2, maxN=0, rm.phix = TRUE). Error learning, sequence inference, and chimera removal were performed as recommended and we used the DADA2 naïve Bayesian classifier method with the SILVA (Quast *et al.*, 2013) version 138.1 training set for taxonomic assignment of the resulting amplicon sequence variants (ASVs). Raw 16S rRNA sequences will be available at the European Nucleotide Archive (project accession # PRJEB52544). For downstream analyses, ASVs not assigned as bacteria, ASVs with less than 20 total reads across the dataset, ASVs present in only one sample, and ASVs assigned as chloroplast or mitochondria

were removed. This yielded ~2 million total bacterial reads from 2574 ASVs with an average of 5152 reads per sample (range 403–50069 reads) after quality filtering.

5.2.5 Statistical analyses

Statistical analyses were conducted in R (version 4.1.2) and visualizations were made using ggplot2 (Wickham, 2016). Diversity metrics were calculated with phyloseq (McMurdie and Holmes, 2013) on samples rarefied to 1000 reads. Differences in alpha diversity between hatchery and outplanted samples were assessed using Welch's t-tests. To test for differences in microbiome composition between host species, hatchery location, cultivation location, month of sampling or between host tissue and surrounding microbial communities, PERMANOVA on Bray-Curtis dissimilarities were conducted with the vegan package (Oksanen *et al.*, 2019) using 999 permutations. The percentage of microbial community turnover for each host species from the BC study was calculated using pairwise sample comparisons of the Jaccard metric between samples from the hatchery and samples from each month of sampling (February, April, June); samples from all cultivation sites were pooled by month. Differences in the percentage of community turnover over time were assessed with Kruskal-Wallis tests.

5.3 Results

To understand microbiome dynamics on cultivated kelp, we first characterized the microbial communities colonizing juvenile kelp sporophytes on seedstring at the hatchery stage. We found species-specific differences in microbiome composition for *Saccharina latissima* and *Alaria marginata* reared in the same hatchery in BC (PERMANOVA: pseudo-F = 5.1239, R^2 = 0.26793, p = 0.001) (Figure 18). Microbiome composition differed significantly between *S.*

latissima sporophytes on seedstring in WA and BC (PERMANOVA: pseudo-F = 15.287, R^2 = 0.649, p = 0.006) (Figure 18). These *S. latissima* originated from different parental sources in different years and were reared in different hatcheries. In the WA hatchery, samples were taken of the surrounding microbial source pools and non-host associated biofilms and showed the microbiome of seedstring kelp was significantly different from bacterial communities in the hatchery seawater and on aquaria surfaces (PERMANOVA: pseudo-F = 5.277, R^2 = 0.540, p = 0.013) (Appendix D - Figure 2). Despite the significant differences between host- and non-host associated microbial communities in the WA hatchery, the magnitude of variation was smaller than the variation between seedstring *S. latissima* microbiome samples from the two different hatcheries, indicating a strong influence of paternal microbiome and/or hatchery microbial source pools on microbiome assembly.

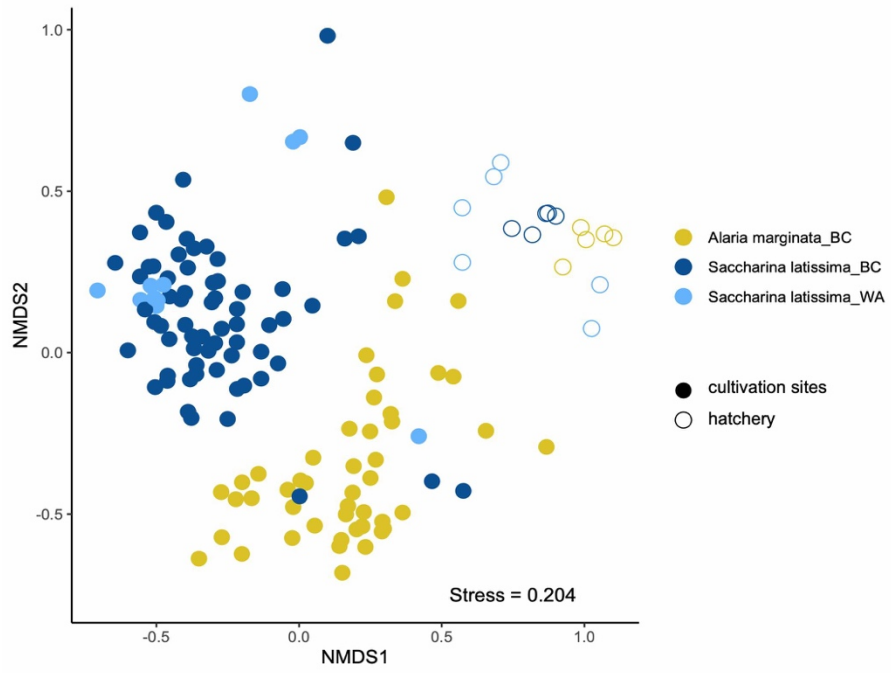

Figure 18. Non-metric multidimensional scaling plot of Bray-Curtis dissimilarity between samples of kelp in the hatchery and after outplanting to cultivation sites.

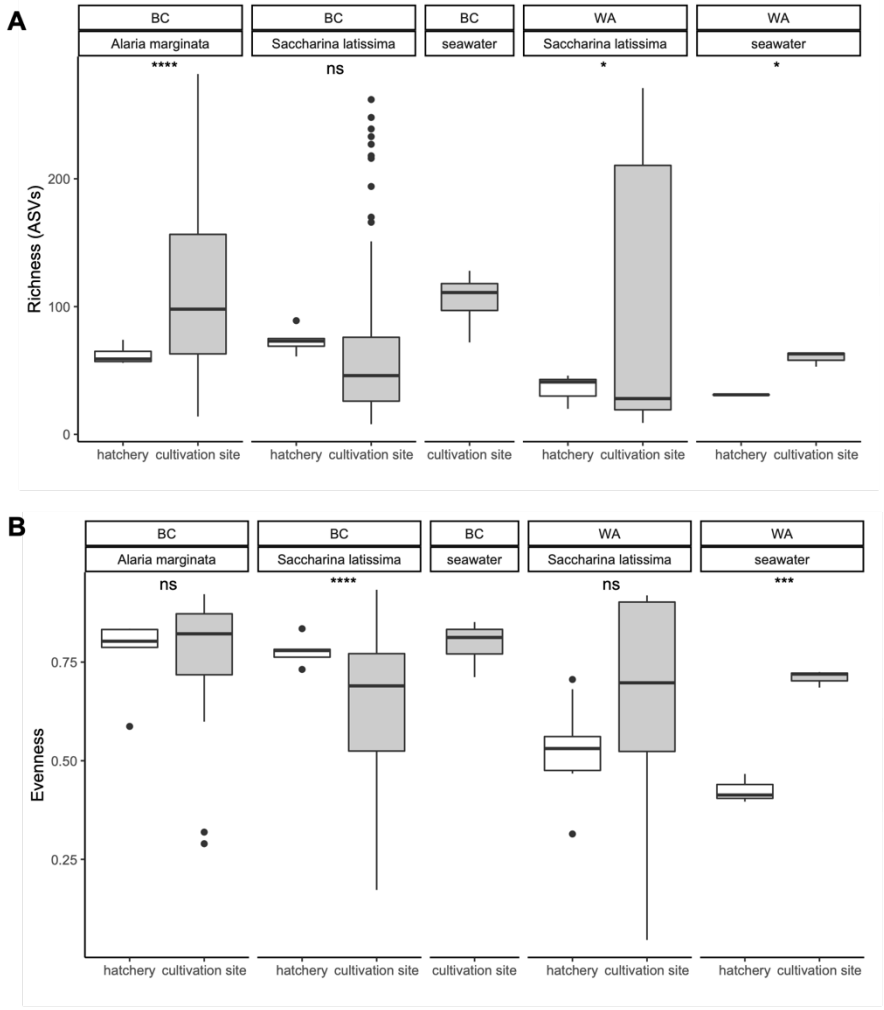

Figure 19. Alpha diversity metrics A) ASV richness and B) evenness between hatchery kelp samples and outplanted kelp samples taken at the cultivation sites. Significant differences in the group means are indicated by asterisks; ns = not significant.

We hypothesized that the microbiome on outplanted kelp would be significantly different from hatchery kelp because outplanted kelp is exposed to more variable microbial source pools in natural seawater. We confirmed alpha diversity was significantly lower in seawater samples (representing the source pool) from the hatchery compared to at the cultivation sites (Figure 19). Microbiome samples of *A. marginata* from the hatchery had lower taxonomic diversity but equal evenness compared to outplanted samples at the cultivation sites. For *S. latissima,* patterns of

alpha diversity between samples from the hatchery and cultivation sites differed between BC and WA (Figure 19). In BC, there was no difference in richness but greater evenness in the microbiome on *S. latissima* from the hatchery compared to on outplants. In WA, both hatchery and outplanted *S. latissima* microbiomes had similar richness and evenness. We observed significant shifts in microbiome composition on both kelp species after outplanting (Table 5) (Figure 18). The microbiome on kelp meristem tissue at cultivation sites was significantly different from source pool microbial communities in the surrounding seawater and non-host biofilms on cultivation lines (PERMANOVA: pseudo-F = 12.325, $R^2 = 0.122$, p = 0.001) (Appendix D - Figure 2). The seawater microbial source pools at the BC cultivation sites were significantly different from one another (PERMANOVA: pseudo-F = 2.042, $R^2 = 0.405$, p = 0.034). In support of our hypothesis, we observed significant microbiome variation explained by cultivation site for outplanted kelp of both species (Table 5) (Figure 20A). For outplanted kelp, there was also a significant effect of time, based on month of sampling, on the microbiome composition (Figure 20B) and a significant interaction between sample month and cultivation site (Table 5).

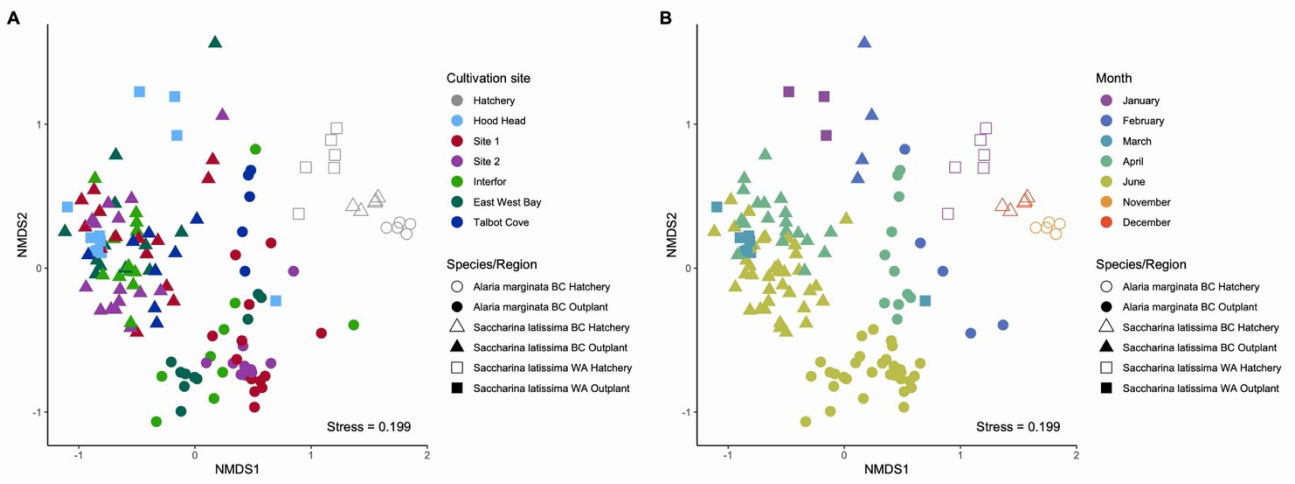

Figure 20. Non-metric multidimensional scaling plot of Bray-Curtis dissimilarity between samples of kelp in the hatchery and after outplanting to cultivation sites. The same plot is shown with samples colored by A) cultivation site and B) month of sampling.

	pseudo-F value	R^2	p-value
Hatchery seedstring vs outplant meristem			
Saccharina latissima	12.27	0.126	**0.001**
Alaria marginata	5.81	0.104	**0.001**
Outplanted *Saccharina latissima*			
Sample month	5.05	0.185	**0.001**
Cultivation location	3.28	0.12	**0.001**
Sample month * cultivation location	2.42	0.134	**0.001**
Outplanted *Alaria marginata*			
Sample month	6.15	0.153	**0.001**
Cultivation location	5.34	0.265	**0.001**
Sample month * cultivation location	2.76	0.137	**0.001**

Table 5. Results of PERMANOVA on Bray-Curtis dissimilarity showing factors associated with microbiome variation in *Saccharina latissima* and *Alaria marginata* corresponding to PCoA plot in Figure 20.
.

To quantify the extent of microbiome change over time from the hatchery to the cultivation sites, we calculated the percent of microbial community turnover in each month of sampling using pairwise sample comparisons of the Jaccard metric. On average, less than 2% of ASVs were maintained from the hatchery to the first sampling, which was two months after

outplanting. The microbiome on outplanted kelp became significantly more different from the hatchery microbiome over time, with less than 0.5% of ASVs from the hatchery found on outplanted kelp at the final sampling in June (Figure 21). The ASVs that persisted from the hatchery to the cultivation sites included members of *Colwellia, Sphingorhabdus* and unassigned Saprospiraceae on *S. latissima* (Appendix D - Figure 3). For *A. marginata*, the persistent ASVs included unassigned members of Rhodobacteraceae and Saprospiraceae as well as *Sulfitobacter* and *Paraglaciecola* (Appendix D - Figure 4). These persistent ASVs were generally found in low relative abundance on outplanted hosts (Appendix D - Figure 3 and 4). No ASVs were detected with 100% prevalence over time on either host species. The most prevalent ASV on *A. marginata* was an ASV from the genus *Lewinella* detected at 55% sample prevalence. The most prevalent ASVs on *S. latissima* were ASVs from the genera *Litorimonas* and *Persicirhabdus* detected at 75% sample prevalence.

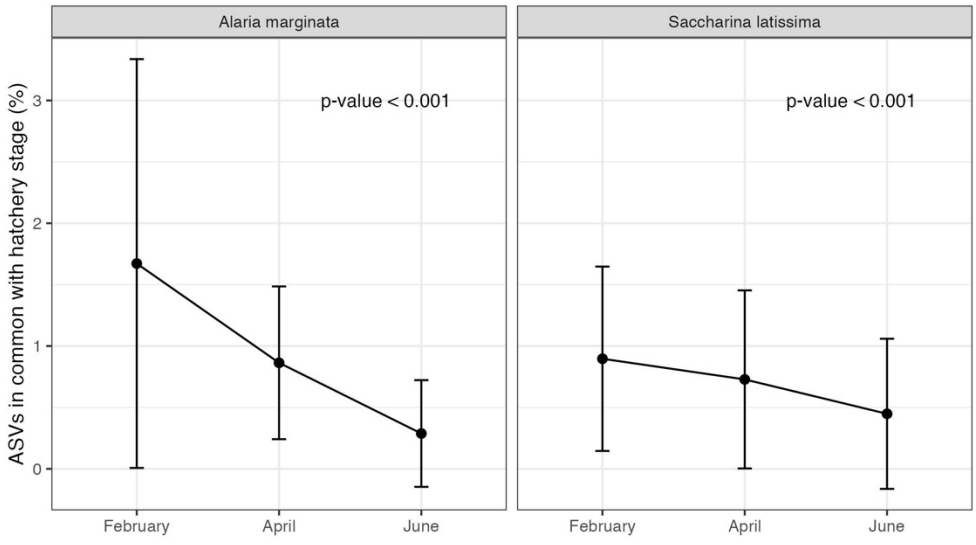

Figure 21. Percentage of total bacterial ASVs shared between the microbiome of kelp in the hatchery and on outplanted kelp at each month of sampling. Points represent the mean and standard deviation of pairwise sample comparisons using the Jaccard metric. P-values indicate significant differences by month based on Kruskal-Wallis tests.

5.4 Discussion

This research aimed to 1) characterize the extent and predictability of microbiome change throughout the kelp cultivation process and to 2) understand the contribution of host species and abiotic conditions to microbiome variation in cultivated kelps. Based on research from terrestrial crop plants (Barret *et al.*, 2015; Walsh *et al.*, 2021) and marine foundation species like corals (Damjanovic *et al.*, 2019), we expected the early life stages of cultivated kelp, in controlled hatchery settings, to be an ideal target for microbiome manipulation.

We found kelp cultivated on seedstring in two hatcheries had unique microbiomes. This is consistent with a recent study on the cultivated kelp *Saccharina japonica,* which found compositional differences in the microbiome of hatchery kelp compared to the microbial communities on reproductive parental sorus tissue and outplanted juvenile sporophytes (Han *et al.*, 2021). We noted that there was less variation between kelp and non-host-associated microbial communities in the same hatchery than between microbiomes of *S. latissima* cultivated in different hatcheries, suggesting that hatchery microbial source pools play an important role in microbiome assembly. It is likely the release of kelp spores in the hatchery facilitates transmission of microbial taxa from the parental sorus tissue to the early life stages of kelp either directly or horizontally through the water column by modifying the species pool in the hatchery, similarly to the findings from Chen and Parfrey (2018). Further studies are needed to characterize hatchery microbial communities in the absence of kelp tissue or in the presence of antibiotics to deepen our understanding of how cultivation methods influence the assembly of hatchery microbial source pools and the microbiome of developing kelp. The lack of research on gametophyte and juvenile sporophyte kelp microbiomes, combined with our findings, highlights

the need for studies on the contribution of horizontal and vertical transmission to kelp microbiome assembly.

We found *S. latissima* and *A. marginata*, kelp from different families reared in the same hatchery with the same or similar seawater microbial source pools, were colonized by distinct microbial taxa. Host species-specificity is commonly observed in the microbiome of mature, sympatric wild kelp (Weigel and Pfister, 2019) and other macroalgae (Lemay *et al.*, 2020). While the inclusion of these two host species in our study design was opportunistic, it presented a unique opportunity to examine microbiome assembly on kelps with different tissue properties and life history strategies (Schiel and Foster, 2006), known to be associated with distinct microbiome compositions (Lemay *et al.*, 2018). The strong role of host-species identity in the hatchery indicates that vertical transmission from parental tissue, host genetics or host biochemistry (Wood *et al.*, 2022) may contribute to the selective assembly of kelp microbiomes.

Discovering potential microbiome-derived benefits to the host and determining how these benefits are affected by the transition from controlled settings to field cultivation sites, where abiotic conditions and biotic interactions vary, is a key priority in the field of microbiome manipulation (Sessitsch *et al.*, 2019). Studies on wild populations of brown macroalgae have found that portions of the microbiome can be maintained when hosts are transplanted to different locations with new microbial source pools (Campbell *et al.*, 2015; Davis *et al.*, 2021). We speculated that kelp-microbe associations persisting from the hatchery to the cultivation sites would indicate the potential for hatchery-stage microbiome manipulation to have lasting effects on the host. A small number of ASVs from the hatchery were present on hosts after outplanting, despite large overall shifts in microbiome composition at the cultivation sites. The ASVs from the hatchery found on outplanted kelp, including members of Rhodobacteraceae and

Saprospiraceae, are common in kelp and macroalgal microbiomes (Weigel and Pfister, 2019; Lemay *et al.*, 2020, 2021). They are likely well adapted to host associated niches (e.g. metabolizing host-derived compounds (Florez *et al.*, 2017; Schultz-Johansen *et al.*, 2018)) and may produce antimicrobial compounds (Wiese *et al.*, 2009) that could shape microbiome composition and successional dynamics. *Sulfitobacter* and members of Rhodobacteraceae synthesize vitamin B12 and growth promoting hormones (Simon *et al.*, 2017) which could be also be important to kelp growth and cultivation outcomes. It is also possible that these frequently co-occurring taxa are parasitic or context-dependent pathogens. For example, a member of the Rhodobacteraceae, *Nautella italica* R11, is known to cause bleaching disease in some red macroalgae at high temperatures (Case *et al.*, 2011). Either way, these bacteria are interesting targets to isolate and test for their effects on kelp growth and other metrics of cultivation success using experimental co-culturing approaches.

Our findings indicate microbial communities on juvenile kelp sporophytes reared in controlled hatcheries may be highly susceptible to outcompetition by microbial colonizers from new microbial source pools. Newly grown meristematic kelp tissue generally has lower microbial diversity (Weigel and Pfister, 2019; Lemay *et al.*, 2021) and microbial cell density (Ramírez-Puebla *et al.*, 2022) which could facilitate the establishment of introduced microbial colonizers on juvenile kelp sporophytes. Both the composition, timing, and the quantity of microbial inoculants used in manipulation trials may be important in determining successful establishment and persistence of beneficial taxa on outplanted kelp (Aleklett *et al.*, 2022). Also, while these early colonizing taxa may not persist throughout host development, they may shape community successional trajectories that impact host biology and cultivation outcomes over time via priority effects (Maignien *et al.*, 2014; Fukami, 2015).

We documented significant microbiome variation corresponding to the month of sampling for both outplanted kelp species. This temporal signal, combined with the low number of ASVs prevalent across the datasets, indicates microbiome turnover or community succession is a predominant feature of the cultivated kelp microbiome. Similar seasonal turnover has been observed in the microbiome on wild kelp populations (Lachnit *et al.*, 2011; Weigel and Pfister, 2019) and other brown macroalgae (Serebryakova *et al.*, 2018; Davis et al. *in review*). We expect seasonal turnover is associated with changes in the seawater microbial community combined with selective colonization influenced by host growth and tissue chemistry. Kelps exhibit seasonal variation in tissue composition and polysaccharide production (Schiener *et al.*, 2015; Starko *et al.*, 2018) which could preferentially select microbial colonizers with different metabolic preferences over time (Lachnit *et al.*, 2013; Rickert *et al.*, 2016). Understanding how the consistent temporal microbiome dynamics we observed 1) affects microbially-mediated cultivation outcomes and 2) influences the timescale appropriate for establishing or detecting change using microbiome manipulation will be essential moving forward.

5.5 Conclusion

In conclusion, we show that host identity and microbial source pools are correlated to microbiome composition in cultivated kelp. We provide a baseline understanding of temporal microbiome dynamics throughout the kelp cultivation process. Our findings are encouraging for future research aimed at identifying specific microbial taxa or consortia that can improve kelp growth or resistance to disease and other stressors. by demonstrating the hatchery stage is a viable target for microbiome manipulation.

Chapter 6: Conclusion

Host-microbiome interactions are important to the health of marine organisms and ecosystem functioning. Understanding the impacts of changing ocean conditions on specific hosts or entire coastal ecosystems thus requires insights on the stability of host-microbiome associations. The results presented here indicate that microbiomes of healthy marine foundation species exhibit consistent temporal turnover under natural conditions (Chapter 2 & 5). Three brown macroalgal species from distinct phylogenetic lineages, in both intertidal and subtidal habitats, showed significant microbiome change correlated to the month of sampling. In *Fucus distichus*, strong seasonal turnover was evident despite inter-individual variation in microbiome composition and population-wide differences in host growth rates and developmental stages (Chapter 2). For *Saccharina latissima* and *Alaria marginata*, significant monthly turnover in microbiome composition was observed at distinct cultivation sites across multiple years (Chapter 5). These findings are in line with patterns observed in seawater (Cram *et al.*, 2015; Ward *et al.*, 2017) and diverse marine (Sieburth and Tootle, 1981; Lachnit *et al.*, 2011; Bierlich *et al.*, 2018; Glasl *et al.*, 2020) and terrestrial hosts (Grady *et al.*, 2019; Kolodny *et al.*, 2019). The proclivity for turnover in the microbiomes of diverse marine foundation species is significant for two reasons. First, the microbiome is often proposed to be a sentinel for host health and environmental change (Glasl *et al.*, 2017, 2019; Trevathan-Tackett *et al.*, 2019). Future studies should be aware of seasonality in developing microbiome-based indicators or drawing conclusions about microbiome dissimilarity from samples taken at different points in time. Second, natural turnover indicates the established microbiome can acquire new taxa or replace existing taxa over time. Colonization and establishment of new microbes that are better adapted

to the prevailing environmental conditions could help maintain important host-microbiome interactions under predicted climate change (Voolstra and Ziegler, 2020).

Through experimental manipulations, I show the timescale for microbiome stability versus change differs. In the short-term, i.e., hours to days, the microbiome may resist colonization from new microbial source pools (Chapter 3). Over longer timescales, i.e., weeks to months, the microbiome of marine foundation species restructures significantly (Chapter 4 & 5). In transplant studies of the California mussel, *Mytilus californianus*, the epibiotic shell microbiome showed significant differentiation along elevation gradients in the intertidal after two to three months (Chapter 4). Similarly, microbiomes of the cultivated kelps, *Saccharina latissima* and *Alaria marginata,* were significantly altered by exposure to natural seawater communities two months after outplanting from the hatchery (Chapter 5). The timescales of microbiome stability versus change provide important ecological context for interactions within the microbiome as well as microbiome assembly and succession on individual hosts. For example, potential bacterial colonizers that are selected for by the contemporary abiotic conditions may be slow to outcompete existing, established members of the microbiome, leading to perceived resistance to change on short time scales. On longer timescales, new microbial colonizers have the potential to coexist with or outcompete existing members of the microbiome leading to detectable community succession.

I also explored the influence of local abiotic conditions on the microbiome at single points in time. I show regional sites, which are home to different *F. distichus* phenotypes, had significantly different seawater microbial source pools as well as unique *F. distichus* microbiome compositions (Chapter 3). Hatchery raised juvenile *S. latissima* and *A. marginata* acquired site-specific microbiomes as they matured at different open-ocean cultivation locations (Chapter 5),

demonstrating site-specific differences can arise even when individuals start with roughly the same microbiome composition. Site-specific differences within the two kelp species were not, however, the most significant predictor of microbiome variation. I show microbiome variation within a population of *F. distichus*, depends on the host's location within randomly selected quadrats (Chapter 2). There was greater microbiome similarity among hosts within the same quadrat than in different quadrats. These local differences could be correlated with the measured quadrat-level variation in temperature, or other unmeasured abiotic factors that varied across the *F. distichus* bed. Further, experimentally changing the position of California mussels within the extent of their natural bed, was associated with microbiome differentiation across an elevation gradient in the intertidal zone (Chapter 4). Intertidal elevation is positively correlated with abiotic stress (Connell, 1972), providing support for within-population microbiome differentiation also being correlated to shifts in local abiotic conditions. These findings are aligned with previous observational and experimental studies in subtidal marine foundation species, such as seagrass (Ettinger *et al.*, 2017; O'Connor *et al.*, 2022) and kelp (Pfister *et al.*, 2019), where distinct microbiome compositions were found on host individuals in the interior versus at the edge of seagrass or kelp beds. In these studies, microbiome variation across host beds is attributed to differences in water chemistry, current, and other local conditions. Taken together, my findings suggest abiotic factors play a role in structuring regional microbial source pools and also contribute to within-population microbiome variation.

Local abiotic factors can also indirectly influence the microbiome via changes in host condition (Marzinelli *et al.*, 2018). In this research I attempted to examine the specific contribution of host factors to microbiome composition. I show host species identity strongly shapes the microbiome of two co-cultivated kelps; consistent with findings from wild macroalgal

communities (Lemay *et al.*, 2020). *Saccharina latissima* and *Alaria marginata* had unique microbiome compositions when grown in the same controlled hatchery settings, with roughly the same microbial source pool (Chapter 5). The species-specific differences became more pronounced when the kelps were outplanted to cultivation sites with high diversity, natural microbial source pools. There is emerging evidence that host phenotypes or genotypes play a role in host-microbiome associations across a range of marine (Griffiths *et al.*, 2019; Jackrel *et al.*, 2020; Wood *et al.*, 2022) and terrestrial hosts (Kwong *et al.*, 2017; Fitzpatrick *et al.*, 2018; Wagner, 2021). The mechanisms of host-specific microbiome assembly are unknown and complicated by interactions with the environment, but likely related to biochemical and morphological traits, life history, and/or vertical transmission. Results from the cultivated kelp study (Chapter 5) could suggest a contribution of the parental microbiome to early microbiome assembly but additional experimental studies are needed to confirm microbiome heritability. The kelp hatchery is an ideal target for future research on horizontal versus vertical transmission of the microbiome because the parental kelp sorus tissue microbiome (pseudo-vertical source) and hatchery seawater microbial community (horizontal source) can be characterized independently to understand the contribution of each to the microbiome on early life stages of kelp.

Variation within host species-specific microbiomes is common (Marzinelli *et al.*, 2015; Thomas *et al.*, 2016; van Oppen and Blackall, 2019) and the factors driving variation are poorly understood (Trevathan-Tackett *et al.*, 2019). Disentangling the contribution of abiotic and biotic factors to within-population microbiome variation is challenging because these factors are often correlated. For example, host developmental phenology is linked to seasonal abiotic cues. I tried to decouple the effects of seasonal factors from host development by sampling the microbiome of juvenile and mature *F. distichus* individuals concurrently for almost one year. I show host size

and reproductive status are significant predictors of *F. distichus* microbiome composition, independent of time of the year (Chapter 2). Changes in host biochemistry or morphology may associated with size and reproductive status may favor specific microbial taxa. For example, distinct microbiomes are associated with heteromorphic life stages in the red algal genus *Mastocarpus* (Lemay *et al.*, 2018). The extent to which different microbial taxa perform distinct functional roles associated with host ontogeny, as in some coral (Bernasconi *et al.*, 2019; Epstein *et al.*, 2019) and amphibian hosts (Kueneman *et al.*, 2015), remains to be determined.

I explicitly tested the effect of host biology on microbiome assembly in *M. californianus* by examining the shell microbiome of paired live and experimentally killed mussels. Surprisingly, the shell microbiome was not different between live and killed hosts (Chapter 4) indicating that host biology is not a strong predictor of microbiome composition in this system. I hypothesize that within-species filtering of the microbiome depends on metabolically active surfaces. For example, tissues of marine macroalgae, sponges, and animals are metabolically active; they exude carbon compounds, secondary metabolites or elicit immune responses that can promote or deter microbial colonization (Saha *et al.*, 2011a; Longford *et al.*, 2019; Woodhams *et al.*, 2020; Posadas *et al.*, 2021). In comparison, the organic periostracum of mussel shells is biogenic but probably not highly active metabolically (Checa, 2000). Similarly, seagrass leaves, which are coated in a waxy cuticle, appear to be less selective surfaces for microbial colonization compared to root tissues which actively secrete carbohydrates (Ettinger *et al.*, 2017; Fahimipour *et al.*, 2017). Thus, the degree of biological or physiological activity of a host surface may influence the level of determinism in microbiome assembly.

I hypothesize that priority effects play a role in establishing and maintaining individual microbiome differences, even in the context of predictable temporal succession. Priority effects

arise when early colonizing taxa change resource availability or local conditions in a way that impacts which taxa can subsequently establish in a community (Fukami, 2015). Priority effects have been shown to play an essential role in the assembly of the phyllosphere and rhizosphere microbiome in plants (Carlström *et al.*, 2019; Leopold and Busby, 2020) and the carbon-rich phycosphere surrounding phytoplankton cells (Majzoub *et al.*, 2019). The surface of macroalgae, being rich in photosynthetic exudates, is analogous to the phycosphere, phyllosphere or rhizosphere and results across studies in this work are aligned with priority effects shaping the microbiome on macroalgal hosts (Nappi *et al.*, 2022). For example, priority effects are likely at play for established microbiomes that resist colonization by microbes from new microbial source pools in transplanted *F. distichus* (Chapter 3). The maintenance of individual differences within the *F. distichus* population over time is also indicative of early colonizers shaping successional trajectory via priority effects (Chapter 2). To explicitly test for priority effects in marine hosts, additional experiments are needed.

An exciting avenue of future research is to understand if priority effects in microbiome assembly and succession can influence microbiome functioning and have consequential impacts on the host, especially related to the ability to respond to environmental change. For example, priority effects may ensure that essential microbial functions are sustained even in suboptimal environmental conditions (Rosado *et al.*, 2019). If functionally similar environmental microbes with greater abiotic tolerances can establish within or replace members of a pre-existing microbiome this could enable hosts to broaden their realized ecological niche. Priority effects may also play an important role in preventing disease (Litvak and Bäumler, 2019; Longford *et al.*, 2019) and fouling (Nasrolahi *et al.*, 2012; Goecke *et al.*, 2013) in marine foundation species. Kelp cultivation (Chapter 5) is an ideal system to further explore the role of priority effects on

microbiome assembly and to test for potential benefits to the host. Specific experiments could be conducted to: 1) test the contribution of the parental kelp microbiome to gametophyte and sporophyte microbiome assembly in the hatchery using different parental populations and sterilized versus unsterilized sorus tissue; 2) inoculate specific bacteria taxa during spore release and quantify the establishment of inoculated bacteria in microbiome and measure the persistence of inoculated taxa in the microbiome after outplanting or exposure to other environmental change; 3) assess beneficial effects of inoculated bacteria on host growth, abiotic tolerances, or influence over microbiome succession in natural seawater or defined microbial source pools; 4) challenge known microbiome compositions with pathogens or fouling organisms to detect protective effects of the microbiome; 5) establish a consistent minimal microbiome in culture (e.g. using antibiotics) which can be used to explore microbiome functions under different abiotic conditions or biotic interactions with introduced bacteria. These future research directions will enhance our ability to predict how climate change will affect the microbiome of important marine species and their ecosystem functions. They are also necessary in the development of microbiome-based strategies to support marine conservation and sustainable aquaculture.

In conclusion, I show that abiotic factors and host identity are broad selective filters for microbiome assembly on coastal foundation species. Within a host species, local abiotic conditions and host physiological state are correlated with microbiome variation. Consistent community turnover, despite individual variability, occurs across a range of hosts and habitats suggesting marine hosts have the capacity to acquire new microbes over time. It is possible these new colonizers are better adapted to the prevailing abiotic conditions. I propose that priority effects maintain variation between individual microbiomes despite temporally consistent, seasonal succession. The findings presented here make a significant contribution to identifying

and understanding the factors structuring the microbiome of marine foundation species. This foundational knowledge represents an important step towards microbiome-based approaches for monitoring, restoring, and cultivating ecologically and economically important marine species in changing oceans.

Bibliography

Adair, K.L. and Douglas, A.E. (2017) Making a microbiome: the many determinants of host-associated microbial community composition. *Curr Opin Microbiol* **35**: 23–29.

Ahmed, H.I., Herrera, M., Liew, Y.J., and Aranda, M. (2019) Long-term temperature stress in the Coral Model Aiptasia supports the "anna Karenina principle" for bacterial microbiomes. *Front Microbiol* **10**: 975.

Aleklett, K., Rosa, D., Pickles, B.J., and Hart, M.M. (2022) Community Assembly and Stability in the Root Microbiota During Early Plant Development. *Front Microbiol* **13**:.

Alster, C.J., Weller, Z.D., and von Fischer, J.C. (2018) A meta-analysis of temperature sensitivity as a microbial trait. *Glob Chang Biol* **24**: 4211–4224.

Van Alstyne, K.L. (1988) Herbivore grazing increases polyphenolic defenses in the intertidal brown alga Fucus distichus. *Ecology* **69**: 655–663.

Van Alstyne, K.L., McCarthy, J.J., Hustead, C.L., and Kearns, L.J. (1999) Phlorotannin allocation among tissues of northeastern Pacific kelps and rockweeds. *J Phycol* **35**: 483–492.

Anderson, C.I.H. and Scott, G.W. (1998) The Occurrence of Distinct Morphotypes within a Population of Fucus Spiralis . *J Mar Biol Assoc United Kingdom* **78**: 1003–1006.

Ang, P. 0 (1991) Natural dynamics of a Fucus distichus (Phaeophyceae, Fucales) population: reproduction and recruitment.

Apprill, A. (2017) Marine Animal Microbiomes: Toward Understanding Host–Microbiome Interactions in a Changing Ocean. *Front Mar Sci* **4**: 222.

Apprill, A., Mcnally, S., Parsons, R., and Weber, L. (2015) Minor revision to V4 region SSU rRNA 806R gene primer greatly increases detection of SAR11 bacterioplankton. *Aquat Microb Ecol* **75**: 129–137.

Armstrong, E., Rogerson, A., and Leftley, J.W. (2000) Utilisation of seaweed carbon by three surface-associated heterotrophic protists, Stereomyxa ramosa, Nitzschia alba and Labyrinthula sp. *Aquat Microb Ecol*.

Azam, F. and Malfatti, F. (2007) Microbial structuring of marine ecosystems. *Nat Rev Microbiol 2007 510* **5**: 782–791.

Balakirev, E.S., Krupnova, T.N., and Ayala, F.J. (2012) Symbiotic Associations in the

Phenotypically-Diverse Brown Alga Saccharina japonica. *PLoS One* **7**: e39587.

Barret, M., Briand, M., Bonneau, S., Préveaux, A., Valière, S., Bouchez, O., et al. (2015) Emergence shapes the structure of the seed microbiota. *Appl Environ Microbiol* **81**: 1257–1266.

Bengtsson, M., Sjøtun, K., and Øvreås, L. (2010) Seasonal dynamics of bacterial biofilms on the kelp Laminaria hyperborea. *Aquat Microb Ecol* **60**: 71–83.

Bengtsson, M., Sjøtun, K., Storesund, J., and Øvreås, J. (2011) Utilization of kelp-derived carbon sources by kelp surface-associated bacteria. *Aquat Microb Ecol* **62**: 191–199.

Bengtsson, M.M. and Øvreås, L. (2010) Planctomycetes dominate biofilms on surfaces of the kelp Laminaria hyperborea. *BMC Microbiol* **10**: 261.

Bernasconi, R., Stat, M., Koenders, A., Paparini, A., Bunce, M., and Huggett, M.J. (2019) Establishment of coral-bacteria symbioses reveal changes in the core bacterial community with host ontogeny. *Front Microbiol* **10**: 1529.

Bers, A. V., Prendergast, G.S., Zürn, C.M., Hansson, L., Head, R.M., and Thomason, J.C. (2005) A comparative study of the anti-settlement properties of mytilid shells. *Biol Lett* **2**: 88–91.

Bers, A.V., D'Souza, F., Klijnstra, J.W., Willemsen, P.R., and Wahl, M. (2006) Chemical defence in mussels: Antifouling effect of crude extracts of the periostracum of the blue mussel Mytilus edulis. *Biofouling* **22**: 251–259.

Bierlich, K.C., Miller, C., DeForce, E., Friedlaender, A.S., Johnston, D.W., and Apprill, A. (2018) Temporal and regional variability in the skin microbiome of humpback whales along the Western Antarctic Peninsula. *Appl Environ Microbiol* **84**:.

Biggs, C.R., Yeager, L.A., Bolser, D.G., Bonsell, C., Dichiera, A.M., Hou, Z., et al. (2020) Does functional redundancy affect ecological stability and resilience? A review and meta-analysis. *Ecosphere* **11**: e03184.

Blanchette, C.A. (1997) Size and Survival of Intertidal Plants in Response to Wave Action: A Case Study with Fucus Gardneri. *Ecology* **78**: 1563.

Bower, S.M., Korrûbel, J.L., and Webb, S.. (2002) Phototrophic Endolith Invasion of Mussel Shells. *Synopsis Infect Dis Parasites Commer Exploit Shellfish*.

Bruhn, A., Tørring, D.B., Thomsen, M., Canal-Vergés, P., Nielsen, M.M., Rasmussen, M.B., et al. (2016) Impact of environmental conditions on biomass yield, quality, and bio-mitigation capacity of Saccharina latissima. *Aquac Environ Interact* **8**: 619–636.

Burge, C.A., Kim, C.J.S., Lyles, J.M., and Harvell, C.D. (2013) Special Issue Oceans and

Humans Health: The Ecology of Marine Opportunists. *Microb Ecol* **65**: 869–879.

Burke, C., Steinberg, P., Rusch, D., Kjelleberg, S., and Thomas, T. (2011) Bacterial community assembly based on functional genes rather than species. *Proc Natl Acad Sci* **108**: 14288–14293.

Cáceres, M. De and Legendre, P. (2009) Associations between species and groups of sites: indices and statistical inference. *Ecology* **90**: 3566–3574.

Callahan, B.J., McMurdie, P.J., Rosen, M.J., Han, A.W., Johnson, A.J.A., and Holmes, S.P. (2016) DADA2: High-resolution sample inference from Illumina amplicon data. *Nat Methods* **13**: 581–583.

Campbell, Alexandra H, Marzinelli, E.M., Gelber, J., and Steinberg, P.D. (2015) Spatial variability of microbial assemblages associated with a dominant habitat-forming seaweed. *Front Microbiol* **6**: 230.

Campbell, Alexandra H., Marzinelli, E.M., Gelber, J., and Steinberg, P.D. (2015) Spatial variability of microbial assemblages associated with a dominant habitat-forming seaweed. *Front Microbiol* **6**: 230.

Campbell, A.H., Vergés, A., and Steinberg, P.D. (2014) Demographic consequences of disease in a habitat-forming seaweed and impacts on interactions between natural enemies. *Ecology* **95**: 142–152.

Capistrant-Fossa, K.A., Morrison, H.G., Engelen, A.H., Quigley, C.T.C., Morozov, A., Serrão, E.A., et al. (2021) The microbiome of the habitat-forming brown alga Fucus vesiculosus (Phaeophyceae) has similar cross-Atlantic structure that reflects past and present drivers1. *J Phycol* **57**: 1681–1698.

Carlström, C.I., Field, C.M., Bortfeld-Miller, M., Müller, B., Sunagawa, S., and Vorholt, J.A. (2019) Synthetic microbiota reveal priority effects and keystone strains in the Arabidopsis phyllosphere. *Nat Ecol Evol* **3**: 1445–1454.

Carrier, T.J. and Reitzel, A.M. (2018) Convergent shifts in host-associated microbial communities across environmentally elicited phenotypes. *Nat Commun* **9**: 1–9.

Case, R.J., Longford, S.R., Campbell, A.H., Low, A., Tujula, N., Steinberg, P.D., and Kjelleberg, S. (2011) Temperature induced bacterial virulence and bleaching disease in a chemically defended marine macroalga. *Environ Microbiol* **13**: 529–537.

Casey, J.M., Connolly, S.R., and Ainsworth, T.D. (2015) Coral transplantation triggers shift in microbiome and promotion of coral disease associated potential pathogens. *Sci Rep* **5**: 11903.

Chakraborty, K., Thilakan, B., and Raola, V.K. (2017) Antimicrobial polyketide furanoterpenoids from seaweed-associated heterotrophic bacterium Bacillus subtilis MTCC 10403. *Phytochemistry* **142**: 112–125.

Checa, A. (2000) A new model for periostracum and shell formation in Unionidae (Bivalvia, Mollusca). *Tissue Cell* **32**: 405–416.

Chen, M.Y. and Parfrey, L.W. (2018) Incubation with macroalgae induces large shifts in water column microbiota, but minor changes to the epibiota of co-occurring macroalgae. *Mol Ecol* **27**: 1966–1979.

Chow, C.-E.T., Sachdeva, R., Cram, J.A., Steele, J.A., Needham, D.M., Patel, A., et al. (2013) Temporal variability and coherence of euphotic zone bacterial communities over a decade in the Southern California Bight. *ISME J 2013 712* **7**: 2259–2273.

Chow, C.E.T., Kim, D.Y., Sachdeva, R., Caron, D.A., and Fuhrman, J.A. (2013) Top-down controls on bacterial community structure: microbial network analysis of bacteria, T4-like viruses and protists. *ISME J 2014 84* **8**: 816–829.

Christie, H., Norderhaug, K., and Fredriksen, S. (2009) Macrophytes as habitat for fauna. *Mar Ecol Prog Ser* **396**: 221–233.

Cleary, D.F.R. and Polónia, A.R.M. (2018) Bacterial and archaeal communities inhabiting mussels, sediment and water in Indonesian anchialine lakes. *Antonie Van Leeuwenhoek* **111**: 237–257.

Cleary, D.F.R., Swierts, T., Coelho, F.J.R.C., Polónia, A.R.M., Huang, Y.M., Ferreira, M.R.S., et al. (2019) The sponge microbiome within the greater coral reef microbial metacommunity. *Nat Commun* **10**: 1–12.

Clouse, K.M. and Wagner, M.R. (2021) Plant Genetics as a Tool for Manipulating Crop Microbiomes: Opportunities and Challenges. *Front Bioeng Biotechnol* **9**:.

Comeau, André M, Douglas, G.M., and Langille, M.G.I. (2017) Microbiome Helper: a Custom and Streamlined Workflow for Microbiome Research. *mSystems* **2**: e00127-16.

Comeau, André M., Douglas, G.M., and Langille, M.G.I. (2017) Microbiome Helper: a Custom and Streamlined Workflow for Microbiome Research. *mSystems* **2**:.

Comeau, A.M., Li, W.K.W., Tremblay, J.-É., Carmack, E.C., and Lovejoy, C. (2011) Arctic Ocean Microbial Community Structure before and after the 2007 Record Sea Ice Minimum. *PLoS One* **6**: e27492.

Connell, J.H. (1972) Community Interactions on Marine Rocky Intertidal Shores. *Annu Rev Ecol Syst* **3**: 169–192.

Coyer, J.A., Hoarau, G., Beszteri, B., Pearson, G., and Olsen, J.L. (2009) Expressed sequence tag-derived polymorphic SSR markers for Fucus serratus and amplification in other species of Fucus. *Mol Ecol Resour* **9**: 168–170.

Coyte, K.Z., Schluter, J., and Foster, K.R. (2015) The ecology of the microbiome: Networks, competition, and stability. *Science* **350**: 663–666.

Cram, J.A., Chow, C.E.T., Sachdeva, R., Needham, D.M., Parada, A.E., Steele, J.A., and Fuhrman, J.A. (2015) Seasonal and interannual variability of the marine bacterioplankton community throughout the water column over ten years. *ISME J* **9**: 563–580.

Damjanovic, K., Van Oppen, M.J.H., Menéndez, P., and Blackall, L.L. (2019) Experimental inoculation of coral recruits with marine bacteria indicates scope for microbiome manipulation in Acropora tenuis and Platygyra daedalea. *Front Microbiol* **10**: 1702.

Dando, P.R., Southward, A.J., and Southward, E.C. (1986) Chemoautotrophic symbionts in the gills of the bivalve mollusc Lucinoma borealis and the sediment chemistry of its habitat. *Proc R Soc London Ser B Biol Sci* **227**: 227–247.

Dang, H. and Lovell, C.R. (2016) Microbial Surface Colonization and Biofilm Development in Marine Environments. *Microbiol Mol Biol Rev* **80**: 91–138.

Datta, M.S., Sliwerska, E., Gore, J., Polz, M.F., and Cordero, O.X. (2016) Microbial interactions lead to rapid micro-scale successions on model marine particles. *Nat Commun* **7**: 11965.

Davis, K.M., Mazel, F., and Wegener Parfrey, L. (2021) The microbiota of intertidal macroalgae *Fucus distichus* is site-specific and resistant to change following transplant. *Environ Microbiol* 1462-2920.15496.

Dethier, M.N. and Williams, S.L. (2009) Seasonal stresses shift optimal intertidal algal habitats. *Mar Biol* **156**: 555–567.

Díez-Vives, C., Taboada, S., Leiva, C., Busch, K., Hentschel, U., and Riesgo, A. (2020) On the way to specificity - Microbiome reflects sponge genetic cluster primarily in highly structured populations. *Mol Ecol* mec.15635.

Dittami, S.M., Duboscq-Bidot, L., Perennou, M., Gobet, A., Corre, E., Boyen, C., and Tonon, T. (2016) Host–microbe interactions as a driver of acclimation to salinity gradients in brown algal cultures. *ISME J* **10**: 51–63.

Dogs, M., Wemheuer, B., Wolter, L., Bergen, N., Daniel, R., Simon, M., and Brinkhoff, T. (2017) Rhodobacteraceae on the marine brown alga Fucus spiralis are abundant and show physiological adaptation to an epiphytic lifestyle. *Syst Appl Microbiol* **40**: 370–382.

Duarte, B., Martins, I., Rosa, R., Matos, A.R., Roleda, M.Y., Reusch, T.B.H., et al. (2018)

Climate change impacts on seagrass meadows and macroalgal forests: An integrative perspective on acclimation and adaptation potential. *Front Mar Sci* **5**: 190.

Dufrêne, M. and Legendre, P. (1997) Speces assemblages and indicator species: the need for a flexible asymmetrical approach. *Ecol Monogr* **67**: 345–366.

Dunphy, C.M., Gouhier, T.C., Chu, N.D., and Vollmer, S. V. (2019) Structure and stability of the coral microbiome in space and time. *Sci Rep* **9**: 1–13.

Egan, S. and Gardiner, M. (2016) Microbial dysbiosis: Rethinking disease in marine ecosystems. *Front Microbiol* **7**: 991.

Egan, S., Harder, T., Burke, C., Steinberg, P., Kjelleberg, S., and Thomas, T. (2013) The seaweed holobiont: understanding seaweed–bacteria interactions. *FEMS Microbiol Rev* **37**: 462–476.

Egan, S., Thomas, T., Holmström, C., and Kjelleberg, S. (2000) Phylogenetic relationship and antifouling activity of bacterial epiphytes from the marine alga Ulva lactuca. *Environ Microbiol* **2**: 343–7.

Ellison, A.M. (2019) Foundation Species, Non-trophic Interactions, and the Value of Being Common. *ISCIENCE* **13**: 254–268.

Epstein, H.E., Torda, G., Munday, P.L., and van Oppen, M.J.H. (2019) Parental and early life stage environments drive establishment of bacterial and dinoflagellate communities in a common coral. *ISME J* **13**: 1635–1638.

Ettinger, C.L., Voerman, S.E., Lang, J.M., Stachowicz, J.J., and Eisen, J.A. (2017) Microbial communities in sediment from Zostera marina patches, but not the Z. marina leaf or root microbiomes, vary in relation to distance from patch edge. *PeerJ* **2017**: e3246.

Fahimipour, A.K., Kardish, M.R., Lang, J.M., Green, J.L., Eisen, J.A., and Stachowicz, J.J. (2017) Globalscale structure of the eelgrass microbiome. *Appl Environ Microbiol* **83**:.

Faria, M., Bordin, N., Kizina, J., Harder, J., Devos, D., and Lage, O.M. (2018) Planctomycetes attached to algal surfaces: Insight into their genomes. *Genomics* **110**: 231–238.

Fitzpatrick, C.R., Copeland, J., Wang, P.W., Guttman, D.S., Kotanen, P.M., and Johnson, M.T.J. (2018) Assembly and ecological function of the root microbiome across angiosperm plant species. *Proc Natl Acad Sci U S A* **115**: E1157–E1165.

Florez, J.Z., Camus, C., Hengst, M.B., and Buschmann, A.H. (2017) A Functional Perspective Analysis of Macroalgae and Epiphytic Bacterial Community Interaction. *Front Microbiol* **8**: 2561.

Forbord, S., Steinhovden, K.B., Rød, K.K., Handå, A., and Skjermo, J. (2018) Cultivation protocol for Saccharina latissima. *Protoc macroalgae Res* **2**: 1–4.

French, E., Kaplan, I., Iyer-Pascuzzi, A., Nakatsu, C.H., and Enders, L. (2021) Emerging strategies for precision microbiome management in diverse agroecosystems. *Nat Plants 2021 73* **7**: 256–267.

Fries, L. (1984) Induction of plantlets in axenically cultivated rhizoids of *Fucus spiralis*. *Can J Bot* **62**: 1616–1620.

Fries, L. (1993) Vitamin B12 Heterotrophy in Fucus spiralis and Ascophyllum nodosum (Fucales, Phaeophyta) in Axenic Cultures. *Bot Mar* **36**: 5–8.

Frölicher, T.L., Fischer, E.M., and Gruber, N. (2018) Marine heatwaves under global warming. *Nat 2018 5607718* **560**: 360–364.

Fukami, T. (2015) Historical Contingency in Community Assembly: Integrating Niches, Species Pools, and Priority Effects. *Annu Rev Ecol Evol Syst* **46**: 1–23.

Gehman, A.L.M. and Harley, C.D.G. (2019) Symbiotic endolithic microbes alter host morphology and reduce host vulnerability to high environmental temperatures. *Ecosphere* **10**: e02683.

Ghaderiardakani, F., Coates, J.C., and Wichard, T. (2017) Bacteria-induced morphogenesis of Ulva intestinalis and Ulva mutabilis (Chlorophyta): a contribution to the lottery theory. *FEMS Microbiol Ecol* **93**:.

Ghaderiardakani, F., Quartino, M.L., and Wichard, T. (2020) Microbiome-Dependent Adaptation of Seaweeds Under Environmental Stresses: A Perspective. *Front Mar Sci* **7**:.

Gilbert, J.A., Steele, J.A., Caporaso, J.G., Steinbrück, L., Reeder, J., Temperton, B., et al. (2012) Defining seasonal marine microbial community dynamics. *ISME J* **6**: 298–308.

Glasl, B., Bourne, D.G., Frade, P.R., Thomas, T., Schaffelke, B., and Webster, N.S. (2019) Microbial indicators of environmental perturbations in coral reef ecosystems. *Microbiome* **7**: 1–13.

Glasl, B., Herndl, G.J., and Frade, P.R. (2016) The microbiome of coral surface mucus has a key role in mediating holobiont health and survival upon disturbance. **10**: 2280–2292.

Glasl, B., Robbins, S., Frade, P.R., Marangon, E., Laffy, P.W., Bourne, D.G., and Webster, N.S. (2020) Comparative genome-centric analysis reveals seasonal variation in the function of coral reef microbiomes. *ISME J* **14**: 1435–1450.

Glasl, B., Webster, N.S., and Bourne, D.G. (2017) Microbial indicators as a diagnostic tool for

assessing water quality and climate stress in coral reef ecosystems. *Mar Biol 2017 1644* **164**: 1–18.

Goecke, F., Labes, A., Wiese, J., and Imhoff, J.F. (2013) Phylogenetic analysis and antibiotic activity of bacteria isolated from the surface of two co-occurring macroalgae from the Baltic Sea. *Eur J Phycol* **48**: 47–60.

Grady, K.L., Sorensen, J.W., Stopnisek, N., Guittar, J., and Shade, A. (2019) Assembly and seasonality of core phyllosphere microbiota on perennial biofuel crops. *Nat Commun 2019 101* **10**: 1–10.

Grebe, G.S., Byron, C.J., Gelais, A.S., Kotowicz, D.M., and Olson, T.K. (2019) An ecosystem approach to kelp aquaculture in the Americas and Europe. *Aquac Reports* **15**: 100215.

Greyson-Gaito, C.J., Bartley, T.J., Cottenie, K., Jarvis, W.M.C., Newman, A.E.M., and Stothart, M.R. (2020) Into the wild: Microbiome transplant studies need broader ecological reality. *Proc R Soc B Biol Sci* **287**: 20192834.

Griffiths, S.M., Antwis, R.E., Lenzi, L., Lucaci, A., Behringer, D.C., Butler, M.J., and Preziosi, R.F. (2019) Host genetics and geography influence microbiome composition in the sponge Ircinia campana. *J Anim Ecol* **88**: 1684–1695.

Halat, L., Galway, M.E., Gitto, S., and Garbary, D.J. (2015) Epidermal shedding in *Ascophyllum nodosum* (Phaeophyceae): seasonality, productivity and relationship to harvesting. *Phycologia* **54**: 599–608.

Halpern, B.S., Walbridge, S., Selkoe, K.A., Kappel, C. V., Micheli, F., D'Agrosa, C., et al. (2008) A global map of human impact on marine ecosystems. *Science* **319**: 948–952.

Han, Q., Zhang, X., Chang, L., Xiao, L., Ahmad, R., Saha, M., et al. (2021) Dynamic shift of the epibacterial communities on commercially cultivated Saccharina japonica from mature sporophytes to sporelings and juvenile sporophytes. *J Appl Phycol* **33**: 1171–1179.

Haring, R., Dethier, M., and Williams, S. (2002) Desiccation facilitates wave-induced mortality of the intertidal alga Fucus gardneri. *Mar Ecol Prog Ser* **232**: 75–82.

Harley, C.D.G. (2008) Tidal dynamics, topographic orientation, and temperature-mediated mass mortalities on rocky shores. *Mar Ecol Prog Ser* **371**: 37–46.

Harley, C.D.G. and Helmuth, B.S.T. (2003) Local- and regional-scale effects of wave exposure, thermal stress, and absolute versus effective shore level on patterns of intertidal zonation. *Limnol Oceanogr* **48**: 1498–1508.

Harley, C.D.G., Hughes, A.R., Hultgren, K.M., Miner, B.G., Sorte, C.J.B., Thornber, C.S., et al. (2006) The impacts of climate change in coastal marine systems. *Ecol Lett* **9**: 228–241.

Harris, R.M.B., Beaumont, L.J., Vance, T.R., Tozer, C.R., Remenyi, T.A., Perkins-Kirkpatrick, S.E., et al. (2018) Biological responses to the press and pulse of climate trends and extreme events. *Nat Clim Chang* **8**: 579–587.

Heisterkamp, I.M., Schramm, A., Larsen, L.H., Svenningsen, N.B., Lavik, G., de Beer, D., and Stief, P. (2013) Shell biofilm-associated nitrous oxide production in marine molluscs: processes, precursors and relative importance. *Environ Microbiol* **15**: 1943–1955.

Helmuth, B.S.T. and Hofmann, G.E. (2001) Microhabitats, thermal heterogeneity, and patterns of physiological stress in the rocky intertidal zone. **201**: 374–384.

Hemmi, A., Mainen, A., Jormalainen, V., and Honkanen, T. (2005) Responses of growth and phlorotannins in Fucus vesiculosus to nutrient enrichment and herbivory. *Aquat Ecol* 201–211.

Hernandez-Agreda, A., Gates, R.D., and Ainsworth, T.D. (2017) Defining the Core Microbiome in Corals' Microbial Soup. *Trends Microbiol* **25**: 125–140.

Hernandez-Agreda, A., Leggat, W., Bongaerts, P., Herrera, C., and Ainsworth, T.D. (2018) Rethinking the coral microbiome: Simplicity exists within a diverse microbial biosphere. *MBio* **9**: 812–830.

Hibbing, M.E., Fuqua, C., Parsek, M.R., and Peterson, S.B. (2010) Bacterial competition: Surviving and thriving in the microbial jungle. *Nat Rev Microbiol* **8**: 15–25.

Jackrel, S.L., Yang, J.W., Schmidt, K.C., and Denef, V.J. (2020) Host specificity of microbiome assembly and its fitness effects in phytoplankton. *ISME J* **15**: 774–788.

James, A.K., English, C.J., Nidzieko, N.J., Carlson, C.A., and Wilbanks, E.G. (2020) Giant kelp microbiome altered in the presence of epiphytes. *Limnol Oceanogr Lett* **5**: 354–362.

Ji, P., Zhang, Y., Wang, J., and Zhao, F. (2017) MetaSort untangles metagenome assembly by reducing microbial community complexity. *Nat Commun 2017 81* **8**: 1–14.

Johannesson, K., Forslund, H., Capetillo, N., Kautsky, L., Johansson, D., Pereyra, R.T., and Råberg, S. (2012) Phenotypic variation in sexually and asexually recruited individuals of the Baltic Sea endemic macroalga Fucus radicans: in the field and after growth in a common-garden. *BMC Ecol* **12**: 2.

Joux, F., Jeffrey, W.H., Lebaron, P., and Mitchell, D.L. (1999) Marine bacterial isolates display diverse responses to UV-B radiation. *Appl Environ Microbiol* **65**: 3820–3827.

Kaehler, S. (1999) Incidence and distribution of phototrophic shell-degrading endoliths of the brown mussel Perna perna. *Mar Biol* **135**: 505–514.

Keser, M. and Larson, B.R. (1984) Colonization and growth dynamics of three species of Fucus. *Mar Ecol Prog Ser* **15**: 125–134.

Kirchman, D.L. (2016) Growth Rates of Microbes in the Oceans. *Ann Rev Mar Sci* **8**: 285–309.

Kolodny, O., Weinberg, M., Reshef, L., Harten, L., Hefetz, A., Gophna, U., et al. (2019) Coordinated change at the colony level in fruit bat fur microbiomes through time. *Nat Ecol Evol* **3**: 116–124.

Krumhansl, K.A., Okamoto, D.K., Rassweiler, A., Novak, M., Bolton, J.J., Cavanaugh, K.C., et al. (2016) Global patterns of kelp forest change over the past half-century. **29**: 13785–13790.

Kucera, H. and Saunders, G.W. (2008) Assigning morphological variants of *Fucus* (Fucales, Phaeophyceae) in Canadian waters to recognized species using DNA barcoding. *Botany* **86**: 1065–1079.

Kueneman, J.G., Woodhams, D.C., Van Treuren, W., Archer, H.M., Knight, R., and McKenzie, V.J. (2015) Inhibitory bacteria reduce fungi on early life stages of endangered Colorado boreal toads (Anaxyrus boreas). *ISME J 2016 104* **10**: 934–944.

Kumar, V., Zozaya-Valdes, E., Kjelleberg, S., Thomas, T., and Egan, S. (2016) Multiple opportunistic pathogens can cause a bleaching disease in the red seaweed *Delisea pulchra*. *Environ Microbiol* **18**: 3962–3975.

Kwong, W.K., Medina, L.A., Koch, H., Sing, K.W., Soh, E.J.Y., Ascher, J.S., et al. (2017) Dynamic microbiome evolution in social bees. *Sci Adv* **3**:.

Lachnit, T., Fischer, M., Künzel, S., Baines, J.F., and Harder, T. (2013) Compounds associated with algal surfaces mediate epiphytic colonization of the marine macroalga *Fucus vesiculosus*. *FEMS Microbiol Ecol* **84**: 411–420.

Lachnit, T., Meske, D., Wahl, M., Harder, T., and Schmitz, R. (2011) Epibacterial community patterns on marine macroalgae are host-specific but temporally variable. *Environ Microbiol* **13**: 655–665.

Lachnit, T., Wahl, M., and Harder, T. (2010) Isolated thallus-associated compounds from the macroalga *Fucus vesiculosus* mediate bacterial surface colonization in the field similar to that on the natural alga. *Biofouling* **26**: 247–255.

Lage, O.M. and Bondoso, J. (2014) Planctomycetes and macroalgae, a striking association. *Front Microbiol* **5**: 267.

Laurin, V., Labbé, N., Parent, S., Juteau, P., and Villemur, R. (2008) Microeukaryote diversity in a marine methanol-fed fluidized denitrification system. *Microb Ecol* **56**: 637–648.

Lemay, M.A., Chen, M.Y., Mazel, F., Hind, K.R., Starko, S., Keeling, P.J., et al. (2020) Morphological complexity affects the diversity of marine microbiomes. *ISME J* 1–15.

Lemay, M.A., Davis, K.M., Martone, P.T., and Wegener Parfrey, L. (2021) Kelp-associated microbiota are structured by host anatomy. *J Phycol* jpy.13169.

Lemay, M.A., Martone, P.T., Hind, K.R., Lindstrom, S.C., and Wegener Parfrey, L. (2018) Alternate life history phases of a common seaweed have distinct microbial surface communities. *Mol Ecol* **27**: 3555–3568.

Lemay, M.A., Martone, P.T., Keeling, P.J., Burt, J.M., Krumhansl, K.A., Sanders, R.D., and Wegener Parfrey, L. (2018) Sympatric kelp species share a large portion of their surface bacterial communities. *Environ Microbiol* **20**: 658–670.

Leopold, D.R. and Busby, P.E. (2020) Host Genotype and Colonist Arrival Order Jointly Govern Plant Microbiome Composition and Function. *Curr Biol* **30**: 3260-3266.e5.

Li, J., Majzoub, M.E., Marzinelli, E.M., Dai, Z., Thomas, T., and Egan, S. (2021) Bacterial controlled mitigation of dysbiosis in a seaweed disease. *ISME J 2021* 1–10.

Li, Y.F., Chen, Y.W., Xu, J.K., Ding, W.Y., Shao, A.Q., Zhu, Y.T., et al. (2019) Temperature elevation and Vibrio cyclitrophicus infection reduce the diversity of haemolymph microbiome of the mussel Mytilus coruscus. *Sci Reports 2019 91* **9**: 1–10.

Li, Y.F., Yang, N., Liang, X., Yoshida, A., Osatomi, K., Power, D., et al. (2018) Elevated seawater temperatures decrease microbial diversity in the gut of Mytilus coruscus. *Front Physiol* **9**: 839.

Lichstein, J.W. (2006) Multiple regression on distance matrices: a multivariate spatial analysis tool. *Plant Ecol 2006 1882* **188**: 117–131.

Lin, J.D., Lemay, M.A., and Wegener Parfrey, L. (2018) Diverse Bacteria Utilize Alginate Within the Microbiome of the Giant Kelp Macrocystis pyrifera. *Front Microbiol* **9**: 1914.

Litvak, Y. and Bäumler, A.J. (2019) The founder hypothesis: A basis for microbiota resistance, diversity in taxa carriage, and colonization resistance against pathogens. *PLOS Pathog* **15**: e1007563.

Longford, S.R., Campbell, A.H., Nielsen, S., Case, R.J., Kjelleberg, S., and Steinberg, P.D. (2019) Interactions within the microbiome alter microbial interactions with host chemical defences and affect disease in a marine holobiont. *Sci Rep* **9**: 1–13.

van der Loos, L.M., Eriksson, B.K., and Falcão Salles, J. (2019) The Macroalgal Holobiont in a Changing Sea. *Trends Microbiol* **27**: 635–650.

Louca, S., Jacques, S.M.S., Pires, A.P.F., Leal, J.S., Srivastava, D.S., Parfrey, L.W., et al. (2017) High taxonomic variability despite stable functional structure across microbial communities. *Nat Ecol Evol* **1**: 15.

Louca, S., Jacques, S.M.S., Pires, A.P.F., Leal, J.S., Srivastava, D.S., Parfrey, L.W., et al. (2016) High taxonomic variability despite stable functional structure across microbial communities. *Nat Ecol Evol* **1**: 0015.

Louca, S., Parfrey, L.W., and Doebeli, M. (2016) Decoupling function and taxonomy in the global ocean microbiome. *Science* **353**: 1272–1277.

Louca, S., Polz, M.F., Mazel, F., Albright, M.B.N., Huber, J.A., O'Connor, M.I., et al. (2018) Function and functional redundancy in microbial systems. *Nat Ecol Evol* **2**: 936–943.

Lubchenco, J. (1980) Algal Zonation in the New England Rocky Intertidal Community: An Experimental Analysis. *Ecology* **61**: 333–344.

Lundberg, D.S., Yourstone, S., Mieczkowski, P., Jones, C.D., and Dangl, J.L. (2013) Practical innovations for high-throughput amplicon sequencing. *Nat Methods 2013 1010* **10**: 999–1002.

Lynch, J.B. and Hsiao, E.Y. (2019) Microbiomes as sources of emergent host phenotypes. *Science* **365**: 1405–1409.

Maignien, L., DeForce, E.A., Chafee, M.E., Murat Eren, A., and Simmons, S.L. (2014) Ecological Succession and Stochastic Variation in the Assembly of Arabidopsis thaliana Phyllosphere Communities. *MBio* **5**:.

Majzoub, M.E., Beyersmann, P.G., Simon, M., Thomas, T., Brinkhoff, T., and Egan, S. (2019) Phaeobacter inhibens controls bacterial community assembly on a marine diatom. *FEMS Microbiol Ecol* **95**: 60.

Marcelino, V.R. and Verbruggen, H. (2016) Multi-marker metabarcoding of coral skeletons reveals a rich microbiome and diverse evolutionary origins of endolithic algae. *Sci Reports 2016 61* **6**: 1–9.

Marquet, N., Nicastro, Katy R, Gektidis, Marcos, Mcquaid, Christopher D, Pearson, Gareth A, Serrão, Ester A, et al. (2013) Comparison of phototrophic shell-degrading endoliths in invasive and native populations of the intertidal mussel Mytilus galloprovincialis. *Biol Invasions* **15**: 1253–1272.

Marshall, K., Joint, I., Callow, M.E., and Callow, J.A. (2006) Effect of Marine Bacterial Isolates on the Growth and Morphology of Axenic Plantlets of the Green Alga Ulva linza. *Microb Ecol* **52**: 302–310.

Marshall, W.L. and Berbee, M.L. (2010) Population-Level Analyses Indirectly Reveal Cryptic Sex and Life History Traits of Pseudoperkinsus tapetis (Ichthyosporea, Opisthokonta): A Unicellular Relative of the Animals. *Mol Biol Evol* **27**: 2014–2026.

Martin, M. (2011) Cutadapt removes adapter sequences from high-throughput sequencing reads. *EMBnet.journal* **17**: 10–12.

Martin, M., Barbeyron, T., Martin, R., Portetelle, D., Michel, G., and Vandenbol, M. (2015) The Cultivable Surface Microbiota of the Brown Alga Ascophyllum nodosum is Enriched in Macroalgal-Polysaccharide-Degrading Bacteria. *Front Microbiol* **6**: 1487.

Martinez Arbizu, P. (2020) pairwiseAdonis: Pairwise multilevel comparison using adonis.

Marzinelli, E.M., Campbell, A.H., Zozaya Valdes, E., Vergés, A., Nielsen, S., Wernberg, T., et al. (2015) Continental-scale variation in seaweed host-associated bacterial communities is a function of host condition, not geography. *Environ Microbiol* **17**: 4078–4088.

Marzinelli, E.M., Qiu, Z., Dafforn, K.A., Johnston, E.L., Steinberg, P.D., and Mayer-Pinto, M. (2018) Coastal urbanisation affects microbial communities on a dominant marine holobiont. *npj Biofilms Microbiomes* **4**: 1–7.

Mayer Pinto, M., Bishop, M., Dethier, M., Hyndes, G.A., Huggett, M.J., Lavery, P.S., et al. (2021) Kelp-Associated Microbes Facilitate Spatial Subsidy in a Detrital-Based Food Web in a Shoreline Ecosystem.

McFall-Ngai, M.J. and Ruby, E.G. (1991) Symbiont recognition and subsequent morphogenesis as early events in an animal-bacterial mutualism. *Science* **254**: 1491–1494.

McMurdie, P.J. and Holmes, S. (2013) phyloseq: An R Package for Reproducible Interactive Analysis and Graphics of Microbiome Census Data. *PLoS One* **8**: e61217.

Meistertzheim, A.-L., Nugues, M.M., Quéré, G., and Galand, P.E. (2017) Pathobiomes Differ between Two Diseases Affecting Reef Building Coralline Algae. *Front Microbiol* **8**: 1686.

Mensch, B., Neulinger, S.C., Graiff, A., Pansch, A., Künzel, S., Fischer, M.A., and Schmitz, R.A. (2016) Restructuring of Epibacterial Communities on Fucus vesiculosus forma mytili in Response to Elevated pCO2 and Increased Temperature Levels. *Front Microbiol* **7**: 434.

Miller, A.W. and Richardson, L.L. (2015) Emerging coral diseases: a temperature-driven process? *Mar Ecol* **36**: 278–291.

Minich, J.J., Morris, M.M., Brown, M., Doane, M., Edwards, M.S., Michael, T.P., and Dinsdale, E.A. (2018) Elevated temperature drives kelp microbiome dysbiosis, while elevated carbon dioxide induces water microbiome disruption. *PLoS One* **13**: e0192772.

Morris, M.M., Haggerty, J.M., Papudeshi, B.N., Vega, A.A., Edwards, M.S., and Dinsdale, E.A. (2016) Nearshore pelagic microbial community abundance affects recruitment success of giant kelp, Macrocystis pyrifera. *Front Microbiol* **7**: 1800.

Moulton, O.M., Altabet, M.A., Beman, J.M., Deegan, L.A., Lloret, J., Lyons, M.K., et al. (2016) Microbial associations with macrobiota in coastal ecosystems: patterns and implications for nitrogen cycling. *Front Ecol Environ* **14**: 200–208.

Mueller, R., Fischer, A.M., Bolch, C.J.S., and Wright, J.T. (2015) Environmental correlates of phenotypic variation: do variable tidal regimes influence morphology in intertidal seaweeds? *J Phycol* **51**: 859–871.

Musella, M., Wathsala, R., Tavella, T., Rampelli, S., Barone, M., Palladino, G., et al. (2020) Tissue-scale microbiota of the Mediterranean mussel (Mytilus galloprovincialis) and its relationship with the environment. *Sci Total Environ* **717**: 137209.

Nappi, J., Goncalves, P., Khan, T., Majzoub, M.E., Grobler, A.S., Marzinelli, E.M., et al. (2022) Differential priority effects impact taxonomy and functionality of host-associated microbiomes. *Mol Ecol*.

Nasrolahi, A., Stratil, S.B., Jacob, K.J., and Wahl, M. (2012) A protective coat of microorganisms on macroalgae: inhibitory effects of bacterial biofilms and epibiotic microbial assemblages on barnacle attachment. *FEMS Microbiol Ecol* **81**: 583–595.

Ndhlovu, A., McQuaid, C.D., Nicastro, K.R., and Zardi, G.I. (2021) Community succession in phototrophic shell-degrading endoliths attacking intertidal mussels. *J Molluscan Stud* **87**: 36.

Neu, A.T., Allen, E.E., and Roy, K. (2021) Do host-associated microbes show a contrarian latitudinal diversity gradient? Insights from Mytilus californianus, an intertidal foundation host. *J Biogeogr* **48**: 2839–2852.

Neu, A.T., Hughes, I. V., Allen, E.E., and Roy, K. (2021) Decade-scale stability and change in a marine bivalve microbiome. *Mol Ecol* **30**: 1237–1250.

Noisette, F. and Hurd, C. (2018) Abiotic and biotic interactions in the diffusive boundary layer of kelp blades create a potential refuge from ocean acidification. *Funct Ecol* **32**: 1329–1342.

Nyholm, S. V. and McFall-Ngai, M.J. (2021) A lasting symbiosis: how the Hawaiian bobtail squid finds and keeps its bioluminescent bacterial partner. *Nat Rev Microbiol 2021 1910* **19**: 666–679.

O'Connor, M.I., Griffiths, G., Sanders-Smith, R., Hessing-Lewis, M., Davis, K.M., Forbes, C., et al. (2022) A reciprocal transplant experiment sheds new light on a classic marine seagrass-

algal symbiosis and suggests influence of epiphytic symbiont on seagrass microbiota. *Aquat Bot* 103511.

Offret, C., Paulino, S., Gauthier, O., Chateau, K., Bidault, A., Corporeau, C., et al. (2020) The marine intertidal zone shapes oyster and clam digestive bacterial microbiota. *FEMS Microbiol Ecol* **96**: 78.

Okamoto, N., Keeling, P.J., Leander, B.S., and Tai, V. (2022) Microbial communities in sandy beaches from the three domains of life differ by microhabitat and intertidal location. *Mol Ecol* **31**: 3210–3227.

Oksanen, J., Blanchet, F.G., Friendly, M., Kindt, R., Legendre, P., Mcglinn, D., et al. (2019) vegan: Community Ecology Package.

de Oliveira, L.S., Tschoeke, D.A., Magalhães Lopes, A.C.R., Sudatti, D.B., Meirelles, P.M., Thompson, C.C., et al. (2017) Molecular Mechanisms for Microbe Recognition and Defense by the Red Seaweed *Laurencia dendroidea*. *mSphere* **2**: e00094-17.

van Oppen, M.J.H. and Blackall, L.L. (2019) Coral microbiome dynamics, functions and design in a changing world. *Nat Rev Microbiol 2019 179* **17**: 557–567.

Paine, R.T. (1966) Food Web Complexity and Species Diversity. *Am Nat* **100**: 65–75.

Paine, R.T. (1974) Intertidal community structure : Experimental studies on the relationship between a dominant competitor and its principal predator. *Oecologia* **15**: 93–120.

Paix, B., Carriot, N., Barry-Martinet, R., Greff, S., Misson, B., Briand, J.F., and Culioli, G. (2020) A Multi-Omics Analysis Suggests Links Between the Differentiated Surface Metabolome and Epiphytic Microbiota Along the Thallus of a Mediterranean Seaweed Holobiont. *Front Microbiol* **11**: 494.

Paix, B., Othmani, A., Debroas, D., Culioli, G., and Briand, J.F. (2019) Temporal covariation of epibacterial community and surface metabolome in the Mediterranean seaweed holobiont Taonia atomaria. *Environ Microbiol* **21**: 3346–3363.

Palinska, K.A., Abed, R.M.M., Vogt, J.C., Radtke, G., and Golubic, S. (2017) Microbial Endoliths on East Adriatic Limestone Coast: Morphological vs. Molecular Diversity. *http://dx.doi.org/101080/0149045120171297512* **34**: 903–915.

Pantos, O., Bongaerts, P., Dennis, P.G., Tyson, G.W., and Hoegh-Guldberg, O. (2015) Habitat-specific environmental conditions primarily control the microbiomes of the coral Seriatopora hystrix. *ISME J* **9**: 1916–1927.

Parada, A.E., Needham, D.M., and Fuhrman, J.A. (2016) Every base matters: assessing small subunit rRNA primers for marine microbiomes with mock communities, time series and

global field samples. *Environ Microbiol* **18**: 1403–1414.

Parrot, D., Blümel, M., Utermann, C., Chianese, G., Krause, S., Kovalev, A., et al. (2019) Mapping the Surface Microbiome and Metabolome of Brown Seaweed Fucus vesiculosus by Amplicon Sequencing, Integrated Metabolomics and Imaging Techniques. *Sci Rep* **9**: 1–17.

Pavia, H., Toth, G.B., Lindgren, A., and Åberg, P. (2003) Intraspecific variation in the phlorotannin content of the brown alga Ascophyllum nodosum. *Phycologia* **42**: 378–383.

Pearson, Gareth A, Hoarau, Galice, Lago-Leston, Asuncion, Coyer, James A, Kube, Michael, Reinhardt, R., et al. (2010) An Expressed Sequence Tag Analysis of the Intertidal Brown Seaweeds Fucus serratus (L.) and F. vesiculosus (L.) (Heterokontophyta, Phaeophyceae) in Response to Abiotic Stressors. *Mar Biotechnol* **12**: 195–213.

Pernice, M., Raina, J.B., Rädecker, N., Cárdenas, A., Pogoreutz, C., and Voolstra, C.R. (2019) Down to the bone: the role of overlooked endolithic microbiomes in reef coral health. *ISME J 2019 142* **14**: 325–334.

Pfister, C.A. (2007) Intertidal invertebrates locally enhance primary production. *Ecology* **88**: 1647–1653.

Pfister, C.A. and Altabet, M.A. (2019) Enhanced microbial nitrogen transformations in association with macrobiota from the rocky intertidal. *Biogeosciences* **16**: 193–206.

Pfister, C.A., Altabet, M.A., and Weigel, B.L. (2019) Kelp beds and their local effects on seawater chemistry, productivity, and microbial communities. *Ecology* **100**: e02798.

Pfister, C.A., Gilbert, J.A., and Gibbons, S.M. (2014) The role of macrobiota in structuring microbial communities along rocky shores. *PeerJ* **2014**: e631.

Phelps, C.M., McMahon, K., Bissett, A., Bernasconi, R., Steinberg, P.D., Thomas, T., et al. (2021) The surface bacterial community of an Australian kelp shows cross-continental variation and relative stability within regions. *FEMS Microbiol Ecol* **97**:.

Pierce, M.L. and Ward, J.E. (2019) Gut Microbiomes of the Eastern Oyster (Crassostrea virginica) and the Blue Mussel (Mytilus edulis): Temporal Variation and the Influence of Marine Aggregate-Associated Microbial Communities . *mSphere* **4**:.

Place, S.P., Menge, B.A., and Hofmann, G.E. (2012) Transcriptome profiles link environmental variation and physiological response of Mytilus californianus between Pacific tides. *Funct Ecol* **26**: 144–155.

Pollock, F.J., McMinds, R., Smith, S., Bourne, D.G., Willis, B.L., Medina, M., et al. (2018) Coral-associated bacteria demonstrate phylosymbiosis and cophylogeny. *Nat Commun* **9**: 1–

13.

Posadas, N., Baquiran, J.I.P., Nada, M.A.L., Kelly, M., and Conaco, C. (2021) Microbiome diversity and host immune functions influence survivorship of sponge holobionts under future ocean conditions. *ISME J 2021 161* **16**: 58–67.

Pratte, Z.A., Patin, N. V., McWhirt, M.E., Caughman, A.M., Parris, D.J., and Stewart, F.J. (2018) Association with a sea anemone alters the skin microbiome of clownfish. *Coral Reefs* **37**: 1119–1125.

Qiu, Z., Coleman, M.A., Provost, E., Campbell, A.H., Kelaher, B.P., Dalton, S.J., et al. (2019) Future climate change is predicted to affect the microbiome and condition of habitat-forming kelp. *Proc R Soc B Biol Sci* **286**: 20181887.

Quast, C., Pruesse, E., Yilmaz, P., Gerken, J., Schweer, T., Yarza, P., et al. (2013) The SILVA ribosomal RNA gene database project: improved data processing and web-based tools. *Nucleic Acids Res* **41**: D590–D596.

Quigley, C.T.C., Capistrant-Fossa, K.A., Morrison, H.G., Johnson, L.E., Morozov, A., Hertzberg, V.S., and Brawley, S.H. (2020) Bacterial Communities Show Algal Host (Fucus spp.)/Zone Differentiation Across the Stress Gradient of the Intertidal Zone. *Front Microbiol* **11**: 2256.

R Core Team (2019) R: A language and environment for statistical computing.

Raimundo, I., Silva, R., Meunier, L., Valente, S.M., Lago-Lestón, A., Keller-Costa, T., and Costa, R. (2021) Functional metagenomics reveals differential chitin degradation and utilization features across free-living and host-associated marine microbiomes. *Microbiome* **9**: 1–18.

Ramírez-Puebla, S.T., Weigel, B.L., Jack, L., Schlundt, C., Pfister, C.A., and Mark Welch, J.L. (2022) Spatial organization of the kelp microbiome at micron scales. *Microbiome* **10**: 52.

Rao, D., Webb, J.S., and Kjelleberg, S. (2006) Microbial colonization and competition on the marine alga Ulva australis. *Appl Environ Microbiol* **72**: 5547–5555.

Redmond, S., Green, L., Yarish, C., Kim, J., and Neefus, C. (2014) New England Seaweed Culture Handbook. *Seaweed Cultiv*.

Rickert, E., Lenz, M., Barboza, F.R., Gorb, S.N., and Wahl, M. (2016) Seasonally fluctuating chemical microfouling control in Fucus vesiculosus and Fucus serratus from the Baltic Sea. *Mar Biol* **163**: 203.

Rickert, Esther, Wahl, M., Link, H., Richter, H., and Pohnert, G. (2016) Seasonal Variations in Surface Metabolite Composition of Fucus vesiculosus and Fucus serratus from the Baltic

Sea. *PLoS One* **11**: e0168196.

Risely, A. (2020) Applying the core microbiome to understand host–microbe systems. *J Anim Ecol* **89**: 1549–1558.

Robbins, S.J., Song, W., Engelberts, J.P., Glasl, B., Slaby, B.M., Boyd, J., et al. (2021) A genomic view of the microbiome of coral reef demosponges. *ISME J 2021 156* **15**: 1641–1654.

Rohde, S., Molis, M., and Wahl, M. (2004) Regulation of anti-herbivore defence by Fucus vesiculosus in response to various cues. *J Ecol* **92**: 1011–1018.

Rosado, P.M., Leite, D.C.A., Duarte, G.A.S., Chaloub, R.M., Jospin, G., Nunes da Rocha, U., et al. (2019) Marine probiotics: increasing coral resistance to bleaching through microbiome manipulation. *ISME J* **13**: 921–936.

Rosenfeld, J.S. (2002) Functional redundancy in ecology and conservation. *Oikos* **98**: 156–162.

Roth-Schulze, A.J., Pintado, J., Zozaya-Valdés, E., Cremades, J., Ruiz, P., Kjelleberg, S., and Thomas, T. (2018) Functional biogeography and host specificity of bacterial communities associated with the Marine Green Alga *Ulva* spp. *Mol Ecol* **27**: 1952–1965.

Roth-Schulze, A.J., Zozaya-Valdés, E., Steinberg, P.D., and Thomas, T. (2016) Partitioning of functional and taxonomic diversity in surface-associated microbial communities. *Environ Microbiol* **18**: 4391–4402.

Rothrock, M.J. and Garcia-Pichel, F. (2005) Microbial diversity of benthic mats along a tidal desiccation gradient. *Environ Microbiol* **7**: 593–601.

Rubiolo, J.A., Botana, L.M., and Martínez, P. (2019) Insights into Mussel Microbiome. In *Microbial Communities in Aquaculture Ecosystems*. Springer International Publishing, pp. 95–120.

Sacristán-Soriano, O., Winkler, M., Erwin, P., Weisz, J., Harriott, O., Heussler, G., et al. (2019) Ontogeny of symbiont community structure in two carotenoid-rich, viviparous marine sponges: comparison of microbiomes and analysis of culturable pigmented heterotrophic bacteria. *Environ Microbiol Rep* **11**: 249–261.

Saha, M., Ferguson, R.M.W., Dove, S., Künzel, S., Meichssner, R., Neulinger, S.C., et al. (2020) Salinity and Time Can Alter Epibacterial Communities of an Invasive Seaweed. *Front Microbiol* **10**: 2870.

Saha, M., Rempt, M., Grosser, K., Pohnert, G., and Weinberger, F. (2011a) Surface-associated fucoxanthin mediates settlement of bacterial epiphytes on the rockweed Fucus vesiculosus. *Biofouling* **27**: 423–433.

Saha, M., Rempt, M., Grosser, K., Pohnert, G., and Weinberger, F. (2011b) Surface-associated fucoxanthin mediates settlement of bacterial epiphytes on the rockweed *Fucus vesiculosus*. *Biofouling* **27**: 423–433.

Saha, M., Rempt, M., Stratil, S.B., Wahl, M., Pohnert, G., and Weinberger, F. (2014) Defence Chemistry Modulation by Light and Temperature Shifts and the Resulting Effects on Associated Epibacteria of Fucus vesiculosus. *PLoS One* **9**: e105333.

Saha, M. and Wahl, M. (2013) Seasonal variation in the antifouling defence of the temperate brown alga Fucus vesiculosus. *Biofouling* **29**: 661–668.

Saha, M. and Weinberger, F. (2019) Microbial "gardening" by a seaweed holobiont: Surface metabolites attract protective and deter pathogenic epibacterial settlement. *J Ecol* **107**: 2255–2265.

Säwström, C., Hyndes, G.A., Eyre, B.D., Huggett, M.J., Fraser, M.W., Lavery, P.S., et al. (2016) Coastal connectivity and spatial subsidy from a microbial perspective. *Ecol Evol* **6**: 6662–6671.

Schellenberg, L. and Clarke, L.J. (2020) Spatial structure of marine host-associated microbiomes: effect of taxonomy, species traits, and study design. *Front Mar Sci* **7**: 146.

Schiel, D.R. and Foster, M.S. (2006) The Population Biology of Large Brown Seaweeds: Ecological Consequences of Multiphase Life Histories in Dynamic Coastal Environments. *http://dx.doi.org/101146/annurev.ecolsys37091305110251* **37**: 343–372.

Schiener, P., Black, K.D., Stanley, M.S., and Green, D.H. (2015) The seasonal variation in the chemical composition of the kelp species Laminaria digitata, Laminaria hyperborea, Saccharina latissima and Alaria esculenta. *J Appl Phycol* **27**: 363–373.

Schonbeck, M. and Norton, T.A. (1978) Factors controlling the upper limits of fucoid algae on the shore. *J Exp Mar Bio Ecol* **31**: 303–313.

Schultz-Johansen, M., Bech, P.K., Hennessy, R.C., Glaring, M.A., Barbeyron, T., Czjzek, M., and Stougaard, P. (2018) A Novel Enzyme portfolio for red algal polysaccharide degradation in the marine bacterium Paraglaciecola hydrolytica S66T encoded in a sizeable polysaccharide utilization locus. *Front Microbiol* **9**: 839.

Scott, G.W., Hull, S.L., Hornby, S.E., Hardy, F.G., and Owens, N.J.P. (2001) Phenotypic variation in Fucus spiralis (Phaeophyceae): Morphology, chemical phenotype and their relationship to the environment. *Eur J Phycol* **36**: 43–50.

Serebryakova, A., Aires, T., Viard, F., Serrão, E.A., and Engelen, A.H. (2018) Summer shifts of bacterial communities associated with the invasive brown seaweed Sargassum muticum are

location and tissue dependent. *PLoS One* **13**: e0206734.

Sessitsch, A., Pfaffenbichler, N., and Mitter, B. (2019) Microbiome Applications from Lab to Field: Facing Complexity. *Trends Plant Sci* **24**: 194–198.

Seuront, L., Nicastro, K.R., Zardi, G.I., and Goberville, E. (2019) Decreased thermal tolerance under recurrent heat stress conditions explains summer mass mortality of the blue mussel Mytilus edulis. *Sci Reports 2019 91* **9**: 1–14.

Shade, A. and Handelsman, J. (2012) Beyond the Venn diagram: The hunt for a core microbiome. *Environ Microbiol* **14**: 4–12.

Shade, A., Peter, H., Allison, S.D., Baho, D.L., Berga, M., Bürgmann, H., et al. (2012) Fundamentals of microbial community resistance and resilience. *Front Microbiol* **3**: 417.

Sharp, K.H., Pratte, Z.A., Kerwin, A.H., Rotjan, R.D., and Stewart, F.J. (2017) Season, but not symbiont state, drives microbiome structure in the temperate coral Astrangia poculata. *Microbiome* **5**: 120.

Sieburth, J.M. and Tootle, J.L. (1981) Seasonality of microbial fouling on Ascophyllum nodosum (L.) Lejol., Fucus vesiculosus (L.), Polysiphonia lanosa (L.) Tandy and Chondrus cripus Stackh. *J Phycol* **17**: 57–64.

Simon, M., Scheuner, C., Meier-Kolthoff, J.P., Brinkhoff, T., Wagner-Döbler, I., Ulbrich, M., et al. (2017) Phylogenomics of Rhodobacteraceae reveals evolutionary adaptation to marine and non-marine habitats. **11**: 1483–1499.

Singh, R.P., Kumari, P., and Reddy, C.R.K. (2015) Antimicrobial compounds from seaweeds-associated bacteria and fungi. *Appl Microbiol Biotechnol* **99**: 1571–1586.

Smale, D.A. and Wernberg, T. (2013) Extreme climatic event drives range contraction of a habitat-forming species. *Proc R Soc B Biol Sci* **280**:.

Starko, S., Mansfield, S.D., and Martone, P.T. (2018) Cell wall chemistry and tissue structure underlie shifts in material properties of a perennial kelp. *Eur J Phycol* **53**: 307–317.

Stone, B.W.G. and Jackson, C.R. (2021) Seasonal Patterns Contribute More Towards Phyllosphere Bacterial Community Structure than Short-Term Perturbations. *Microb Ecol* **81**: 146–156.

Stopnisek, N. and Shade, A. (2021) Persistent microbiome members in the common bean rhizosphere: an integrated analysis of space, time, and plant genotype. *ISME J* 1–15.

Stratil, S.B., Neulinger, S.C., Knecht, H., Friedrichs, A.K., and Wahl, M. (2013) Temperature-driven shifts in the epibiotic bacterial community composition of the brown macroalga

Fucus vesiculosus. *Microbiologyopen* **2**: 338–349.

Sunagawa, S., Coelho, L.P., Chaffron, S., Kultima, J.R., Labadie, K., Salazar, G., et al. (2015) Structure and function of the global ocean microbiome. *Science* **348**:.

Sweet, M.J. and Bulling, M.T. (2017) On the Importance of the Microbiome and Pathobiome in Coral Health and Disease. *Front Mar Sci* **4**: 9.

Tamames, J. and Puente-Sánchez, F. (2019) SqueezeMeta, a highly portable, fully automatic metagenomic analysis pipeline. *Front Microbiol* **10**: 3349.

Tan, T.T., Song, S.L., Poong, S.W., Ward, G.M., Brodie, J., and Lim, P.E. (2020) The effect of grazing on the microbiome of two commercially important agarophytes, Gracilaria firma and G. salicornia (Gracilariaceae, Rhodophyta). *J Appl Phycol* **32**: 2549–2559.

Tapia, J.E., González, B., Goulitquer, S., Potin, P., and Correa, J.A. (2016) Microbiota Influences Morphology and Reproduction of the Brown Alga Ectocarpus sp. *Front Microbiol* **7**: 197.

Tarquinio, F., Bourgoure, J., Koenders, A., Laverock, B., Säwström, C., and Hyndes, G.A. (2018) Microorganisms facilitate uptake of dissolved organic nitrogen by seagrass leaves. *ISME J 2018 1211* **12**: 2796–2800.

Teagle, H., Hawkins, S.J., Moore, P.J., and Smale, D.A. (2017) The role of kelp species as biogenic habitat formers in coastal marine ecosystems. *J Exp Mar Bio Ecol* **492**: 81–98.

Thomas, T., Moitinho-Silva, L., Lurgi, M., Björk, J.R., Easson, C., Astudillo-García, C., et al. (2016) Diversity, structure and convergent evolution of the global sponge microbiome. *Nat Commun 2016 71* **7**: 1–12.

Thompson, L.R., Sanders, J.G., McDonald, D., Amir, A., Ladau, J., Locey, K.J., et al. (2017) A communal catalogue reveals Earth's multiscale microbial diversity. *Nature* **551**: 457–463.

Trevathan-Tackett, S.M., Sherman, C.D.H., Huggett, M.J., Campbell, A.H., Laverock, B., Hurtado-McCormick, V., et al. (2019) A horizon scan of priorities for coastal marine microbiome research. *Nat Ecol Evol* **3**: 1509–1520.

Ugarelli, K., Chakrabarti, S., Laas, P., and Stingl, U. (2017) The Seagrass Holobiont and Its Microbiome. *Microorganisms* **5**: 81.

Uren Webster, T.M., Rodriguez-Barreto, D., Castaldo, G., Gough, P., Consuegra, S., and Garcia de Leaniz, C. (2020) Environmental plasticity and colonisation history in the Atlantic salmon microbiome: A translocation experiment. *Mol Ecol* **29**: 886–898.

Vezzulli, L., Stagnaro, L., Grande, C., Tassistro, G., Canesi, L., and Pruzzo, C. (2018)

Comparative 16SrDNA Gene-Based Microbiota Profiles of the Pacific Oyster (Crassostrea gigas) and the Mediterranean Mussel (Mytilus galloprovincialis) from a Shellfish Farm (Ligurian Sea, Italy). *Microb Ecol* **75**: 495–504.

Vollmers, J., Frentrup, M., Rast, P., Jogler, C., and Kaster, A.-K. (2017) Untangling Genomes of Novel Planctomycetal and Verrucomicrobial Species from Monterey Bay Kelp Forest Metagenomes by Refined Binning. *Front Microbiol* **8**: 472.

Voolstra, C.R. and Ziegler, M. (2020) Adapting with Microbial Help: Microbiome Flexibility Facilitates Rapid Responses to Environmental Change. *BioEssays* **42**: 2000004.

Wagner, M.R. (2021) Prioritizing host phenotype to understand microbiome heritability in plants. *New Phytol* **232**: 502–509.

Wahl, M., Jormalainen, V., Eriksson, B.K., Coyer, J.A., Molis, M., Schubert, H., et al. (2011) Stress Ecology in Fucus: Abiotic, Biotic and Genetic Interactions. In *Advances in marine biology*. pp. 37–105.

Walsh, C.M., Becker-Uncapher, I., Carlson, M., and Fierer, N. (2021) Variable influences of soil and seed-associated bacterial communities on the assembly of seedling microbiomes. *ISME J 2021 159* **15**: 2748–2762.

Wang, L., English, M.K., Tomas, F., and Muellera, R.S. (2021) Recovery and Community Succession of the Zostera Marina Rhizobiome after Transplantation. *Appl Environ Microbiol* **87**: 1–16.

Wang, Z., Tsementzi, D., Williams, T.C., Juarez, D.L., Blinebry, S.K., Garcia, N.S., et al. (2020) Environmental stability impacts the differential sensitivity of marine microbiomes to increases in temperature and acidity. *ISME J* 1–10.

Ward, C.S., Yung, C.M., Davis, K.M., Blinebry, S.K., Williams, T.C., Johnson, Z.I., and Hunt, D.E. (2017) Annual community patterns are driven by seasonal switching between closely related marine bacteria. *ISME J* **11**: 1412–1422.

Weigel, B.L. and Erwin, P.M. (2017) Effects of reciprocal transplantation on the microbiome and putative nitrogen cycling functions of the intertidal sponge, Hymeniacidon heliophila. *Sci Rep* **7**: 1–12.

Weigel, B.L. and Erwin, P.M. (2016) Intraspecific variation in microbial symbiont communities of the sun sponge, Hymeniacidon heliophila, from intertidal and subtidal habitats. *Appl Environ Microbiol* **82**: 650–658.

Weigel, B.L. and Pfister, C.A. (2020) Oxygen metabolism shapes microbial settlement on photosynthetic kelp blades compared to artificial kelp substrates. *Environ Microbiol Rep*

1758-2229.12923.

Weigel, B.L. and Pfister, C.A. (2019) Successional Dynamics and Seascape-Level Patterns of Microbial Communities on the Canopy-Forming Kelps Nereocystis luetkeana and Macrocystis pyrifera. *Front Microbiol* **10**: 346.

Wickham, H. (2016) ggplot2: elegant graphics for data analysis, springer.

Wiese, J., Thiel, V., Nagel, K., Staufenberger, T., and Imhoff, J.F. (2009) Diversity of antibiotic-active bacteria associated with the brown alga Laminaria saccharina from the Baltic Sea. *Mar Biotechnol* **11**: 287–300.

Wilkins, L.G.E., Leray, M., O'Dea, A., Yuen, B., Peixoto, R.S., Pereira, T.J., et al. (2019) Host-associated microbiomes drive structure and function of marine ecosystems. *PLoS Biol* **17**: e3000533.

Wood, G., Marzinelli, E.M., Coleman, M.A., Campbell, A.H., Santini, N.S., Kajlich, L., et al. (2019) Restoring subtidal marine macrophytes in the Anthropocene: trajectories and future-proofing. *Mar Freshw Res* **70**: 936–951.

Wood, G., Steinberg, P.D., Campbell, A.H., Vergés, A., Coleman, M.A., Marzinelli, E.M., and Russell, J. (2022) Host genetics, phenotype and geography structure the microbiome of a foundational seaweed. *Mol Ecol* **00**: 1–18.

Woodhams, D.C., Bletz, M.C., Becker, C.G., Bender, H.A., Buitrago-Rosas, D., Diebboll, H., et al. (2020) Host-associated microbiomes are predicted by immune system complexity and climate. **21**: 1–20.

Woznica, A. and King, N. (2018) Lessons from simple marine models on the bacterial regulation of eukaryotic development. *Curr Opin Microbiol* **43**: 108–116.

Wright, J.T., Williams, S.L., and Dethier, M.N. (2004) No zone is always greener: Variation in the performance of Fucus gardneri embryos, juveniles and adults across tidal zone and season. *Mar Biol* **145**: 1061–1073.

Wu, S., Ou, H., Liu, T., Wang, D., and Zhao, J. (2018) Structure and dynamics of microbiomes associated with the marine sponge Tedania sp. during its life cycle. *FEMS Microbiol Ecol* **94**: 55.

Yoshitake, K., Kimura, G., Sakami, T., Watanabe, T., Taniuchi, Y., Kakehi, S., et al. (2021) Development of a time-series shotgun metagenomics database for monitoring microbial communities at the Pacific coast of Japan. *Sci Reports 2021 111* **11**: 1–13.

Yung, C.M., Vereen, M.K., Herbert, A., Davis, K.M., Yang, J., Kantorowska, A., et al. (2015) Thermally adaptive tradeoffs in closely related marine bacterial strains. *Environ Microbiol*

17: 2421–2429.

Zardi, G.I., Nicastro, K.R., McQuaid, C.D., and Gektidis, M. (2009) Effects of Endolithic Parasitism on Invasive and Indigenous Mussels in a Variable Physical Environment. **4**:.

Zardi, G.I., Nicastro, K.R., Mcquaid, C.D., Ng, T.P.T., Lathlean, J., and Seuront, L. (2016) Enemies with benefits: parasitic endoliths protect mussels against heat stress. *Sci Rep* **6**: 1–8.

Zhang, F., Jonas, L., Lin, H., and Hill, R.T. (2019) Microbially mediated nutrient cycles in marine sponges. *FEMS Microbiol Ecol* **95**: 155.

Zhang, R., Chang, L., Xiao, L., Zhang, X., Han, Q., Li, N., et al. (2020) Diversity of the epiphytic bacterial communities associated with commercially cultivated healthy and diseased Saccharina japonica during the harvest season. *J Appl Phycol* **32**: 2071–2080.

Zhang, Ying, Yang, Q., Ling, J., Long, L., Huang, H., Yin, J., et al. (2021) Shifting the microbiome of a coral holobiont and improving host physiology by inoculation with a potentially beneficial bacterial consortium. *BMC Microbiol* **21**: 1–14.

Ziegler, M., Grupstra, C.G.B., Barreto, M.M., Eaton, M., BaOmar, J., Zubier, K., et al. (2019) Coral bacterial community structure responds to environmental change in a host-specific manner. *Nat Commun* **10**: 1–11.

Ziegler, M., Seneca, F.O., Yum, L.K., Palumbi, S.R., and Voolstra, C.R. (2017) Bacterial community dynamics are linked to patterns of coral heat tolerance. *Nat Commun* **8**:.

Zozaya-Valdes, E., Egan, S., and Thomas, T. (2015a) A comprehensive analysis of the microbial communities of healthy and diseased marine macroalgae and the detection of known and potential bacterial pathogens. *Front Microbiol* **6**: 146.

Zozaya-Valdes, E., Egan, S., and Thomas, T. (2015b) A comprehensive analysis of the microbial communities of healthy and diseased marine macroalgae and the detection of known and potential bacterial pathogens. *Front Microbiol* **6**: 146.

Zozaya-Valdés, E., Roth-Schulze, A.J., Egan, S., and Thomas, T. (2017) Microbial community function in the bleaching disease of the marine macroalgae *Delisea pulchra*. *Environ Microbiol* **19**: 3012–3024.

Appendices

Appendix A - Chapter 2: Supplementary Information

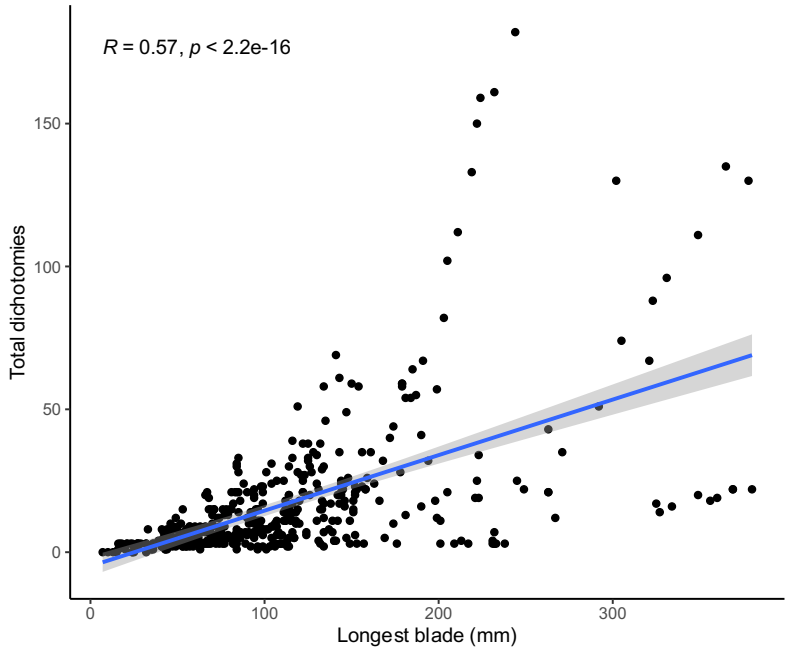

Appendix A - Figure 1. Correlation between length of the longest blade (mm) and total dichotomies for measured individuals in the *Fucus distichus* population.

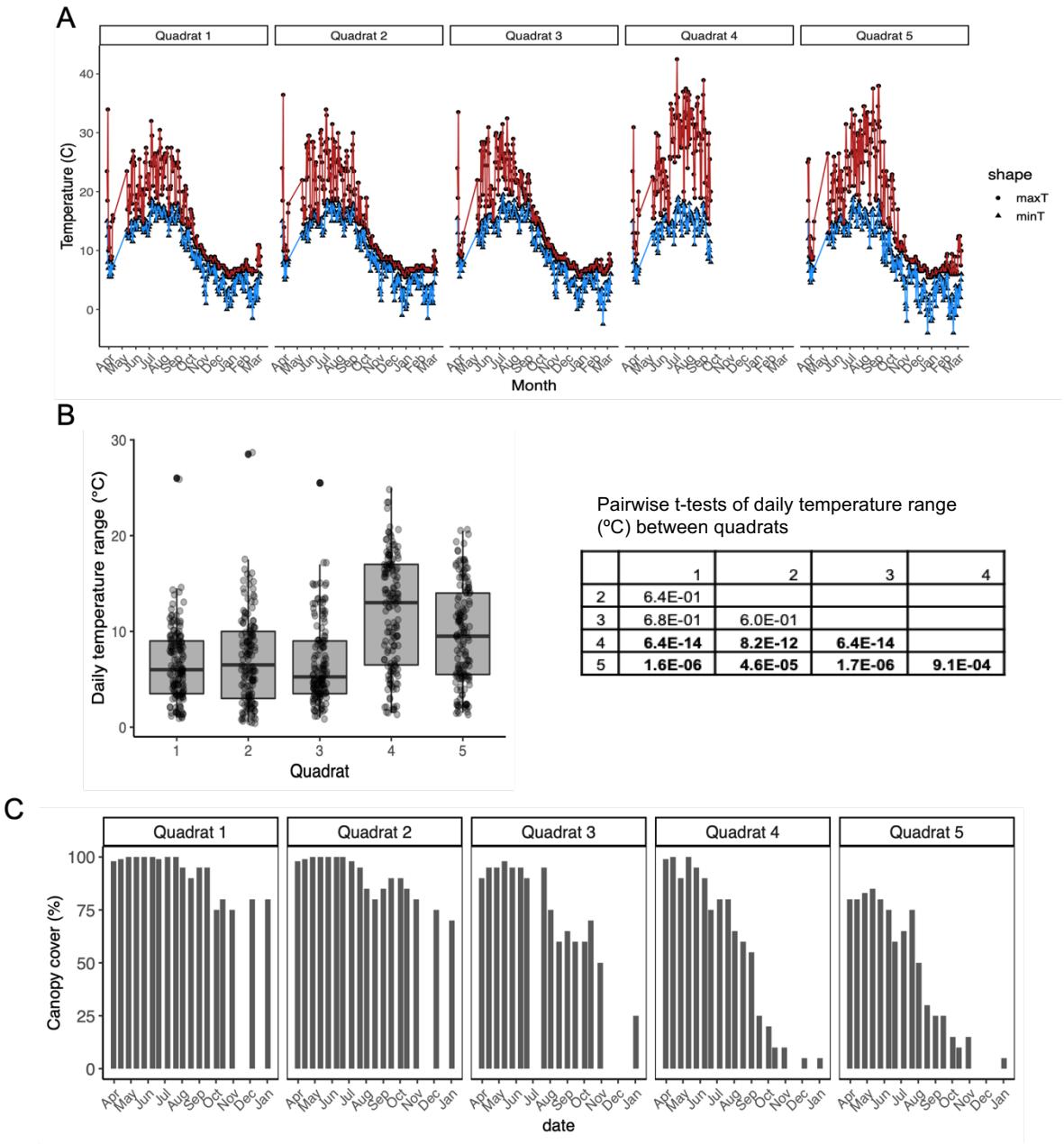

	1	2	3	4
2	6.4E-01			
3	6.8E-01	6.0E-01		
4	**6.4E-14**	**8.2E-12**	**6.4E-14**	
5	**1.6E-06**	**4.6E-05**	**1.7E-06**	**9.1E-04**

Appendix A - Figure 2. Variability in temperature and host canopy cover over time among quadrats.

A) Seasonality in maximum and minimum daily temperature values recorded by iButton temperature loggers in each quadrat. B) Summary of daily temperature ranges and table of p-values from pairwise t-tests between quadrats with significant differences in bold. C) Percent *F. distichus* canopy cover in each quadrat over time.

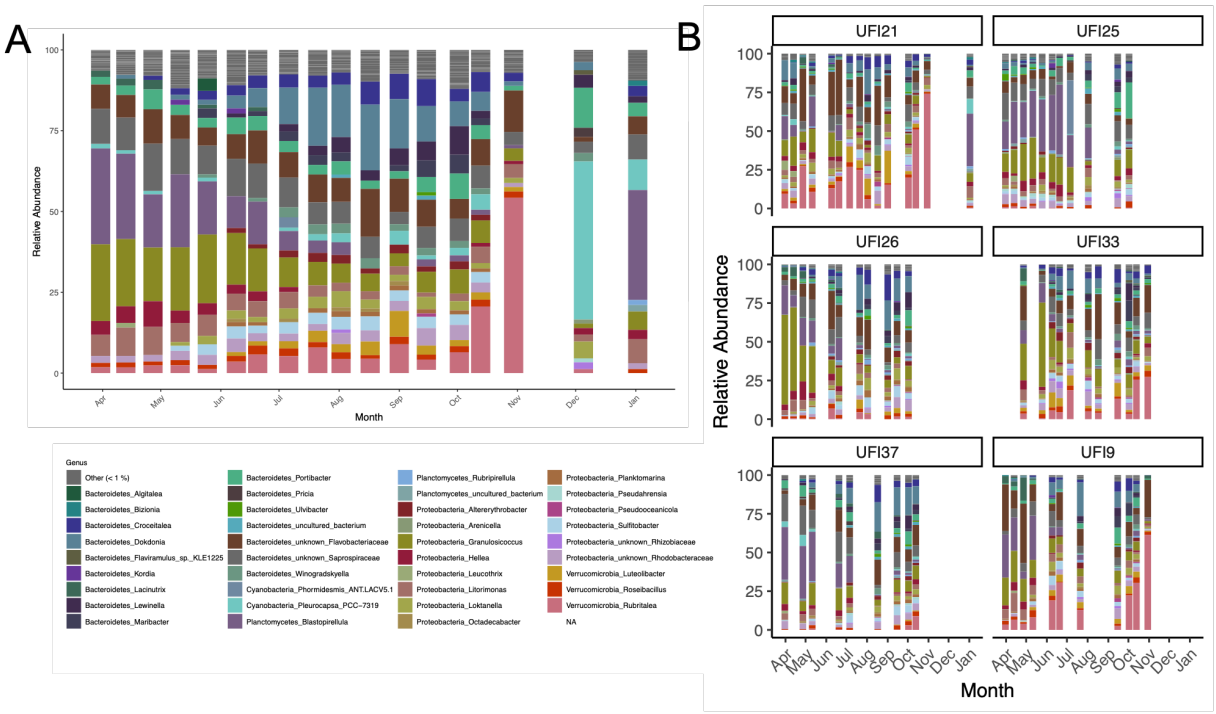

Appendix A - Figure 3. Relative abundance of dominant bacteria genera over time on *Fucus distichus.* Barplots are summarized A) across the population at each timepoint and B) on focal individuals over time.

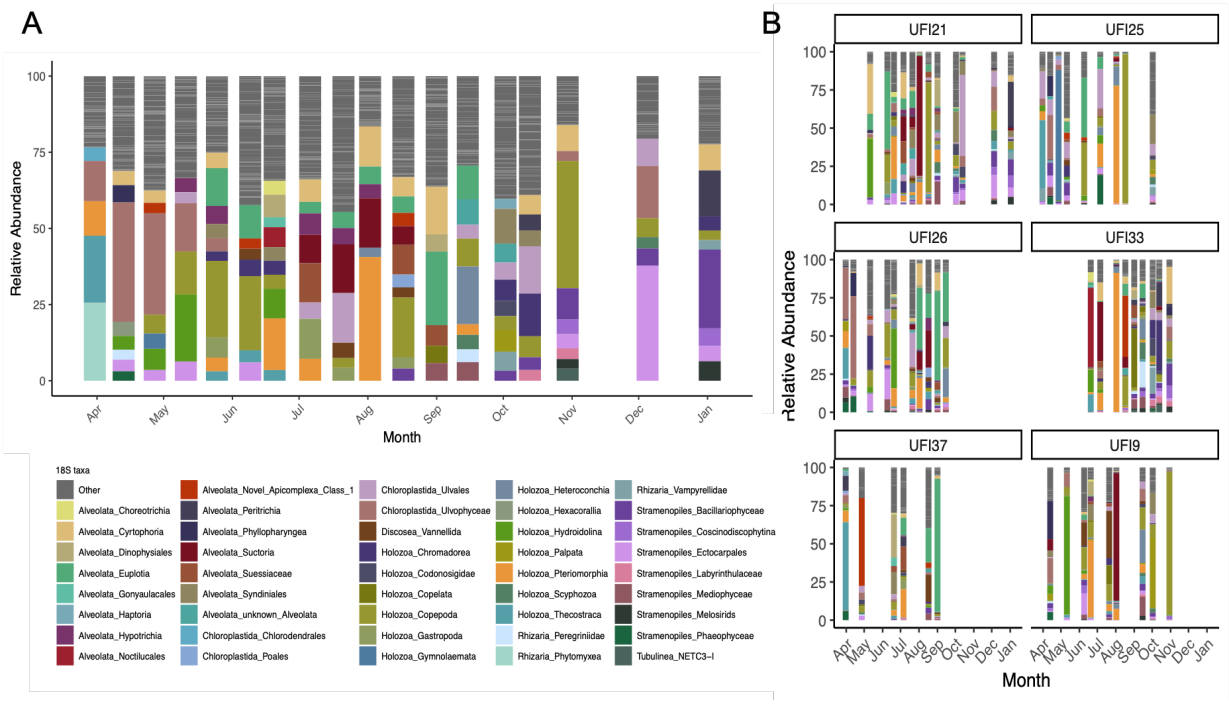

Appendix A - Figure 4. Relative abundance of dominant eukaryote taxa over time on *Fucus distichus*. Barplots are summarized A) across the population at each timepoint and B) on focal individuals over time.

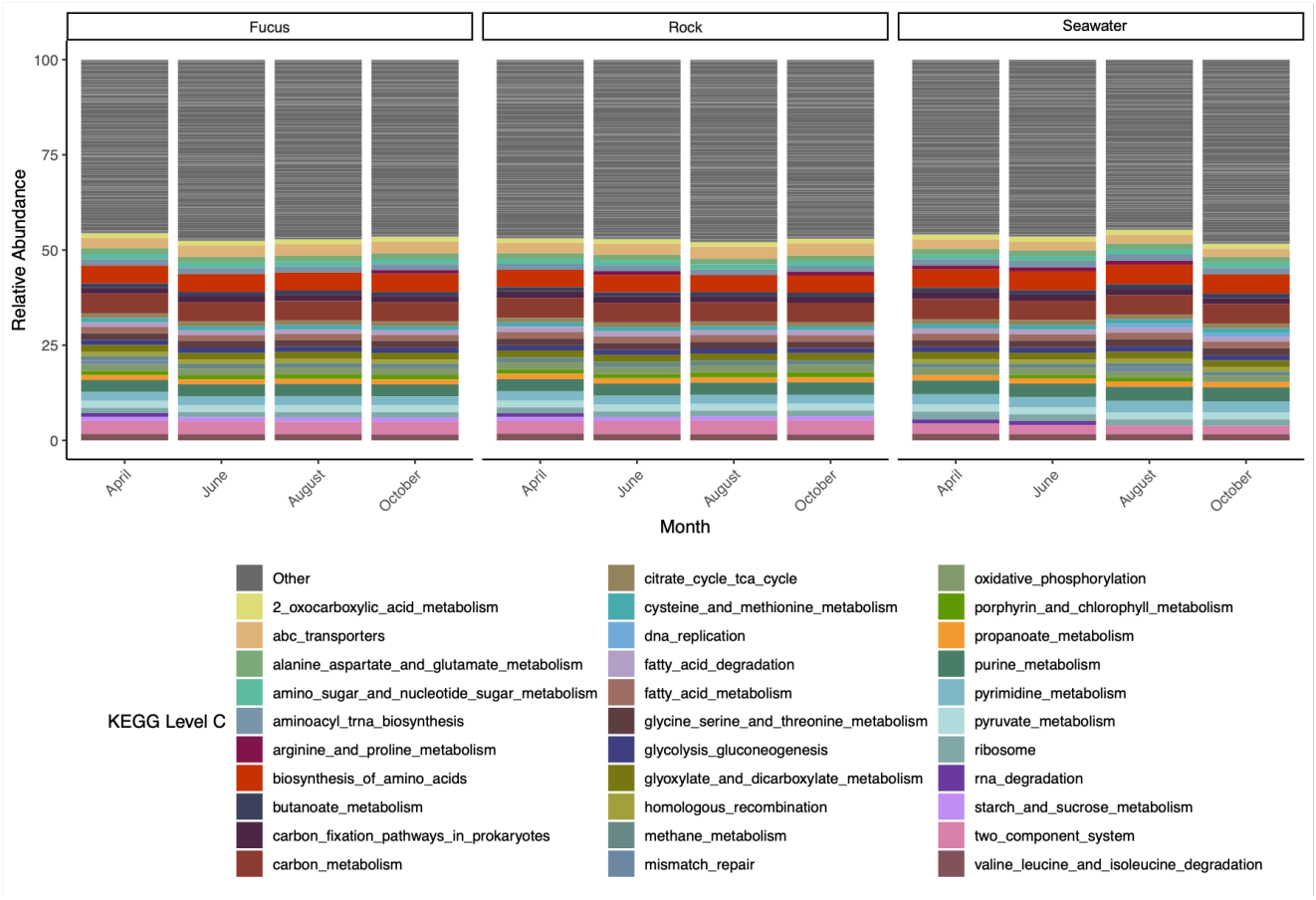

Appendix A - Figure 5. Relative abundance of the most abundant KEGG level C categories summarized by habitat type. Bars represent summary values of samples from each month.

	Df	SumsOfSqs	F Model	R2	p-value	p-adjusted
Pairwise 16S						
Fucus vs Rock	1	0.254	326.236	0.497	0.001	0.003
Fucus vs Water	1	0.281	321.144	0.535	0.001	0.003
Rock vs Water	1	0.053	416.657	0.726	0.001	0.003
Pairwise 18S						
Fucus vs Rock	1	0.017	29.839	0.096	0.001	0.003
Fucus vs Water	1	0.031	57.207	0.192	0.001	0.003
Rock vs Water	1	0.028	64.965	0.289	0.001	0.003
Pairwise Metagenomics						
Fucus vs Rock	1	0.099	8.444	0.199	0.001	0.003
Fucus vs Water	1	0.282	20.617	0.392	0.001	0.003
Rock vs Water	1	0.242	18.432	0.480	0.001	0.003

Appendix A - Table 1. Pairwise PERMANOVA analysis of microbiome beta-diversity (Bray-Curtis) between habitat types.

16S rRNA gene					
Group F. distichus: 29 genera					
	A	B	IndVal statistic	p-value	significance
Blastopirellula	0.95	0.98	0.964	0.001	***
Granulosicoccus	0.82	1	0.906	0.001	***
Litorimonas	0.81	0.97	0.888	0.001	***
Croceitalea	0.91	0.84	0.876	0.001	***
Rubritalea	0.9	0.82	0.859	0.001	***
Roseibacillus	0.75	0.98	0.858	0.001	***
Hellea	0.81	0.79	0.801	0.001	***
Dokdonia	0.67	0.88	0.765	0.001	***
Octadecabacter	0.76	0.73	0.745	0.001	***
unknown_Flavobacteriaceae	0.55	1	0.742	0.001	***
Bdellovibrio	0.95	0.57	0.738	0.001	***
unknown_Rhodobacteraceae	0.54	1	0.731	0.001	***
Peredibacter	0.77	0.7	0.731	0.001	***
Loktanella	0.73	0.72	0.722	0.002	**
unknown_Saprospiraceae	0.51	1	0.714	0.001	***
Altererythrobacter	0.68	0.7	0.69	0.003	**
Winogradskyella	0.56	0.77	0.658	0.009	**
Luteolibacter	0.9	0.47	0.652	0.002	**
unknown_21	0.74	0.56	0.645	0.003	**
unknown_Micavibrionaceae	0.72	0.57	0.637	0.003	**
unknown_NS11-12_marine_group	0.55	0.67	0.608	0.007	**
Group rock substrate: 73 genera					
	A	B	IndVal statistic	p-value	significance
Phormidesmis_ANT.LACV5.1	0.97	0.97	0.972	0.001	***
Pleurocapsa_PCC-7319	0.93	1	0.963	0.001	***
Truepera	0.99	0.85	0.92	0.001	***
Lewinella	0.81	1	0.9	0.001	***
unknown_Hyphomonadaceae	0.8	0.99	0.887	0.001	***
unknown_Sphingomonadaceae	0.84	0.91	0.873	0.001	***
Pseudahrensia	0.79	0.96	0.87	0.001	***
Algimonas	0.77	0.94	0.848	0.001	***
unknown_Rhodothermaceae	0.84	0.85	0.847	0.001	***
Kordia	0.91	0.72	0.809	0.001	***
unknown_Phycisphaeraceae	0.97	0.61	0.769	0.001	***
unknown_Rhizobiaceae	0.61	0.94	0.756	0.001	***
Rubrivirga	0.93	0.6	0.744	0.001	***
Ilumatobacter	0.59	0.85	0.708	0.001	***
unknown_Micavibrionales	0.59	0.82	0.698	0.002	**
Portibacter	0.52	0.93	0.693	0.008	**
Hyphomonas	0.91	0.52	0.688	0.001	***
Robiginitomaculum	0.69	0.66	0.675	0.001	***
Tunicatimonas	0.91	0.49	0.671	0.001	***
Rubricoccus	0.82	0.54	0.662	0.001	***
unknown_Rubinisphaeraceae	0.69	0.63	0.659	0.001	***
Parasphingopyxis	0.99	0.43	0.655	0.001	***
Rubidimonas	0.96	0.43	0.645	0.001	***
Pibocella	0.95	0.4	0.618	0.001	***
Group seawater: 75 genera					
	A	B	IndVal statistic	p-value	significance
NS4_marine_group	1	1	1	0.001	***
unknown_SAR86_clade	1	1	1	0.001	***
NS5_marine_group	1	1	1	0.001	***
Amylibacter	0.99	1	0.997	0.001	***
Formosa	0.99	1	0.993	0.001	***
Ascidiaceihabitans	1	0.94	0.972	0.001	***
unknown_SAR116_clade	1	0.94	0.972	0.001	***
NS3a_marine_group	1	0.94	0.972	0.001	***
Clade_Ia	1	0.94	0.971	0.001	***
Synechococcus_CC9902	1	0.94	0.971	0.001	***
Planktomarina	0.94	1	0.967	0.001	***
Candidatus_Actinomarina	1	0.89	0.942	0.001	***
NS2b_marine_group	0.99	0.89	0.94	0.001	***
OM43_clade	0.99	0.89	0.94	0.001	***
OM60(NOR5)_clade	0.99	0.89	0.936	0.001	***
Pseudohongiella	1	0.83	0.913	0.001	***
Tenacibaculum	0.83	1	0.911	0.001	***
unknown_Cryomorphaceae	0.73	1	0.857	0.001	***
Ulvibacter	0.73	1	0.854	0.001	***
unknown_Marine_Group_II	1	0.72	0.85	0.001	***
SAR92_clade	1	0.72	0.85	0.001	***
RS62_marine_group	1	0.72	0.849	0.001	***
unknown_NS9_marine_group	0.78	0.89	0.832	0.001	***
Flavicella	0.98	0.67	0.808	0.001	***
Fluviicola	0.75	0.78	0.765	0.001	***
Polaribacter	0.64	0.89	0.754	0.001	***
Luminiphilus	1	0.56	0.745	0.001	***
Pseudoalteromonas	0.82	0.67	0.739	0.001	***
Burkholderia-Caballeronia-Paraburkholderia	1	0.5	0.707	0.001	***
Candidatus_Aquiluna	1	0.5	0.707	0.001	***
IS-44	1	0.5	0.707	0.001	***
unknown_Kordiimonadales	1	0.5	0.707	0.001	***
XZXXH163	1	0.5	0.707	0.001	***
Marinoscillum	0.99	0.5	0.703	0.001	***
Candidatus_Tenderia	0.99	0.5	0.702	0.001	***
Colwellia	0.79	0.56	0.664	0.001	***
Lutibacter	0.82	0.5	0.639	0.001	***
unknown_Clade_II	1	0.39	0.624	0.001	***
unknown_Crocinitomicaceae	0.7	0.56	0.622	0.001	***
Draconibacterium	0.98	0.39	0.618	0.001	***
Halioglobus	0.96	0.39	0.611	0.001	***
Significance: '***' 0.001 '**' 0.01 '*' 0.05 '.' 0.1 ' ' 1					

Appendix A - Table 2. Indicator analysis (IndVal) results by habitat type for 16S rRNA amplicon sequences aggregated at the genus level. Significant results with an Indval statistic > 0.6 are presented.

18S rRNA gene					
Group F. distichus: 21 genera					
	A	B	IndVal statistic	p-value	significance
Ulvophyceae_sp._RCC4620	0.90165	0.57143	0.718	0.001	***
Ulvella	0.9032	0.47253	0.653	0.001	***
Harpacticoida	0.63693	0.65934	0.648	0.003	**
Halothrix	0.68885	0.53846	0.609	0.001	***
Group rock substrate: 51 genera					
	A	B	IndVal statistic	p-value	significance
Scrupocellaria_maderensis	0.98365	0.7549	0.862	0.001	***
Ectocarpales	0.88455	0.79412	0.838	0.001	***
Monostroma	0.93762	0.65686	0.785	0.001	***
Blidingia	0.97343	0.58824	0.757	0.001	***
Sessilia	0.71675	0.77451	0.745	0.001	***
Pseudoperkinsus	0.62026	0.76471	0.689	0.001	***
Parvamoeba	0.79546	0.54902	0.661	0.001	***
Navicula	0.6698	0.64706	0.658	0.001	***
Achnanthes_sp._p346	0.88276	0.4902	0.658	0.001	***
unknown_Vampyrellidae	0.74874	0.5	0.612	0.001	***
Group seawater: 160 genera					
	A	B	IndVal statistic	p-value	significance
Calanoida	0.98046	0.98333	0.982	0.001	***
Gyrodinium	0.9312	0.95	0.941	0.001	***
Haplozoon	0.97697	0.81667	0.893	0.001	***
Oikopleuridae	0.92306	0.85	0.886	0.001	***
Teleaulax_acuta	0.97733	0.61667	0.776	0.001	***
unknown_Teleaulax	1	0.6	0.775	0.001	***
Myrionecta	0.99634	0.6	0.773	0.001	***
Spionida	0.6855	0.83333	0.756	0.001	***
Cryptocaryon	0.94271	0.6	0.752	0.001	***
unknown_Prasinophytae	0.98957	0.55	0.738	0.001	***
Syndiniales_Group_I	0.58724	0.91667	0.734	0.001	***
Protoperidinium	0.94054	0.51667	0.697	0.001	***
Chaetoceros	0.72117	0.66667	0.693	0.001	***
Thalassiosira	0.82778	0.55	0.675	0.001	***
unknown_Embryophyta	0.85108	0.5	0.652	0.001	***
Strombidium	0.65267	0.65	0.651	0.001	***
Stolidobranchia	0.93566	0.45	0.649	0.001	***
Ulva	0.73971	0.56667	0.647	0.001	***
Warnowia	0.91051	0.45	0.64	0.001	***
Veneroida	0.45102	0.85	0.619	0.001	***
unknown_Mamiellophyceae	1	0.38333	0.619	0.001	***
Syndiniales_Group_II	0.80585	0.46667	0.613	0.001	***
Helicostomella	0.86386	0.43333	0.612	0.001	***
Opheliidae	0.87611	0.41667	0.604	0.001	***
Cyclopoida	0.8409	0.43333	0.604	0.001	***
Significance: '***' 0.001 '**' 0.01 '*' 0.05 '.' 0.1 ' ' 1					

Appendix A - Table 3. Indicator analysis (IndVal) results by habitat type for 18S rRNA amplicon sequences aggregated at the genus level. Significant results with an Indval statistic > 0.6 are presented.

Group F. distichus: 102 KEGGs					
	A	B	IndVal statistic	p-value	significance
biosynthesis_of_12_14_and_16_membered_macrolides	0.73	0.96	0.836	0.001	***
aflatoxin_biosynthesis	0.57	1	0.757	0.001	***
biosynthesis_of_type_ii_polyketide_backbone	0.56	1	0.748	0.001	***
ecm_receptor_interaction	0.55	1	0.744	0.001	***
flavone_and_flavonol_biosynthesis	0.51	1	0.717	0.001	***
bacterial_chemotaxis	0.51	1	0.716	0.001	***
sesquiterpenoid_and_triterpenoid_biosynthesis	0.5	1	0.706	0.003	**
fluorobenzoate_degradation	0.49	1	0.7	0.001	***
Group rock substrate: 79 KEGGs					
	A	B	IndVal statistic	p-value	significance
acridone_alkaloid_biosynthesis	1	0.92	0.957	0.001	***
photosynthesis_antenna_proteins	0.9	1	0.95	0.001	***
regulation_of_autophagy	0.74	1	0.86	0.001	***
isoflavonoid_biosynthesis	0.72	1	0.85	0.001	***
cutin_suberine_and_wax_biosynthesis	0.71	1	0.844	0.001	***
brassinosteroid_biosynthesis	0.75	0.92	0.83	0.001	***
type_i_polyketide_structures	0.67	1	0.82	0.001	***
nonribosomal_peptide_structures	0.66	1	0.81	0.001	***
leishmaniasis	0.66	1	0.81	0.001	***
non_homologous_end_joining	0.62	1	0.785	0.001	***
proteasome	0.57	1	0.754	0.002	**
biosynthesis_of_siderophore_group_nonribosomal_peptides	0.56	1	0.747	0.001	***
spliceosome	0.55	1	0.739	0.002	**
sphingolipid_signaling_pathway	0.54	1	0.733	0.001	***
staphylococcus_aureus_infection	0.53	1	0.73	0.002	**
glycosaminoglycan_biosynthesis chondroitin_sulfate_dermatan_sulfate	0.53	1	0.727	0.004	**
vibrio_cholerae_infection	0.53	1	0.726	0.001	***
meiosis_yeast	0.52	1	0.723	0.001	***
plant_hormone_signal_transduction	0.51	1	0.712	0.001	***
malaria	0.51	1	0.712	0.026	*
mtor_signaling_pathway	0.51	1	0.712	0.038	*
nitrotoluene_degradation	0.5	1	0.709	0.001	***
cell_cycle_yeast	0.5	1	0.705	0.007	**
glycosylphosphatidylinositolgpi_anchor_biosynthesis	0.49	1	0.703	0.01	**
diterpenoid_biosynthesis	0.49	1	0.702	0.001	***
Group seawater: 4 KEGGs					
	A	B	IndVal statistic	p-value	significance
glycosphingolipid_biosynthesis_lacto_and_neolacto_series	0.9177	0.8	0.857	0.001	***
glycosaminoglycan_biosynthesis_keratan_sulfate	0.8433	0.8	0.821	0.001	***
mucin_type_o_glycan_biosynthesis	0.8256	0.8	0.813	0.001	***
cytokine_cytokine_receptor_interaction	0.5734	0.8	0.677	0.008	**
Significance: '***' 0.001 '**' 0.01 '*' 0.05 '.' 0.1 ' ' 1					

Appendix A - Table 4. Indicator analysis (IndVal) results by habitat type for shotgun metagenomic sequences aggregated at KEGG level C. Significant results with an Indval statistic > 0.7 are presented.

Habitat type	n samples	Mean percentage of reads mapped	Variance	sd	Group significance
Fucus distichus	96	80.18	53.07	7.285	a
Rock substrate	48	46.011	118.371	10.88	b
Seawater	40	38.635	123.593	11.117	c

Appendix A - Table 5. Games-Howell post-hoc test for percent of shotgun metagenomic reads mapped according to habitat type.

All Habitats						
	Df	SumsOfSqs	MeanSqs	F Model	R2	p-value
Month	1	0.008047	0.008047	8.005	0.15393	0.001 ***
Residuals	44	0.044232	0.001005		0.84607	
Total	45	0.052279			1	
By Habitat type						
	Df	SumsOfSqs	MeanSqs	F Model	R2	p-value
Fucus distichus						
Month	1	0.0020417	0.002042	3.065	0.12228	0.031 *
Residuals	22	0.0146555	0.000666		0.87772	
Total	23	0.0166973			1	
Rock						
Month	1	0.0012623	0.001262	2.5139	0.20089	0.099 .
Residuals	10	0.0050212	0.000502		0.79911	
Total	11	0.0062835			1	
Seawater						
Month	1	0.0052346	0.005235	23.267	0.74414	0.001 ***
Residuals	8	0.0017998	0.000225		0.25586	
Total	9	0.0070345			1	
Significance: 0 '***' 0.001 '**' 0.01 '*' 0.05 '.' 0.1 ' ' 1						

Appendix A - Table 6. The contribution of time to variation in microbiome functional (KEGG) diversity (Bray-Curtis) for each habitat type using PERMANOVA.

Appendix B - Chapter 3: Supplementary information

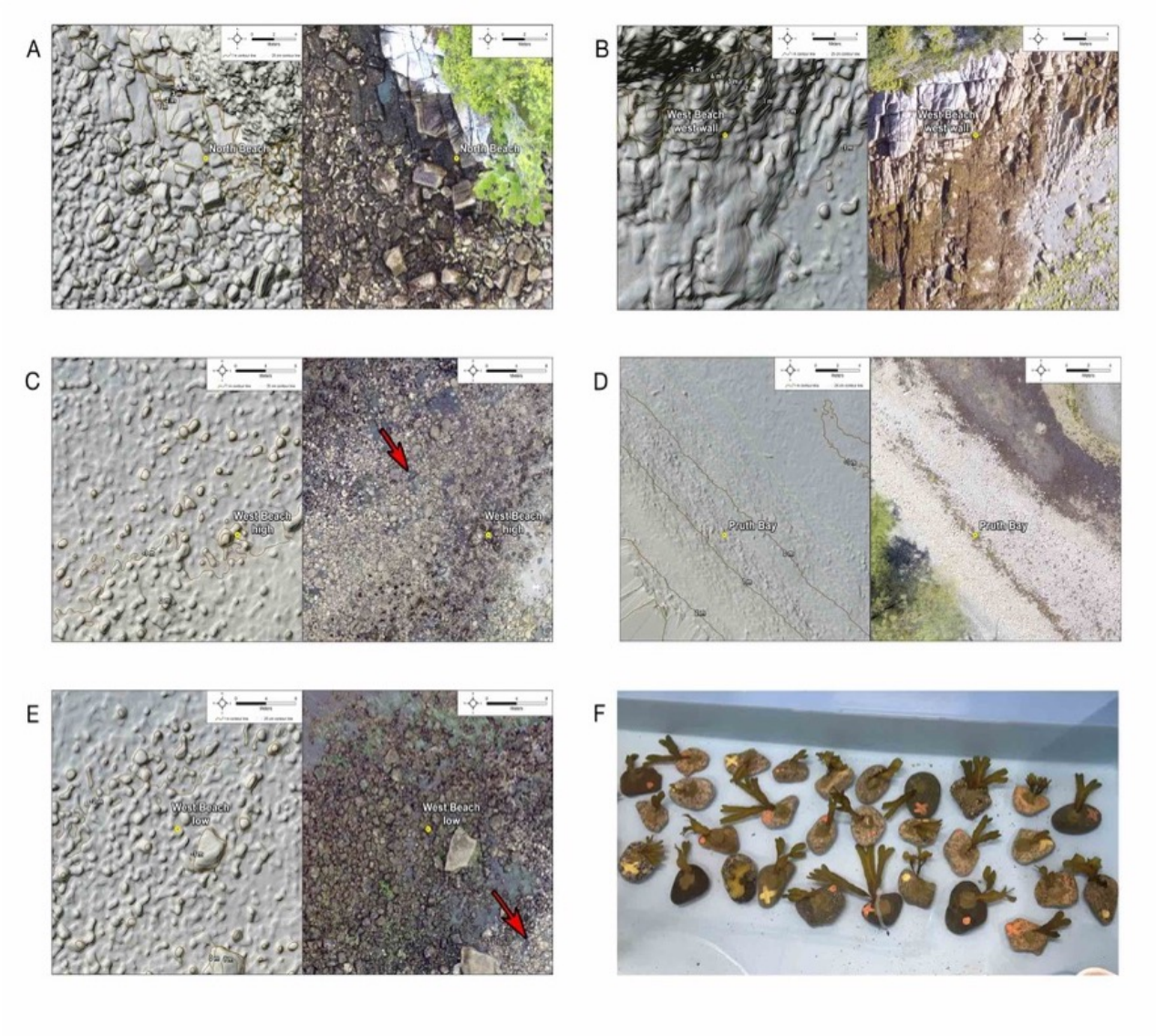

Appendix B - Figure 1. Benthic contour maps and aerial photographs of sampling sites. 0m is the MLLW line and brown contours are every 1m; tan contours are every 0.25m. A) North Beach (NB), morphotype A; B) West Beach west wall (WB west wall), morphotype A; C) West Beach high (WB high, morphotype A; D) Pruth Bay (PB), morphotype B; E) West Beach low (WB low), morphotype C; F) Experimental setup for the common garden. Red arrows in C) and E) indicate zone at WB without *F. distichus* growth, separating morphotypes A and C.

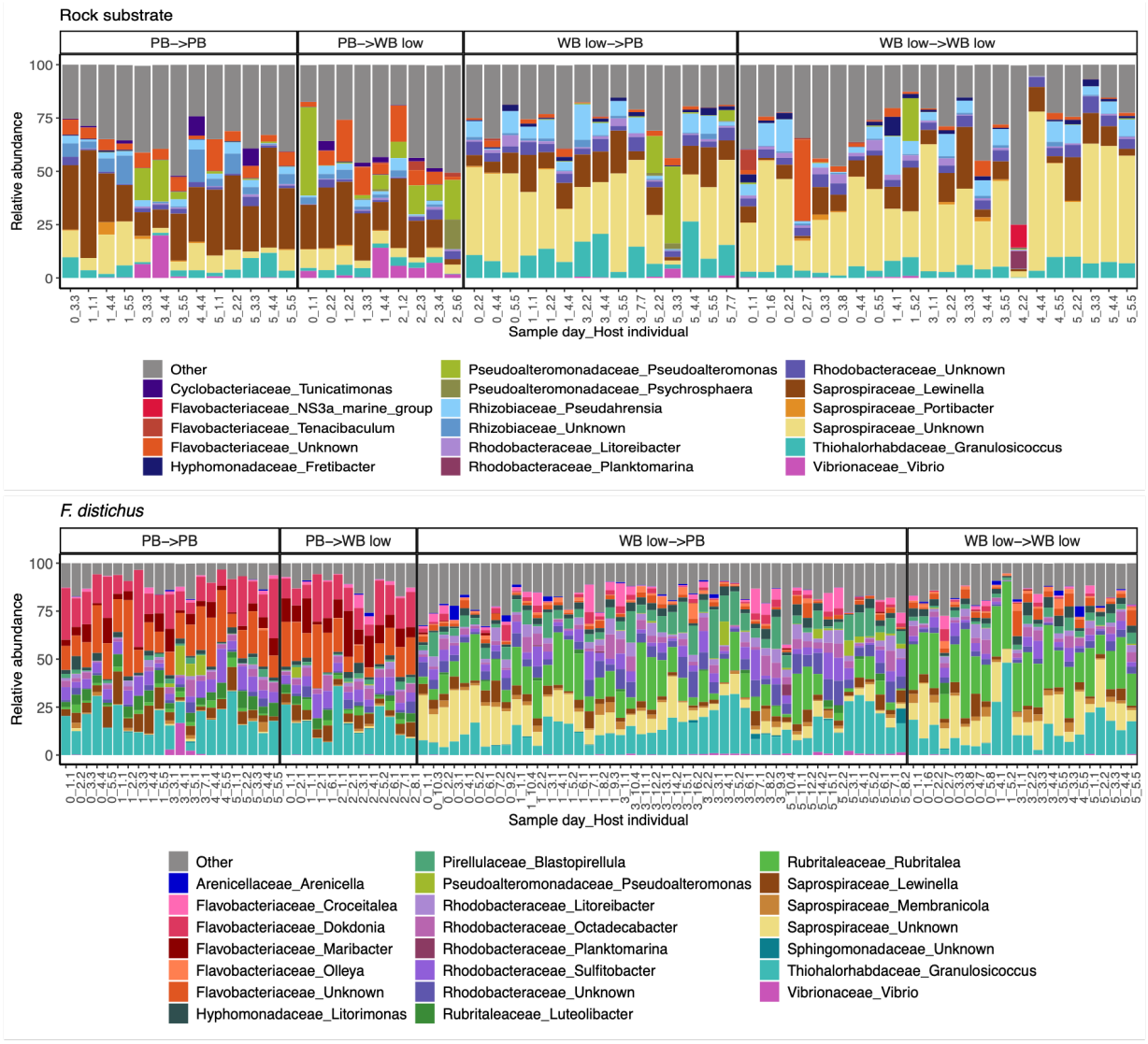

Appendix B - Figure 2. *Fucus distichus* and rock biofilm communities are distinct and stable following transplant to a new environment. Stacked bar plots of the most abundant ASVs on rock substrate and *Fucus distichus* from reciprocal transplant experiment. Each column represents an individual sample; samples are ordered by day of sampling and grouped by site of origin. The first number of x-axis labels is sampling day, the second number is a unique sample identifier.

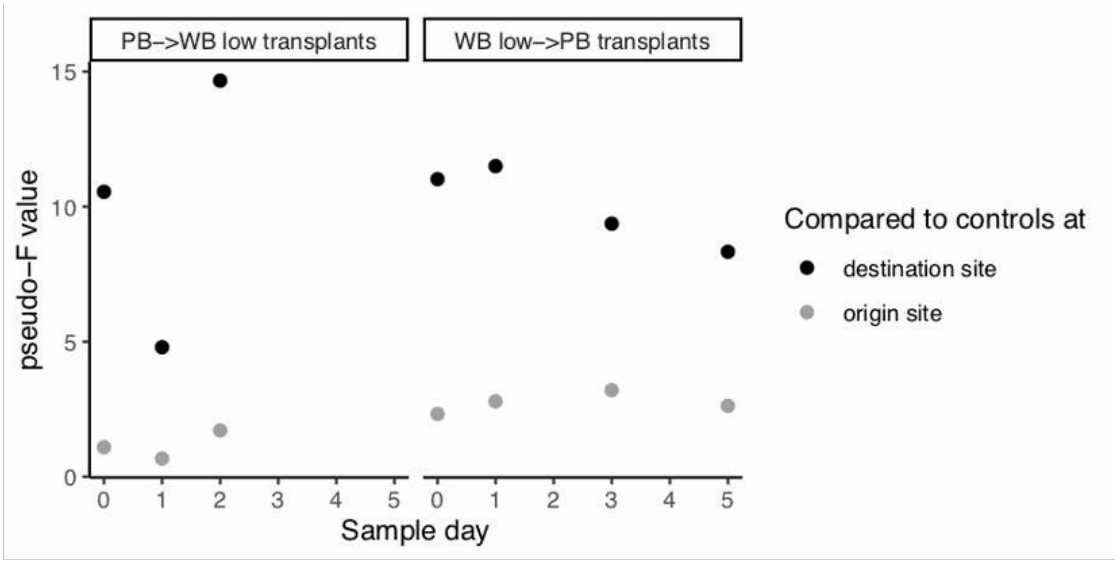

Appendix B - Figure 3. Microbial communities on *F. distichus* transplants do not become more differentiated from unmanipulated controls at the native origin site over time or more similar to controls at destination site over time. ANOVA on linear regressions of pseudo-F values over time for WB low -> PB transplants and controls at the destination site (p-value = 0.054) or origin site (p-value = 0.630); PB -> WB low and controls at the destination site (p-value = 0.728) or origin site (p-value = 0.597).

origin	comparison	beta_metric	group1	group2	n1	n2	p.adjust	p.adjust.signif
PB	within site	jacc	1	5	30	6	0.303	ns
NB	within site	jacc	1	5	20	20	0.535	ns
WB west wall	within site	jacc	1	5	56	12	0.00833	**
WB high	within site	jacc	1	5	42	30	0.336	ns
WB low	within site	jacc	1	5	30	42	7.36E-05	****
PB	between sites	jacc	1	5	156	66	0.000334	***
NB	between sites	jacc	1	5	135	100	0.449	ns
WB west wall	between sites	jacc	1	5	192	84	0.605	ns
WB high	between sites	jacc	1	5	175	114	0.615	ns
WB low	between sites	jacc	1	5	156	126	0.172	ns

Appendix B - Table 1. Pairwise comparisons of compositional dissimilarity (Jaccard) of *Fucus distichus* microbiome samples from within the same site and between a focal site and all other sites at the start (day 1) and end (day 5) of the common garden experiment.

ASV	A	B	indval.stat	p.value	group	Domain	Phylum	Class	Order	Family	Genus	Species	Accession
ASV51	1	1	1	0.001	PB_day.1	Bacteria	Bacteroidetes	Bacteroidia	Flavobacteriales	Flavobacteriaceae	unknown_Flavobacteriaceae	unknown_Flavobacteriaceae	AB476295.1.1444
ASV76	1	1	1	0.001	PB_day.1	Bacteria	Bacteroidetes	Bacteroidia	Chitinophagales	Saprospiraceae	Lewinella	Lewinella sp. HME9321	KF385496.1.1389
ASV93	1	1	1	0.001	WB low_day.1	Bacteria	Planctomycetes	Planctomycetacia	Pirellulales	Pirellulaceae	Blastopirellula	unknown_Blastopirellula	FN822210.1.1536
ASV194	1	1	1	0.001	WB low_day.1	Bacteria	Proteobacteria	Gammaproteobacteria	Arenicellales	Arenicellaceae	Arenicella	unknown_Arenicella	NA
ASV217	1	1	1	0.001	WB low_day.1	Bacteria	Bacteroidetes	Bacteroidia	Chitinophagales	Saprospiraceae	unknown_Saprospiraceae	unknown_Saprospiraceae	JQ196292.1.1351
ASV311	1	1	1	0.001	WB low_day.1	Bacteria	Bacteroidetes	Bacteroidia	Chitinophagales	Saprospiraceae	unknown_Saprospiraceae	unknown_Saprospiraceae	JQ196292.1.1351
ASV320	1	1	1	0.001	WB low_day.1	Bacteria	Proteobacteria	Alphaproteobacteria	Caulobacterales	Hyphomonadaceae	Litorimonas	Litorimonas_cladophorae	JX174422.1.1401
ASV352	1	1	1	0.001	WB low_day.1	Bacteria	Bacteroidetes	Bacteroidia	Chitinophagales	Saprospiraceae	unknown_Saprospiraceae	unknown_Saprospiraceae	JQ196292.1.1351
ASV319	1	1	1	0.001	NB+WB low_day.1	Bacteria	Verrucomicrobia	Verrucomicrobiae	Verrucomicrobiales	Rubritaleaceae	Rubritalea	unknown_Rubritalea	NA
ASV51	1	1	1	0.003	PB_day.5	Bacteria	Bacteroidetes	Bacteroidia	Flavobacteriales	Flavobacteriaceae	unknown_Flavobacteriaceae	unknown_Flavobacteriaceae	AB476295.1.1444
ASV77	1	1	1	0.003	WB low_day.5	Bacteria	Bacteroidetes	Bacteroidia	Chitinophagales	Saprospiraceae	unknown_Saprospiraceae	unknown_Saprospiraceae	AB476226.1.1449
ASV2	1	1	1	0.003	NB+WB low_day.5	Bacteria	Verrucomicrobia	Verrucomicrobiae	Verrucomicrobiales	Rubritaleaceae	Rubritalea	unknown_Rubritalea	JQ196089.1.1359
ASV49	1	1	1	0.003	NB+PB+WB high+WB west wall_day.5	Bacteria	Bacteroidetes	Bacteroidia	Flavobacteriales	Flavobacteriaceae	Dokdonia	unknown_Dokdonia	NA
ASV30	0.9982	1	0.999	0.001	NB+WB high+WB low+WB west wall_day.1	Bacteria	Verrucomicrobia	Verrucomicrobiae	Verrucomicrobiales	Rubritaleaceae	Rubritalea	unknown_Rubritalea	NA
ASV121	0.9986	1	0.999	0.001	WB west wall_day.5	Bacteria	Bacteroidetes	Bacteroidia	Flavobacteriales	Flavobacteriaceae	unknown_Flavobacteriaceae	unknown_Flavobacteriaceae	NA
ASV4	0.9987	1	0.999	0.001	NB+PB+WB high+WB west wall_day.5	Bacteria	Bacteroidetes	Bacteroidia	Flavobacteriales	Flavobacteriaceae	Nonlabens	unknown_Nonlabens	NA
ASV17	0.9924	1	0.996	0.001	NB+WB high+WB low_day.1	Bacteria	Proteobacteria	Gammaproteobacteria	Thiohalorhabdales	Thiohalorhabdaceae	Granulosicoccus	unknown_Granulosicoccus	NA
ASV71	0.9906	1	0.995	0.001	NB+PB+WB high+WB west wall_day.5	Bacteria	Bacteroidetes	Bacteroidia	Flavobacteriales	Flavobacteriaceae	Nonlabens	Nonlabens_aremilitoris	KP769429.1.1309
ASV77	0.9867	1	0.993	0.001	WB low_day.1	Bacteria	Bacteroidetes	Bacteroidia	Chitinophagales	Saprospiraceae	unknown_Saprospiraceae	unknown_Saprospiraceae	AB476226.1.1449
ASV135	0.9835	1	0.992	0.001	PB_day.1	Bacteria	Proteobacteria	Alphaproteobacteria	Rhizobiales	Rhizobiaceae	Roseitalea	Mesorhizobium_sp._DG943	AY2580891.1378
ASV17	0.9836	1	0.992	0.001	NB+WB low_day.5	Bacteria	Proteobacteria	Gammaproteobacteria	Thiohalorhabdales	Thiohalorhabdaceae	Granulosicoccus	unknown_Granulosicoccus	NA
ASV7	0.9796	1	0.99	0.001	NB+PB+WB high+WB west wall_day.1	Bacteria	Proteobacteria	Alphaproteobacteria	Rhodobacterales	Rhodobacteraceae	Sulfitobacter	Sulfitobacter_sp._FS12-3	JQ799973.1.1380
ASV26	0.9789	1	0.989	0.001	WB low_day.1	Bacteria	Bacteroidetes	Bacteroidia	Chitinophagales	Saprospiraceae	unknown_Saprospiraceae	unknown_Saprospiraceae	NA
ASV26	0.9776	1	0.989	0.001	WB low_day.5	Bacteria	Bacteroidetes	Bacteroidia	Chitinophagales	Saprospiraceae	unknown_Saprospiraceae	unknown_Saprospiraceae	NA
ASV2	0.9766	1	0.988	0.001	NB+WB low_day.1	Bacteria	Verrucomicrobia	Verrucomicrobiae	Verrucomicrobiales	Rubritaleaceae	Rubritalea	unknown_Rubritalea	JQ196089.1.1359
ASV153	0.9739	1	0.987	0.001	bests_day.5	Bacteria	Proteobacteria	Deltaproteobacteria	Bdellovibrionales	Bdellovibrionaceae	unknown_OM27_clade	unknown_OM27_clade	FJ905764.1.1375
ASV173	0.9682	1	0.984	0.001	NB+WB low_day.5	Bacteria	Bacteroidetes	Bacteroidia	Chitinophagales	Saprospiraceae	unknown_Saprospiraceae	unknown_Saprospiraceae	JQ196292.1.1351
ASV58	0.9658	1	0.983	0.001	WB low_day.1	Bacteria	Bacteroidetes	Bacteroidia	Chitinophagales	Saprospiraceae	unknown_Saprospiraceae	unknown_Saprospiraceae	FN433362.1.1487
ASV135	0.9667	1	0.983	0.002	PB_day.5	Bacteria	Proteobacteria	Alphaproteobacteria	Rhizobiales	Rhizobiaceae	Roseitalea	Mesorhizobium_sp._DG943	AY2580891.1378
ASV25	0.9624	1	0.981	0.001	NB+PB+WB high_day.1	Bacteria	Bacteroidetes	Bacteroidia	Flavobacteriales	Flavobacteriaceae	Dokdonia	Dokdonia_sp._Hel_1_53	ZS854132.1.1248
ASV4	1	0.9615	0.981	0.001	NB+PB+WB high+WB west wall_day.1	Bacteria	Bacteroidetes	Bacteroidia	Flavobacteriales	Flavobacteriaceae	Nonlabens	unknown_Nonlabens	NA
ASV85	0.9589	1	0.979	0.002	PB_day.5	Bacteria	Verrucomicrobia	Verrucomicrobiae	Verrucomicrobiales	Rubritaleaceae	Luteolibacter	unknown_Luteolibacter	NA
ASV66	0.9564	1	0.978	0.001	WB low_day.1	Bacteria	Proteobacteria	Gammaproteobacteria	Thiohalorhabdales	Thiohalorhabdaceae	Granulosicoccus	unknown_Granulosicoccus	JQ218711.1.1497
ASV66	0.9518	1	0.976	0.001	WB low_day.5	Bacteria	Proteobacteria	Gammaproteobacteria	Thiohalorhabdales	Thiohalorhabdaceae	Granulosicoccus	unknown_Granulosicoccus	JQ218711.1.1497
ASV6	1	0.9524	0.976	0.001	NB+PB+WB high+WB low_day.5	Bacteria	Bacteroidetes	Bacteroidia	Chitinophagales	Saprospiraceae	Lewinella	Lewinella_sp._HME9321	KF385496.1.1389
ASV42	0.9427	1	0.971	0.001	NB_day.1	Bacteria	Proteobacteria	Alphaproteobacteria	Rhodobacterales	Rhodobacteraceae	unknown_Rhodobacteraceae	unknown_Rhodobacteraceae	NA
ASV60	1	0.9333	0.966	0.001	NB+PB+WB low_day.5	Bacteria	Verrucomicrobia	Verrucomicrobiae	Verrucomicrobiales	Rubritaleaceae	unknown_Rubritaleaceae	unknown_Rubritaleaceae	NA
ASV35	0.9303	1	0.965	0.001	NB+WB high_day.1	Bacteria	Proteobacteria	Alphaproteobacteria	Rhodobacterales	Rhodobacteraceae	unknown_Rhodobacteraceae	unknown_Rhodobacteraceae	NA
ASV242	0.9289	1	0.964	0.001	WB high_day.5	Bacteria	Bacteroidetes	Bacteroidia	Flavobacteriales	Flavobacteriaceae	Maribacter	unknown_Maribacter	NA
ASV35	0.9292	1	0.964	0.002	NB+WB high_day.5	Bacteria	Proteobacteria	Alphaproteobacteria	Rhodobacterales	Rhodobacteraceae	unknown_Rhodobacteraceae	unknown_Rhodobacteraceae	NA
ASV25	0.9214	1	0.962	0.002	NB+PB+WB high_day.5	Bacteria	Verrucomicrobia	Verrucomicrobiae	Verrucomicrobiales	Rubritaleaceae	Luteolibacter	unknown_Luteolibacter	NA
ASV27	0.9719	0.9524	0.962	0.006	NB+PB+WB high+WB low_day.5	Bacteria	Proteobacteria	Alphaproteobacteria	Rhodobacterales	Rhodobacteraceae	Litoreibacter	Litoreibacter_halocynthiae	JX644172.1.1420
ASV25	1	0.9231	0.961	0.001	NB+PB+WB high+WB west wall_day.1	Bacteria	Verrucomicrobia	Verrucomicrobiae	Verrucomicrobiales	Rubritaleaceae	Luteolibacter	unknown_Luteolibacter	NA
ASV297	0.9604	0.9615	0.961	0.006	NB+WB high+WB low+WB west wall_day.1	Bacteria	Bacteroidetes	Bacteroidia	Chitinophagales	Saprospiraceae	unknown_Saprospiraceae	unknown_Saprospiraceae	NA
ASV288	0.9226	1	0.961	0.005	PB_day.5	Bacteria	Bacteroidetes	Bacteroidia	Flavobacteriales	Flavobacteriaceae	unknown_Flavobacteriaceae	Formosa_sp._18III/A01/079	AY612758.1.1457
ASV7	0.973	0.9444	0.959	0.04	NB+PB+WB high+WB west wall_day.5	Bacteria	Proteobacteria	Alphaproteobacteria	Rhodobacterales	Rhodobacteraceae	Sulfitobacter	Sulfitobacter_sp._FS12-3	JQ799973.1.1380
ASV41	0.9178	1	0.958	0.004	NB+WB low_day.5	Bacteria	Bacteroidetes	Bacteroidia	Chitinophagales	Saprospiraceae	Membraniciola	Lewinella_sp._CZ-AZ5	JX306763.1.1396
ASV63	0.916	1	0.957	0.001	NB+WB low_day.5	Bacteria	Proteobacteria	Alphaproteobacteria	Caulobacterales	Hyphomonadaceae	Fretibacter	Fretibacter_rubidus	JQ965646.1.1412
ASV3	0.9844	0.9286	0.956	0.001	NB+PB+WB high_day.5	Bacteria	Bacteroidetes	Bacteroidia	Flavobacteriales	Flavobacteriaceae	Dokdonia	Dokdonia_sp._Hel_1_53	ZS854132.1.1248
ASV231	0.9123	1	0.955	0.002	NB+WB low_day.5	Bacteria	Bacteroidetes	Bacteroidia	unknown_Bacteroidia	unknown_Bacteroidia	unknown_Bacteroidia	unknown_Bacteroidia	NA
ASV233	0.9869	0.9231	0.954	0.002	NB+WB high+WB low+WB west wall_day.1	Bacteria	Bacteroidetes	Bacteroidia	Chitinophagales	Saprospiraceae	unknown_Saprospiraceae	unknown_Saprospiraceae	AB476238.1.1449
ASV73	0.9751	0.9333	0.954	0.001	NB+WB high+WB west wall_day.5	Bacteria	Verrucomicrobia	Verrucomicrobiae	Verrucomicrobiales	Rubritaleaceae	unknown_Rubritaleaceae	unknown_Rubritaleaceae	NA
ASV82	0.9091	1	0.953	0.001	NB+WB low_day.1	Bacteria	Proteobacteria	Alphaproteobacteria	Rhodobacterales	Rhodobacteraceae	Octadecabacter	unknown_Octadecabacter	NA
ASV84	1	0.9091	0.953	0.01	NB+WB high+WB low+WB west wall_day.5	Bacteria	Proteobacteria	Alphaproteobacteria	Caulobacterales	Hyphomonadaceae	Litorimonas	Litorimonas_cladophorae	JX174422.1.1401
ASV104	0.8983	1	0.948	0.001	WB high_day.1	Bacteria	Proteobacteria	Alphaproteobacteria	Rhodobacterales	Rhodobacteraceae	unknown_Rhodobacteraceae	unknown_Rhodobacteraceae	NA
ASV374	0.8936	1	0.945	0.001	NB_day.1	Bacteria	Bacteroidetes	Bacteroidia	Cytophagales	Cyclobacteriaceae	Reichenbachiella	Reichenbachiella_sp._MAR_2010_115	ZS854387.1.1280
ASV58	0.9728	0.9167	0.944	0.001	NB+WB low_day.5	Bacteria	Bacteroidetes	Bacteroidia	Chitinophagales	Saprospiraceae	unknown_Saprospiraceae	unknown_Saprospiraceae	FN433362.1.1487
ASV16	0.9606	0.9231	0.942	0.013	NB+PB+WB high+WB west wall_day.1	Bacteria	Proteobacteria	Alphaproteobacteria	Rhodobacterales	Rhodobacteraceae	Octadecabacter	Octadecabacter_temperatus	KF836544.1.1324
ASV84	1	0.8846	0.941	0.002	NB+WB high+WB low+WB west wall_day.1	Bacteria	Proteobacteria	Alphaproteobacteria	Caulobacterales	Hyphomonadaceae	Litorimonas	Litorimonas_cladophorae	JX174422.1.1401
ASV125	0.8835	1	0.94	0.001	WB west wall_day.1	Bacteria	Bacteroidetes	Bacteroidia	Flavobacteriales	Flavobacteriaceae	Olleya	Psychroserpens_sp._FI_9C	KF365476.1.1391
ASV104	0.9793	0.9	0.939	0.001	NB+WB high+WB west wall_day.5	Bacteria	Proteobacteria	Alphaproteobacteria	Rhodobacterales	Rhodobacteraceae	unknown_Rhodobacteraceae	unknown_Rhodobacteraceae	NA
ASV315	0.88	1	0.938	0.003	PB_day.5	Bacteria	Proteobacteria	Alphaproteobacteria	Sphingomonadales	Sphingomonadaceae	Altererythrobacter	mucus_bacterium_91	AY654830.1.1386
ASV5	0.8789	1	0.937	0.003	NB+WB low_day.1	Bacteria	Proteobacteria	Gammaproteobacteria	Thiohalorhabdales	Thiohalorhabdaceae	Granulosicoccus	unknown_Granulosicoccus	JQ218703.1.1493
ASV73	0.9926	0.8846	0.937	0.001	NB+WB high+WB low+WB west wall_day.1	Bacteria	Verrucomicrobia	Verrucomicrobiae	Verrucomicrobiales	Rubritaleaceae	unknown_Rubritaleaceae	unknown_Rubritaleaceae	NA
ASV40	0.8788	1	0.937	0.003	PB_day.5	Bacteria	Proteobacteria	Gammaproteobacteria	Thiohalorhabdales	Thiohalorhabdaceae	Granulosicoccus	unknown_Granulosicoccus	JQ218705.1.1493
ASV121	1	0.875	0.935	0.001	WB west wall_day.1	Bacteria	Bacteroidetes	Bacteroidia	Flavobacteriales	Flavobacteriaceae	unknown_Flavobacteriaceae	unknown_Flavobacteriaceae	NA
ASV703	1	0.875	0.935	0.002	WB west wall_day.1	Bacteria	Bacteroidetes	Bacteroidia	Flavobacteriales	Flavobacteriaceae	Winogradskyella	Winogradskyella_litoriviva	JX174421.1.1448
ASV78	0.9392	0.9286	0.934	0.002	NB+PB+WB high_day.5	Bacteria	Bacteroidetes	Bacteroidia	Chitinophagales	Saprospiraceae	Membraniciola	Lewinella_sp._CZ-AZ5	JX306763.1.1396
ASV798	0.8649	1	0.93	0.002	PB_day.5	Bacteria	Proteobacteria	Alphaproteobacteria	unknown_Alphaproteobacteria	unknown_Alphaproteobacteria	unknown_Alphaproteobacteria	unknown_Alphaproteobacteria	NA
ASV11	0.926	0.9333	0.93	0.003	NB+PB+WB low_day.5	Bacteria	Planctomycetes	Planctomycetacia	Pirellulales	Pirellulaceae	Blastopirellula	unknown_Blastopirellula	JQ198127.1.1339
ASV320	1	0.8571	0.926	0.003	WB low_day.5	Bacteria	Verrucomicrobia	Verrucomicrobiae	Verrucomicrobiales	Rubritaleaceae	unknown_Roseibacillus	unknown_Roseibacillus	NA
ASV320	1	0.8571	0.926	0.002	WB low_day.5	Bacteria	Proteobacteria	Alphaproteobacteria	Caulobacterales	Hyphomonadaceae	Litorimonas	Litorimonas_cladophorae	JX174422.1.1401
ASV338	1	0.8571	0.926	0.002	WB low_day.5	Bacteria	Bacteroidetes	Bacteroidia	Chitinophagales	Saprospiraceae	unknown_Saprospiraceae	unknown_Saprospiraceae	NA
ASV352	1	0.8571	0.926	0.002	WB low_day.5	Bacteria	Bacteroidetes	Bacteroidia	Chitinophagales	Saprospiraceae	unknown_Saprospiraceae	unknown_Saprospiraceae	JQ196292.1.1351
ASV426	1	0.8571	0.926	0.003	WB low_day.5	Bacteria	Proteobacteria	Deltaproteobacteria	unknown_Deltaproteobacteria	unknown_Deltaproteobacteria	unknown_Deltaproteobacteria	unknown_Deltaproteobacteria	NA
ASV459	1	0.8571	0.926	0.002	WB low_day.5	Bacteria	Bacteroidetes	Bacteroidia	Chitinophagales	Saprospiraceae	unknown_Saprospiraceae	unknown_Saprospiraceae	JQ196292.1.1351
ASV583	1	0.8571	0.926	0.003	WB low_day.5	Bacteria	Proteobacteria	Gammaproteobacteria	Thiotrichales	Thiotrichaceae	Leucothrix	unknown_Leucothrix	JQ347498.1.1491
ASV69	1	0.8571	0.926	0.003	NB+PB+WB high_day.5	Bacteria	Bacteroidetes	Bacteroidia	Flavobacteriales	Flavobacteriaceae	Nonlabens	Nonlabens_dokdonensis_DSW-6	CP001397.2039941.204145
ASV298	0.8543	1	0.924	0.004	WB west wall_day.5	Bacteria	Verrucomicrobia	Verrucomicrobiae	Verrucomicrobiales	Rubritaleaceae	Rubritalea	unknown_Rubritalea	NA
ASV110	0.929	0.9167	0.923	0.001	NB+WB high_day.1	Bacteria	Bacteroidetes	Bacteroidia	Chitinophagales	Saprospiraceae	unknown_Saprospiraceae	unknown_Saprospiraceae	NA
ASV111	0.9301	0.9167	0.923	0.002	NB+PB+WB west wall_day.5	Bacteria	Verrucomicrobia	Verrucomicrobiae	Verrucomicrobiales	Rubritaleaceae	Roseibacillus	unknown_Roseibacillus	FJ873322.1.1398
ASV16	0.9573	0.8889	0.922	0.037	NB+PB+WB high+WB west wall_day.5	Bacteria	Proteobacteria	Alphaproteobacteria	Rhodobacterales	Rhodobacteraceae	Octadecabacter	Octadecabacter_temperatus	KF836544.1.1324
ASV116	0.8484	1	0.921	0.002	WB low_day.5	Bacteria	Planctomycetes	Planctomycetacia	Pirellulales	Pirellulaceae	Blastopirellula	unknown_Blastopirellula	NA
ASV180	0.9255	0.9167	0.921	0.003	NB+WB low_day.5	Bacteria	Bacteroidetes	Bacteroidia	Chitinophagales	Saprospiraceae	unknown_Saprospiraceae	unknown_Saprospiraceae	NA
ASV217	0.9869	0.8571	0.92	0.002	WB low_day.5	Bacteria	Bacteroidetes	Bacteroidia	Chitinophagales	Saprospiraceae	unknown_Saprospiraceae	unknown_Saprospiraceae	JQ196292.1.1351
ASV65	1	0.8462	0.92	0.001	PB+WB high+WB west wall_day.5	Bacteria	Bacteroidetes	Bacteroidia	Flavobacteriales	Flavobacteriaceae	unknown_Flavobacteriaceae	unknown_Flavobacteriaceae	NA
ASV37	0.9532	0.8889	0.92	0.012	PB+WB high+WB west wall_day.5	Bacteria	Bacteroidetes	Bacteroidia	Flavobacteriales	Flavobacteriaceae	Winogradskyella	unknown_Winogradskyella	FJ946592.1.1290
ASV5	0.9041	0.9333	0.919	0.012	NB+WB low_day.5	Bacteria	Proteobacteria	Gammaproteobacteria	Thiohalorhabdales	Thiohalorhabdaceae	Granulosicoccus	unknown_Granulosicoccus	JQ218703.1.1493
ASV106	0.9838	0.8571	0.918	0.002	WB low_day.5	Bacteria	Verrucomicrobia	Verrucomicrobiae	Verrucomicrobiales	Rubritaleaceae	Roseibacillus	unknown_Roseibacillus	JQ195958.1.1364
ASV242	0.9734	0.8571	0.913	0.003	WB high_day.1	Bacteria	Bacteroidetes	Bacteroidia	Flavobacteriales	Flavobacteriaceae	Maribacter	unknown_Maribacter	NA
ASV164	1	0.8333	0.913	0.003	WB low_day.1	Bacteria	Bacteroidetes	Bacteroidia	Chitinophagales	Saprospiraceae	unknown_Saprospiraceae	unknown_Saprospiraceae	NA
ASV168	1	0.8333	0.913	0.003	WB low_day.1	Bacteria	Bacteroidetes	Bacteroidia	Chitinophagales	Saprospiraceae	unknown_Saprospiraceae	unknown_Saprospiraceae	AB476226.1.1449
ASV169	1	0.8333	0.913	0.003	WB low_day.1	Bacteria	Verrucomicrobia	Verrucomicrobiae	Verrucomicrobiales	Rubritaleaceae	Roseibacillus	unknown_Roseibacillus	JQ198528.1.1364
ASV372	1	0.8333	0.913	0.003	WB low_day.1	Bacteria	Kiritimatiellaeota	Kiritimatiellae	WCHB1-41	unknown_WCHB1-41	unknown_WCHB1-41	unknown_WCHB1-41	AB661552.1.1484
ASV631	1	0.8333	0.913	0.003	WB low_day.1	Bacteria	Bacteroidetes	Bacteroidia	Chitinophagales	Saprospiraceae	unknown_Saprospiraceae	unknown_Saprospiraceae	JQ197156.1.1348
ASV103	1	0.8333	0.913	0.003	NB+WB low_day.5	Bacteria	Planctomycetes	Planctomycetacia	Pirellulales	Pirellulaceae	Blastopirellula	unknown_Blastopirellula	FN822210.1.1536
ASV359	1	0.8333	0.913	0.002	NB+WB low_day.5	Bacteria	Bacteroidetes	Bacteroidia	Flavobacteriales	Flavobacteriaceae	unknown_Flavobacteriaceae	unknown_Flavobacteriaceae	NA
ASV173	0.8209	1	0.912	0.003	WB low_day.1	Bacteria	Bacteroidetes	Bacteroidia	Chitinophagales	Saprospiraceae	unknown_Saprospiraceae	unknown_Saprospiraceae	JQ196292.1.1351
ASV278	0.981	0.8462	0.911	0.014	NB+WB high+WB low+WB west wall_day.1	Bacteria	Bacteroidetes	Bacteroidia	Chitinophagales	Saprospiraceae	unknown_Saprospiraceae	unknown_Saprospiraceae	FN433362.1.1487
ASV61	0.9929	0.8333	0.91	0.004	NB+WB high+WB low_day.5	Bacteria	Bacteroidetes	Bacteroidia	Flavobacteriales	Flavobacteriaceae	Olleya	Olleya_sp._VCSA23	GQ996384.1.1483
ASV11	0.8758	0.9412	0.908	0.037	NB+PB+WB low_day.1	Bacteria	Planctomycetes	Planctomycetacia	Pirellulales	Pirellulaceae	Blastopirellula	unknown_Blastopirellula	JQ198127.1.1339
ASV311	0.9628	0.8571	0.908	0.003	WB low_day.5	Bacteria	Bacteroidetes	Bacteroidia	Chitinophagales	Saprospiraceae	unknown_Saprospiraceae	unknown_Saprospiraceae	JQ196292.1.1351
ASV6	0.9874	0.8333	0.907	0.006	NB+PB+WB high+WB low_day.1	Bacteria	Bacteroidetes	Bacteroidia	Chitinophagales	Saprospiraceae	Lewinella	Lewinella_sp._HME9321	KF385496.1.1389
ASV103	1	0.8182	0.905	0.001	NB+WB low_day.1	Bacteria	Planctomycetes	Planctomycetacia	Pirellulales	Pirellulaceae	Blastopirellula	unknown_Blastopirellula	FN822210.1.1536
ASV403	1	0.8182	0.905	0.001	NB+WB low_day.1	Bacteria	Bacteroidetes	Bacteroidia	Chitinophagales	Saprospiraceae	unknown_Saprospiraceae	unknown_Saprospiraceae	NA
ASV110	0.9019	0.9091	0.905	0.006	NB+WB high_day.1	Bacteria	Bacteroidetes	Bacteroidia	Chitinophagales	Saprospiraceae	unknown_Saprospiraceae	unknown_Saprospiraceae	NA
ASV385	1	0.8182	0.905	0.036	NB+WB high+WB low+WB west wall_day.5	Bacteria	Bacteroidetes	Bacteroidia	Chitinophagales	Saprospiraceae	Aureispira	Saprospira_sp._CNJ640	AY527410.1.1443
ASV454	0.9646	0.8462	0.903	0.038	NB+WB high+WB low+WB west wall_day.1	Bacteria	Verrucomicrobia	Verrucomicrobiae	Verrucomicrobiales	Rubritaleaceae	Persicirhabdus	unknown_Persicirhabdus	JQ195816.1.1359
ASV93	0.9513	0.8571	0.903	0.003	NB+WB low_day.5	Bacteria	Planctomycetes	Planctomycetacia	Pirellulales	Pirellulaceae	Blastopirellula	unknown_Blastopirellula	FN822210.1.1536
ASV12	0.9491	0.8571	0.902	0.002	PB+WB west wall_day.1	Bacteria	Bacteroidetes	Bacteroidia	Flavobacteriales	Flavobacteriaceae	Maribacter	unknown_Maribacter	NA
ASV65	1	0.8095	0.9	0.003	PB+WB high+WB west wall_day.1	Bacteria	Bacteroidetes	Bacteroidia	Flavobacteriales	Flavobacteriaceae	unknown_Flavobacteriaceae	unknown_Flavobacteriaceae	NA

Appendix B - Table 2. Indicator analysis for ASVs significantly associated with site(s) of origin in the common garden. Specific indicators were identified for each site at initial sampling (day 1) and final sampling (day 5) in common garden as well as for all possible combinations of sites and time points using the indicspecies package in R (Cáceres and Legendre, 2009). The Indval statistic is comprised of A, specificity, and B, fidelity of an ASV.

ASV	A	B	indval.stat	p.value	group	Domain	Phylum	Class	Order	Family	Genus	Species	Accession
ASV26	1	1	1	0.001	WB low	Bacteria	Bacteroidetes	Bacteroidia	Chitinophagales	Saprospiraceae	unknown_Saprospiraceae	unknown_Saprospiraceae	NA
ASV61	1	1	1	0.001	WB low	Bacteria	Bacteroidetes	Bacteroidia	Flavobacteriales	Flavobacteriaceae	Olleya	Olleya_sp._VCSA23	GQ996384.1.1483
ASV66	1	1	1	0.001	WB low	Bacteria	Proteobacteria	Gammaproteobacteria	Thiohalorhabdales	Thiohalorhabdaceae	Granulosicoccus	unknown_Granulosicoccus	JQ218711.1.1497
ASV2	0.9993	1	1	0.001	WB low	Bacteria	Verrucomicrobia	Verrucomicrobiae	Verrucomicrobiales	Rubritaleaceae	Rubritalea	unknown_Rubritalea	JQ196089.1.1359
ASV4	0.998	1	0.999	0.001	PB	Bacteria	Bacteroidetes	Bacteroidia	Flavobacteriales	Flavobacteriaceae	Nonlabens	unknown_Nonlabens	NA
ASV25	0.9978	1	0.999	0.001	PB	Bacteria	Verrucomicrobia	Verrucomicrobiae	Verrucomicrobiales	Rubritaleaceae	Luteolibacter	unknown_Luteolibacter	NA
ASV17	0.9983	1	0.999	0.001	WB low	Bacteria	Proteobacteria	Gammaproteobacteria	Thiohalorhabdales	Thiohalorhabdaceae	Granulosicoccus	unknown_Granulosicoccus	NA
ASV58	0.9946	1	0.997	0.001	WB low	Bacteria	Bacteroidetes	Bacteroidia	Chitinophagales	Saprospiraceae	unknown_Saprospiraceae	unknown_Saprospiraceae	FN433362.1.1487
ASV3	0.9737	1	0.987	0.001	PB	Bacteria	Bacteroidetes	Bacteroidia	Flavobacteriales	Flavobacteriaceae	Dokdonia	Dokdonia_sp._Hel_1_53	JX854132.1.1248
ASV69	0.9617	1	0.981	0.001	PB	Bacteria	Bacteroidetes	Bacteroidia	Flavobacteriales	Flavobacteriaceae	Nonlabens	Nonlabens_dokdonensis_DSW-6	CP001397.2039941.2041454
ASV22	1	0.9524	0.976	0.001	PB	Bacteria	Bacteroidetes	Bacteroidia	Flavobacteriales	Flavobacteriaceae	Maribacter	unknown_Maribacter	NA
ASV85	1	0.9524	0.976	0.001	PB	Bacteria	Verrucomicrobia	Verrucomicrobiae	Verrucomicrobiales	Rubritaleaceae	Luteolibacter	unknown_Luteolibacter	NA
ASV16	0.9404	1	0.97	0.001	PB	Bacteria	Proteobacteria	Alphaproteobacteria	Rhodobacterales	Rhodobacteraceae	Octadecabacter	Octadecabacter_temperatus	KF836544.1.1324
ASV37	1	0.9412	0.97	0.001	WB low	Bacteria	Proteobacteria	Alphaproteobacteria	Rhodobacterales	Rhodobacteraceae	Octadecabacter	Octadecabacter_temperatus	KF836544.1.1324
ASV93	1	0.9412	0.97	0.001	WB low	Bacteria	Planctomycetes	Planctomycetacia	Pirellulales	Pirellulaceae	Blastopirellula	unknown_Blastopirellula	FN822210.1.1536
ASV332	1	0.9412	0.97	0.001	WB low	Bacteria	Bacteroidetes	Bacteroidia	Chitinophagales	Saprospiraceae	unknown_Saprospiraceae	unknown_Saprospiraceae	NA
ASV462	1	0.9412	0.97	0.001	WB low	Bacteria	Bacteroidetes	Bacteroidia	Chitinophagales	Saprospiraceae	unknown_Saprospiraceae	unknown_Saprospiraceae	AB476201.1.1445
ASV453	1	0.9412	0.97	0.001	WB low	Bacteria	Proteobacteria	Gammaproteobacteria	Thiohalorhabdales	Thiohalorhabdaceae	Granulosicoccus	unknown_Granulosicoccus	JQ218703.1.1493
ASV21	0.998	0.9412	0.969	0.001	WB low	Bacteria	Verrucomicrobia	Verrucomicrobiae	Verrucomicrobiales	Rubritaleaceae	Rubritalea	unknown_Rubritalea	NA
ASV5	0.9359	1	0.967	0.001	WB low	Bacteria	Proteobacteria	Gammaproteobacteria	Thiohalorhabdales	Thiohalorhabdaceae	Granulosicoccus	unknown_Granulosicoccus	JQ218703.1.1493
ASV178	0.9921	0.9412	0.966	0.001	WB low	Bacteria	Proteobacteria	Alphaproteobacteria	Sphingomonadales	Sphingomonadaceae	Erythrobacter	Erythrobacter_sp._KLE1221	GU644356.1.1384
ASV12	1	0.9048	0.951	0.001	PB	Bacteria	Bacteroidetes	Bacteroidia	Flavobacteriales	Flavobacteriaceae	Maribacter	unknown_Maribacter	NA
ASV76	1	0.9048	0.951	0.001	PB	Bacteria	Bacteroidetes	Bacteroidia	Chitinophagales	Saprospiraceae	Lewinella	Lewinella_sp._HME9321	KF385496.1.1389
ASV295	1	0.9048	0.951	0.001	PB	Bacteria	Planctomycetes	Phycisphaerae	Phycisphaerales	Phycisphaeraceae	unknown_Phycisphaeraceae	unknown_Phycisphaeraceae	AB491825.1.1502
ASV56	0.9593	0.9412	0.95	0.001	WB low	Bacteria	Proteobacteria	Alphaproteobacteria	Rhodobacterales	Rhodobacteraceae	unknown_Rhodobacteraceae	unknown_Rhodobacteraceae	NA
ASV51	0.9934	0.9048	0.948	0.001	PB	Bacteria	Bacteroidetes	Bacteroidia	Flavobacteriales	Flavobacteriaceae	unknown_Flavobacteriaceae	unknown_Flavobacteriaceae	AB476295.1.1444
ASV116	0.9511	0.9412	0.946	0.001	WB low	Bacteria	Planctomycetes	Planctomycetacia	Pirellulales	Pirellulaceae	Blastopirellula	unknown_Blastopirellula	NA
ASV38	0.95	0.9412	0.946	0.001	WB low	Bacteria	Bacteroidetes	Bacteroidia	Flavobacteriales	Flavobacteriaceae	Nonlabens	Nonlabens_arenilitoris	KP769429.1.1309
ASV97	1	0.8824	0.939	0.001	WB low	Bacteria	Verrucomicrobia	Verrucomicrobiae	Verrucomicrobiales	Rubritaleaceae	Rubritalea	unknown_Rubritalea	JQ347431.1.1350
ASV103	1	0.8824	0.939	0.001	WB low	Bacteria	Planctomycetes	Planctomycetacia	Pirellulales	Pirellulaceae	Blastopirellula	unknown_Blastopirellula	FN822210.1.1536
ASV152	0.92	0.9524	0.936	0.001	PB	Bacteria	Verrucomicrobia	Verrucomicrobiae	Verrucomicrobiales	Rubritaleaceae	Roseibacillus	unknown_Roseibacillus	JQ198528.1.1364
ASV7	0.8607	1	0.928	0.001	PB	Bacteria	Proteobacteria	Alphaproteobacteria	Rhodobacterales	Rhodobacteraceae	Sulfitobacter	Sulfitobacter_sp._FS12-3	JQ799973.1.1380
ASV95	1	0.8571	0.926	0.001	PB	Bacteria	Proteobacteria	Gammaproteobacteria	Thiohalorhabdales	Thiohalorhabdaceae	Granulosicoccus	unknown_Granulosicoccus	JQ218705.1.1493
ASV99	1	0.8571	0.926	0.001	PB	Bacteria	Bacteroidetes	Bacteroidia	Flavobacteriales	Flavobacteriaceae	Psychroserpens	Psychroserpens_sp._ANY4	KT121448.1.1407
ASV177	1	0.8571	0.926	0.001	PB	Bacteria	Bacteroidetes	Bacteroidia	Chitinophagales	Saprospiraceae	Lewinella	Lewinella_sp._HME9321	KF385496.1.1389
ASV57	0.886	0.9524	0.919	0.001	PB	Bacteria	Bacteroidetes	Bacteroidia	Flavobacteriales	Flavobacteriaceae	Winogradskyella	unknown_Winogradskyella	FJ946592.1.1290
ASV29	1	0.8235	0.907	0.001	WB low	Bacteria	Proteobacteria	Alphaproteobacteria	Rhodobacterales	Rhodobacteraceae	Sulfitobacter	alpha_proteobacterium_SF16	GU061130.1.1335
ASV30	1	0.8235	0.907	0.001	WB low	Bacteria	Verrucomicrobia	Verrucomicrobiae	Verrucomicrobiales	Rubritaleaceae	Rubritalea	unknown_Rubritalea	NA
ASV77	1	0.8235	0.907	0.001	WB low	Bacteria	Bacteroidetes	Bacteroidia	Chitinophagales	Saprospiraceae	unknown_Saprospiraceae	unknown_Saprospiraceae	AB476226.1.1449
ASV161	1	0.8235	0.907	0.001	WB low	Bacteria	Proteobacteria	Alphaproteobacteria	Rhodobacterales	Rhodobacteraceae	Loktanella	unknown_Loktanella	NA
ASV169	1	0.8235	0.907	0.001	WB low	Bacteria	Verrucomicrobia	Verrucomicrobiae	Verrucomicrobiales	Rubritaleaceae	Roseibacillus	unknown_Roseibacillus	JQ198528.1.1364
ASV201	1	0.8235	0.907	0.001	WB low	Bacteria	Proteobacteria	Gammaproteobacteria	Thiotrichales	Thiotrichaceae	Leucothrix	unknown_Leucothrix	JQ347498.1.1491
ASV276	1	0.8235	0.907	0.001	WB low	Bacteria	Bacteroidetes	Bacteroidia	Chitinophagales	Saprospiraceae	unknown_Saprospiraceae	unknown_Saprospiraceae	NA
ASV422	1	0.8235	0.907	0.001	WB low	Bacteria	Proteobacteria	Gammaproteobacteria	Thiotrichales	Thiotrichaceae	Leucothrix	unknown_Leucothrix	NA
ASV41	0.8728	0.9412	0.906	0.001	WB low	Bacteria	Bacteroidetes	Bacteroidia	Chitinophagales	Saprospiraceae	Membranicola	Lewinella_sp._CZ-AZ5	JX306763.1.1396
ASV187	0.9943	0.8235	0.905	0.001	WB low	Bacteria	Bacteroidetes	Bacteroidia	Sphingobacteriales	NS11-12_marine_group	unknown_NS11-12_marine_group	unknown_NS11-12_marine_group	AB476256.1.1446
ASV112	1	0.8095	0.9	0.001	PB	Bacteria	Bacteroidetes	Bacteroidia	Chitinophagales	Saprospiraceae	Lewinella	Lewinella_sp._HME9321	KF385496.1.1389

Appendix B - Table 3. Indicator analysis for ASVs on *Fucus distichus* significantly associated with origin sites in the reciprocal transplant experiment. Specific indicators were identified for each site based on initial samples (day 0) and unmanipulated controls at West Beach low or Pruth Bay over the 5 day experiment using the indicspecies package in R (Cáceres and Legendre, 2009). The Indval statistic is comprised of A, specificity, and B, fidelity of an ASV.

Appendix C - Chapter 4: Supplementary information

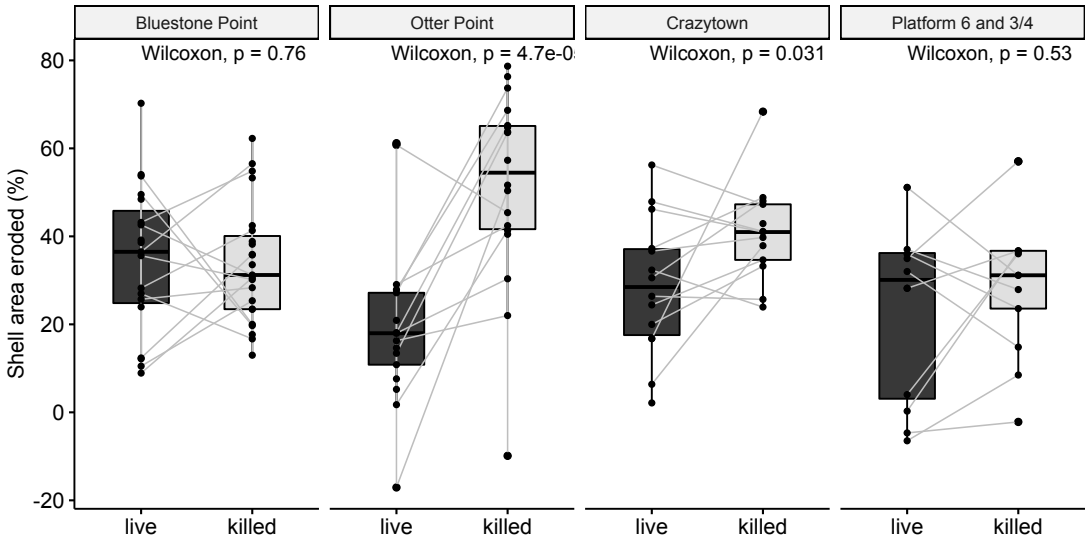

Appendix C - Figure 1. Wilcoxan tests comparing percentage shell erosion for pairs of live and killed transplanted mussels at each site.

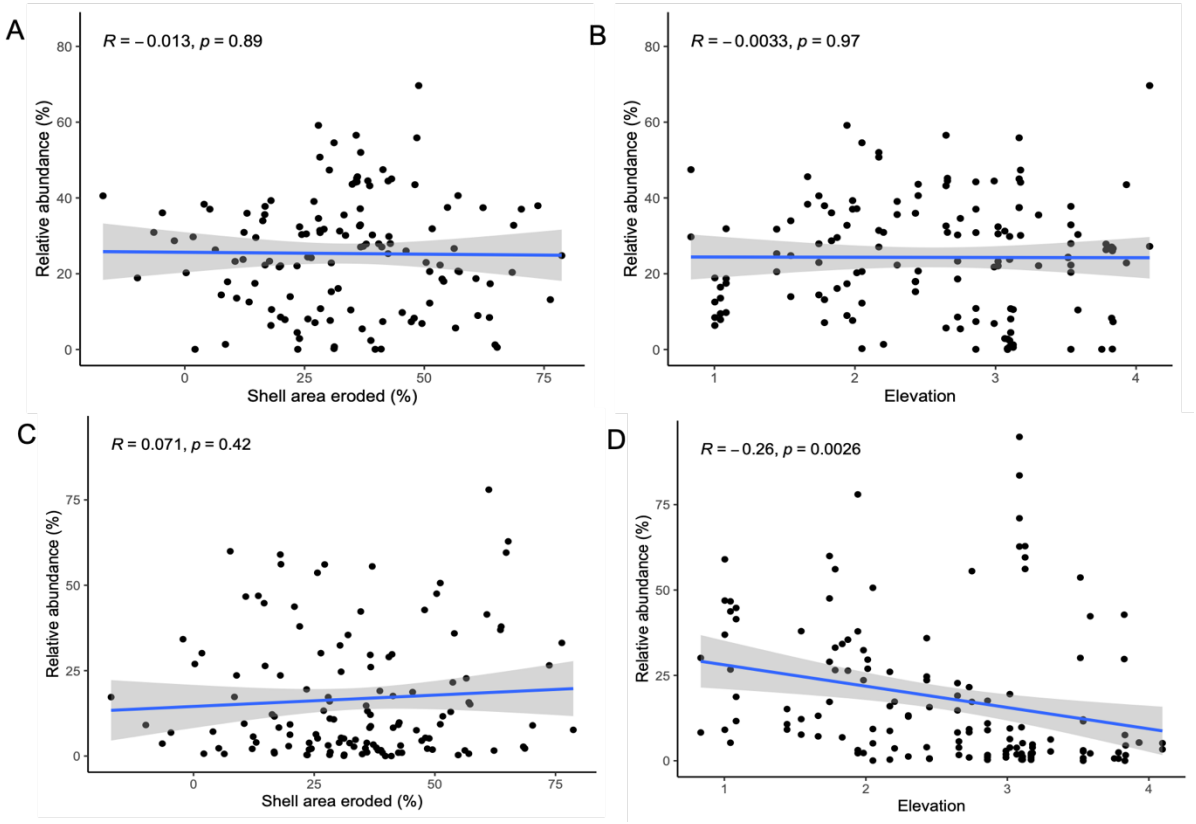

Appendix C - Figure 2. Relative abundance of reads per sample plotted as a function of A) percentage of host mussel shell eroded and B) intertidal elevation for potentially endolithic cyanobacteria and as a function of C) percentage of host mussel shell eroded and D) intertidal elevation for eukaryotic algae (chloroplasts).
Intertidal elevation is expressed as meters above Canadian chart datum.

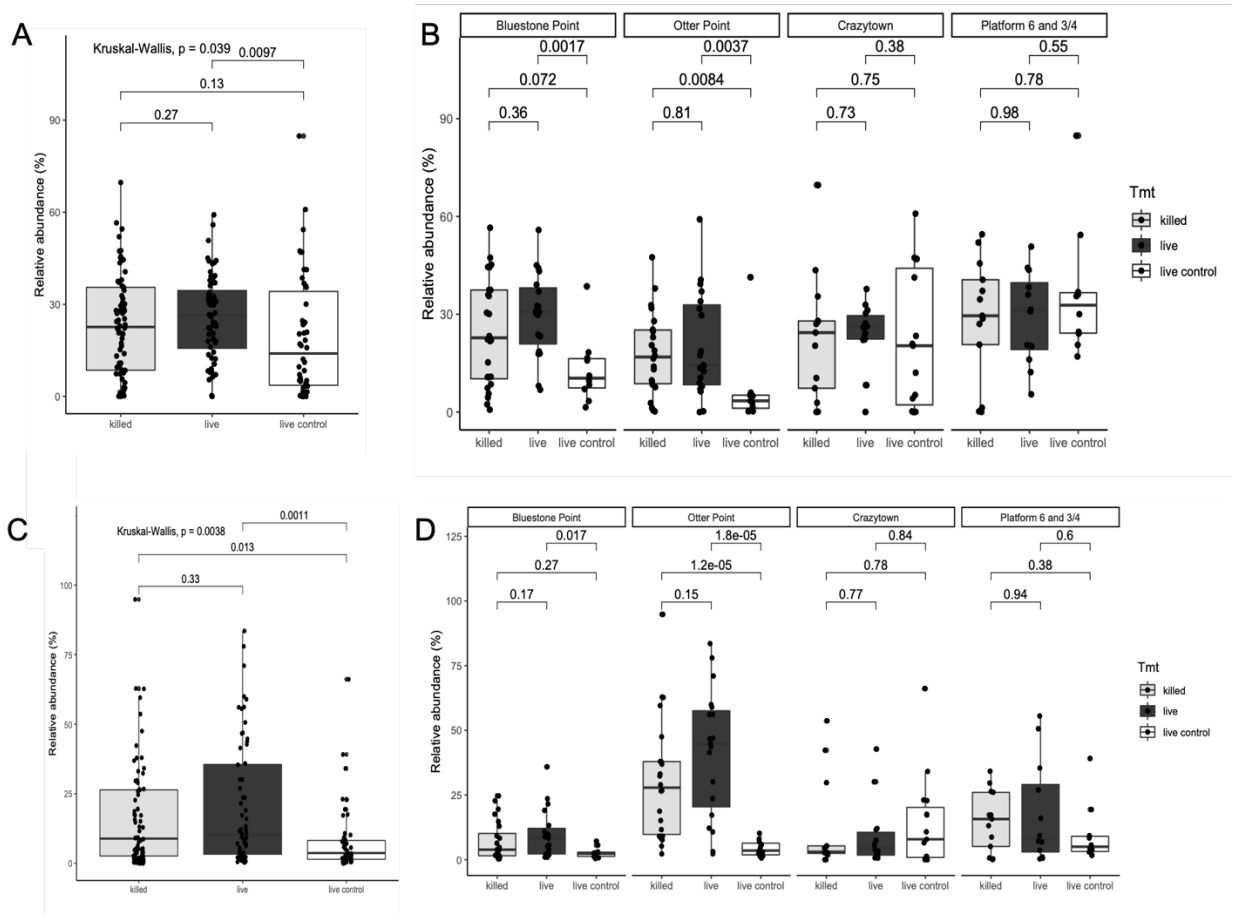

Appendix C - Figure 3. Differences in the relative abundance of potentially endolithic cyanobacteria reads between A) treatments and B) treatments grouped by site. Differences in the relative abundance of chloroplast reads between C) treatments and D) treatments grouped by site. Statistically significant differences based on Kruskal-Wallis tests are displayed above the groups being compared.

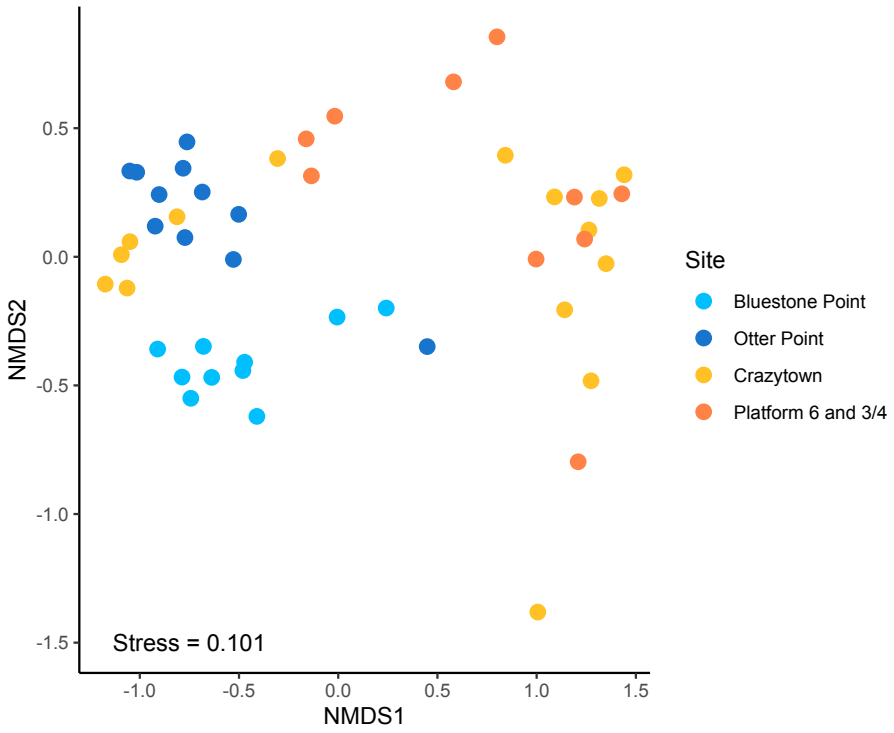

Appendix C - Figure 4. Non-metric multidimensional scaling analysis of Bray-Curtis dissimilarity for microbiome samples of live control mussel shells.

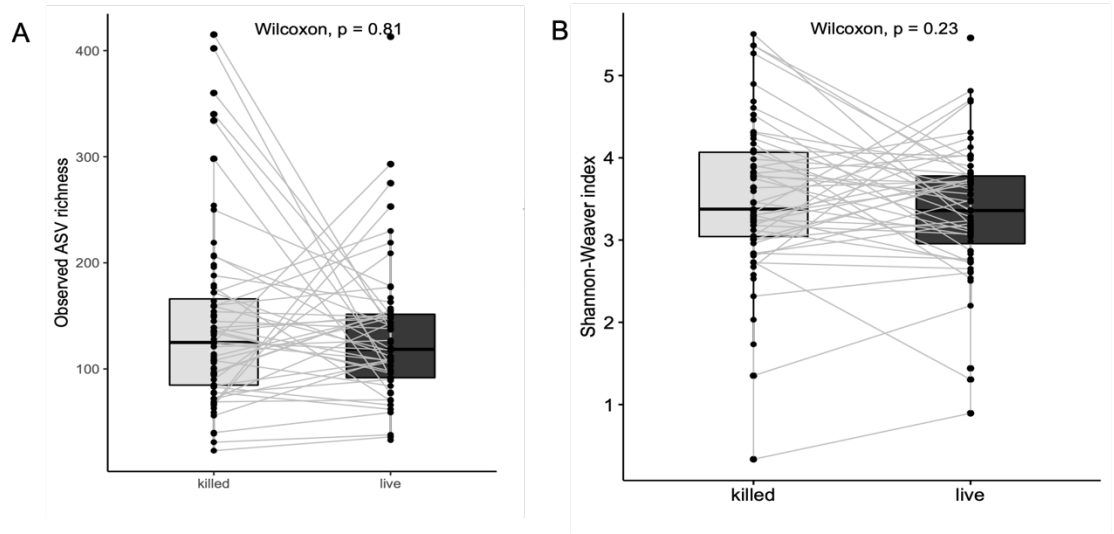

Appendix C - Figure 5. Wilcoxan tests examining differences in A) ASV richness and B) Shannon-Weaver (H') metrics of microbiome alpha diversity between live and killed transplanted mussel shell pairs.

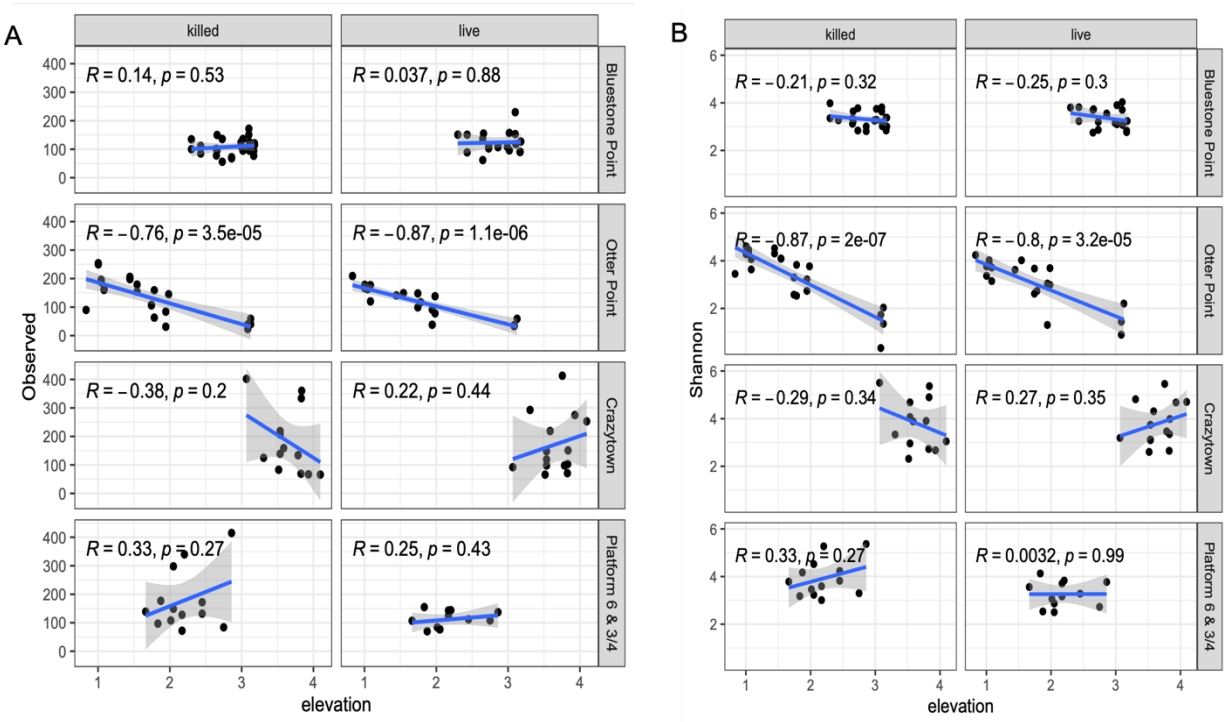

Appendix C - Figure 6. Relationship between elevation in the intertidal zone (expressed as meters above Canadian chart datum) and A) ASV richness and B) Shannon-Weaver (H') metrics of microbiome alpha diversity between live and killed transplanted mussel shell pairs at each site.

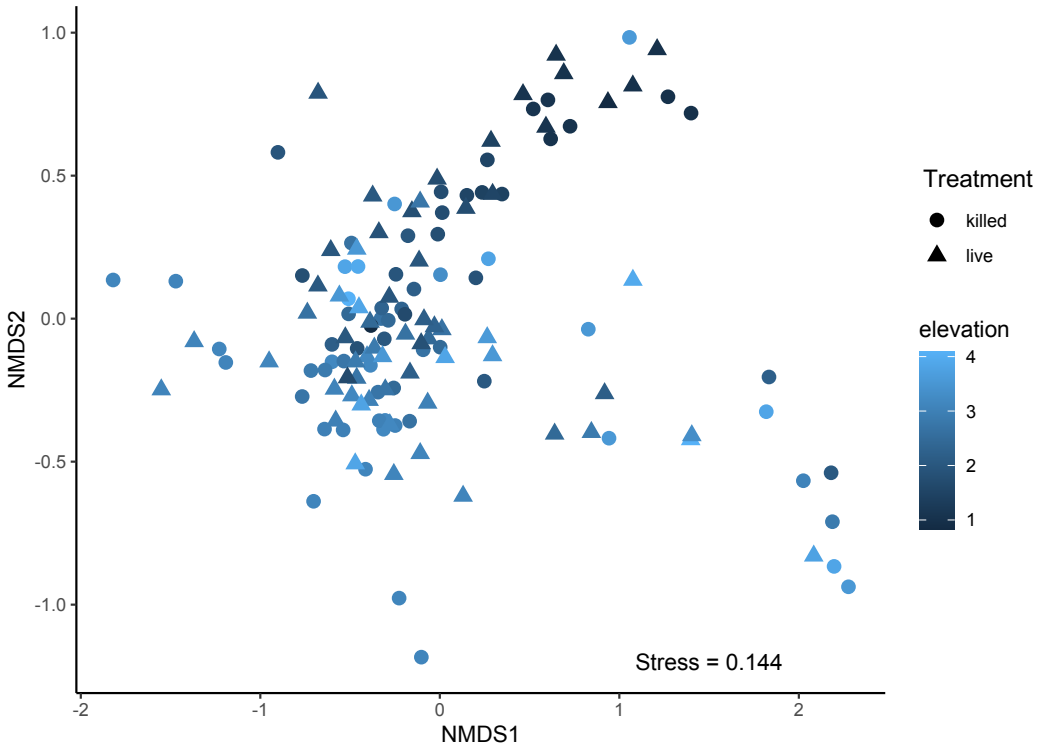

Appendix C - Figure 7. Non-metric multidimensional scaling analysis of Bray-Curtis dissimilarity for transplanted mussel shell microbiome samples by elevation in the intertidal zone expressed continuously as meters above Canadian chart datum.

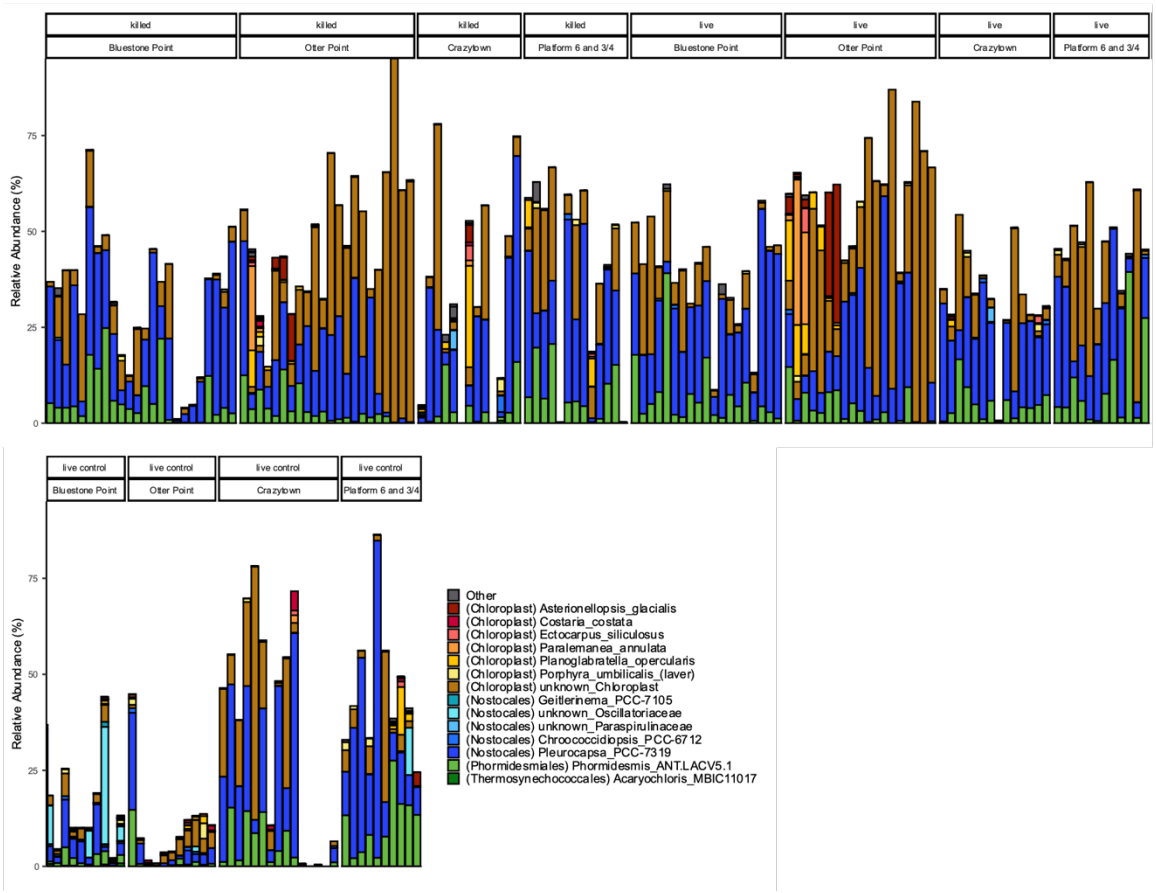

Appendix C - Figure 8. Relative abundance of the dominant cyanobacteria and chloroplast reads across the dataset. Each bar represents an individual mussel sample. Live and killed transplant samples are ordered from left to right by low to high elevation in the intertidal zone

Treatment	Taxa	Specificity (A)	Fidelity (B)	IndVal statistic	p-value
Killed	unknown_Rhodobacteraceae	0.598	1.000	0.774	0.035
	Maribacter	0.710	0.771	0.740	0.026
	unknown_Alphaproteobacteria	0.704	0.600	0.650	0.031
	Zobellia	1.000	0.229	0.478	0.007
	unknown_DEV007	0.868	0.257	0.473	0.024
Treatment	**Taxa**	**Specificity (A)**	**Fidelity (B)**	**IndVal statistic**	**p-value**
Live	Maribius	0.952	0.257	0.495	0.028

Appendix C - Table 1. IndVal results for live versus killed transplants at Otter Point and Crazytown where the percentage of mussel shell eroded was significantly different between transplant treatments.

Site comparison	Df	SumsOfSqs	F Model	R^2	p-value	p-adjusted
Bluestone Point vs Crazytown	1	1.27	3.55	0.134	0.001	**0.006**
Bluestone Point vs Otter Point	1	1.17	3.78	0.166	0.001	**0.006**
Bluestone Point vs Platform 6 and 3/4	1	1.41	4.21	0.19	0.001	**0.006**
Crazytown vs Otter Point	1	1.29	3.69	0.133	0.002	**0.012**
Crazytown vs Platform 6 and 3/4	1	0.575	1.54	0.0629	0.096	0.576
Otter Point vs Platform 6 and 3/4	1	1.58	4.84	0.203	0.001	**0.006**

Appendix C - Table 2. . Pairwise PERMANOVA results of Bray-Curtis dissimilarity by site for the microbiome on live control mussels.

ASV	Sample type	IndVal	Prevalence (A)	Fidelity (B)	Rank1	Rank2	Rank3	Rank4	Rank5	Rank6	Rank7	Accession
ASV85	Live control mussels	0.958543594	0.982908554	0.934782609	Bacteria	Proteobacteria	Alphaproteobacteria	Rhodobacterales	Rhodobacteraceae	NA	NA	NA
ASV125	Live control mussels	0.942626688	0.973168413	0.913043478	Bacteria	Actinobacteria	Acidimicrobiia	Microtrichales	Ilumatobacteraceae	Ilumatobacter	uncultured_bacterium	JQ197530.1.1340
ASV2	Transplanted mussels	0.92741047	0.965838972	0.890510949	Bacteria	Cyanobacteria	Oxyphotobacteria	Chloroplast	uncultured_bacterium	uncultured_bacterium	uncultured_bacterium	NA
ASV6	Transplanted mussels	0.926244519	0.963411971	0.890510949	Bacteria	Bacteroidetes	Bacteroidia	Chitinophagales	Saprospiraceae	Lewinella	Lewinella_sp._HME9321	KF385496.1.1389
ASV18	Transplanted mussels	0.922343268	0.979397002	0.868613139	Bacteria	Proteobacteria	Alphaproteobacteria	Rhizobiales	Rhizobiaceae	uncultured	uncultured_bacterium	AB476277.1.1408
ASV79	Live control mussels	0.920588533	0.999595626	0.847826087	Bacteria	Proteobacteria	Alphaproteobacteria	Rhizobiales	Rhizobiaceae	Pseudahrensia	Pseudahrensia_aquimaris	GU575117.1.1441
ASV149	Live control mussels	0.917966767	0.993910189	0.847826087	Bacteria	Bacteroidetes	Bacteroidia	Flavobacteriales	Flavobacteriaceae	Winogradskyella	NA	NA
ASV4	Transplanted mussels	0.902752606	0.996873489	0.817518248	Bacteria	Proteobacteria	Alphaproteobacteria	Rhizobiales	Rhizobiaceae	NA	NA	NA
ASV168	Live control mussels	0.896854406	1	0.804347826	Bacteria	Bacteroidetes	Bacteroidia	Flavobacteriales	Flavobacteriaceae	Ulvibacter	uncultured_bacterium	JQ287292.1.1482
ASV9	Transplanted mussels	0.896524592	0.974465656	0.824817518	Bacteria	Cyanobacteria	Oxyphotobacteria	Phormidesmiales	Phormidesmiaceae	Phormidesmis_ANT.LACV5.1	NA	NA
ASV16	Transplanted mussels	0.893463637	0.854406141	0.934306569	Bacteria	Proteobacteria	Alphaproteobacteria	Rhizobiales	Rhizobiaceae	Pseudahrensia	Pseudahrensia_aquimaris	GU575117.1.1441
ASV99	Live control mussels	0.891957443	0.963080308	0.826086957	Bacteria	Proteobacteria	Alphaproteobacteria	Rhodobacterales	Rhodobacteraceae	Loktanella	alpha_proteobacterium_SF17A	GU061152.1.1332
ASV259	Live control mussels	0.891946087	0.98908432	0.804347826	Bacteria	Bacteroidetes	Bacteroidia	Chitinophagales	Saprospiraceae	uncultured	uncultured_bacterium	AB476201.1.1445
ASV3	Transplanted mussels	0.889613489	0.994710696	0.795620438	Bacteria	Proteobacteria	Alphaproteobacteria	Rhizobiales	Rhizobiaceae	uncultured	uncultured_bacterium	AB476277.1.1408
ASV137	Live control mussels	0.884651737	1	0.782608696	Bacteria	Bacteroidetes	Bacteroidia	Flavobacteriales	Flavobacteriaceae	Maribacter	NA	NA
ASV36	Transplanted mussels	0.882297725	0.978417896	0.795620438	Bacteria	Proteobacteria	Alphaproteobacteria	Rhodobacterales	Rhodobacteraceae	NA	NA	NA
ASV1	Transplanted mussels	0.87921228	0.860999593	0.897810219	Bacteria	Cyanobacteria	Oxyphotobacteria	Nostocales	Xenococcaceae	Pleurocapsa_PCC-7319	NA	NA
ASV113	Live control mussels	0.872278376	1	0.760869565	Bacteria	Proteobacteria	Alphaproteobacteria	Rhizobiales	Rhizobiaceae	Pseudahrensia	uncultured_marine_bacterium	NA
ASV150	Live control mussels	0.871244301	0.997630432	0.760869565	Bacteria	Bacteroidetes	Bacteroidia	Chitinophagales	Saprospiraceae	uncultured	uncultured_bacterium	NA
ASV191	Live control mussels	0.867099388	0.988160629	0.760869565	Bacteria	Bacteroidetes	Bacteroidia	Flavobacteriales	Flavobacteriaceae	Ulvibacter	Ulvibacter_marinus	KF146346.1.1440
ASV66	Live control mussels	0.865183761	0.800766866	0.934782609	Bacteria	Proteobacteria	Alphaproteobacteria	Rhodobacterales	Rhodobacteraceae	Litoreibacter	Litoreibacter_halocynthiae	DQ644172.1.1420
ASV111	Live control mussels	0.8614041	0.948132863	0.782608696	Bacteria	Bacteroidetes	Bacteroidia	Flavobacteriales	Flavobacteriaceae	Olleya	NA	NA
ASV305	Live control mussels	0.859726954	1	0.719130435	Bacteria	Bacteroidetes	Bacteroidia	Chitinophagales	Saprospiraceae	uncultured	uncultured_bacterium	NA
ASV330	Live control mussels	0.859262789	0.97037991	0.760869565	Bacteria	Proteobacteria	Alphaproteobacteria	Sphingomonadales	Sphingomonadaceae	Altererythrobacter	mucus_bacterium_91	AY654830.1.1386
ASV209	Live control mussels	0.858644803	0.997484156	0.719130435	Bacteria	Bacteroidetes	Bacteroidia	Chitinophagales	Saprospiraceae	uncultured	uncultured_bacterium	AB476288.1.1448
ASV10	Transplanted mussels	0.854471449	0.877426664	0.832116788	Bacteria	Cyanobacteria	Oxyphotobacteria	Nostocales	Xenococcaceae	Pleurocapsa_PCC-7319	NA	NA
ASV152	Live control mussels	0.851780921	0.953554684	0.760869565	Bacteria	Bacteroidetes	Bacteroidia	Chitinophagales	Saprospiraceae	uncultured	uncultured_bacterium	NA
ASV327	Live control mussels	0.846573476	0.999017755	0.717391304	Bacteria	Proteobacteria	Alphaproteobacteria	Sphingomonadales	Sphingomonadaceae	Sphingorhabdus	Sphingomonas_sp._S11-S-1	EU016172.1.1450
ASV300	Live control mussels	0.846130117	0.997971638	0.717391304	Bacteria	Deinococcus-Thermus	Deinococci	Deinococcales	Trueperaceae	Truepera	NA	NA
ASV787	Live control mussels	0.845232286	0.99585486	0.717391304	Bacteria	Proteobacteria	Alphaproteobacteria	Caulobacterales	Hyphomonadaceae	Hyphomonas	NA	NA
ASV275	Live control mussels	0.839123216	0.98151144	0.717391304	Bacteria	Bacteroidetes	Bacteroidia	Chitinophagales	Saprospiraceae	uncultured	uncultured_bacterium	AB476238.1.1449
ASV186	Live control mussels	0.834057656	1	0.695652174	Bacteria	Bacteroidetes	Bacteroidia	Flavobacteriales	Flavobacteriaceae	Maribacter	Maribacter_sp._MGE_SAT_274	DQ854411.1.1342
ASV505	Live control mussels	0.834057656	1	0.695652174	Bacteria	Proteobacteria	Alphaproteobacteria	Rhizobiales	Hyphomicrobiaceae	Filomicrobium	uncultured_marine_bacterium	FN396733.1.1364
ASV32	Transplanted mussels	0.834002022	0.934231705	0.744525547	Bacteria	Bacteroidetes	Bacteroidia	Chitinophagales	Saprospiraceae	Lewinella	Lewinella_sp._HME9321	KF385496.1.1389
ASV205	Live control mussels	0.832999774	0.997464897	0.695652174	Bacteria	Bacteroidetes	Bacteroidia	Flavobacteriales	Flavobacteriaceae	Maribacter	NA	NA
ASV565	Live control mussels	0.832880175	0.997178491	0.695652174	Bacteria	Bacteroidetes	Bacteroidia	Chitinophagales	Saprospiraceae	uncultured	uncultured_bacterium	NA
ASV59	Transplanted mussels	0.829658632	0.952542242	0.722627737	Bacteria	Cyanobacteria	Oxyphotobacteria	Phormidesmiales	Phormidesmiaceae	Phormidesmis_ANT.LACV5.1	Pseudophormidium_sp._ANT.LPE.3	AY493587.1.1466
ASV37	Transplanted mussels	0.825672235	0.983133112	0.693430657	Bacteria	Proteobacteria	Gammaproteobacteria	Thiohalorhabdales	Thiohalorhabdaceae	Granulosicoccus	uncultured_proteobacterium	JQ218705.1.1493
ASV7	Transplanted mussels	0.824319512	0.756844424	0.897810219	Bacteria	Cyanobacteria	Oxyphotobacteria	Nostocales	Xenococcaceae	Pleurocapsa_PCC-7319	NA	NA
ASV674	Live control mussels	0.820922069	1	0.673913043	Bacteria	Chloroflexi	Anaerolineae	Ardenticatenales	uncultured	uncultured_bacterium	uncultured_bacterium	AB491709.1.1401
ASV23	Transplanted mussels	0.818102308	0.965188632	0.693430657	Bacteria	Proteobacteria	Alphaproteobacteria	Caulobacterales	Hyphomonadaceae	Litorimonas	NA	NA
ASV39	Transplanted mussels	0.808075273	0.922258078	0.708029197	Bacteria	Bacteroidetes	Rhodothermia	Rhodothermales	Rhodothermaceae	Rubrivirga	Rubrivirga_profundi	KR108283.1.1462
ASV539	Live control mussels	0.806839015	0.998183434	0.652173913	Bacteria	Bacteroidetes	Bacteroidia	Chitinophagales	Saprospiraceae	uncultured	uncultured_bacterium	JQ197156.1.1348
ASV224	Live control mussels	0.806801875	0.99809154	0.652173913	Bacteria	Proteobacteria	Gammaproteobacteria	Thiohalorhabdales	Thiohalorhabdaceae	Granulosicoccus	uncultured_proteobacterium	JQ218703.1.1493
ASV304	Live control mussels	0.805797323	0.963491259	0.673913043	Bacteria	Proteobacteria	Alphaproteobacteria	Rhodobacterales	Rhodobacteraceae	Sulfitobacter	NA	NA
ASV620	Live control mussels	0.803036647	0.988797379	0.652173913	Bacteria	Proteobacteria	Alphaproteobacteria	Rhodobacterales	Rhodobacteraceae	NA	NA	NA
ASV61	Transplanted mussels	0.801220036	0.966457536	0.664233577	Bacteria	Proteobacteria	Alphaproteobacteria	Rickettsiales	Mitochondria	NA	NA	NA

Appendix C - Table 3. IndVal results for ASVs significantly associated with transplants versus live control mussels for all sites combined.

Appendix D - Chapter 5: Supplementary information

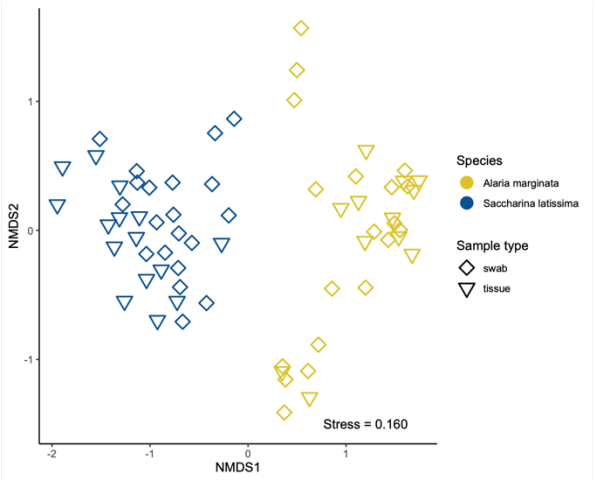

PERMANOVA by sample extraction type

	psuedo-F value	R^2	p-value
Alaria marginata	2.433	0.077	0.01
Saccharina latissima	2.986	0.066	**0.005**

Appendix D - Figure 1. Nonmetric multidimensional scaling plot of Bray-Curtis dissimilarity between bacterial communities on kelp meristem in BC taken by swabbing or by extracting from whole tissue at the final sampling in June 2021 and corresponding PERMANOVA tests.

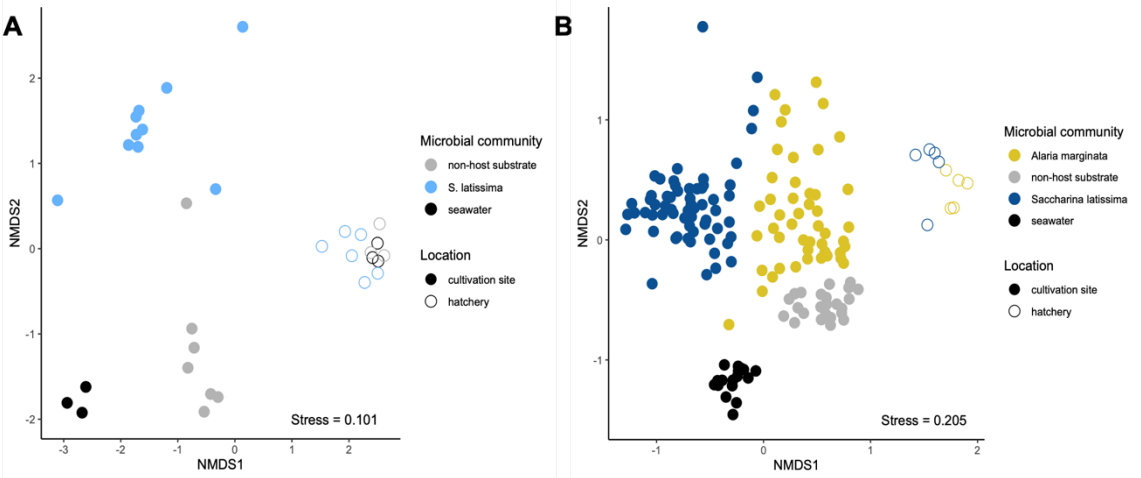

Appendix D - Figure 2. Nonmetric multidimensional scaling plot of Bray-Curtis dissimilarity between bacterial communities on kelp versus in seawater and on non-host substrates (aquaria surfaces or cultivation lines) from the hatchery and cultivation sites in A) Washington and B) British Columbia.

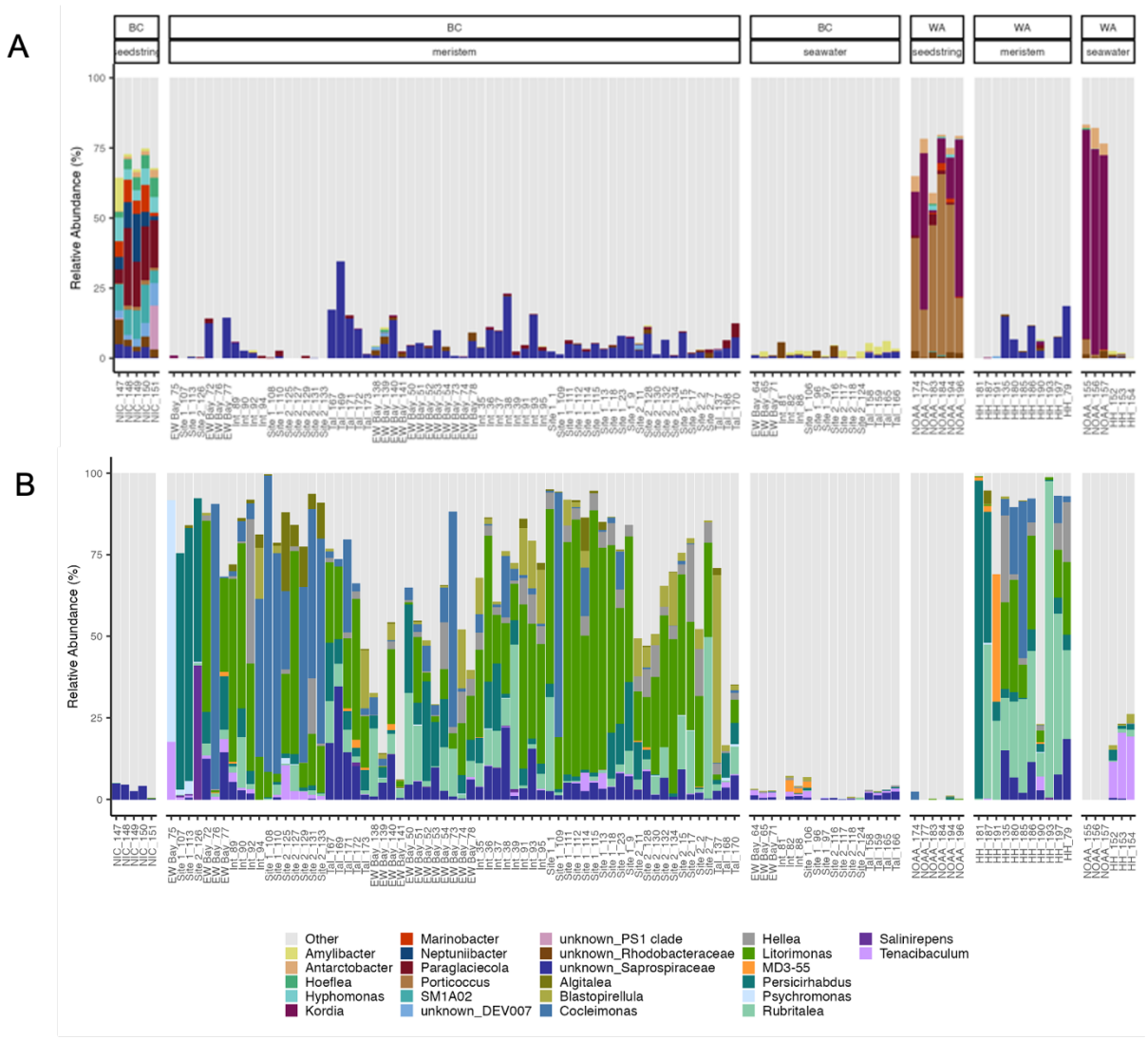

Appendix D - Figure 3. Stacked barplots showing A) the relative abundance of dominant bacterial genera from the hatchery on *Saccharina latissima* seedstring and field cultivated *S. latissima* as well as in the surrounding seawater and B) the dominant bacterial genera from kelp meristematic tissue at the cultivation sites compared to hatchery seedstring and seawater samples. X-axis labels represent sampling site (NIC = BC hatchery, EW Bay = East West Bay, Int = Interfor, Tal = Talbot Cove, NOAA = WA hatchery, HH = Hood Head) and unique sample number. Samples are arranged chronologically by month of sampling.

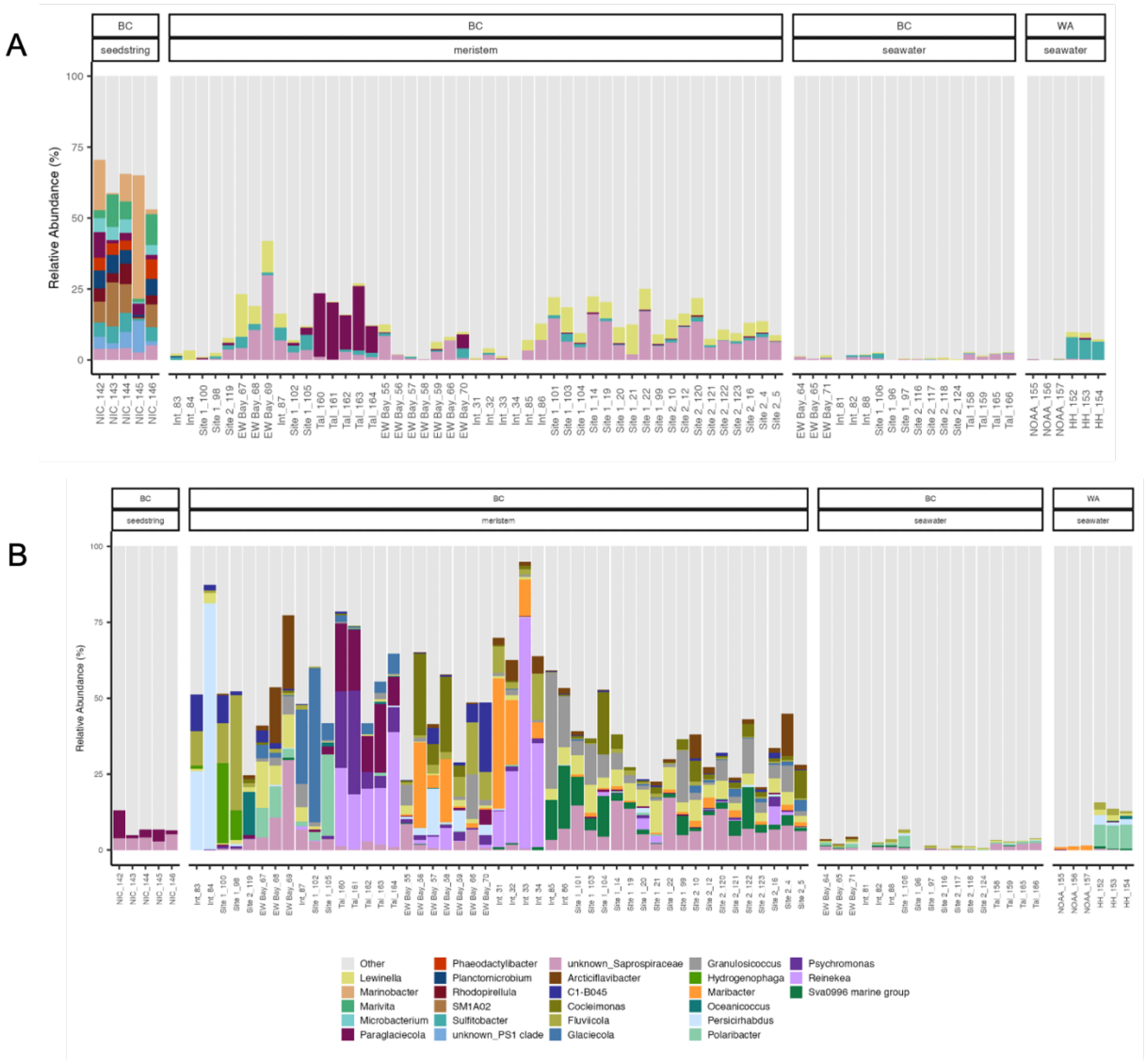

Appendix D - Figure 4. Stacked barplots showing A) the relative abundance of dominant bacterial genera from the hatchery on *Alaria marginata* seedstring and field cultivated *A. marginata* as well as in the surrounding seawater and B) the dominant bacterial genera from kelp meristematic tissue at the cultivation sites compared to hatchery seedstring and seawater samples. X-axis labels represent sampling site (NIC = BC hatchery, EW Bay = East West Bay, Int = Interfor, Tal = Talbot Cove) and unique sample number. Samples are arranged chronologically by month of sampling.